

University of Mississippi

eGrove

Electronic Theses and Dissertations

Graduate School

1-1-2022

LATE-STAGE DIVERSIFICATION OF SELECT NATURAL PRODUCTS â€“ NEW CHEMICAL ENTITIES WITH IMPROVED BIOLOGICAL ACTIVITIES

Moneerah J. Alqahtani

Follow this and additional works at: <https://egrove.olemiss.edu/etd>

Recommended Citation

Alqahtani, Moneerah J., "LATE-STAGE DIVERSIFICATION OF SELECT NATURAL PRODUCTS â€“ NEW CHEMICAL ENTITIES WITH IMPROVED BIOLOGICAL ACTIVITIES" (2022). *Electronic Theses and Dissertations*. 2191.

<https://egrove.olemiss.edu/etd/2191>

This Dissertation is brought to you for free and open access by the Graduate School at eGrove. It has been accepted for inclusion in Electronic Theses and Dissertations by an authorized administrator of eGrove. For more information, please contact egrove@olemiss.edu.

LATE-STAGE DIVERSIFICATION OF SELECT NATURAL PRODUCTS – NEW
CHEMICAL ENTITIES WITH IMPROVED BIOLOGICAL ACTIVITIES

A Dissertation
presented in partial fulfillment of requirements
for the degree of Doctor of Philosophy in Pharmaceutical Sciences
Department of BioMolecular Sciences, Division of Pharmacognosy
The University of Mississippi

by

Moneerah Jarallah S Alqahtani

May 2022

Copyright Moneerah Jarallah S Alqahtani 2022
ALL RIGHTS RESERVED

ABSTRACT

Owing to their complexity, diverse structures and molecular targets, natural products have contributed, and will continue to contribute, to the development and discovery of new drugs. Although natural products provide numerous active compounds, their complex structures and poor pharmacokinetics make meeting the eligibility criteria for clinical trials unfeasible. In order to improve their drug-likeness, structural modification is an effective tool to generate countless natural product-based molecules with potential therapeutics. This proposal entails synthetic efforts towards late-stage diversification of natural products in two projects.

The first study highlights the multi-factorial nature of Alzheimer's disease and brings attention to the importance of the paradigm shift in drug development for Alzheimer's from single-targeted ligands to multi-target directed ligands. Clinical trials have shown that drugs targeting proteins such as amyloid- β and tau failed to slow down or even reverse the progression of Alzheimer's disease. Consequently, we propose the synthesis of small molecules that are hybrids of lipoic and arundic acids. Lipoic acid is a naturally occurring compound that possesses antioxidant, anti-inflammatory, and reactive oxygen species scavenging properties, however, results from studies on its efficacy and potency against Alzheimer's remain inconsistent. Arundic acid, on the other hand, has completed phase II clinical trials for the treatment of multiple neurodegenerative diseases including Alzheimer's, and has displayed *in vitro* and *in vivo* neuroprotective potential. Therefore, by combining the structural features of both lipoic acid and

arundic acid, multi-functional and bivalent ligands were designed. This approach would potentially synergize the anti-oxidative effects of lipoic acid and the neuroprotective traits of arundic acid.

The second study focuses on the search for a new insecticide to control bed bug infestations. With the emergence of insecticide-resistance acquired by bed bugs to commercially available juvenile hormone analogues (JHAs), the increasing evidence of environmental pollution, and risk of chemical exposure, we aimed to design an alternative compound for managing bed bug infestations. By transforming a naturally occurring monoterpene into its C4 elongated conjugate esters, novel compounds were successfully synthesized in one step. Moreover, their impact on the development and reproduction of bed bugs *Cimex lectularius* Linnaeus were tested.

DEDICATION

This dissertation is dedicated to my mother Khairiyah, my sister Mona, and my great grandmother Shareefah.

LIST OF ABBREVIATIONS AND SYMBOLS

NPs: Natural Products

FDA: Food and Drug Administration

MW: Molecular Weight

ADME: Absorption, Distribution, Metabolism, and Excretion

SAR: Structure-Activity-Relationship

GC-MS: Gas Chromatography-Mass Spectrometry

AD: Alzheimer's Disease

A β : Amyloid-Beta

NFTs: Neurofibrillary Tangles

JHAs: Juvenile Hormone Analogues

IGRs: Insect Growth Regulators

APOE E4: E4 Allele of the Apolipoprotein E Gene

APP: Amyloid Precursor Protein

ER: Endoplasmic Reticulum

sAPP: Soluble Fragment of Amyloid Precursor Protein

AICD: APP Intracellular Domain

MAPT: Microtubule-Associated Protein Tau

PHFs: Paired Helical Filaments

Ach: Acetylcholine

AChE: Acetylcholinesterase

AChEIs: Acetylcholinesterase Inhibitors

BuChE: Butyrylcholinesterase

ROS: Reactive Oxygen Species

PUFAs: Polyunsaturated Fatty Acids

IL: Interleukin

TGF- β : Transforming Growth Factor Beta

ALA: Alpha Lipoic Acid

DHLA: Dihydrolipoic Acid

HIV: Human Immunodeficiency Virus

iNOS: Inducible nitric oxide synthase

THF: Tetrahydrofuran

Et₃N: Triethylamine

DMP: Dess-Martin-Periodinane

ANH.: Anhydrous

DMSO: Dimethyl Sulfoxide

LiHMDS: Lithium Bis(Trimethylsilyl)Amide

Pd/C: Palladium on Carbon

EtOAc: Ethyl Acetate

LiOH: Lithium Hydroxide

°C: Degrees Celsius

RT: Room Temperature

M/Z: Mass-to-Charge Ratio

HRESI-MS: High Resolution Electrospray Ionization Mass Spectroscopy

NMR: Nuclear Magnetic Resonance

DEPT: Distortionless Enhancement by Polarization Transfer

IR: Infrared Spectroscopy

DCM: Dichloromethane

Na₂S: Sodium Sulfide

DMF: Dimethylformamide

Calcd: Calculated

MsCl: Methanesulfonyl Chloride

HSQC: Heteronuclear Single Quantum Correlation

KHMDS: Potassium Bis(trimethylsilyl)Amide

NOESY: Nuclear Overhauser Effect Spectroscopy

δ: Chemical Shift

ppm: Parts Per Million

MHz: Megahertz

NaHMDS: Sodium Bis(trimethylsilyl)Amide

R_f: Retardation Factor

DDT: Dichloro-Diphenyl-Trichloroethane

ACKNOWLEDGMENTS

I would like to thank my advisor, Dr. Ikhlas Khan, for giving the opportunity to be in his group and for his continuous support and guidance. I would also like to extend my gratitude to my outstanding committee members: Dr. Samir Ross, Dr. Hoang V. Le, and Dr. Cole Stevens for their valuable feedback and professionalism.

Throughout my Ph.D. journey, I was taught by amazing faculties who inspired me to be a better scientist and helped me develop the skills I need in the field of pharmaceutical sciences. From the department of Biomolecular Sciences: Dr. Daneel Ferreira, Dr. John Rimoldi, Dr. Ziaeddin Madar, Dr. David Colby, and Dr. Paul Boudreau, and from the department of Chemistry: Dr. Jared Delcamp and Dr. Davita Watkins. I am very grateful to have taken a class taught by you. You inspired me to be the teacher I want to be for my future students.

I would like to express my appreciation to those whom I had the opportunity to meet and collaborate with in the National Center for Natural Products Research (NCNPR): Dr. Rehman Junaid, Dr. Ahmed Galal, Dr. Ali Zulfiqar, Dr. John Adams, Dr. Mantasha Idrisi, and Dr. Islam Husain. Thank you for your support and your efforts in helping me with my projects.

My special appreciation goes to Dr. Shuneize Slater. I wish words could express how much grateful I am to you. You helped me develop the skills I needed in the lab and you were too kind to work with me in your free time. Above all, you gave me the honor to collaborate with you and co-author in your research article to debut my very first publication.

I would like to thank Dr. Ismail Hussein and Dr. Lo'ay Almomani for their work ethics and immense assistance during my journey as a student. I also would like to extend my acknowledgment to my superheroes Jennifer Taylor and Sherrie Gussow for their above and beyond performance in making each and every student's needs go as effortless as possible.

I would like to acknowledge my appreciation to King Saud University as well as the Saudi Arabian Cultural Mission (SACM) for granting me this scholarship and amazing opportunity to pursue my dreams.

Finally, I would like to thank my family: my father, my mother, my sister Mona, my brothers –specially Abdullah- and my cats Mitsu, Rasta, and Leo for their support and love.

TABLE OF CONTENTS

ABSTRACT	ii
DEDICATION	iv
LIST OF ABBREVIATIONS AND SYMBOLS.....	v
ACKNOWLEDGMENTS.....	viii
TABLE OF CONTENTS	x
LIST OF FIGURES.....	xiv
LSIT OF SCHEMES.....	xvi
LIST OF TABLES.....	xvii
CHAPTER I.....	1
THE SIGNIFICANT IMPACT OF NATURAL PRODUCT MODIFICATION ON DRUG DEVELOPMENT	1
1. Introduction	1
2. Structural Modulations of Natural Products	2
3. Examples of Synthetic Strategies Used for The Modification of NPs	2
3.1. Structure Simplification	2
3.2. Improving Activity or Selectivity	4
3.3. Protecting Environmental Resources	6
4. Overall Objectives.....	10

4.1. Study-1: Late-stage diversification of lipoic acid:	10
4.2. Specific aim-2: Late-stage diversification of menthone:	11
CHAPTER II	13
INTRODUCTION TO ALZHEIMER'S DISEASE	13
1. Introduction	13
2. Etiology and Hypotheses of Alzheimer's Disease.....	15
2.1. The Amyloid Hypothesis	15
2.2. The Tau Hypothesis	18
2.3. The Cholinergic Hypothesis.....	19
2.4. The Oxidative Stress Hypothesis	20
2.4.1. Protein Oxidation	21
2.4.2. Lipid Oxidation.....	21
2.4.3. DNA Oxidation.....	22
2.5. The Neuro-Inflammation Hypothesis.....	22
3. Treatments of Alzheimer's Disease	23
3.1. Symptomatic Treatments.....	23
3.2. Disease-Modifying Treatments	24
3.3. Alternative Therapies	25
4. The Multi-Target Ligands Paradigm.....	25
CHAPTER III	27

LATE-STAGE DIVERSIFICATION OF LIPOIC AND ARUNDIC ACIDS – SYNTHESIS
OF NOVEL HYBRID CHEMICAL ENTITY WITH POTENTIAL SYNERGISTIC
ANTIOXIDANT AND NEUROPROTECTIVE PROPERTIES 27

1. Introduction 27

 1.1. α -Lipoic Acid 27

 1.2. Arundic Acid 29

2. Innovation 31

3. Approach 31

4. Results and Discussion 35

5. Experimental Section 51

 5.1. General Experimental Procedures 51

 5.2. Synthesis of Compounds 52

CHAPTER IV 90

LATE-STAGE DIVERSIFICATION OF MENTHONE HOMOLOG AS JUVENILE
HORMONE ANALOG AND ITS GROWTH INHIBITING EFFECT AGAINST BED BUGS

90

1. Introduction 90

 1.1. Bed Bugs 90

 1.2. Juvenile Hormone Analogues (JHAs) 92

2. Significance 93

3. Innovation	94
4. Approach.....	94
5. Results and Discussion.....	94
5.1. Synthesis of (AJM-IGR-100).....	94
5.2. IGR Activity.....	97
6. Experimental Procedures.....	102
6.1. Synthesis of (AJM-IGR-100):.....	102
6.2. IGR Activity.....	103
BIBLIOGRAPHY	107
APPENDIX.....	117
VITA	253

LIST OF FIGURES

Figure 1. 1. Structural modification of halichondrin B to eribulin.	3
Figure 1. 2. Structural modification of morphine to fentanyl.	4
Figure 1. 3. Structural modification of vancomycin to telavancin.	5
Figure 1. 4. Structural modification of 3-oxododecanal to sodium new houttuynate.	6
Figure 2. 1. Schematic representation of APP processing in AD.	17
Figure 2. 2. Progress of tau pathology in AD.	19
Figure 3. 1. Chemical structure of both enantiomers of lipoic acid.	28
Figure 3. 2. Chemical structure of (R)-Arundic acid.	30
Figure 3. 3. Illustration of similar structural features of ALA and arundic acid.	31
Figure 3. 4. Structures of proposed compounds.	32
Figure 3. 5. Synthesis of MJS-1	36
Figure 3. 6. Diol protection of 13a into 1,3-dioxane 12a	36
Figure 3. 7. Oxidation of 12 a	37
Figure 3. 8. Horner–Wadsworth–Emmons olefination reaction.	38
Figure 3. 9. Hydrogenation of the di-olefins 10a	38
Figure 3. 10. Hydrolysis of ester 9a	39
Figure 3. 11. Chiral auxiliary incorporation into 8a	39

Figure 3. 12. Diastereoselective alkylation of 7a .	40
Figure 3. 13. Hydrogenation and debenylation of 6a .	45
Figure 3. 14. Mesylation reaction of 4a .	45
Figure 3. 15. The formation of 1,2 dithiolane ring.	46
Figure 3. 16. Synthesis of 19 .	49
Figure 3. 17. Alkylation of 19 .	50
Figure 3. 18. Formation of 20 .	50
Figure 4. 1. The life cycle of a bed bug.	91
Figure 4. 2. Chemical structures of currently used JHAs.	93
Figure 4. 3. Olefination of menthone via HWE reaction.	94
Figure 4. 4. HWE reaction conditions of menthone.	97
Figure 4. 5. Mortality and feeding behavior of 1st instar bed bugs with a novel insect growth regulator.	100
Figure 4. 6. Mortality and feeding behavior of 1st instar bed bugs with a novel insect growth regulator.	101
Figure 4. 7. <i>In vivo</i> residual bioassay: Feeding of bed bugs.	104
Figure 4. 8. <i>In vivo</i> residual bioassay: Exposing 1st instar bed bugs to filter paper treated with IGR.	105

LSIT OF SCHEMES

Scheme 3. 1. Retrosynthetic analysis of 1 (a) and (b) using the first approach.....	32
Scheme 3. 2. Retrosynthetic analysis for the synthesis of compound 1a	33
Scheme 3. 3. Retrosynthetic analysis for the synthesis of compound 1b	34
Scheme 3. 4. Retrosynthetic analysis of 1b using L- menthol for asymmetric alkylation.	35
Scheme 3. 5. Synthesis of 1b	48
Scheme 3. 6. Total synthesis of lipoic acid.....	49

LIST OF TABLES

Table 1. 1. Examples of NPs modifications.....	8
Table 1. 2. Examples of NPs modifications “contd”.....	9
Table 3. 1. Optimization conditions for 12a	37
Table 3. 2. Optimization conditions for 6a	41
Table 3. 3. Optimization conditions for 6a “contd”.....	42
Table 3. 4. Optimization conditions for 6a “contd”.....	43
Table 3. 5. Optimization conditions for 6a “contd”.....	44
Table 3. 6. Optimization conditions for the alkylation of 19	51
Table 4. 1. Optimization conditions for HWE reaction using NaHMDS.....	96
Table 4. 2. Optimization conditions for HWE reaction using KHMDS.....	96
Table 4. 3. Table 4. 2. Optimization conditions for HWE reaction using LiHMDS.....	97

CHAPTER I

THE SIGNIFICANT IMPACT OF NATURAL PRODUCT MODIFICATION ON DRUG DEVELOPMENT

1. Introduction

Natural products (NPs) have historically been the major contributor of drugs for treating a broad-spectrum of human diseases ^{1, 2}. Including plants, animals, microorganisms, and marine organisms, NPs are a great source of biologically active compounds with a variety of biological properties that allow for novel development of synthetic compounds ³.

There are a substantial number of natural drugs on the market, and the number of newer compounds is steadily rising ^{4, 5}. In fact, according to a detailed review recently published in the *Journal of Natural Products*, more than half of the therapeutic agents authorized by the US Food and Drug Administration (FDA) between 1981 and 2019 were derived from NPs or their synthetic analogues ⁶. Pure unaltered NPs represented 3.8% with 71 total drugs ⁶. In addition, other categories of natural products were included in the review such as botanical drugs (coded NB, with 14 total drugs, 0.8%), natural product derivatives (coded ND, with 356 total drugs, 18.9%), synthetic drugs made by total synthesis with a pharmacophore of a NP (coded *S, with 272 total drugs, 14.4%), and mimic of natural products (coded NM, with 424 total drugs, 22.5%) ⁶.

2. Structural Modulations of Natural Products

NPs commonly feature advantageous and diverse scaffolds, structural complexity, and profuse stereochemistry^{7,8}. However, due to their limited potency, harmful and adverse effects, and poor physicochemical aspects, most natural compounds cannot be used as drugs⁹. In order to optimize their therapeutic effects, lower their toxicities, and modify their physicochemical properties, structural modulations are highly imperative¹⁰⁻¹². Examples on successful structural modification of NPs and the strategies utilized to obtain more refined molecules can be briefly summarized as follows.

3. Examples of Synthetic Strategies Used for The Modification of NPs

3.1. Structure Simplification

Simplified methods are usually used to remove structurally irrelevant features, especially when dealing with large and complex compounds. The majority of NPs have a relatively high MW and a complicated framework, resulting in a poor ADME profile¹³. Moreover, failure to generate drug-like NP derivatives may cause difficulties in the synthetic process¹³. Therefore, molecular dissection while sustaining the structure-activity-relationship (SAR) is unquestionably the best tool for removing the limiting factors that restrict the development of NP-based drugs which exhibit improved drug-likeness and are more synthetically accessible as well^{3,4}.

The marine NP, Halichondrin B, is reported to have antiproliferative activity similar to other antitubulin drugs¹⁴, yet with a distinctive mechanism of interaction with tubulin¹⁵. This anticancer agent has a MW of 1111.3 and is comprised of two moieties: a polyether with 18 chiral atoms, and a macrolide with 12 chiral atoms³. The two moieties are connected vis C-29 and C-30, in which C-30 is linked to a lactone group that is susceptible to hydrolyzation, releasing the macrolide moiety and ultimately losing the activity¹⁶. To solve this problem, the oxygen atom of

the lactone group was replaced with a methylene group¹⁶. This approach prevented the hydrolysis of the ester at the lactone linkage and also maintained the conformation unaltered. In addition, to increasing its solubility while forming a salt, an amino group was introduced at the terminal of the side chain as a solubilizing group¹⁶. Collectively, these modifications resulted in the total synthesis of a simpler molecule, eribulin, with 19 chiral atoms and a MW of 729.9, (**Figure 1.1**)¹⁷. In 2010, eribulin was approved by the FDA for the treatment of metastatic breast cancer and again in 2016 for soft tissue sarcoma¹⁸.

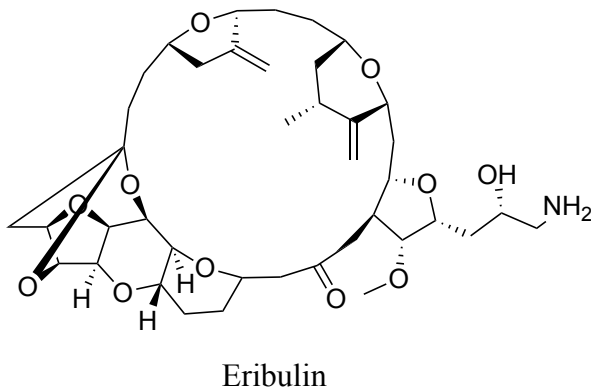
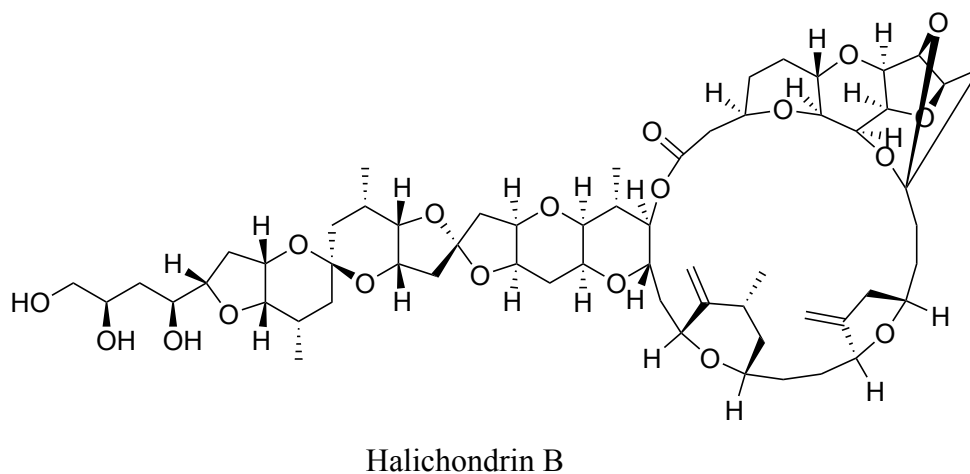


Figure 1. 1. Structural modification of halichondrin B to eribulin.

The synthesis of NPs occurs with high stereochemical specificity in organisms via the process of enzymatic catalysis, providing compounds with chiral centers, and/or cis/trans configurations. Those chiral centers not contributing in target binding should be changed as much as feasible to their non-chiral analogues. The popular analgesic morphine, for example, has five fused rings and five chiral centers^{19,20}. After structural alterations, such as the removal of the B, C, and E rings, the synthetic analgesic, fentanyl, is a considerably simpler non-chiral analogue, **(Figure 1.2)**²¹. In 1998, fentanyl was granted the approval by FDA to treat the breakthrough pain in patients with cancer as the first pain medicine²².

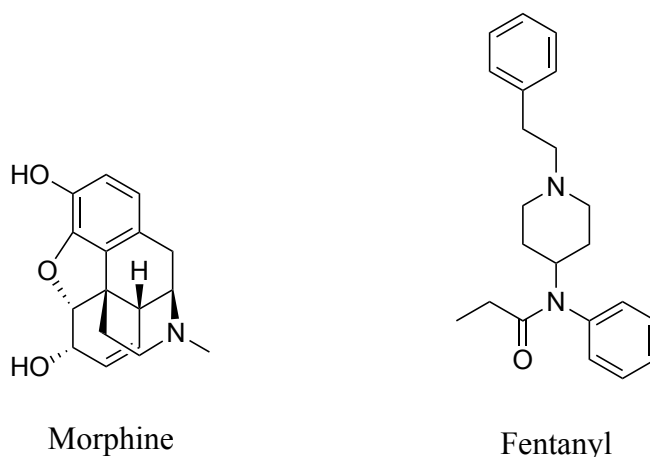


Figure 1. 2. Structural modification of morphine to fentanyl.

3.2. Improving Activity or Selectivity

The natural antibiotic, vancomycin, is a known antibacterial used for a number of infections caused by methicillin-resistant *Staphylococcus aureus* (MRSA)^{23, 24}. This large glycopeptide antibiotic is a hydrophilic molecule, is capable of preventing the synthesis of bacterial cell wall²⁵ as well as the cross-linking of the N-acetylmuramic acid/N-acetylglucosamine (NAM/NAG) polymers²⁶. Vancomycin exerts its effects through the formation of 5 hydrogen bonds with the (D-alanyl-D-alanine) moieties of the cell wall peptides NAM and NAG²⁷. However, resistance to

vancomycin has emerged due to alteration in the peptidoglycan terminal (D-alanyl-D-alanine) being replaced with (D-alanyl-D-lactate)²⁸, resulting in low binding affinity to the cell wall precursor (D-alanyl-D-alanine), and a successful formation of cross-links²⁹. For that reason, telavancin, a semi-synthetic second generation antibiotic was developed with unique multifunctional mechanism of actions. It inhibits the process of transpeptidation, disrupting the integrity of cell membrane and the synthesis of cell wall³⁰.

The strategy execution during the synthesis of telavancin involved the introduction of a long aliphatic chain into the amino-sugar component of, which adheres in the lipophilic membrane, improving its stability and affinity for peptidoglycan in the target environment³⁰. Furthermore, to optimize the hydrophilic-lipophilic properties, a polar component amino-phosphonic acid is tethered to the biphenyl moiety, (Figure 1.3)³⁰. In 2009, FDA announced the approval of telavancin for the treatment of complicated skin infections, and again in 2013 for treating bacterial pneumonia³¹.

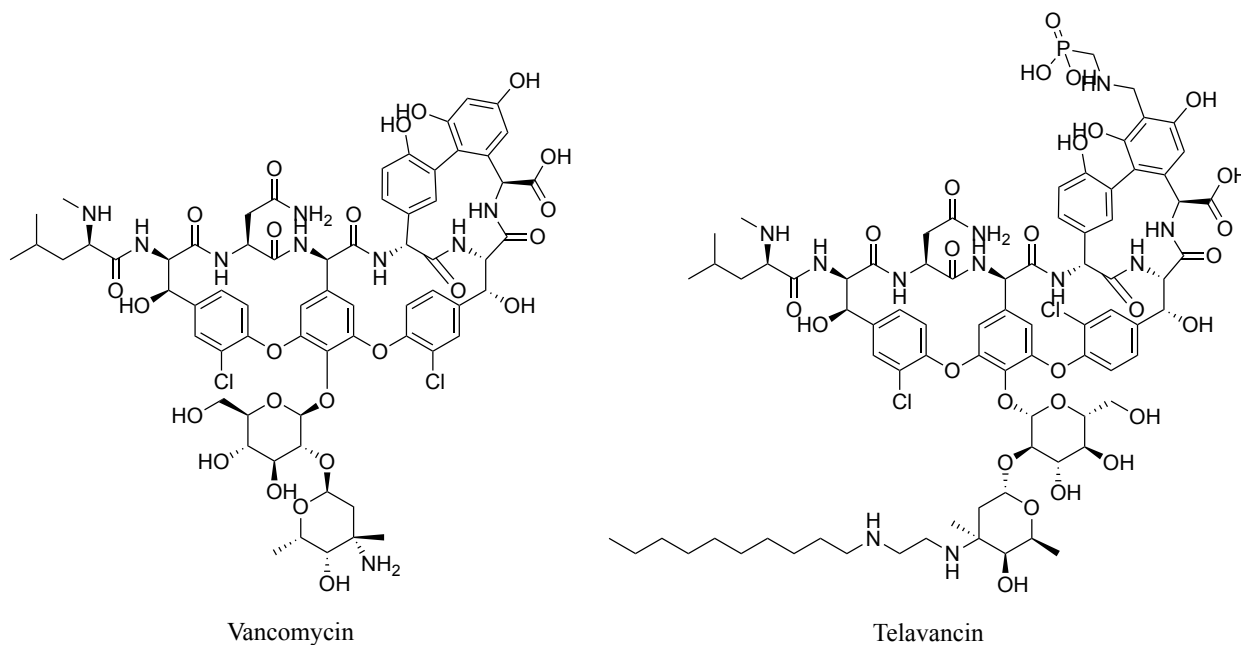


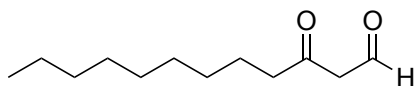
Figure 1. 3. Structural modification of vancomycin to telavancin.

3.3. Protecting Environmental Resources

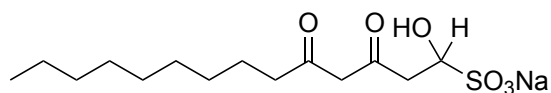
Limitations such as seasonal availability and low yield make obtaining NPs from separation often a challenging and time demanding task, and generally inefficient³². In this context, synthetic tools like semi- and total synthesis of NPs may have an immense influence on the development of various novel synthetic methodologies³. One example is the development of the antibacterial agent, houttuynium. The plant *Houttuynia Cordala*, known in the traditional Chinese medicine for treating colpitis in women³³. However, this plant thrives in damp to wet soil that is partially submerged in water and subjected to the heat of the sun, therefore, it is unavailable during the winter seasons³⁴.

It is important to remember that medicinal development cannot be done at the expense of natural resources and the environment, hence, the volatile oil houttuynin (3-oxododecanal/decanoyl acetaldehyde), was extracted by a group of scientists from the Chinese Academy of Medical Sciences (CAMS), and reported it as the main constituent of the volatile oily mixture via GC–MS tool³⁵. Following the structural characterization of 3-oxododecanal, its total synthesis was easily accomplished from simple starting materials. Furthermore, by using sodium bisulfite in a reaction, 3-oxododecanal was converted into the corresponding sodium bisulfite adduct, namely sodium new houttuynonate (SNH) with a substantial increased solubility,³⁶

(Figure 1.4).



3-oxododecanal



Sodium new houttuynonate (SNH)

Figure 1. 4. Structural modification of 3-oxododecanal to sodium new houttuynonate.

More examples of successful structural modulation of natural compounds by applying synthetic strategies with the purpose of optimizing their biological and therapeutic potential for clinical applications are listed in **Table 1.1 and 1.2**.

Table 1. 1. Examples of NPs modifications.

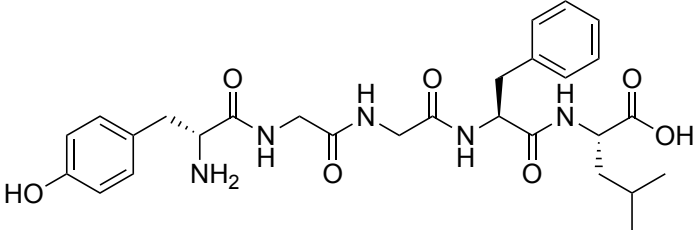
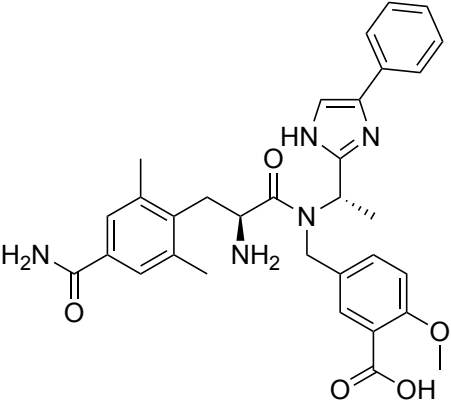
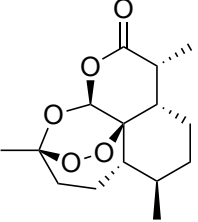
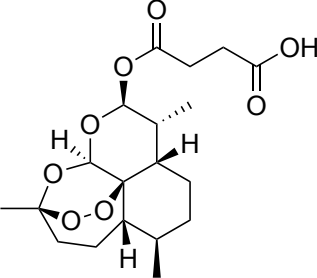
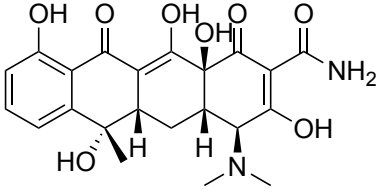
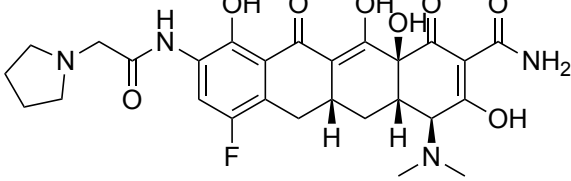
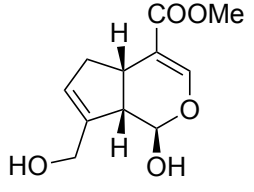
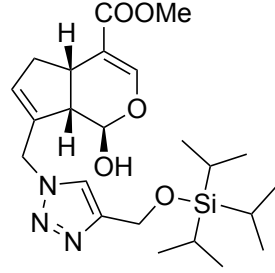
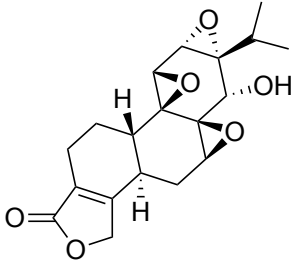
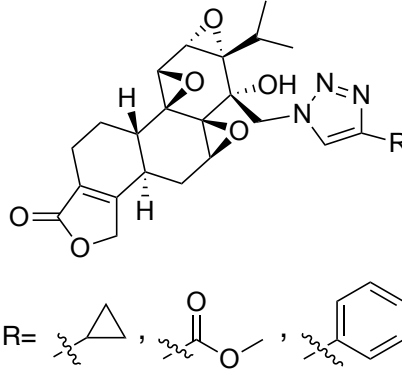
Natural product	Synthetically modified natural product	The purpose of modification	Reference
 <p data-bbox="478 740 625 773">Enkephalin</p>	 <p data-bbox="1077 748 1234 781">Eluxadoline</p>	<p data-bbox="1413 337 1654 513">To increase activity and metabolic stability</p>	<p data-bbox="1776 337 1801 354">37</p>
 <p data-bbox="478 1162 625 1195">Artemisinin</p>	 <p data-bbox="1083 1154 1230 1187">Artesunate</p>	<p data-bbox="1419 829 1650 1005">To Improve physico-chemical properties</p>	<p data-bbox="1776 829 1801 846">38</p>

Table 1. 2. Examples of NPs modifications “contd”.

 <p>Tetracycline</p>	 <p>Eravacycline</p>	<p>Synthesis-driven drug discovery</p>	<p>39</p>
 <p>Genipin</p>	 <p>Genipin-triazole</p>	<p>To increase potency and improve cytotoxicity</p>	<p>40</p>
 <p>Triptolide</p>	 <p>C14-triazole subs. epi-triptolide derivatives</p>	<p>To reduce toxicity</p>	<p>41</p>

4. Overall Objectives

As evidenced by previous examples of successful modification of NPs, we can affirm that NPs, for decades, have been utilized as the source of inspiration for scientists to develop compounds with profoundly unique structural features and optimized quality. Moreover, synthetic chemistry can also be used to generate a wide range of natural product-based analogues with potential therapeutics and improved overall drug-likeness. ***Our central hypothesis*** is following a simple homologous functionalization of privileged natural product scaffolds will yield new chemical entities with improved biological properties. This dissertation entails our synthetic efforts towards late-stage diversification of natural products in two studies:

4.1. Study-1: Late-stage diversification of lipoic acid:

From accessible materials, natural products can be modulated from being single-targeted ligands to multi-targeted ligands, providing superior pharmacological potency and better understanding of the pathogenesis underlying complex diseases, particularly Alzheimer's disease (AD). AD is a persistent neurodegenerative disease that causes permanent cognitive impairment and a constant deterioration in the ability to handle daily activities independently, leading to serious life - threatening complications^{42,43}. Over the years, researches have mostly concentrated on two hallmarks: amyloid-beta (A β) protein and hyperphosphorylated tau protein neurofibrillary tangles (NFTs)⁴⁴. Despite the colossal investment in disease-modifying drugs aiming to target either A β or Tau proteins, they continue to fail with more setbacks than successful treatment⁴⁴. Other factors including neuro-inflammation and oxidative stress are currently considered as hallmarks of the disorder, but little is known about their contributions to the pathology and whether each factor is regarded as a cause or a bystander⁴⁵⁻⁴⁷. Up-to-date, there is no conclusive cure for

AD, and most of the approved drugs are merely used for symptomatic purposes to improve cognitive performance and quality of life ⁴⁸.

Our research emphasizes the multifactorial nature of AD; thus, the importance of the paradigm shift in drug development for AD from single-targeted ligands to multi-target directed ligands. Hereby, by combining the structural features of the natural antioxidant —lipoic acid, and the synthetic neuroprotective agent —arundic acid, hybrid small molecules of multifunctional ligands were designed. This approach will improve the overall antioxidative and neuroprotective traits of novel lipoic acid analogues.

4.2. Specific aim-2: Late-stage diversification of menthone:

Besides therapeutics, natural products applications can be used for protecting human health and reducing environmental pollution and hazards ⁴⁹. Bed bugs (*Cimex lectularius* L.) are reported the most in urban areas and have raised many concerns regarding the public and environmental health ^{50, 51}. The bugs survive solely on the blood of humans and animals causing skin rashes, bleeding, inflammation, as well as psychological impacts including sleep difficulties, anxiety, and stress as a result of the continuous and overwhelming infestations ^{52, 53}. Thus far, there are two commercially available juvenile hormone analogues (JHAs), namely methoprene and hydroxyphenoxypyrene ⁵¹. JHAs are insect growth regulators (IGRs) that act by mimicking insect juvenile hormone, a pivotal developmental hormone that plays a critical role in regulating insect's life-cycle, keeping insects in immature stages, and preventing their reproduction ⁵⁴. Despite the fact that JHAs are favored because of their demonstrated effectiveness and minimal toxicity to non-arthropods, their efficacy for bed bug control is ambiguous ⁵⁵.

Because certain bed bug strains have acquired resistance to common insecticides ^{56, 57}, JHAs have only exhibited insecticidal activity when used at greater rates than those recommended on the label ⁵¹. Eventually, observations such as aquatic toxicity and human overexposure to insecticides via inhalation or skin contact have been reported ⁵⁸. Hence, this part of the dissertation focuses on developing a novel natural product-derived analogue as an IGR for managing bed bugs with preferable safety profile compared to other available IGRs.

Overall, our research provides insights on how natural products can be used as a foundation for the development of novel natural product-derived analogues using a range of approaches. These novel analogues can lead to the development of new chemical entities with improved activity for treating complex ailments as well as enhancing human health and the quality of environment.

To address our hypothesis, two specific aims will be conducted: **specific aim 1:** synthesis of novel hybrid of lipoic and arundic acids with potential synergistic antioxidant and neuroprotective properties, and **specific aim 2:** synthesis of menthone homolog as insect growth regulator and analyze its impact against (*Cimex lectularius L.*). The details of each aim are represented in chapters (III) and (IV), respectively.

CHAPTER II

INTRODUCTION TO ALZHEIMER'S DISEASE

1. Introduction

AD is one of the most progressive neurodegenerative disorders that causes irreversible memory impairment and continuous decline in carrying out daily tasks independently, which results in severe complications and death ^{42, 43}. In 2021, the number of Americans living with Alzheimer's dementia is estimated to be 6.2 million with 5.3% of people age 65-74, 13.8% of people age 75-84, and 34.6% are age 85 and older ⁵⁹. As the size of the elderly population continues to grow, the number of cases in the U.S. will increase rapidly as well ⁵⁹.

Throughout the years, studies and reviews were primarily dedicated for two major biological hallmarks: the accumulation of amyloid-beta protein fragments outside neurons in the brain and neurofibrillary tangles of hyperphosphorylated tau protein inside neurons ⁴⁴. These changes are accompanied by synapse loss, mitochondrial damage, and the death of neurons ⁴⁴. Symptoms of AD worsens as plaques and tangles build up and damage the neurons ⁴⁴. Common symptoms of AD include memory loss with attention and language deficits, disorientation, hallucination, and difficulty with self-care ⁶⁰.

Alzheimer's can be split into two groups: sporadic AD when the exact cause is not well-defined and familial AD in which a dominant gene was inherited that speeds up the progression of the disease ^{61,62}. Sporadic AD is often referred to as late-onset Alzheimer's and it accounts for the vast majority of cases ⁶³. The percentage of people with AD increases drastically with age: 17% of people age 65-74 and 83% of people 75-85 and over ⁵⁹, thus ageing is considered the greatest risk factor for developing late-onset Alzheimer's ⁶⁴. Familial Alzheimer's, on the other hand, is often called early-onset Alzheimer's and it accounts for 5-10% of cases and can be caused by multiple gene mutations ^{65,66}.

In addition to age, researchers have identified several genes that contribute to increasing the risk of AD. It has been shown that inheriting one $\epsilon 4$ allele of the apolipoprotein E gene (*ApoE e4*) strengthens the impact of developing late-onset Alzheimer's ⁶⁷. In fact, those who inherit two copies of the $\epsilon 4$ allele, one from each parent, have 8-12 risk fold ⁶⁸. Apolipoprotein E helps breaking down beta-amyloid, however it appears that the $\epsilon 4$ allele is less effective than other alleles, such as ApoE $\epsilon 2$, which indicates that beta-amyloid plaques are more likely to evolve ⁶⁹. Mutations in the *PSEN-1* or *PSEN-2* genes on chromosome 14 or chromosome 1, respectively, have been linked to an increased likelihood of developing early-onset Alzheimer's ⁷⁰. These genes encode for presenilin 1 (PS-1) and presenilin 2 (PS-2) proteins, both are subunits of γ -secretase ^{61,70}. Such mutations can alter the location where γ -secretase cuts amyloid precursor protein (APP), thus producing different length of beta-amyloid molecules that are known to clump up and ultimately form plaques. Trisomy 21 (Down syndrome), is another known genetic cause of Alzheimer's and it involves having an extra copy of chromosome 21 ^{70,71}. The gene responsible for producing APP is located on chromosome 21 ⁷², this implies that people with Down syndrome have an extra APP gene and more likely to have an increased expression of APP, therefore an

increased amount of amyloid plaques aggregation ^{71, 72}. In consequence, familial AD often advances by age 40 in patients with Down syndrome ⁷¹.

2. Etiology and Hypotheses of Alzheimer's Disease

Despite the apparent thorough analysis of the etiology and pathology of AD, owing to its complicated pathological characteristics, the exact underlying mechanism has yet to be completely understood. However, the two main pathological hallmarks of AD are the deposition of A β peptides and the accumulation of NFTs ⁴⁴. These have been known as being at the core of the pathogenesis of AD. After all, the lack of information about the exact cause of the disease has hindered the development of effective new drugs.

In addition to A β and NFTs, other contributing factors have been hypothesized in order to find a clear explanation of the underlying mechanism of AD. Above all, the loss of cholinergic functions has served as the basis for developing therapies and most of the drugs currently approved by the United States Food and Drugs Administration (US FDA) are the products of this hypothesis ⁷³. Other hypotheses such as neuro-inflammation and oxidative stress have recently gained increasing interest and attention from researchers and considered as hallmarks of the disorder, but little is known about their contributions to the pathology, and whether each factor is regarded as a cause or a bystander ⁴⁵⁻⁴⁷. AD is a complex set of defects that cannot be explained based on a single hypothesis, but rather a combination of other cellular events that account for the disease's development and progression.

2.1. The Amyloid Hypothesis

The amyloid hypothesis postulates that imbalanced A β production, aggregation and clearance, leads to plaque aggregation followed by a series of biochemical events that eventually advance into AD ⁷⁴. The starting point for amyloid plaques is amyloid precursor protein, which is

made inside the cell and becomes imbedded on the surface of many cell structures- the plasma membrane, Golgi apparatus, endoplasmic reticulum (ER), endosome, lysosome and mitochondria⁷⁵. Mutations in APP gene disrupt the normal process of which APP is cleaved, leading to the formation of toxic proteins particularly in early onset AD⁷⁶. APP undergoes sequential proteolytic cleavage by three specific secretase enzymes⁷⁶. These enzymes are called β -secretase, γ -secretase and α -secretase⁷⁶. APP processing may follow one of two pathways that have very different consequences for the cell, depending on which enzyme is involved and the segment of APP where the cleaving occurs.

Under normal conditions, the non-amyloidogenic pathway, APP is cleaved by the metalloprotease α -secretase close to the outer cellular membrane releasing a soluble fragment of amyloid precursor protein (sAPP α), which has beneficial properties, such as promoting neuronal growth and survival^{76, 77}. Next, the remaining fragment of APP, a C-terminal fragment (C83), is cleaved by γ -secretase resulting in the formation of p3 peptide (3 kDa) and generation of APP intracellular domain (AICD)^{76, 78}.

In the harmful pathway, the amyloidogenic pathway, β -secretase first cleaves the APP molecule in close proximity of the transmembrane domain, releasing soluble fragment of APP (sAPP β) from the cell and C-terminal fragment (C99)^{76, 78}. The membrane-bound C99 fragment is subsequently cleaved by γ -secretase leading to the formation of APP intracellular domain (AICD) and releasing A β peptide fragment in the extracellular space⁷⁶. A β peptides tend to bind to more A β peptides, other proteins and cellular material are then incorporated, ultimately forming the well-known AD-characteristic amyloid plaques, **(Figure 2.1)**^{76, 78}.

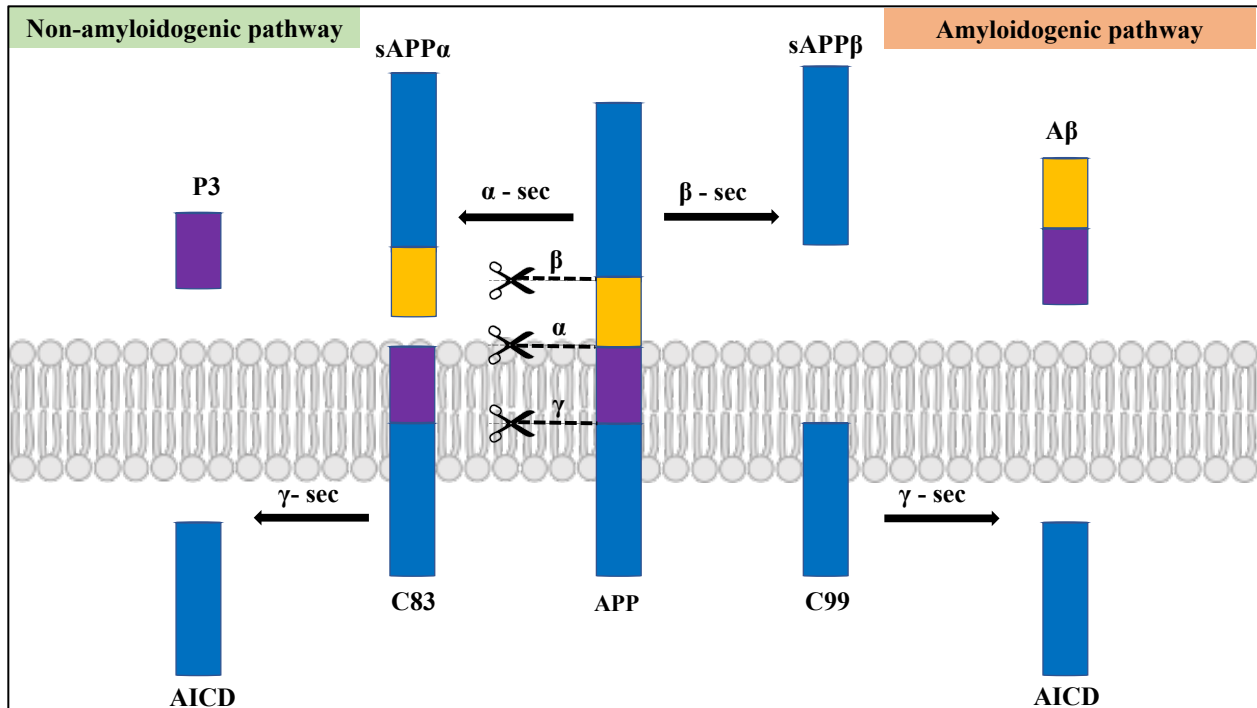


Figure 2. 1. Schematic representation of APP processing in AD.

The amyloid cascade hypothesis is argued against by evidence from several experimental and clinical trials. In some cases, large quantities of amyloid aggregates could be found in the brain with little if any clinical AD symptoms; therefore, amyloid alone is not sufficient to cause the disease ⁷⁹. Transgenic mice with a defective variant of human APP gene along with a mutated form of presenilin 1 and 2 generate significant amounts of amyloid in their brain notwithstanding their poor performance in spatial memory tests (such as the Morris water maze), they never develop any of the well-known AD pathologies ⁸⁰. Furthermore, transgenic mice expressing only amyloid- β peptide without APP expression, produce a substantial amount of amyloid- β without cognitive decline, hence this data provides a clear indication that A β alone is not adequate to trigger AD symptoms and pathology ⁸¹.

2.2. The Tau Hypothesis

The Tau theory suggests that neurotoxic accumulation of neurofibrillary tangles in the brain eventually causes neuronal loss and synaptic dysfunction, leading to neurodegeneration⁸².⁸³ The formation of neurofibrillary tangles starts when Microtubule-Associated Protein Tau (MAPT), known for its role in stabilizing internal microtubules and transporting nutrients in neurons⁸³, begins to undergo a number of post-translational modifications including phosphorylation⁸⁴. When tau is phosphorylated, it helps supporting microtubules by binding to them⁸⁵. In AD, an irregularly significant number of additional phosphate molecules bind to tau and as a result of this hyperphosphorylation, tau loses its ability to promote microtubule assembly and aggregates with more tau threads to form paired helical filaments (PHFs) and NFTs, (**Figure 2.2**)^{83, 85}. In the process, microtubules disintegrate and become destabilized, which destroys the neurons' ability to interact with each other⁸⁴. This collapse triggers a cascade of events that progressively display in the symptoms of AD⁸⁵.

Although the amyloid theory postulated that tau accumulation occurs downstream of A β aggregation⁸³, the brains of patients with mild dementia and no pathology of A β were found to have tau tangles^{83, 85}. In addition, tau pathology associates with the advancement and severity of AD more closely than A β plaque load does⁸⁶. While A β plaques can appear in the brains of people who do not encounter neurodegeneration, the same cannot apply for NFTs that are found in frontotemporal dementia as well as other tauopathies^{84, 85}. Perhaps it is because amyloid plaques are formed in the extracellular space while tau tangles develop inside neurons where axonal transport may be significantly impaired.

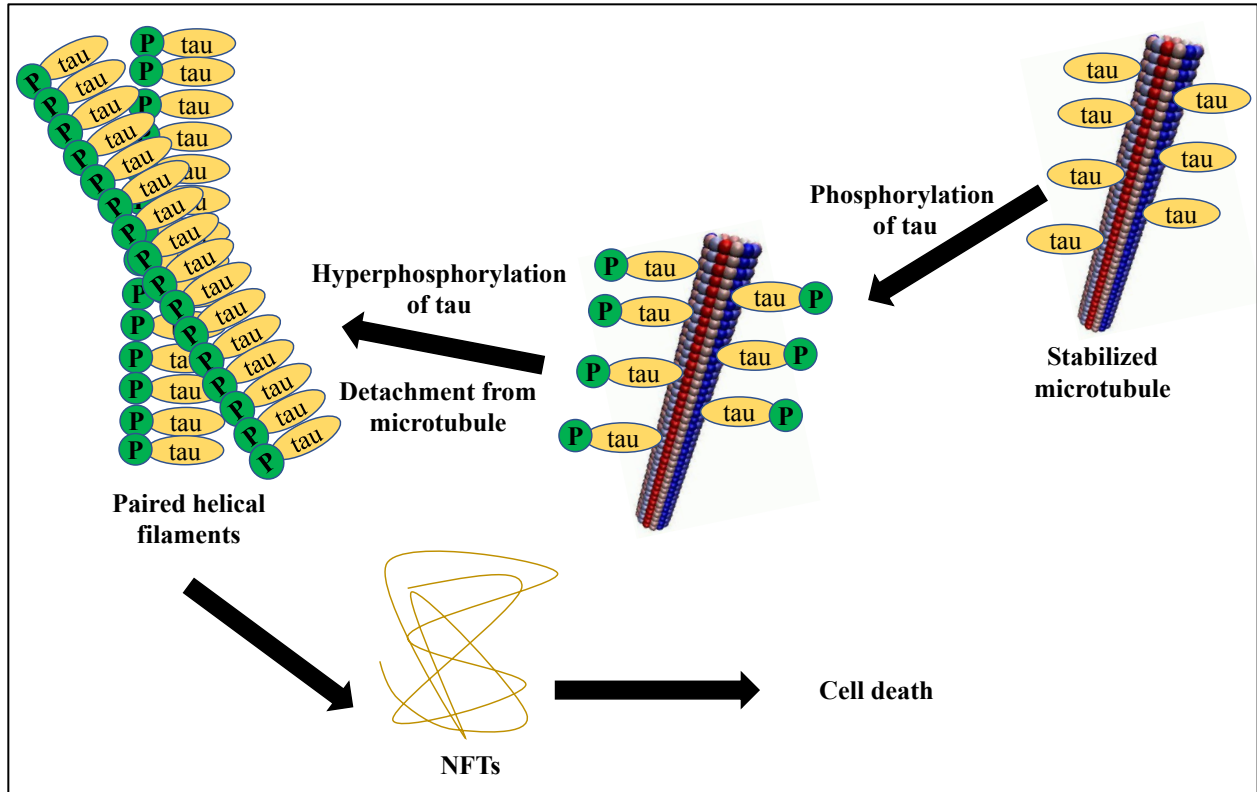


Figure 2. 2. Progress of tau pathology in AD.

2.3. The Cholinergic Hypothesis

The cholinergic hypothesis, which is already known to be classical at present, is the basis behind the use of acetylcholinesterase inhibitors (AChEIs) as treatment for AD. The first hypothesis proposes that the loss of cholinergic neurons that thereafter contributes to dysfunction of cholinergic activity can play a role in memory loss and subsequent cognitive deficits (often observed in the brain of AD patients) ⁸⁷.

Acetylcholine (ACh) is an organic molecule produced in cholinergic neurons by the enzyme choline acetyltransferase from choline and acetyl-CoA chemicals ⁸⁸. Acetylcholine is a key component of the central nervous system, supporting cognitive functions from the basal forebrain through the hippocampal and cortex areas ⁸⁹. Additionally, it has muscle-activating properties in

the peripheral nervous system⁸⁸. This neurotransmitter is hydrolyzed by two major cholinesterase enzymes, acetylcholinesterase (AChE) and butyrylcholinesterase (BuChE)⁹⁰. This process promotes healthy cell signaling and ensures that overstimulation of the neurons is avoided⁸⁹.

It is well known that the levels of AChE near amyloid plaques and NFTs rise significantly with each stage of the illness, and it has been postulated that AChE may interact directly with A β to promote plaque production^{82,90}. Consequently, using AChEIs or modulating other cholinergic receptors (muscarinic and nicotinic ACh) can lead to enhanced acetylcholine concentrations in the brain, increased cholinergic transmission, and eventually restoration of cholinergic function, resulting in a decrease in the severe lack of cognitive function^{89,91}. This hypothesis contributed to the rise of the only currently approved drugs to treat AD by the FDA, namely (tacrine, donepezil, rivastigmine and galanthamine)⁹².

2.4. The Oxidative Stress Hypothesis

Oxidative stress refers to the lack of balance between antioxidants and pro-oxidants, in which the oxidants are overly produced or the dysfunction of antioxidants⁹³. This imbalance causes a buildup of reactive oxygen species (ROS) and other free radicals, which can affect main cellular components; such as lipids, proteins, and DNA, and it may result in cellular apoptosis^{94,95}.

Under normal conditions of cellular metabolism and numerous functions, in order to maintain cellular homeostasis, radical superoxide ($O_2^{\cdot-}$) and the non-radical hydrogen peroxide (H_2O_2) oxidants are produced. In the presence of catalytic iron or copper ions, excessive production of ($O_2^{\cdot-}$) and (H_2O_2) can cause tissue damage, which frequently triggers the formation of the highly reactive hydroxyl radical (OH^{\cdot}) and other oxidants (43,44,45). As a result, because metal facilitates redox reactions, one of the most important forms of antioxidant

defense is collecting and distributing iron in aspects that do not catalyze the forming of reactive radicals, as is often the case during tissue damage, when iron availability increases, potentially speeding up free radical reactions^{94,95}.

There is compelling evidence that brain tissue in Alzheimer's patients is subjected to oxidative stress throughout the time of the disorder⁹³. Age is the paramount risk factor for AD⁹⁴, which is associated to the free radical theory. The oxidative stress in AD can be manifested through specific markers comprising proteins oxidation, lipids oxidation, and DNA oxidation⁹⁶.

2.4.1. Protein Oxidation

The attack of ROS on protein's side-chains results in the oxidation of the amino acid hydroxyls and the generation of a load of aldehyde and ketone derivatives that can then attack amino acids to generate protein based-carbonyls, a mechanism known as protein carbonylation^{93,96}. Reactive carbonyl moieties are higher in the frontal and parietal lobes, as well as the hippocampus, as a result of this oxidation⁹⁶. Protein carbonylation has been proposed as a useful indicator of the extent of oxidative damage to proteins, which has been linked to oxidative stress and Alzheimer's disease^{93,94,96}.

2.4.2. Lipid Oxidation

Lipid peroxidation contributes to oxidative stress by ROS mediated damage to the side chains of lipids found in the brain⁹⁶. A hydrogen atom is removed from the methylene carbon as part of the process⁹⁶. The molecule's susceptibility increases as the number of double bonds increases⁹⁴. As a result, polyunsaturated fatty acids (PUFAs) are more vulnerable to peroxidation. Moreover, products of lipid peroxidation and lipoperoxidation of membranes are elevated in the frontal/temporal cortex and hippocampus regions of the brain, and are significantly induced by A β

and NFTs ^{94, 96}. Thus, lipid peroxidation is linked to the neuronal damage in AD and is a special marker in neurodegeneration ⁹⁵.

2.4.3. DNA Oxidation

Oxidative stress causes DNA bases to be sensitive to hydroxylation, protein carbonylation, and nitration ⁹⁷. In Alzheimer's disease, brain ROS causes calcium influx via glutamate receptors, prompting an excitotoxic cascade that leads to apoptosis ^{97, 98}. When oxygen combines with uncontrolled redox-active metals, reactive oxygen species (ROS) are produced ⁹⁸. Increased levels of 8-hydroxy-2-deoxyguanosine (8OHdG) and 8-hydroxyguanosine (8OHD) reflect DNA and RNA oxidation ^{97, 98}. These markers have also been observed in A β plaques and NFTs in AD brains ^{97, 98}.

Additionally, research studies reveal that consuming antioxidants in the diet lowers the risk of Alzheimer's disease ⁹⁹. Antioxidants often have the capacity to prevent amyloid accumulation as well ⁹⁹. Accordingly, antioxidant treatment is beginning to gain the researchers' interest as a promising strategy to target AD

2.5. The Neuro-Inflammation Hypothesis

In the central nervous system, there is clear evidence of astrogliosis and microgliosis along with other inflammation-related indicators present in AD brain tissue ¹⁰⁰⁻¹⁰². Hyper-activation of astrocytes and microglia is associated in the progression and development of AD giving their role as the primary effectors of the innate immunity ^{101, 102}. When compared to normal individuals, these cells exhibit up to 5 times the activity and concentration in the proximity of amyloid plaques and NFTs in AD patients ¹⁰³. The impact of these cells on the neurotoxicity or synaptotoxicity is highly influenced by any disproportion in their protective and detrimental functions. Furthermore, increased S100B expression has been observed in the brains of individuals with AD ¹⁰⁴.

It was proposed that S100B abundance is amplified in reactive astrocytes and microglia co-localized with β amyloid plaques, where escalating production of IL-1 by activated microglia has also been detected ¹⁰⁵. The phenomenon starts when diffuse deposits of β amyloid first stimulate and trigger IL-1 β -secreting microglia, which promote astrocytes and activate astrocyte-derived S100B production ^{104, 105}. This self-producing neuroinflammatory loop induces both activated microglia and astrocytes to produce more proinflammatory cytokines such as IL-1 β , TGF- β , IL-12, and IL-18 and other acute-phase reactants ¹⁰⁶. Eventually, supraphysiological levels of toxic oxyradicals and nitric oxide are produced ¹⁰⁶. In addition to increasing inflammatory responses, these pro-inflammatory substances are prone to causing further indirect neuronal damage in the AD brain ^{104, 105}. Recently, a growing research is moving in the direction towards the use of anti-inflammatory drugs as a therapeutic approach aimed at neurodegenerative diseases, especially AD ¹⁰⁷.

3. Treatments of Alzheimer's Disease

With the goal of intervening with the disease's progression, most of the drugs in development are disease-modifying, in the notion of that these therapies aim at the pathological stages that lead to AD, whereas all of the present FDA-approved drugs are symptomatic therapies ^{108, 109}.

3.1. Symptomatic Treatments

The term "symptomatic" is used to describe drugs that improved cognition or controlled neuropsychiatric symptoms without affecting the underlying factors that lead to cell death in AD ¹¹⁰.

There are three types of drugs that are approved to treat the disease in different stages. The first type is Cholinesterase inhibitors, this includes Donepezil (Aricept®), Rivastigmine (Exelon®),

and Galantamine (Razadyne®) ⁴³. An additional drug that belongs to this class and was the first FDA-approved AChEI is Tacrine (Cognex®), however, it was taken off market in 2013 due to hepatotoxicity ¹¹¹. The second type is Glutamate regulators with with only one drug, named Memantine (Namenda®) ⁴³. Lastly, the third type is a combination of Cholinesterase inhibitor + glutamate regulator, Donepezil and memantine ⁴³.

Clinical trials have confirmed their positive benefits on improving cognitive functions compared to placebo in the treatment of AD ¹¹². Unfortunately, the beneficial effects are often short-term and the disease continues to advance because none of these drugs have been proven to halt or delay the course of AD, emphasizing the disease's complicated pathophysiology ^{43, 112}.

3.2. Disease-Modifying Treatments

The terminology "disease-modifying" refers to therapies that aim to modify the underlying biology of AD and create neuroprotection, typically via a number of different mechanisms ¹¹³. Almost two decades of research was dedicated, and still is, mainly towards A β plaques through different approaches: β or γ - secretase inhibitors, α - secretase activators, anti A β aggregation, production, and deposition ^{43, 113-115}. In addition, many studies were invested in developing drugs that target NFTs of tau protein with either its aggregation or hyperphosphorylation ¹¹⁶. Nonetheless, disease-modifying strategies for AD have consistently failed in preclinical and clinical trials, despite the massive efforts and investments in the research of AD-modifying therapeutics ¹¹⁷. As a consequence, treatment failures attributed to these hypotheses show that these hypotheses may not be adequate to understand and explain the pathogenesis of AD.

Regardless, it is worth mentioning that in June 2021, the U.S. FDA granted an accelerated approval to Aducanumab (Aduhelm™) for the treatment of AD as the first disease-modifying drug since 2003¹¹⁸. Aduhelm is an anti-amyloid antibody intravenous infusion acts on the reduction of amyloid beta plaque in the brain¹¹⁸. This major breakthrough has received mixed views and opinions because the approval of this drug is solely based on a surrogate endpoint that requires an additional post-approval trial to further confirm that Aduhelm indeed provides the anticipated clinical benefits.

3.3. Alternative Therapies

As a consequence of the repeated nonfulfillment of drugs that are related to A β deposits and tau tangles hypotheses, alternative approaches are being considered as new strategies to target AD. For instance, antioxidants, anti-inflammation, neuroprotective agents, type II diabetes drugs, p38a kinase inhibitors, ketone body elevators, antiviral drug, as well as drugs promoting vascular risk reduction and cholesterol removal from the brain^{43, 119, 120}. However, due to their limited progress and lack of efficacy in clinical trials, it was suggested that it is time to finally consider unconventional methods of developing therapeutics for AD^{43, 119, 120}.

4. The Multi-Target Ligands Paradigm

As previously stated, Alzheimer's is a complex disorder involving a variety of pathogenic processes. Therefore, designing a one compound for a single target appears as an outdated principle. In many conditions, the "single ligand, single target" paradigm attains its purpose, but when dealing with multifactorial disorders such Alzheimer's, molecules that are aimed at a single target may not be clinically effective¹²¹.

In chapter III, we describe our efforts towards developing novel molecules for AD. Our research urges the recognition of the multi-factorial nature of AD and undertakes the multi-target directed ligands approach. By combining the structural features of two compounds that exhibit antioxidant and neuroprotective activities, bivalent ligands were designed.

CHAPTER III

LATE-STAGE DIVERSIFICATION OF LIPOIC AND ARUNDIC ACIDS – SYNTHESIS OF NOVEL HYBRID CHEMICAL ENTITY WITH POTENTIAL SYNERGISTIC ANTIOXIDANT AND NEUROPROTECTIVE PROPERTIES

1. Introduction

1.1. α -Lipoic Acid

Alpha lipoic acid (ALA) is a compound present in mitochondria, essential for a variety of enzymatic functions, often known as 1,2-dithiolane-3-pentanoic acid or thioctic acid^{122, 123}. Reed isolated ALA in 1951 from processed liver, and it was first used in clinical practice in 1959 to treat acute poisoning by *Amanita phalloides*, popularly known as death cap (from mushrooms)¹²². ALA is an organosulfur molecule found in nature and formed by plants, animals, and humans¹²³. Moreover, it is a cofactor for several enzyme complexes involved in cell energy production in the Krebs cycle, and it plays a key part in numerous chemical processes^{123, 124}.

α -Lipoic acid can be oxidized or reduced since it has two thiol groups. Dihydrolipoic acid is the reduced form (DHHLA)¹²⁵. Because ALA is a chiral molecule with one asymmetrical carbon atom, it can exist in two enantiomers¹²⁶. S-lipoic acid is a synthetic isomer with no significant activity¹²⁶.

On the other hand, only R-lipoic acid is the naturally occurring isomer in some food and endogenously synthesized, making it the isomer responsible for the biological activities of ALA^{124, 126}. Supplements of lipoic acid contain both isomers in a racemic mixture (\pm) without the need to resolve the S-isomer since it does not have any recorded adverse effects, **(Figure 3.1)**¹²⁴.

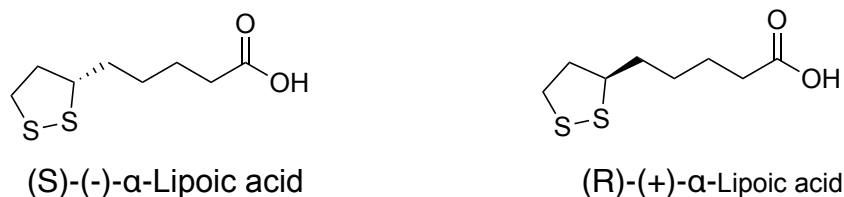


Figure 3. 1. Chemical structure of both enantiomers of lipoic acid.

Although alpha-lipoic acid is commonly considered as a healthy element in our diets¹²⁶, it has yet to be approved by the FDA as a supplement for any health-related purposes. Reportedly, the “universal antioxidant” has significantly shown both physiological and pharmacological properties¹²⁷. For example, in cases of heavy metal poisoning (Pb, Hg, As, Se) in animal tissues, it exhibits curative and protective effects¹²⁸. Furthermore, ALA appears to have the potential in managing diabetes, which is one of the most useful applications of lipoic acid¹²⁹. It is permitted as part of a therapy plan for diabetic patients in some countries¹²⁹.

Most importantly, ALA has received considerable recognition for its potential to hinder the pathogenesis or progression of AD, mainly for its antioxidant activities^{130, 131}. It has shown to activate choline acetyltransferase, therefore increasing the production of acetylcholine¹²⁴. It was also found to increase the uptake of glucose which helps produce more acetylcholine from acetyl-CoA¹²⁴. Moreover, it acts as a metal chelator, chelating toxic redox-active transition metals that are found to stabilize and promote the aggregation of amyloid plaques, suggesting that LA can reduce the amyloid burden and enhance its extraction in AD cases^{124, 132}. Additionally, LA is able

to scavenge free radicals and decrease the levels of pro-inflammatory cytokines such as IL-1, IL-6, TNF and iNOS, making it a great anti-inflammatory as well as antioxidant for individuals with AD that usually express elevated levels of free radical and cytokines^{124 133}. Furthermore, Joseph F Quinn et.al, investigated the effect of LA on the Tg2576 mice, a transgenic model of AD-associated cerebral amyloidosis^{124, 134}. In the study, the authors were able to illustrate that LA-treated Tg2576 mice displayed superior performance in the Morris water maze experiment than untreated Tg2576 mice in terms of learning and memory retention¹³⁴. However, the reduction in memory deficit was not accompanied with the observation of reduced levels of amyloid plaques¹³⁴.

Altogether, clinical trials of lipoic acid in various neurological disorders have revealed promising benefits, nonetheless, these findings were supported by low quality trials. Further research is required to provide sufficient evidence of the above effects of LA and to explore its full antioxidant potential.

1.2. Arundic Acid

ONO-2506, (R) -(-)-2-propyloctanoic acid, or arundic acid, is a neuroprotective agent due to its effects on activated glial cells, astrocytes and microglia¹³⁵. It exerts its neuroprotective activity by the inhibition of S100B synthesis, a calcium-binding protein^{135, 136}. It was discovered by Ono Pharmaceutical Co., Ltd., (Mishima, Osaka, Japan) as a synthetic compound, **(Figure 3.2)** during a random screening process and was found to ameliorate astrocytes function¹³⁵. Moreover, it has shown inhibitory effects both *in-vitro* and *in-vivo* of activated glial-induced synthesis of S100B, and has completed phase-II of clinical trials for the treatment of various neurodegenerative diseases such AD and amyotrophic lateral sclerosis¹³⁶.

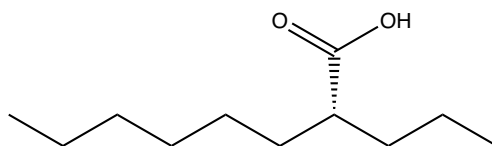


Figure 3. 2. Chemical structure of (R)-Arundic acid.

As mentioned in chapter II, the synthesis and levels of S100B is upregulated in brains with AD pathology ¹³⁷. In Tg APP_{sw} mice, a transgenic mouse model of AD, the overexpression of S100B from reactive gliosis -astrocytosis and microgliosis- precedes the formation of β -amyloid plaques ¹³⁷. Additionally, nuclear factor-kB, a major transcription factor in many inflammatory reactions, is also activated by S100B protein ¹³⁷. In a study conducted by the lab of Takashi Mori, it was concluded that arundic acid attenuated the levels of S100B protein, S100B-associated β -amyloid peptide, and the deposition of β -amyloid ¹³⁶. In addition, a substantial amelioration in β -amyloid plaque-associated reactive astrocytosis and microgliosis was reported in the arundic acid-treated Tg APP_{sw}, compared to the vehicle-treated mice ¹³⁶. If the AD-like pathology in these mice is indicative of the clinical ailment, these results propose that inhibiting S100B synthesis might be an innovative and beneficial therapeutic strategy, specifically for slowing disease progression and/or delaying its onset. Based on these findings, arundic acid is suggested to be a promising therapeutic drug for AD that warrants further investigation ^{136, 138}.

Collectively, these findings point to the need for further exploration of the role of antioxidants and neuroprotective agents as disease-modifying therapeutics. Our research instigates considering unconventional perspectives for therapeutic approaches towards a disease with multifactorial nature. In this context, we rationalize the hybridization of lipoic and arundic acids to endow the novel hybrids with improved antioxidant and neuroprotective properties. For a multifactorial disease, a multi-target directed ligands appear to be a more plausible strategy than

the single-target directed ligands that have yet to be effective in treating or even slowing down the disease's progression.

2. Innovation

The key aspects of innovation in this study is the incorporation of a propyl moiety α to the carboxylic acid group in lipoic acid to provide novel hybrids with the potential of synergistic neuroprotective and antioxidant effects. Hybridizing the similar structural features of a natural antioxidant with the synthetic inhibitor of S100B is a matter that has not been done and explored before, (**Figure 3.3**). In addition, we were able to take advantage of our scheme for a novel synthesis of both antipodes of lipoic acid starting from enantiomerically pure intermediate ester through a sequence of chemical transformations reported in the literature with some modifications.

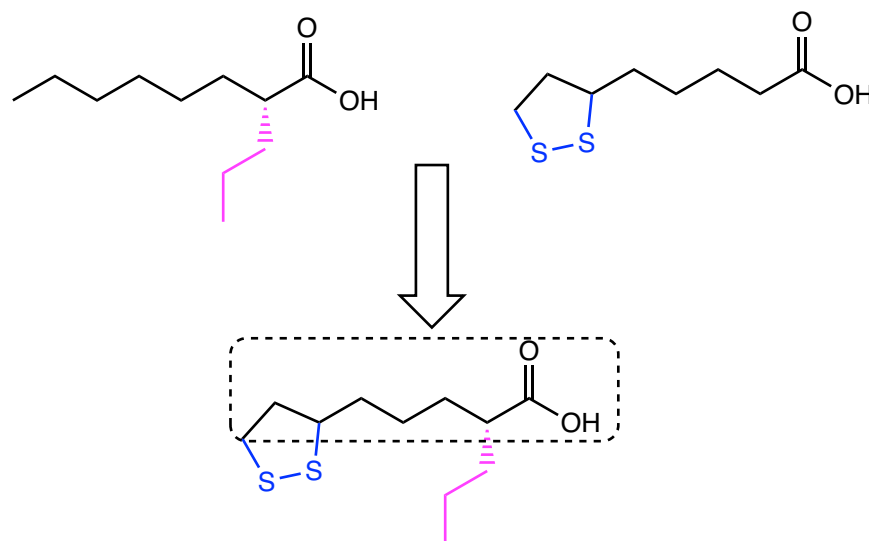


Figure 3. 3. Illustration of similar structural features of ALA and arundic acid.

3. Approach

Taken into consideration that it is only the (R) enantiomer of arundic acid that exhibits inhibitory activity against S100B protein, and that both enantiomers of ALA are available in over-

the-counter dietary supplements as a racemic mixture, we aimed for the synthesis of two diastereomers both having the R configuration α to the carboxylic acid, similar to that of arundic acid, with stereoisomeric variation at C6 of lipoic acid unit to provide **1a** and **1b**, (**Figure 3.4**).

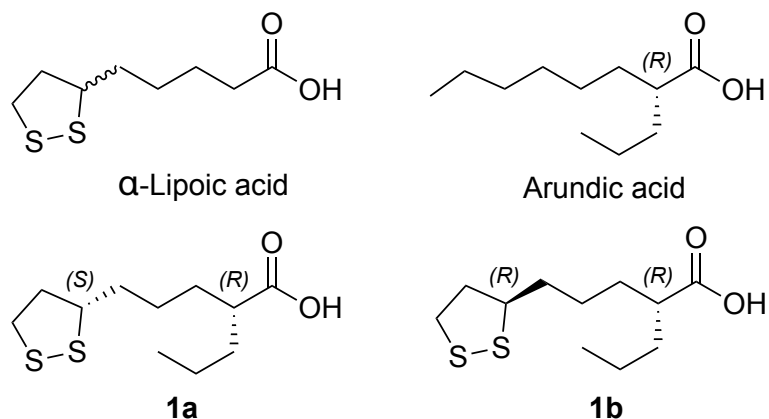
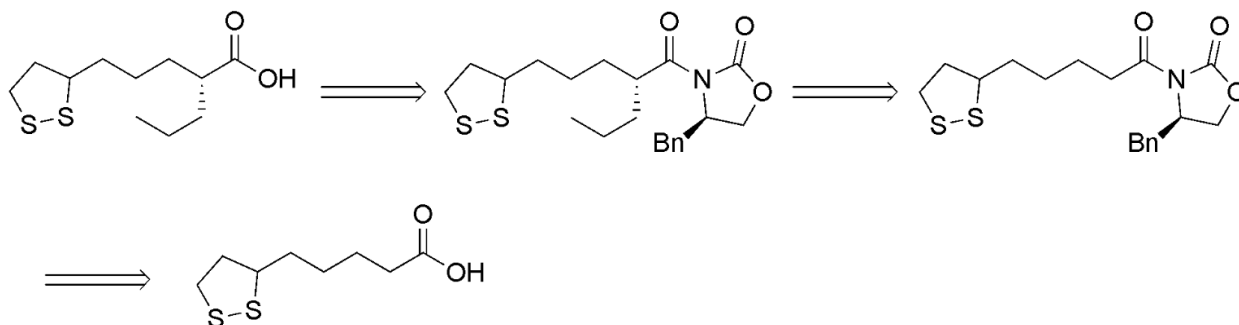


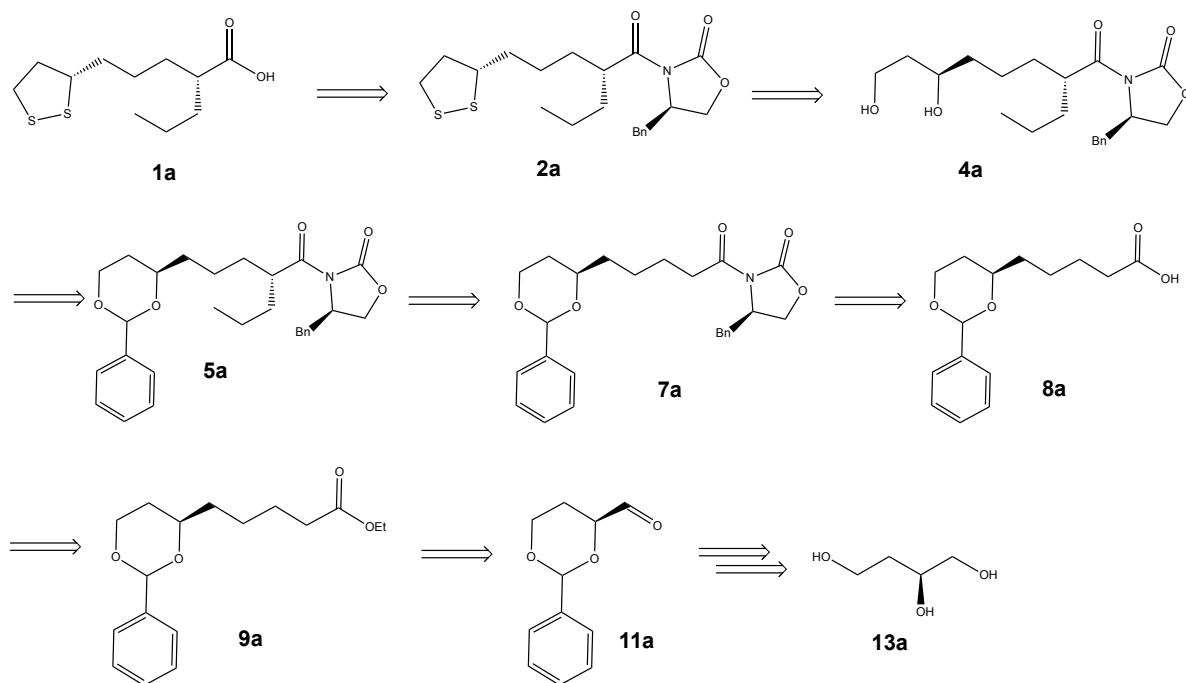
Figure 3. 4. Structures of proposed compounds.

From there, we first aimed to design a short and efficient synthetic route for the synthesis of **1**, starting from affordable enantiomerically pure (S)-(-)- or (R)-(+)-lipoic acid tethered to a commercially available Evans oxazolidinone as a chiral auxiliary for the asymmetric alkylation reaction, followed by the hydrolysis of alkylated products to give **1a** or **1b**, respectively, (**Scheme 3.1**).

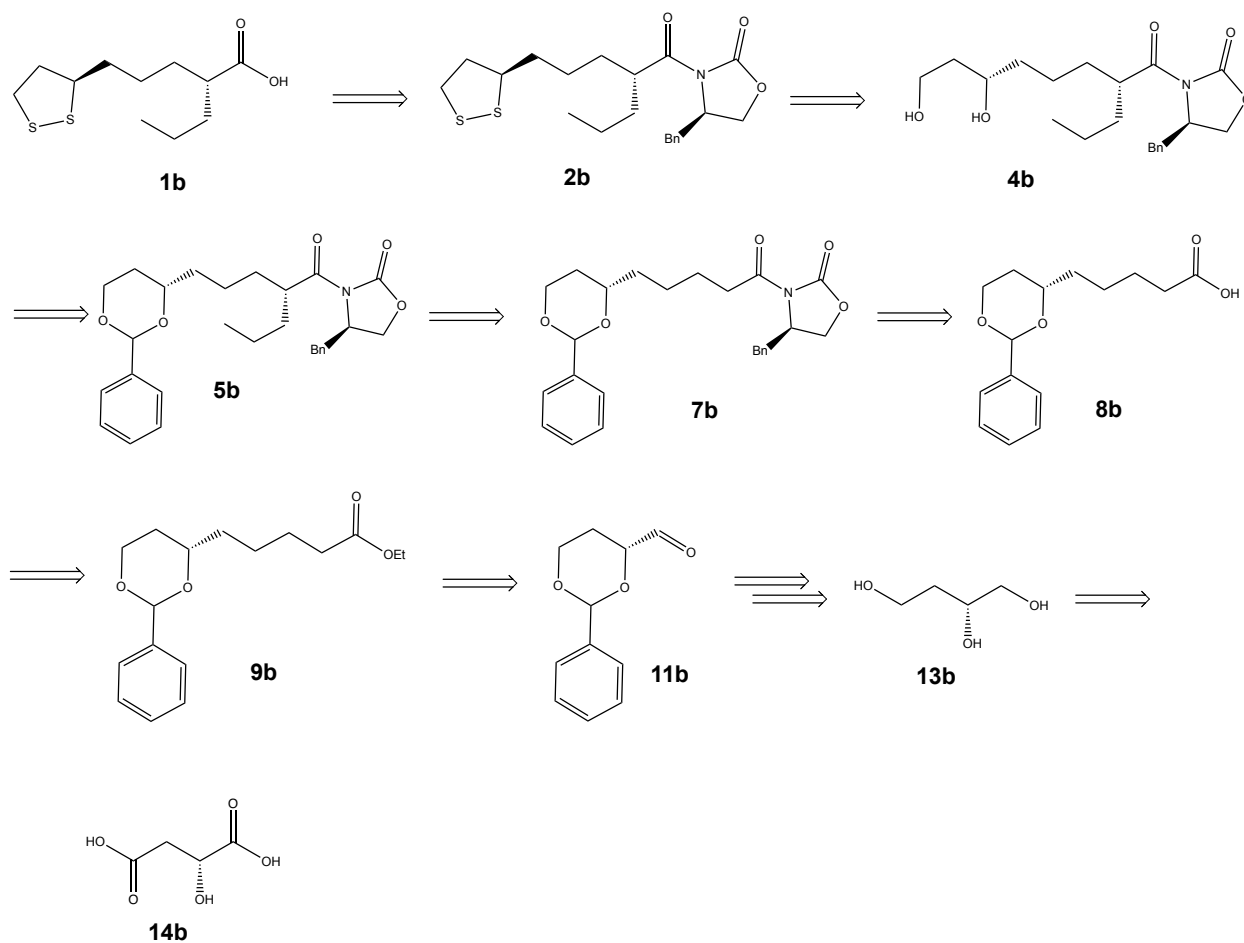


Scheme 3. 1. Retrosynthetic analysis of 1 (a) and (b) using the first approach.

As for the second approach, we attempted to employ 1,2,4-butanetriol chiron as our starting material in the synthesis process to control, and maintain, the chirality at C6 of lipoic acid unit while performing chemical transformations that will result in the desired chirality at C2 position. We proposed that compound **1a** will be obtained by the removal of chiral auxiliary group from **2a** which in turn will be made from the corresponding diol **4a** through a di-mesylated intermediate. The diol **4a** will then be prepared from the acetal deprotection of **5a**, which is a product resulted from a diastereoselective alkylation of **7a** that will be made by a covalent coupling of chiral auxiliary to compound **8a**. Compound **8a** will be achieved from the hydrolysis of the ester **9a** which will be made ready from the olefination followed by hydrogenation of aldehyde **11a** that will eventually disconnect into the enantiomerically pure C4 building block starting material (S)-1,2,4-butanetriol **13a** through appropriately designed chemical reactions, (Scheme 3.2). By using the same analogy, compound **1b** will be achieved from (R)-1,2,4-butanetriol **13b** via the reduction of its precursor (R)-malic acid **14b**, (Scheme 3.3).

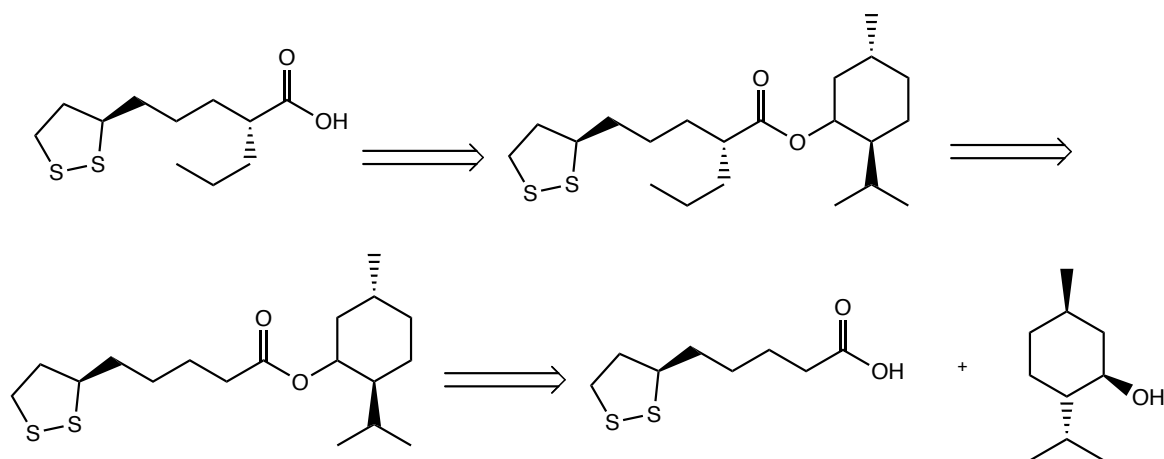


Scheme 3. 2. Retrosynthetic analysis for the synthesis of compound 1a.



Scheme 3. 3. Retrosynthetic analysis for the synthesis of compound 1b.

In terms of adopting a short and effective synthetic route, the third -and final- strategy is similar to the first. We postulated that using L-menthol as a chiral auxiliary will result in a preferred asymmetric and diastereoselective alkylation of the corresponding menthyl lipiate derivative when using a pure enantiomer of lipoic acid as the starting material. Our retrosynthetic analysis for **1b** disconnects the menthyl lipiate **19** into R-lipoic acid and L-menthol that could be assembled by simple esterification reaction followed by asymmetric alkylation, and finally ester hydrolysis to provide the final desired product **1b**, (Scheme 3.4).



Scheme 3. 4. Retrosynthetic analysis of **1b using L- menthol for asymmetric alkylation.**

4. Results and Discussion

We attempted the synthesis of **1b** by using the first approach which involves tethering (R)-(+)-lipoic acid to a commercially available chiral auxiliary Evans oxazolidinone, as the first step of the synthesis. Lipoic acid was dissolved in THF and treated with the base Et_3N and pivaloyl chloride at $-20\text{ }^\circ\text{C}$, followed by LiCl and (4R)-benzyloxazolidin-2-one to afford **MJS-1** in 79% isolated yield, (**Figure 3.5**). Next, the second step includes the asymmetric alkylation of **MJS-1** (C-C bond formation in alpha position to the carbonyl). However, this step failed to obtain the alkylated derivative of **MJS-1** despite our efforts to monitor the reaction conditions by screening several parameters, such as different bases, alkylating reagents, temperatures, and reaction duration. Subsequently, the third-and last- step, that includes the removal of the chiral auxiliary to ultimately furnish the desired product **1b** was not achievable. Similarly, the synthesis of **1a** was carried out starting from (S)-(-)-lipoic acid with successful attachment of chiral auxiliary and no alkylation of the product was attained.

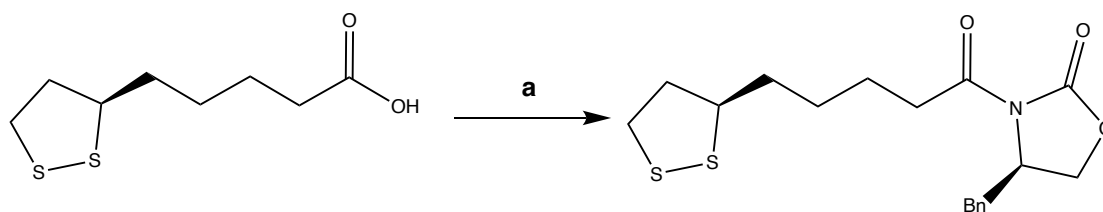


Figure 3. 5. Synthesis of MJS-1.

Reagents and conditions: **a-1)** triethylamine, pivaloyl chloride, 20°C, 2 h, THF; **a-2)** LiCl, (4R)-benzyloxazolidin- 2-one, 0 °C – rt, 4 h, 79%.

Moving forward to the second approach, the synthesis of **1a** started with a regioselective protection of the enantiopure (S)-1,2,4-butanetriol **13a** in the presence of benzaldehyde dimethyl acetal, triethylamine, and a catalytic amount of camphorsulfonic acid at room temperature to give the acetal compound 1,3-dioxan **12a** in excellent yield, (**Figure 3.6**). Optimization conditions for this reaction are listed in **Table 3.1**.

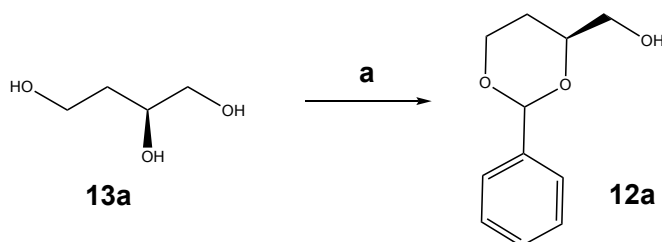


Figure 3. 6. Diol protection of 13a into 1,3-dioxane 12a.

Reagents and conditions: **a)** PhCH(OMe)₂, CSA, CH₂Cl₂, Et₃N, rt, 16 h, 92%.

Table 3. 1. Optimization conditions for 12a.

Entry	Reagent	Catalyst	Base (TEA)	Temp/Duration	% Yield
1	1 equiv. benzaldehyde dimethyl acetal	0.03 equiv. p-toluenesulfonic acid	0.1 equiv.	rt/ 12 h	45% ^a
2	1.2 equiv. benzaldehyde dimethyl acetal	0.05 equiv. p-toluenesulfonic acid	0.1 equiv.	rt/ 16 h	51% ^a
3	1 equiv. benzaldehyde dimethyl acetal	0.03 equiv. camphorsulfonic acid	0.1 equiv.	rt/ 12 h	63% ^a
4	1.2 equiv. benzaldehyde dimethyl acetal	0.05 equiv. camphorsulfonic acid	0.1 equiv.	rt/ 16 h	92% ^a

^a = yields reported for isolated compounds.

Next, **12a** was subjected to oxidation reaction in which the alcohol functional group was transformed into the aldehyde derivative **11a**. The oxidation of **12a** was attempted via Dess-Martin-Periodinane (DMP) and Swern oxidation reactions, (**Figure 3.7**). Only the swern oxidation was able to furnish the aldehyde **11a** in a quantitative yield after purification.

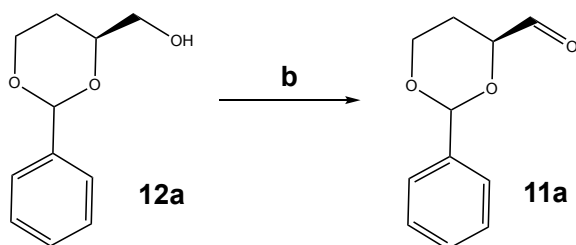


Figure 3. 7. Oxidation of 12 a.

Reagents and conditions: **b**) DMP oxidation: DMP, anh. CH₂Cl₂, 0 °C, no reaction.

Swern oxidation: **b-i**) (COCl)₂, DMSO, CH₂Cl₂; **b-ii**) Et₃N, -78 °C to rt, quantitative.

The resulting aldehyde **11a** was then reacted with Horner–Wadsworth–Emmons reagent and LiHMDS at -78 °C to produce the di-olefins **10a** as a mixture of inseparable cis and trans isomers, (Z:E) equaled 8:92, respectively, (**Figure 3.8**). The mixture did not require further purification in order to separate the two isomers, because in the next step which involves the saturation of both isomers, one compound **9a** will eventually be produced. Consequently, the saturation of the di-olefins **10a** was carried out by using palladium in the form of Pd/C as a hydrogenation catalyst under H₂ atmosphere for 24 h at room temperature to provide the corresponding saturated ester **9a** in 40% overall yield (with respect to alcohol **12a**), (**Figure 3.9**).

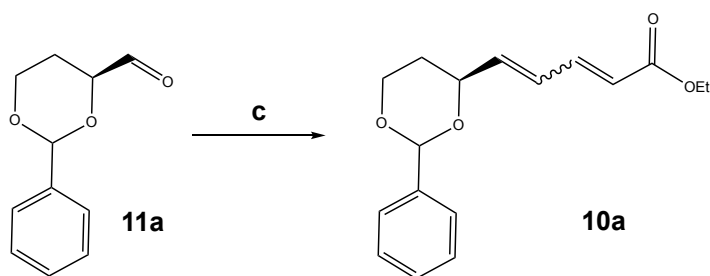


Figure 3. 8. Horner–Wadsworth–Emmons olefination reaction.

Reagents and conditions: **c**) LiHMDS, THF, triethyl 4-phosphonocrotonate, 0 °C, 2h.

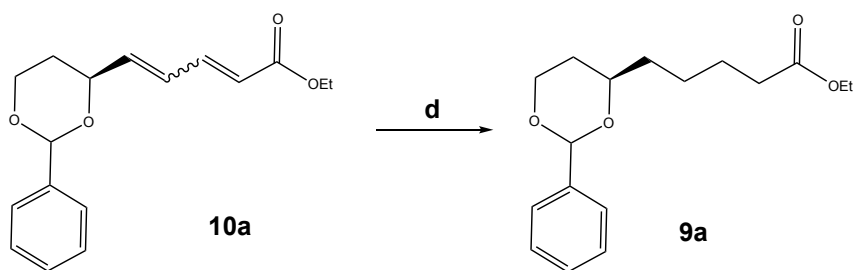


Figure 3. 9. Hydrogenation of the di-olefins 10a.

Reagents and conditions: **d**) Pd/C (cat.), EtOAc, H₂, rt, 24 h, 40% for **9a** (based on **12a**).

Subsequently, hydrolysis of ester **9a** was achieved with 4 M LiOH/H₂O solution in THF for 24 h at room temperature to give the acid **8a** in 63% yield, (**Figure 3.10**). Next, in order to control the stereoselectivity in the alkylation reaction, the acid **8a** was then treated with Et₃N and pivaloyl chloride in the presence of anhydrous THF at -20 °C for 2 h, followed by LiCl and readily available oxazolidinone chiral auxiliary to afford **7a** in 80% yield, (**Figure 3.11**).

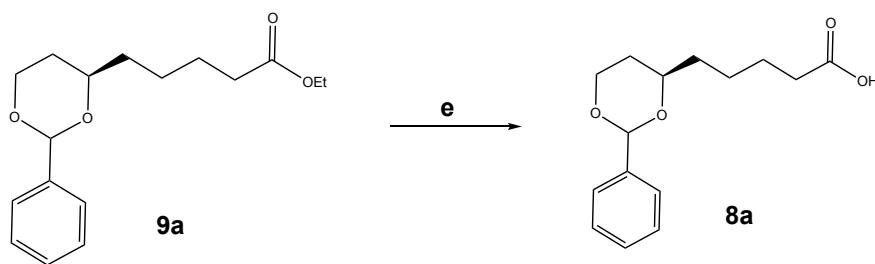


Figure 3. 10. Hydrolysis of ester 9a.

Reagents and conditions: **e**) 4 M LiOH/H₂O, THF, rt, 24 h, 63%.

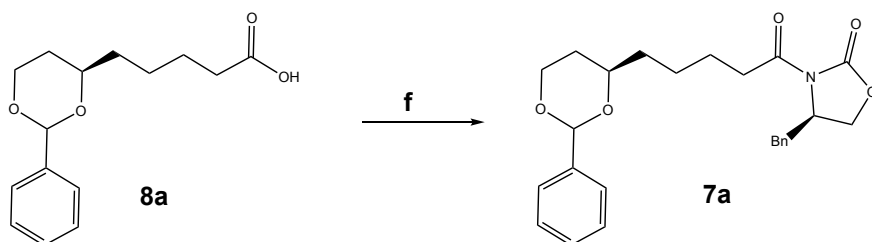


Figure 3. 11. Chiral auxiliary incorporation into 8a.

Reagents and conditions: **f-i**) TEA, pivaloyl chloride, THF, -20°C, 2h; **f-ii**) LiCl, (R)-4-Benzyl-2-oxazolidinone, 0 °C - rt, 2h, 80%.

Diastereoselective alkylation of **7a** was then carried out by deprotonation with LiHMDS at 0 °C to form a rigidly chelated enolate that was alkylated by allyl bromide in which the least hindered diastereoface is preferred to deliver **6a** with 63% isolated yield, (**Figure 3.12**). By

employing the oxazolidinone chiral auxiliary in the previous step, the desired stereogenic center at C2 was created successfully. It is worth mentioning that this step required much time, resources, and efforts to achieve the synthesis of **6a**. A plenty of trials were attempted using different combinations of bases, alkylating reagents, and reaction's temperatures and durations for the product to be finally synthesized, (**Table 3.2-3.5**).

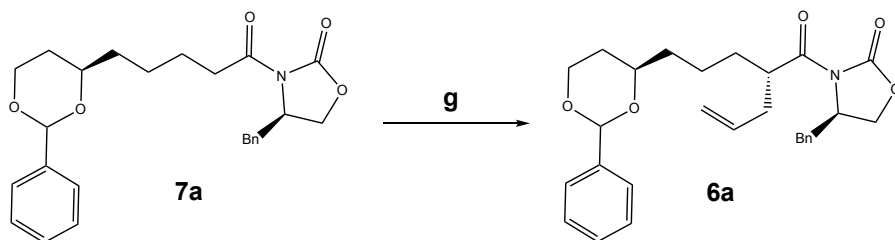


Figure 3. 12. Diastereoselective alkylation of 7a.

Reagents and conditions: **g-i)** LiHMDS, THF, 0 °C, 1h; **g-ii)** C₃H₅Br, 63%.

Table 3. 2. Optimization conditions for 6a.

Entry	Base	Alkylating reagent	Temp.	Duration	Remarks
1	KHMDS	C ₃ H ₇ Br	-78 °C	30 min.	No reaction
2				1 h	No reaction
3			-20 °C	30 min.	No reaction
4				1 h	No reaction
5			0 °C	30 min.	No reaction
6				1 h	No reaction
7			rt	30 min.	SM
8				1 h	SM
9		C ₃ H ₅ Br	-78 °C	30 min.	No reaction
10				1 h	No reaction
11			-20 °C	30 min.	SM
12				1 h	SM
13			0 °C	30 min.	No reaction
14				1 h	SM
15			rt	30 min.	SM
16				1 h	SM
17		C ₃ H ₅ I	-78 °C	30 min.	No reaction
18				1 h	No reaction
19			-20 °C	30 min.	No reaction
20				1 h	No reaction

Table 3. 3. Optimization conditions for 6a “contd”.

Entry	Base	Alkylating reagent	Temp.	Duration	Remarks
21	KHMDS	C ₃ H ₅ I	0 °C	30 min.	No reaction
22				1 h	No reaction
23			rt	30 min.	SM
24				1 h	SM
25	NaHMDS	C ₃ H ₇ Br	-78 °C	30 min.	No reaction
26				1 h	No reaction
27			-20 °C	30 min.	SM
28				1 h	No reaction
29			0 °C	30 min.	No reaction
30				1 h	No reaction
31			rt	30 min.	No reaction
32				1 h	No reaction
33		C ₃ H ₅ Br	-78 °C	30 min.	No reaction
34				1 h	No reaction
35			-20 °C	30 min.	No reaction
36				1 h	No reaction
37			0 °C	30 min.	SM
38				1 h	SM
39			rt	30 min.	No reaction
40				1 h	No reaction

Table 3. 4. Optimization conditions for 6a “contd”.

Entry	Base	Alkylating reagent	Temp.	Duration	Remarks	
41	NaHMDS	C ₃ H ₅ I	-78 °C	30 min.	No reaction	
42				1 h	No reaction	
43			-20 °C	30 min.	No reaction	
44				1 h	No reaction	
45			0 °C	30 min.	No reaction	
46				1 h	No reaction	
47			rt	30 min.	No reaction	
48				1 h	No reaction	
49	LiHMDS	C ₃ H ₇ Br	-78 °C	30 min.	No reaction	
50				1 h	No reaction	
51			-20 °C	30 min.	SM	
52				1 h	No reaction	
53			0 °C	30 min.	SM	
54				1 h	Trace	
55			rt	30 min.	No reaction	
56				1 h	No reaction	
57			C ₃ H ₅ I	-78 °C	30 min.	Complex mixture
58					1 h	No reaction
59				-20 °C	30 min.	SM
60					1 h	No reaction

Table 3. 5. Optimization conditions for 6a “contd”.

Entry	Base	Alkylating reagent	Temp.	Duration	Remarks
61	LiHMDS	C ₃ H ₅ I	0 °C	30 min.	SM
62				1 h	Trace
63			rt	30 min.	Complex mixture
64				1 h	No reaction
65		C ₃ H ₅ Br	-78 °C	30 min.	SM
66				1 h	No reaction
67			-20 °C	30 min.	SM
68				1 h	SM
69			0 °C	30 min.	38% isolated yield.
70				1 h	63% isolated yield, dr> 85%
71			rt	30 min.	SM
72				1 h	No reaction

Reduction of the double bond followed by debenzoylation of **6a** resulted in the diol **4a** in 92% yield using hydrogenation conditions as previously mentioned for compound **9a**, (**Figure 3.13**). Afterwards, mesylation of **4a** was achieved in quantitative yield when **4a** was treated with MsCl and Et₃N in anhydrous DCM at 0 °C to afford the corresponding dimesylated derivative **3a**, (**Figure 3.14**), which next was directly subjected to dry conditions with Na₂S and sulfur in anhydrous DMF for 24 h at 85-90 °C to afford a 1,2 dithiolane derivative **15** in poor yield, 12%, (**Figure 3.15**).

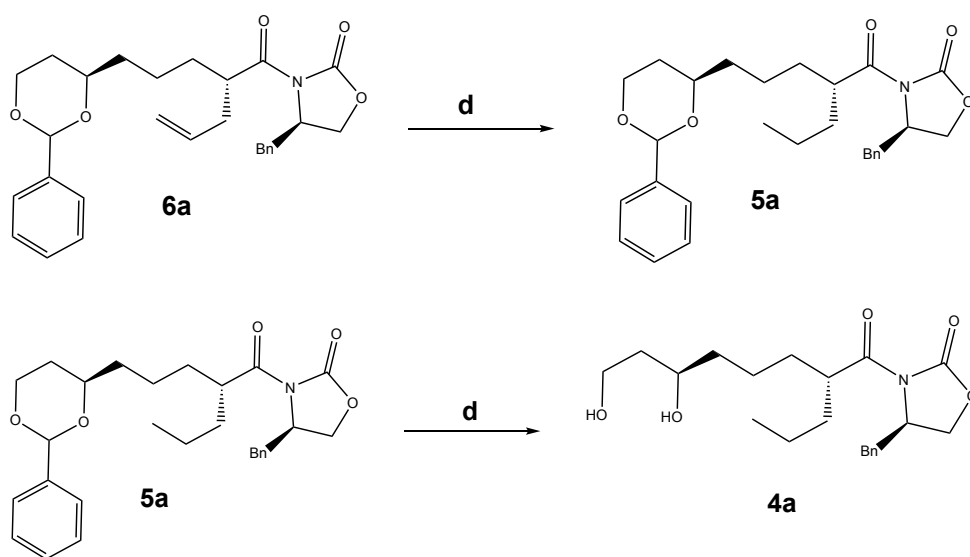


Figure 3. 13. Hydrogenation and debenzoylation of 6a.

Reagents and conditions: **d**) Pd/C (cat.), EtOAc, H₂, rt, 24 h, 92% for **4a** (based on **6a**).

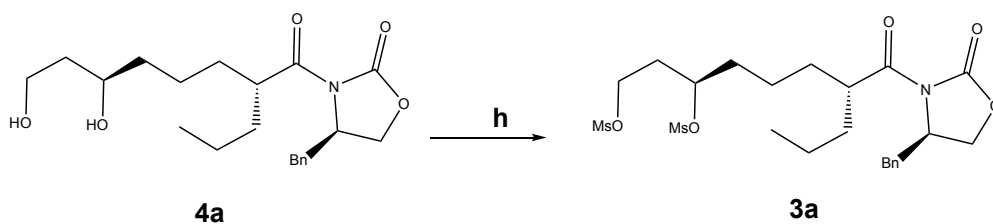


Figure 3. 14. Mesylation reaction of 4a.

Reagents and conditions: **h**) MsCl, Et₃N, CH₂Cl₂, 0 °C, 1h, quantitative.

From NMR data, we were able to characterize the chemical structure to be **2a**, however, results from HRESIMS were not in agreement with our findings, (**Figure 3.15**). The HRESIMS showed fragment ions at (m/z 424.16254 $[M+H]^+$ for $C_{21}H_{30}NO_4S_2$, calcd. 424.16107) and an ion at (m/z 446.14513 $[M+Na]^+$ for $C_{21}H_{29}NNaO_4S_2$, calcd. 446.14301) which are + 15.99 than $[M+H]^+$ and $[M+Na]^+$ for the expected product **2a**, indicating that oxidation to one of the sulfur atoms might have occurred to form compound **15** whether during the reaction, purification, or sample handling. Besides sulfur susceptibility to oxidation and reaction's poor yield, compound **15** exhibited poor solubility in most solvents which made it difficult to carry out to the next step or to perform further analytical experiments.

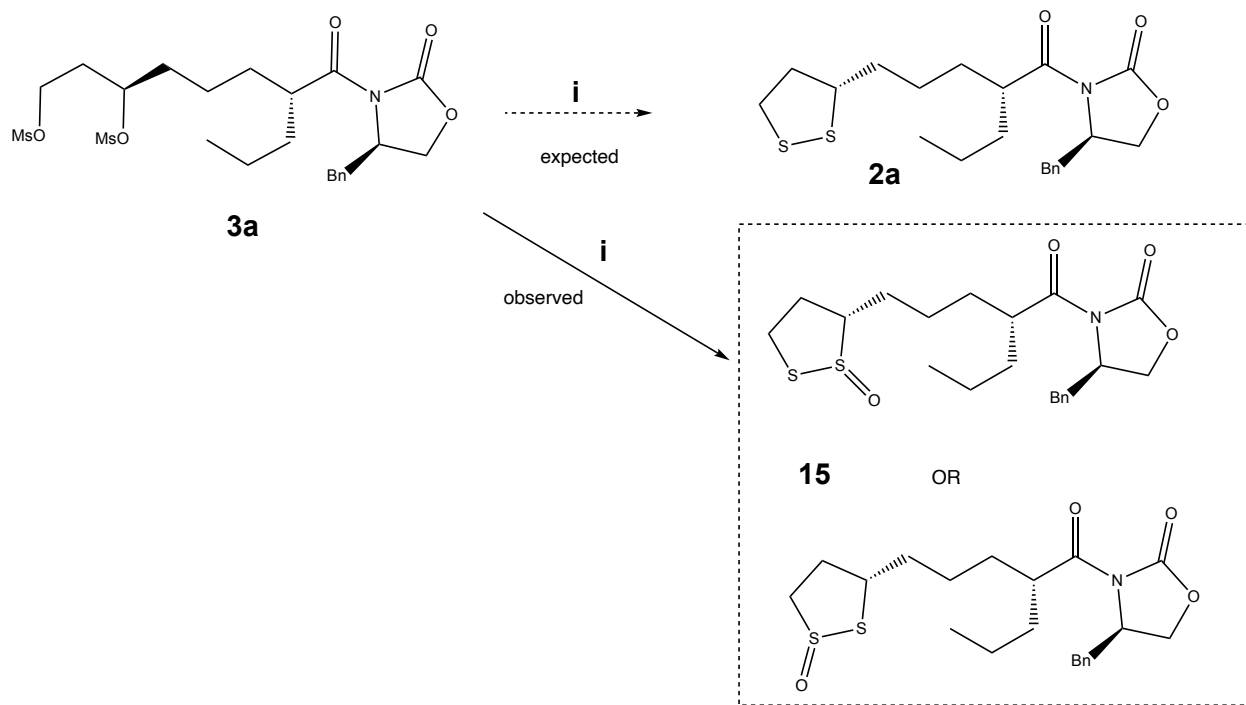
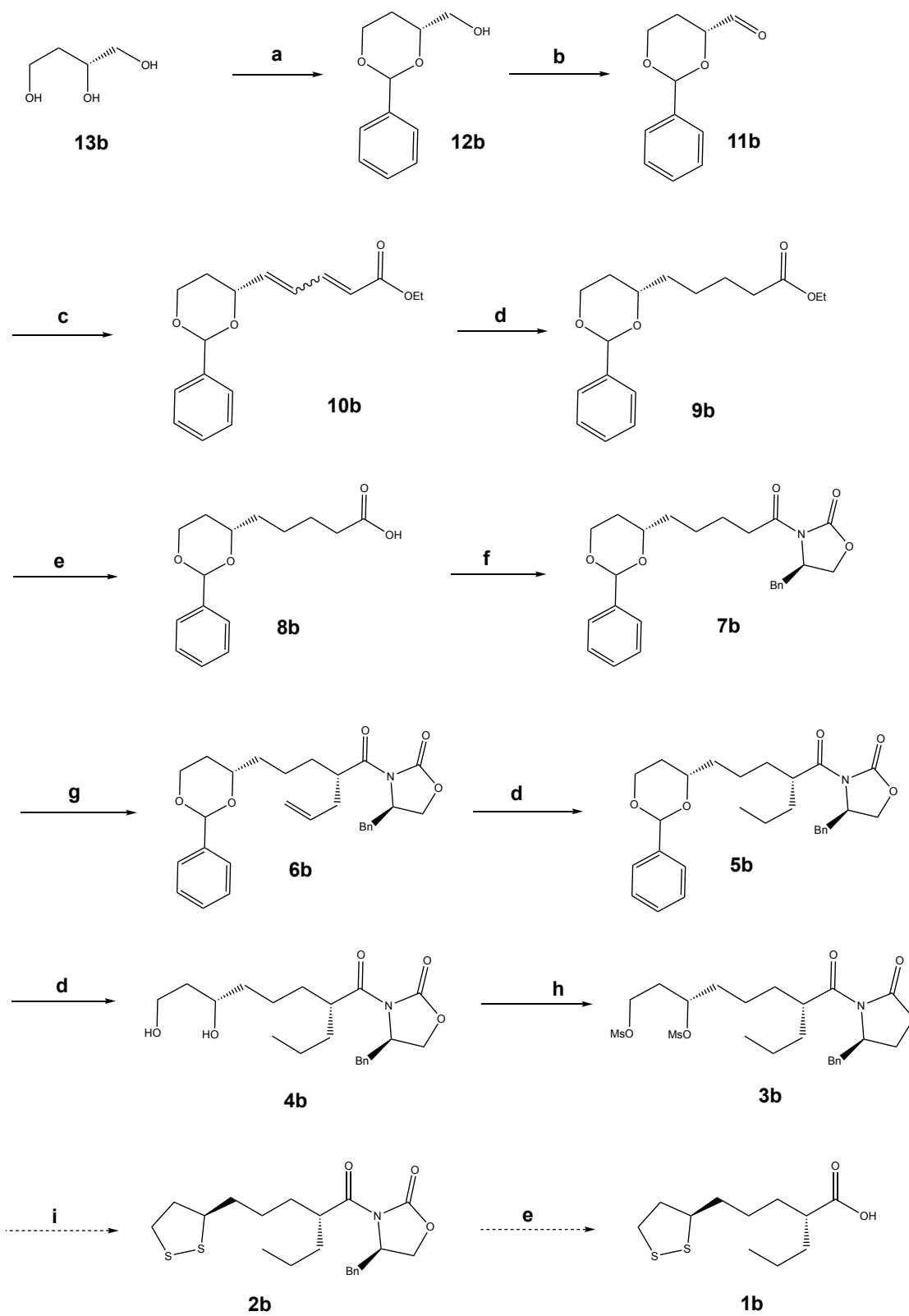


Figure 3. 15. The formation of 1,2 dithiolane ring.

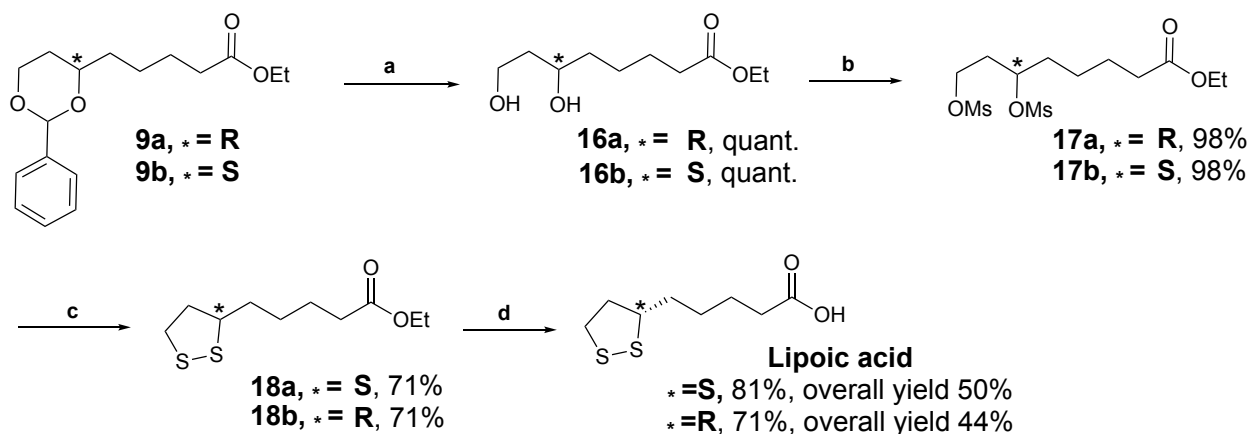
Reagents and conditions: **i**) Na_2S , S, DMF, 85-90 °C, 24 h, 12% for **15**.

By using the same synthetic strategy for **1a**, the synthesis of **1b** was carried out starting from the precursor (R)-malic acid **14b** and following the exact designed reactions for **1a**. Unfortunately, after affording the dimesylated product **3b**, further progress in the synthesis failed as the next steps that involve formation of 1,2 dithiolane ring, and consequently, amide hydrolysis did not result in complete synthesis of **1b**, (**Scheme 3.5**).

In addition to the proposed hybrids, we were able to take advantage of this scheme for a novel synthesis of both antipodes of lipoic acid starting from the enantiomerically pure intermediate ester **9** (as indicated by asterisk) through a sequence of chemical transformations reported in the literature with some modifications, (**Scheme 3.6**).



Scheme 3.5. Synthesis of **1b**.



Scheme 3. 6. Total synthesis of lipoic acid.

Reagents and conditions: **a)** Pd/C (cat.), EtOAc, H₂, rt, 24 h; **b)** MsCl, Et₃N, CH₂Cl₂, 0 °C, 1h; **c)** Na₂S, S, DMF, 85-90 °C, 24 h; **d)** 4 M LiOH/H₂O, THF, rt, 24 h.

Lastly, we pursued the synthesis of the proposed hybrids with one last approach to tackle the difficulties we encountered with previous approaches. In this approach, the use of L-menthol as a chiral auxiliary tethered to enantiomerically pure lipoic acid will afford diastereoisomers upon alkylation that are easy to separate. In addition, this scheme not only offers a short and efficient strategy, it utilizes affordable material as well as it makes use of another natural product in the synthesis process. Consequently, R-lipoic acid and L-menthol in pyridine as the base were treated with diethyl chlorophosphate at room temperature for 30 minutes before raising the temperature to 70 °C for 20 h to provide the ester **19** in 32% isolated yield, (**Figure 3.16**).

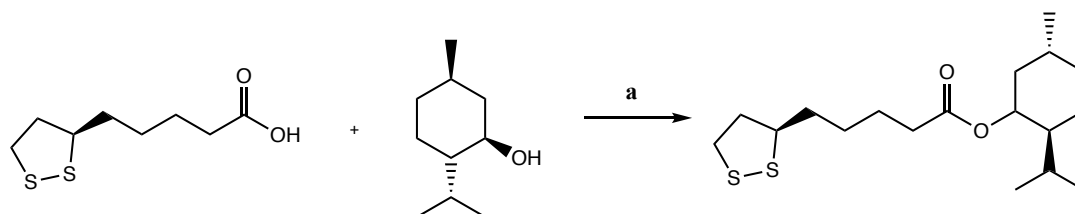


Figure 3. 16. Synthesis of 19.

Reagents and conditions: **a)** pyridine, (C₂H₅O)₂P(O)Cl, rt for 30 min, 70 °C for 20 h, 32%

Next, we attempted to alkylate the ester **19** by treating it with the base LiHMDS at 0 °C and allyl iodide to form the alkylated derivative of the ester, (**Figure 3.17**). However, NMR data revealed the alkylation reaction provided compound **20** instead of the expected compound, (**Figure 3.18**). The reaction's duration upon the addition of the base was optimized to avoid the ring opening, closing, and dialkylation mechanism, giving similar results each time, (**Table 3.6**).

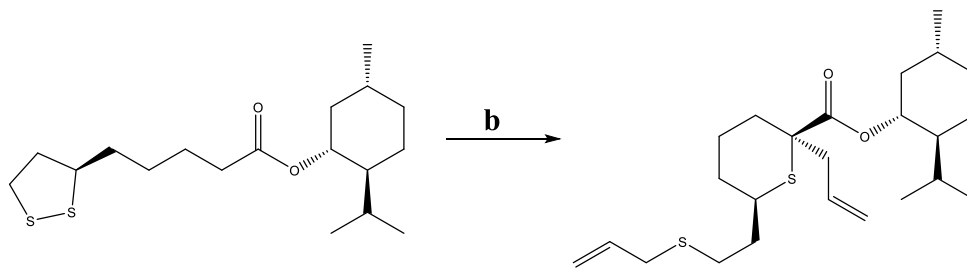


Figure 3. 17. Alkylation of 19.

Reagents and conditions: **b-i)** LiHMDS, THF, 0 °C, 30 minutes; **b-ii)** C₃H₅I, 0 °C, 1 h, 52%.

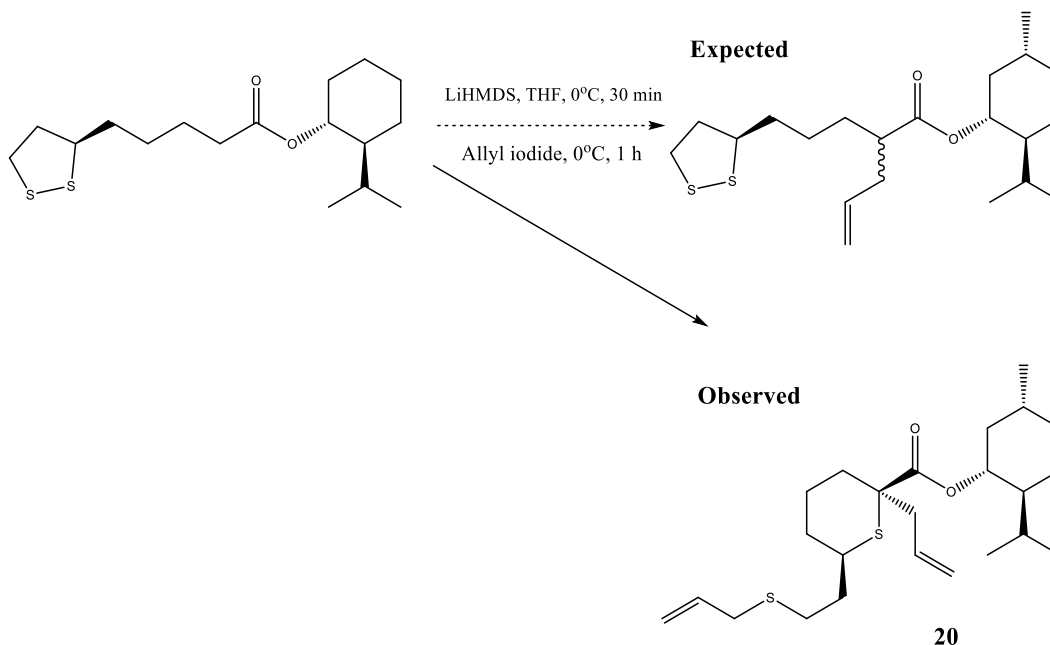


Figure 3. 18. Formation of 20.

Table 3. 6. Optimization conditions for the alkylation of 19.

Base/Duration	Alkylating reagent/Duration	Comments
LiHMDS/ 1h	C ₃ H ₅ I/1 h	20
	C ₃ H ₅ I/ 30 minutes	20
LiHMDS/ 30 minutes	C ₃ H ₅ I/1 h	20
	C ₃ H ₅ I/ 30 minutes	20

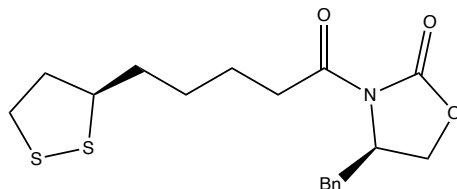
5. Experimental Section

5.1. General Experimental Procedures

All reactions were conducted under argon atmosphere except for hydrogenation and debenzylolation reactions, in which they were performed in hydrogen gas environment. Glassware and magnetic stir bars were oven-dried prior each reaction. All solvents were distilled before use. All commercially available reactants and reagents were purchased from Sigma-Aldrich[®] and Fisher Scientific and were used without additional purification. To monitor reactions progress, thin layer chromatography (TLC) plates (F₂₅₄ aluminum support silica gel 60 matrix, 200 μm thickness, 10-12 μm pore size) were used and the progress was visualized by UV absorption at 254 nm, iodine or phosphomolybdic acid staining, or a combination of the two. Flash silica gel 60-120 mesh SiO₂ was used for column chromatographic purification. The ¹H NMR and ¹³C NMR spectra were recorded on Bruker AU III 400 or 500 MHz NMR spectrometers in CDCl₃ or D₂O solvents. IR spectra were recorded on Agilent Technologies infrared spectrophotometer model Cary 630 FTIR. An Agilent MS TOF 1100 series with electrospray ionization was used to acquire the HRESIMS data.

5.2. Synthesis of Compounds

- Preparation of (R)-3-(5-((R)-1,2-dithiolan-3-yl)pentanoyl)-4-benzyloxazolidin-2-one (**MJS-1**):



Procedure: To a stirred solution of R-lipoic acid (5 g, 24.23 mmol) in THF (200 mL) was added triethylamine (6.76 mL, 48.47 mmol) followed pivaloyl chloride (2.98 mL, 24.23 mmol) at -20 °C. After being stirred for 2 h, LiCl (1.20 g, 28.38 mmol) and (4R)-benzyloxazolidin-2-one (3.87 g, 21.83 mmol) were added and the mixture was allowed to warm up to 0 °C and then to room temperature slowly and was stirred for an additional 4 h. The mixture was concentrated, and residue was partitioned between 5% aqueous KHSO₄ (200 mL) and ethyl acetate (500 mL). The organic layer was washed with 1 M sodium bicarbonate (2x100 mL) and brine (100 mL) and then dried over anhydrous magnesium sulfate and concentrated. The residue was purified by column chromatography using normal phase silica gel (n-hexane/ethyl acetate 2:1 to 1:1) to give **MJS-1** (6.31 g) as a yellow oil.

Molecular Formula: C₁₈H₂₃NO₃S₂

Yield: 79%

Rf: 0.31 (n-hexane/ethyl acetate 8:2).

IR v_{max}, (neat, cm⁻¹): 2924, 2858, 1777, 1697, 1386, 762, 702.

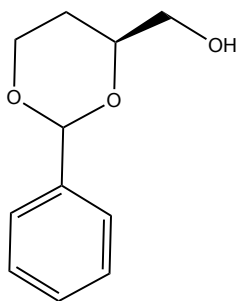
¹H NMR (400 MHz, Chloroform-d): δ 7.41 – 7.25 (m, 3H), 7.28 – 7.19 (m, 2H), 4.70 (ddt, J = 10.4, 7.0, 3.3 Hz, 1H), 4.28 – 4.15 (m, 2H), 3.62 (dq, J = 8.4, 6.4 Hz, 1H), 3.32 (dd, J = 13.4, 3.4 Hz, 1H), 3.27 – 3.09 (m, 2H), 3.08 – 2.87 (m, 2H), 2.79 (dd, J = 13.4, 9.6 Hz, 1H), 2.50 (dtd, J =

13.0, 6.6, 5.4 Hz, 1H), 1.95 (dq, $J = 12.7, 6.9$ Hz, 1H), 1.75 (dt, $J = 13.8, 11.5, 5.8$ Hz, 4H), 1.67 – 1.61 (m, 1H), 1.62 – 1.47 (m, 1H).

^{13}C NMR (101 MHz, Chloroform-*d*): δ 173.02, 153.47, 135.26, 129.42, 128.97, 127.38, 66.23, 56.36, 55.16, 40.24, 38.52, 37.95, 35.33, 34.67, 28.73, 23.98.

HRESIMS *m/z*: 366.11970 $[\text{M}+\text{H}]^+$ (calcd. for $\text{C}_{18}\text{H}_{24}\text{NO}_3\text{S}_2$, 366.11920), 388.10214 $[\text{M}+\text{Na}]^+$ (calcd. for $\text{C}_{18}\text{H}_{23}\text{NNaO}_3\text{S}_2$, 388.10114), 404.09704 $[\text{M}+\text{K}]^+$ (calcd. for $\text{C}_{18}\text{H}_{23}\text{KNO}_3\text{S}_2$, 404.07508).

- Preparation of (2*S*,4*S*)-4-(Hydroxymethyl)-2-phenyl-1,3-dioxane (**12a**):



Procedure: (S)-1,2,4-Butanetriol (2.50 g, 23.56 mmol) and benzaldehyde dimethylacetal (3.80 g, 24.97 mmol) in dry dichloromethane (80 mL) were stirred at room temperature in the presence of camphorsulfonic acid (273.62 mg, 1.18 mmol). After the mixture had been stirred for 16 h, triethylamine (238.39 mg, 2.36 mmol) was added and the solvents were removed under reduced pressure. The product **12a** (4.20 g) was obtained after column chromatography on silica gel (n-hexane/ethyl acetate 2:1 to 1:1) as a colorless oil.

Molecular Formula: $\text{C}_{11}\text{H}_{14}\text{O}_3$

Yield: 92%

R_f: 0.41 (n-hexane/ethyl acetate 4:6).

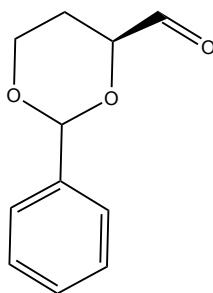
IR ν_{max} , (neat, cm^{-1}): 3391, 3030, 2924, 2858, 1716, 752.

¹H NMR (400 MHz, Chloroform-*d*): δ 7.41 – 7.15 (m, 5H), 5.38 (s, 1H), 4.13 (d, $J = 11.4$ Hz, 1H), 3.87 – 3.75 (m, 2H), 3.57 – 3.42 (m, 2H), 2.27 (s, 1H), 1.81 – 1.66 (m, 1H), 1.27 (d, $J = 13.2$ Hz, 1H).

¹³C NMR (101 MHz, Chloroform-*d*): δ 138.28, 128.86, 128.17, 126.05, 101.16, 77.48, 66.52, 65.50, 26.73.

HRESIMS m/z : 195.10169 [M+H]⁺ (calcd. for C₁₁H₁₅O₃, 195.10156), 217.08416 [M+Na]⁺ (calcd. for C₁₁H₁₄NaO₃, 217.08350), 411.17729 [2M+Na]⁺ (calcd. for C₂₂H₂₈NaO₆, 411.17779).

- Preparation of (2*S*,4*S*)-4-Formyl-2-phenyl-1,3-dioxane (**11a**):



Procedure: A solution of dry DMSO (3.56 mL, 50.17 mmol) in dichloromethane (26 mL) was added dropwise, at -78 °C under argon, to a solution of oxalyl chloride (2 mL, 23.35 mmol) in dichloromethane (50 mL). After the mixture had been stirred for 12 min, a solution of alcohol **12a** (4.2 g, 21.62 mmol) in dichloromethane (25 mL) was added dropwise. The mixture was stirred at -78 °C for 30 min and was then treated with triethylamine (14.23 mL, 102.06 mmol). After a further 5 min the cooling bath was removed, water (100 mL) was added, and the mixture was allowed to warm up to room temperature. The phases were separated, the aqueous phase was extracted with dichloromethane (3x100 mL), and the combined organic extracts were washed with saturated ammonium chloride solution (250 mL) and water (250 mL) and dried over anhydrous Na₂SO₄.

Evaporation of the solvents afforded crude aldehyde **11a** (5.1 g) as a colorless oil. The product was used in the next step without purification. An aliquot was purified for analytical purposes.

Molecular Formula: C₁₁H₁₂O₃

Yield: quantitative

Rf: 0.58 (n-hexane/ethyl acetate 7:3).

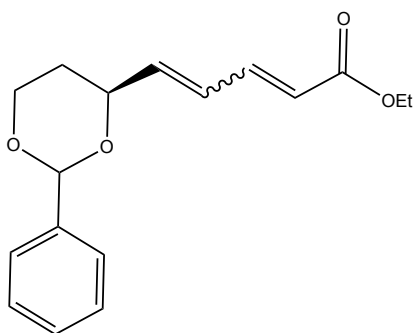
IR v_{max}, (neat, cm⁻¹): 2910, 2874, 1713, 751.

¹H NMR (400 MHz, Chloroform-d): δ 9.75 (d, J = 0.7 Hz, 1H), 7.59 – 7.34 (m, 5H), 5.63 (s, 1H), 4.43 – 4.33 (m, 2H), 4.09 – 3.98 (m, 1H), 2.08 – 1.92 (m, 1H), 1.88 – 1.77 (m, 1H).

¹³C NMR (101 MHz, Chloroform-d): δ 200.55, 137.68, 129.25, 128.40, 126.13, 101.21, 80.40, 66.51, 25.94.

HRESIMS m/z: 193.08645 [M+H]⁺ (calcd. for C₁₁H₁₃O₃, 193.08591), 407.14211 [2M+Na]⁺ (calcd. for C₂₂H₂₄NaO₆, 407.14649).

- Preparation of ethyl (2E,4E)-5-((2S,4S)-2-phenyl-1,3-dioxan-4-yl) penta-2,4-dienoate (**10a**):



Procedure: Lithium bis(trimethylsilyl) amide (1.0 M in THF, 66.33 mL, 66.33 mmol) was added slowly to a solution of Triethyl 4-phosphonocrotonate (14.71 mL, 66.33 mmol) in 30 mL THF at 0 °C. The resulting dark orange solution was stirred at 0 °C for an additional 30 min before the dropwise addition of aldehyde **11a** (5.1 g, 26.53 mmol) in 10 mL THF. The mixture was stirred

for 2h, and then left to warm at room temperature. The reaction was quenched with saturated aqueous ammonium chloride (75 mL) and extracted with EtOAc (3 x 80 mL). The combined organic layers were washed with water (2 x 100 mL) and with brine (100 mL), dried with anhydrous Na₂SO₄, filtered, and concentrated in vacuum. Evaporation of the solvents afforded crude olefins **10a** as a yellow oil that was used directly for the next reaction. The product was used in the next step without purification. An aliquot was purified for analytical purposes.

Molecular Formula: C₁₇H₂₀O₄

Rf: for major isomer = 0.33 and for minor isomer = 0.44 (n-hexane/ethyl acetate 8:2).

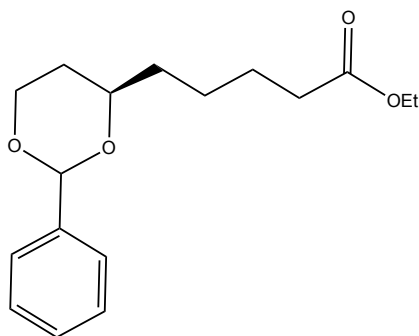
IR v_{max}, (neat, cm⁻¹): 2989, 2848, 1705, 1645, 1611, 700, 747.

¹H NMR (500 MHz, Chloroform-*d*): δ 7.58 – 7.35 (m, 5H), 7.30 (dd, J = 15.4, 11.1 Hz, 1H), 6.47 (dd, J = 15.4, 11.2 Hz, 1H), 6.17 (dd, J = 15.4, 5.0 Hz, 1H), 5.94 (d, J = 15.4 Hz, 1H), 5.60 (s, 1H), 4.56 – 4.48 (m, 1H), 4.32 (dd, J = 11.7, 4.7 Hz, 1H), 4.22 (q, J = 7.1 Hz, 2H), 4.02 (td, J = 12.0, 2.5 Hz, 1H), 1.95 (qd, J = 12.3, 4.6 Hz, 1H), 1.65 (d, J = 13.3 Hz, 1H), 1.31 (t, J = 7.2 Hz, 3H).

¹³C NMR (126 MHz, Chloroform-*d*): δ 166.89, 143.69, 140.85, 138.34, 128.97, 128.32, 127.89, 126.15, 122.09, 101.23, 76.34, 66.81, 60.41, 31.10, 14.32.

HRESIMS *m/z*: 289.14190 [M+H]⁺ (calcd. for C₁₇H₂₁O₄, 289.14343), 311.12655 [M+Na]⁺ (calcd. for C₁₇H₂₀NaO₄, 311.12537).

- Preparation of ethyl 5-((2*S*,4*R*)-2-phenyl-1,3-dioxan-4-yl) pentanoate (**9a**):



Procedure: To a stirred solution of crude olefins **10a** in ethyl acetate (250 mL) was added a catalytic amount of 10% Pd/C and stirred under H₂ atmosphere at room temperature for 24 h. The progress of the reaction was monitored by TLC. After completion, the reaction was stopped and filtered over celite bed, and the celite bed was washed with ethyl acetate. All the organic layers were combined and concentrated on a rotavaporator to give a crude residue. Purification of the crude residue was carried out by silica gel column chromatography using (n-hexane/ethyl acetate 80:20) to give **9a** (1.67 g) as a yellow oil.

Molecular Formula: C₁₇H₂₄O₄

Yield: 40% (based on **12a**)

Rf: 0.51 (n-hexane/ethyl acetate 8:2).

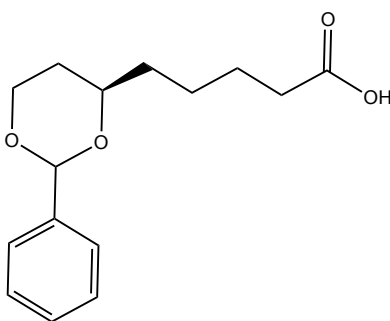
IR v_{max}, (neat, cm⁻¹): 2939, 2857, 1729, 749, 698.

¹H NMR (400 MHz, Chloroform-*d*): δ 7.57 – 7.27 (m, 5H), 5.50 (s, 1H), 4.24 (ddd, J = 11.4, 5.1, 1.3 Hz, 1H), 4.13 (q, J = 7.2 Hz, 2H), 3.93 (td, J = 12.0, 2.6 Hz, 1H), 3.87 – 3.75 (m, 1H), 2.33 (t, J = 7.4 Hz, 2H), 1.86 – 1.72 (m, 1H), 1.72 – 1.61 (m, 3H), 1.61 – 1.36 (m, 4H), 1.25 (t, J = 7.1 Hz, 3H).

¹³C NMR (126 MHz, Chloroform-*d*): δ 173.69, 138.87, 128.64, 128.19, 126.02, 101.12, 76.96, 67.07, 60.23, 35.66, 34.28, 31.33, 24.89, 24.57, 14.27.

HRESIMS m/z : 293.17473 $[M+H]^+$ (calcd. for $C_{17}H_{25}O_4$, 293.17473), 315.15620 $[M+Na]^+$ (calcd. for $C_{17}H_{24}NaO_4$, 315.15667).

- Preparation of 5-((2S,4R)-2-phenyl-1,3-dioxan-4-yl) pentanoic acid (**8a**):



Procedure: LiOH (0.67 g) dissolved in 7mL H_2O (4M) was added to a solution of **9a** (1.6 g) in THF (14 mL). The reaction mixture was stirred at rt for 24 h. The mixture was concentrated and the resulting aqueous solution was slowly acidified with 3M HCl under ice bath. The mixture was extracted with EtOAc (3 x 10 mL), dried over anhydrous Na_2SO_4 , and concentrated. Purification of the crude residue was carried out by silica gel column chromatography using (n-hexane/ethyl acetate 8:2) to give the acid **8a** as a white oil (1g).

Molecular Formula: $C_{15}H_{20}O_4$

Yield: 63%

Rf: 0.20 (n-hexane/ethyl acetate 8:2).

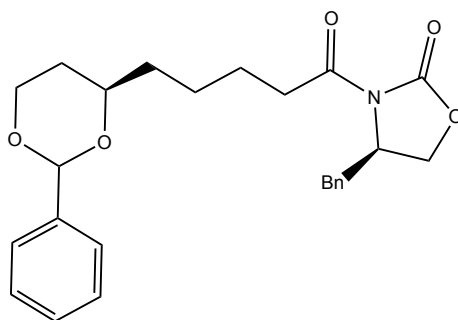
IR ν_{max} , (neat, cm^{-1}): 3300-2500, 2920, 1700, 1598, 825, 743.

1H NMR (400 MHz, Chloroform- d): δ 7.56 – 7.36 (m, 5H), 5.53 (s, 1H), 4.30 (ddd, $J = 11.4, 5.1, 1.3$ Hz, 1H), 3.98 (td, $J = 12.0, 2.6$ Hz, 1H), 3.91 – 3.81 (m, 1H), 2.40 (t, $J = 7.4$ Hz, 2H), 1.91 – 1.78 (m, 1H), 1.78 – 1.70 (m, 2H), 1.70 – 1.61 (m, 2H), 1.58 – 1.51 (m, 2H), 1.51 – 1.42 (m, 1H).

^{13}C NMR (101 MHz, Chloroform-*d*): δ 179.74, 138.78, 128.69, 128.23, 126.05, 101.17, 76.96, 67.08, 35.61, 33.99, 31.31, 24.60, 24.51.

HRESIMS *m/z*: *z* 265.14125 $[\text{M}+\text{H}]^+$ (calcd. for $\text{C}_{15}\text{H}_{21}\text{O}_4$, 265.14343), 287.12418 $[\text{M}+\text{Na}]^+$ (calcd. for $\text{C}_{15}\text{H}_{20}\text{NaO}_4$, 287.12537), 263.12612 $[\text{M}-\text{H}]^-$ (calcd. for $\text{C}_{15}\text{H}_{19}\text{O}_4$, 263.12888).

- Preparation of (R)-4-benzyl-3-(5-((2S,4R)-2-phenyl-1,3-dioxan-4-yl) pentanoyl) oxazolidin-2-one (**7a**):



Procedure: To a stirred solution of **8a** (1.0 g, 3.78 mmol) in THF (40 mL) was added TEA (1.2 mL, 8.60 mmol) followed pivaloyl chloride (0.64 mL, 5.16 mmol) at $-20\text{ }^\circ\text{C}$. After being stirred for 2 h, LiCl (186 mg, 4.47 mmol) and (4R)-benzyloxazolidin-2-one (609 mg, 3.44 mmol) were added. The mixture was allowed to warm to $0\text{ }^\circ\text{C}$ and then to room temperature slowly and was stirred for an additional 4 h. The mixture was concentrated, and residue was partitioned between 5% aqueous KHSO_4 (20 mL) and ethyl acetate (50 mL). The organic layer was washed with 1 M sodium bicarbonate ($2 \times 10\text{ mL}$) and brine (10 mL) and then dried over anhydrous magnesium sulfate and concentrated. Purification of the crude residue was carried out by silica gel column chromatography using (n-hexane/ethyl acetate 8:2) to give to give **7a** (1.26 g) as a colorless oil.

Molecular Formula: $\text{C}_{25}\text{H}_{29}\text{NO}_5$

Yield: 80%

Rf: 0.33 (n-hexane/ethyl acetate 8:2).

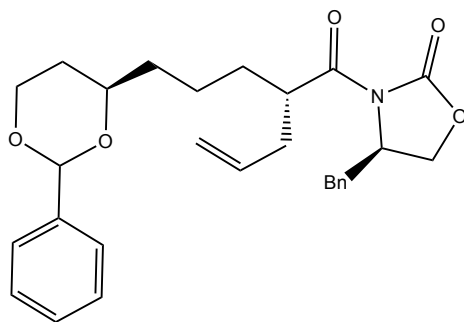
IR v_{max}, (neat, cm⁻¹): 2935, 2864, 1785, 1696, 739, 701.

¹H NMR (500 MHz, Chloroform-*d*): δ 7.57 – 7.18 (m, 10H), 5.54 (s, 1H), 4.73 – 4.64 (m, 1H), 4.30 (ddd, *J* = 11.4, 5.1, 1.4 Hz, 1H), 4.24 – 4.15 (m, 2H), 4.08 – 3.94 (m, 1H), 3.93 – 3.83 (m, 1H), 3.32 (dd, *J* = 13.4, 3.4 Hz, 1H), 3.08 – 2.90 (m, 2H), 2.78 (dd, *J* = 13.4, 9.6 Hz, 1H), 1.91 – 1.75 (m, 3H), 1.75 – 1.71 (m, 1H), 1.70 – 1.63 (m, 1H), 1.63 – 1.56 (m, 2H), 1.56 – 1.47 (m, 1H).

¹³C NMR (126 MHz, Chloroform-*d*): δ 173.20, 153.47, 138.85, 135.30, 129.42, 128.97, 128.64, 128.21, 127.36, 126.03, 101.15, 76.99, 67.10, 66.19, 55.17, 37.94, 35.74, 35.50, 31.36, 24.57, 24.16.

HRESIMS *m/z*: 424.21273 [M+H]⁺ (calcd. for C₂₅H₃₀NO₅, 424.21184), 446.19462 [M+Na]⁺ (calcd. for C₂₅H₂₉NNaO₅, 446.19378), 462.19044 [M+K]⁺ (calcd. for C₂₅H₂₉KNO₅, 462.16772).

- Preparation of (R)-4-benzyl-3-((S)-2-(3-((2S,4R)-2-phenyl-1,3-dioxan-4-yl) propyl) pent-4-enoyl) oxazolidin-2-one (**6a**):



Procedure: 15 mL THF was added to **7a** (1.2 g, 2.83 mmol) under argon at 0 °C. Lithium bis(trimethylsilyl) amide (1.0 M in THF, 7.08 mL, 7.08 mmol) was then added dropwise and the mixture was left for 1 h. Then, freshly distilled allyl bromide (1.23 mL, 14.17 mmol) was added and reaction was monitored via TLC. Once the starting material is totally converted to product, 15 mL NH₄Cl was added and mixture was allowed to warm up to rt. Then mixture was extracted by EtOAc (2x 25 mL), organic layer was washed with 25 mL brine, dried over anhydrous Na₂SO₄

and concentrated in vacuum. Purification of the crude residue was carried out by silica gel column chromatography using (n-hexane/ethyl acetate 9.5:0.5) to give **6a** (830 mg) as a colorless oil.

Molecular Formula: C₂₈H₃₃NO₅

Yield: 63%

Rf: 0.40 (n-hexane/ethyl acetate 8:2).

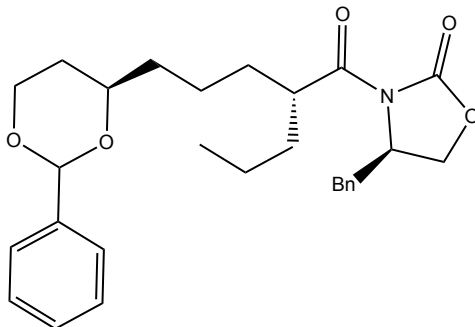
IR v_{max}, (neat, cm⁻¹): 2941, 2854, 1787, 1699, 723, 700.

¹H NMR (500 MHz, Chloroform-d): δ 7.57 – 7.22 (m, 10H), 5.93 – 5.80 (m, 1H), 5.51 (s, 1H), 5.16 – 5.05 (m, 2H), 4.74 – 4.62 (m, 1H), 4.28 (ddd, J = 11.4, 5.0, 1.4 Hz, 1H), 4.16 – 4.06 (m, 2H), 4.04 – 3.91 (m, 2H), 3.91 – 3.81 (m, 1H), 3.31 (dd, J = 13.3, 3.4 Hz, 1H), 2.69 (dd, J = 13.4, 9.9 Hz, 1H), 2.57 – 2.46 (m, 1H), 2.44 – 2.31 (m, 1H), 1.88 – 1.76 (m, 2H), 1.76 – 1.65 (m, 1H), 1.65 – 1.55 (m, 2H), 1.55 – 1.44 (m, 2H), 1.51 – 1.28 (m, 1H).

¹³C NMR (126 MHz, Chloroform-d): δ 176.03, 153.29, 138.98, 135.53, 135.31, 129.53, 129.06, 128.77, 128.31, 127.43, 126.17, 117.37, 101.27, 77.02, 67.21, 66.03, 55.63, 42.39, 38.21, 36.86, 35.96, 31.41, 31.34, 22.69.

HRESIMS m/z: 464.24360 [M+H]⁺ (calcd. for C₂₈H₃₄NO₅, 464.24314), 486.22713 [M+Na]⁺ (calcd. for C₂₈H₃₃NNaO₅, 486.22508).

- Preparation of (R)-4-benzyl-3-((R)-5-((2S,4R)-2-phenyl-1,3-dioxan-4-yl)-2-propylpentanoyl)oxazolidin-2-one (**5a**):



Procedure: To a solution of **6a** (820 mg) in EtOAc (40 mL) was added a catalytic amount of 10% Pd/C and stirred under H₂ atmosphere at room temperature for 24 h. The mixture was filtered through a pad of celite and the pad was washed with EtOAc (50 mLx2). The filtrate was concentrated to provide a clean crude of **5a** (821 mg) as a colorless oil.

Molecular Formula: C₂₈H₃₅NO₅

Yield: quantitative

Rf: 0.42 (n-hexane/ethyl acetate 8:2).

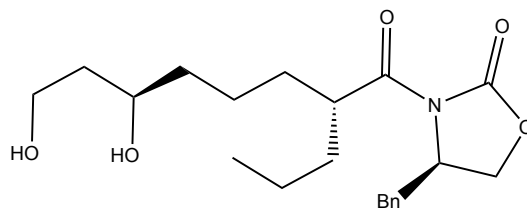
IR v_{max}, (neat, cm⁻¹): 2937, 2862, 1786, 1698, 721, 700.

¹H NMR (500 MHz, Chloroform-d): δ 7.57 – 7.22 (m, 10H), 5.51 (s, 1H), 4.69 (ddt, J = 10.4, 6.7, 3.1 Hz, 1H), 4.28 (ddd, J = 11.4, 5.1, 1.4 Hz, 1H), 4.16 – 4.06 (m, 2H), 3.97 (td, J = 12.0, 2.6 Hz, 1H), 3.90 – 3.82 (m, 2H), 3.33 (dd, J = 13.3, 3.3 Hz, 1H), 2.73 (dd, J = 13.3, 9.9 Hz, 1H), 1.90 – 1.76 (m, 2H), 1.82 – 1.65 (m, 3H), 1.63 – 1.51 (m, 4H), 1.51 – 1.41 (m, 1H), 1.41 – 1.26 (m, 2H), 0.96 (t, J = 7.3 Hz, 3H).

¹³C NMR (126 MHz, Chloroform-d): δ 176.84, 153.19, 138.88, 135.41, 129.42, 128.95, 128.66, 128.19, 127.33, 126.06, 101.16, 76.87, 67.11, 65.89, 55.49, 42.56, 38.07, 35.90, 34.66, 31.79, 31.24, 22.67, 20.37, 14.25.

HRESIMS m/z: 466.25876 [M+H]⁺ (calcd. for C₂₈H₃₆NO₅, 466.25879), 488.24521 [M+Na]⁺ (calcd. for C₂₈H₃₅NNaO₅, 488.24073), 483.28510 [M+NH₄]⁺ (calcd. for C₂₈H₃₉N₂O₅, 483.28534).

- Preparation of (R)-4-benzyl-3-((2R,6R)-6,8-dihydroxy-2-propyloctanoyl) oxazolidin-2-one (4a):



Procedure: To a solution of **5a** (810 mg) in EtOAc (40 mL) was added a catalytic amount of 10% Pd/C and stirred under H₂ atmosphere at room temperature for 24 h. The mixture was filtered through a pad of celite and the pad was washed with EtOAc (50 mLx2). The filtrate was concentrated to provide a clean crude of **4a** (607 mg) as a colorless oil.

Molecular Formula: C₂₁H₃₁NO₅

Yield: 92% (based on **6a**)

Rf: 0.22 (n-hexane/ethyl acetate 2:8).

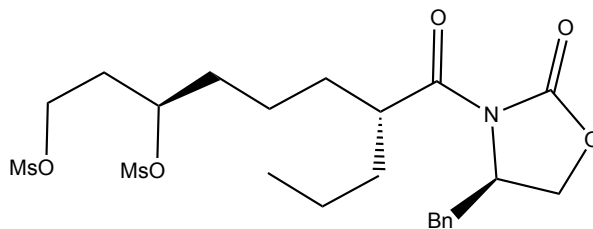
IR v_{max}, (neat, cm⁻¹): 3600-3100, 2924, 2868, 1791, 1696, 702.

¹H NMR (400 MHz, Chloroform-d): δ 7.35 – 7.22 (m, 5H), 4.77 – 4.66 (m, 1H), 4.25 – 4.11 (m, 2H), 3.89 – 3.75 (m, 4H), 3.32 (dd, J = 13.3, 3.4 Hz, 1H), 2.81 (sbr, 2H), 2.72 (dd, J = 13.3, 9.8 Hz, 1H), 1.80 – 1.55 (m, 4H), 1.62 – 1.38 (m, 4H), 1.45 – 1.33 (m, 3H), 1.36 – 1.24 (m, 1H), 0.94 (t, J = 7.3 Hz, 3H).

¹³C NMR (101 MHz, Chloroform-d): δ 176.95, 153.32, 135.34, 129.40, 128.94, 127.32, 71.60, 65.99, 61.49, 55.46, 42.57, 38.29, 38.04, 37.59, 34.70, 31.80, 23.27, 20.36, 14.21.

HRESIMS m/z: 378.22903 [M+H]⁺ (calcd. for C₂₁H₃₂NO₅, 378.22749), 400.21144 [M+Na]⁺ (calcd. for C₂₁H₃₁NNaO₅, 400.20943), 777.43251 [2M+Na]⁺ (calcd. for C₄₂H₆₂N₂NaO₁₀, 777.42965), 412.18206 [M+Cl]⁻ (calcd. for C₂₁ClH₃₁NO₅, 412.18962).

- Preparation of (3R,7R)-7-((R)-4-benzyl-2-oxooxazolidine-3-carbonyl) decane-1,3-diyl dimethanesulfonate (**3a**):



Procedure: To a stirred solution of **4a** (590 mg, 1.56 mmol) in anhydrous dichloromethane (30 mL) were added Et₃N (1.09 mL, 7.81 mmol) and MsCl (0.278.22 mL, 3.59 mmol) at 0 °C. The progress of the reaction was monitored by TLC. After completion, the reaction mixture was poured into aqueous NaHCO₃ (2%, 30 mL) and extracted with DCM (2x30 mL). The combined organic extracts were washed with brine, dried over anhydrous Na₂SO₄, filtered, and concentrated under reduced pressure to give a clean crude **3a** in an excellent yield (825 mg) as a yellow oil. The crude compound was utilized directly in the next reaction.

Molecular Formula: C₂₃H₃₅NO₉S₂

Rf: 0.66 (n-hexane/ethyl acetate 2:8).

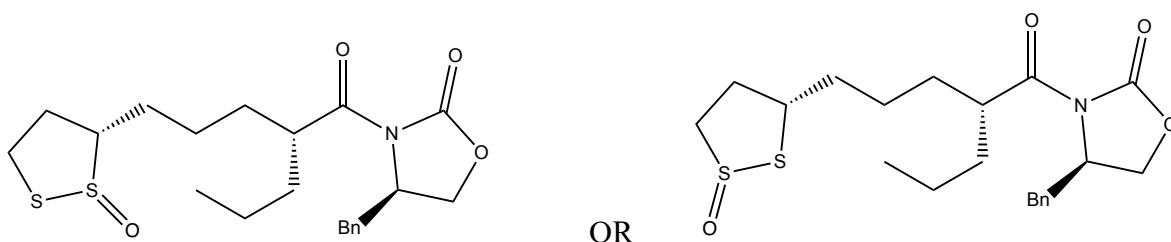
IR v_{max}, (neat, cm⁻¹): 2976, 2872, 1789, 1699.

¹H NMR (400 MHz, Chloroform-d): δ 7.36 – 7.21 (m, 5H), 4.91 – 4.82 (m, 1H), 4.75 – 4.68 (m, 1H), 4.36 – 4.30 (m, 2H), 4.28 – 4.08 (m, 2H), 3.88 – 3.81 (m, 1H), 3.31 (dd, J = 13.1, 3.2 Hz, 1H), 3.05 (d, J = 1.1 Hz, 6H), 2.73 (dd, J = 13.3, 9.8 Hz, 1H), 2.17 – 2.04 (m, 2H), 1.81 – 1.24 (m, 10H), 0.94 (t, J = 7.3 Hz, 3H).

¹³C NMR (101 MHz, Chloroform-d): δ 176.44, 153.33, 135.39, 129.40, 128.93, 127.31, 78.61, 66.04, 65.65, 55.42, 42.19, 38.63, 38.05, 37.40, 34.67, 34.63, 34.00, 31.30, 22.32, 20.36, 14.18.

HRESIMS m/z : 534.18709 $[M+H]^+$ (calcd. for $C_{23}H_{36}NO_9S_2$, 534.18259), 556.16643 $[M+Na]^+$ (calcd. for $C_{23}H_{35}NNaO_9S_2$, 556.16453), 572.13763 $[M+K]^+$ (calcd. for $C_{23}H_{35}KNO_9S_2$, 572.13847), 551.20917 $[M+NH_4]^+$ (calcd. for $C_{23}H_{39}N_2O_9S_2$, 551.20914).

- Preparation of (4R)-4-benzyl-3-((2R)-5-((3S)-2-oxido-1,2-dithiolan-3-yl)-2-propylpentanoyl)oxazolidin-2-one OR (4R)-4-benzyl-3-((2R)-5-((3S)-1-oxido-1,2-dithiolan-3-yl)-2-propylpentanoyl)oxazolidin-2-one (**15**):



Procedure: A mixture of dimesylate (265.34 μmol), finely powdered sodium sulfide (23.61 mg, 302.49 μmol), and sulfur (9.7 mg, 302.49 μmol) in anhydrous DMF (1.5 mL) were heated at 85–90 $^{\circ}\text{C}$ for 24 h. The reaction mixture was diluted with cold water, extracted with EtOAc (2x10 mL) and the combined organic fractions were washed with brine, dried over anhydrous Na_2SO_4 , filtered and concentrated under reduced pressure. Purification of the crude residue was carried out by silica gel column chromatography using (n-hexane/dichloromethane 4:6) to give **15** (13 mg) as a yellowish resin.

Molecular Formula: $C_{21}H_{29}NO_4S_2$

Yield: 12%

Rf: 18 (n-hexane/dichloromethane 4:6).

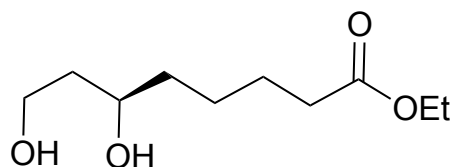
^1H NMR (400 MHz, Chloroform-d): δ 7.40 – 7.21 (m, 5H), 4.78 – 4.67 (m, 1H), 4.27 – 4.13 (m, 2H), 3.91 – 3.79 (m, 1H), 3.58 (dq, $J = 8.4, 6.4$ Hz, 1H), 3.34 (dd, $J = 13.3, 3.4$ Hz, 1H), 3.25 – 3.07 (m, 2H), 2.73 (dd, $J = 13.2, 9.9$ Hz, 1H), 2.46 (dtd, $J = 12.2, 6.6, 5.6$ Hz, 1H), 1.94 (dq, $J =$

12.8, 6.9 Hz, 1H), 1.89 – 1.61 (m, 2H), 1.69 – 1.48 (m, 1H), 1.55 (ddd, $J = 8.8, 5.9, 3.9$ Hz, 1H), 1.48 (d, $J = 29.9$ Hz, 3H), 1.53 – 1.39 (m, 2H), 1.39 – 1.25 (m, 1H), 0.95 (t, $J = 7.3$ Hz, 3H).

^{13}C NMR (101 MHz, Chloroform-*d*): δ 176.65, 153.19, 135.40, 129.41, 128.95, 127.33, 77.25, 65.98, 56.45, 55.52, 42.26, 40.33, 38.50, 38.09, 34.90, 31.58, 27.07, 20.34, 14.22.

HRESIMS m/z : 424.16254 $[\text{M}+\text{H}]^+$ (calcd. for $\text{C}_{21}\text{H}_{30}\text{NO}_4\text{S}_2$, 424.16107), 446.14513 $[\text{M}+\text{Na}]^+$ (calcd. for $\text{C}_{21}\text{H}_{29}\text{NNaO}_4\text{S}_2$, 446.14301).

- Preparation of ethyl (R)-6,8-dihydroxyoctanoate (**16a**):



Procedure: To a stirred solution of **9a** (130 mg, 444.63 μmol) in ethyl acetate (5 mL) was added a catalytic amount of 10% Pd (30 mg) and stirred under an H_2 atmosphere at room temperature for 24 h. The progress of the reaction was monitored by TLC. After completion, the reaction was stopped and filtered over celite bed, and the celite bed was washed with ethyl acetate. All the organic layers were combined and concentrated on a rotavaporator to give a crude residue. Purification of the crude residue was carried out by silica gel column chromatography using (n-hexane/ethyl acetate 1:1) to give **16a** (90 mg) as a colorless oil.

Molecular Formula: $\text{C}_{10}\text{H}_{20}\text{O}_4$

Yield: quantitative

Rf: 0.30 (n-hexane/ethyl acetate 2:8).

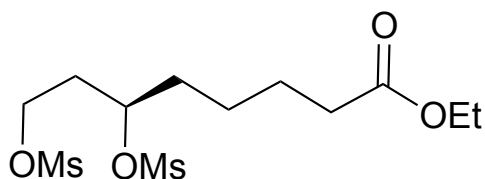
IR ν_{max} , (neat, cm^{-1}): 3397, 2944, 2887, 1702.

¹H NMR (400 MHz, Chloroform-*d*): δ 4.07 (q, $J = 7.1$ Hz, 2H), 3.85 – 3.76 (m, 2H), 3.77 – 3.70 (m, 1H), 3.47 (s, 2H), 2.26 (t, $J = 7.4$ Hz, 2H), 1.70 – 1.53 (m, 4H), 1.52 – 1.38 (m, 3H), 1.38 – 1.29 (m, 1H), 1.20 (t, $J = 7.1$ Hz, 3H).

¹³C NMR (101 MHz, Chloroform-*d*): δ 174.05, 71.37, 61.36, 60.40, 38.36, 37.29, 34.28, 25.07, 24.83, 14.26.

HRESIMS m/z : 205.143253 [M+H]⁺ (calcd. for C₁₀H₂₁O₄, 205.14343), 227.12745 [M+Na]⁺ (calcd. for C₁₀H₂₀NaO₄, 227.12537).

- Preparation of ethyl (R)-6,8-dimesyloxy octanoate (**17a**):



Procedure: To a solution of the diol **16a** (80 mg, 391.65 μ mol) in anhydrous dichloromethane (3 mL) were added triethylamine (0.273 mL, 1.96 mmol) and methanesulfonyl chloride (70 μ L, 900.79 μ mol) at 0 °C and stirred for 1 h at the same temperature. The reaction mixture was poured into aqueous sodium hydrogen carbonate and extracted with dichloromethane (2x5 mL). The combined organic extracts were washed with brine, dried over anhydrous Na₂SO₄, filtered and concentrated under reduced pressure. The crude oily compound was purified by silica gel column chromatography using (n-hexane/ethyl acetate 1:1) as an eluent to afford 6, 8 dimesylate **17a** (140 mg) as a colorless oil.

Molecular Formula: C₁₂H₂₄O₈S₂

Yield: 98%

Rf: 0.62 (n-hexane/ethyl acetate 2:8).

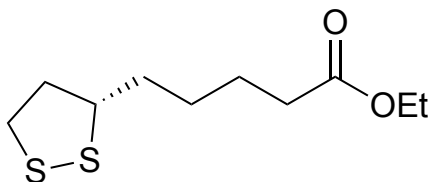
IR v_{max}, (neat, cm⁻¹): 3025, 2957, 1715, 1181.

¹H NMR (400 MHz, Chloroform-d): δ 4.93 – 4.84 (m, 1H), 4.42 – 4.29 (m, 2H), 4.13 (q, J = 7.1 Hz, 2H), 3.06 (d, J = 1.4 Hz, 6H), 2.33 (t, J = 7.3 Hz, 2H), 2.20 – 2.00 (m, 2H), 1.88 – 1.58 (m, 4H), 1.52 – 1.38 (m, 2H), 1.26 (t, J = 7.1 Hz, 3H).

¹³C NMR (101 MHz, Chloroform-d): δ 173.31, 78.56, 65.62, 60.36, 38.65, 37.41, 34.60, 33.98, 33.90, 24.48, 24.21, 14.24.

HRESIMS m/z: 361.09952 [M+H]⁺ (calcd. for C₁₂H₂₅O₈S₂, 361.09853), 383.08783 [M+Na]⁺ (calcd. for C₁₂H₂₄NaO₈S₂, 383.08047), 378.12553 [M+NH₄]⁺ (calcd. for C₁₂H₂₈NO₈S₂, 378.12508), 399.05523 [M+K]⁺ (calcd. for C₁₂H₂₄KO₈S₂, 399.05441), 395.06927 [M+Cl]⁻ (calcd. for C₁₂ClH₂₄O₈S₂, 395.06066).

- Preparation of ethyl S-(-)-lipoate or [ethyl (5S)-5-(1,2-dithiolan-3yl) pentanoate] (**18a**):



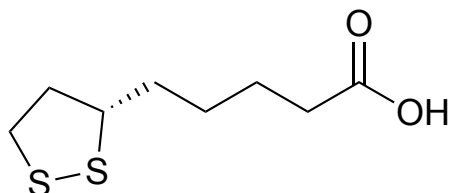
Procedure: A mixture of dimesylate **17a** (120 mg, 332.93 μmol), finely powdered sodium sulfide (30 mg, 379.54 μmol) and sulfur (13 mg, 379.54 μmol) in anhydrous dimethylformamide (2 mL) were heated at 85-90 °C for 24 h. The reaction mixture was diluted with cold water, extracted with EtOAc (2x5 mL) and the combined organic fractions were washed with brine, dried over anhydrous Na₂SO₄, filtered and concentrated under reduced pressure. The residue was purified by silica gel column chromatography using (n-hexane/ethyl acetate 1:1) as an eluent to afford **18a** (56 mg) as a light-yellow oil.

Molecular Formula: C₁₀H₁₈O₂S₂

Yield: 71%

Rf: Rf= 0.81 (n-hexane/ethyl acetate 6:4).

- Preparation of (S)-5-(1,2-dithiolan-3-yl)-pentanoic acid or **(S)-lipoic acid**:



Procedure: To a stirred solution of **18a** (45 mg, 192.00 μmol) in THF (1 mL) was added aqueous LiOH (3 M, 1 mL) and stirred at rt for 24 h. THF was evaporated in a rotavaporator and the aqueous layer was acidified carefully with 6 M HCl to pH 2. The product was extracted with dichloromethane (2x5 mL) and the combined organic phases were dried over anhydrous Na_2SO_4 , filtered, and concentrated on a rotavaporator to afford a crude residue. The resulting residue was purified by flash column chromatography (silica gel) using n-hexane/ethyl acetate 85:15 as an eluent, to afford **(S)-lipoic acid** (32 mg) as a yellow solid.

Molecular Formula: $\text{C}_8\text{H}_{14}\text{O}_2\text{S}_2$

Yield: 81%

Rf: 0.22 (n-hexane/ethyl acetate 8:2).

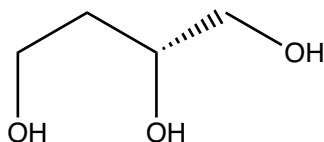
IR ν_{max} , (neat, cm^{-1}): 3024, 2919, 1697, 721.

^1H NMR (400 MHz, Chloroform-*d*): δ 3.66 – 3.54 (m, 1H), 3.27 – 3.09 (m, 2H), 2.56 – 2.46 (m, 1H), 2.40 (t, $J = 7.4$ Hz, 2H), 2.01 – 1.87 (m, 1H), 1.82 – 1.67 (m, 4H), 1.67 – 1.41 (m, 2H).

^{13}C NMR (101 MHz, Chloroform-*d*): δ 178.77, 56.29, 40.23, 38.52, 34.60, 33.65, 28.68, 24.41.

HRESIMS m/z : 229.03268 $[\text{M}+\text{Na}]^+$ (calcd. for $\text{C}_8\text{H}_{14}\text{NaO}_2\text{S}_2$, 229.03273), 245.02744 $[\text{M}+\text{K}]^+$ (calcd. for $\text{C}_8\text{H}_{14}\text{KO}_2\text{S}_2$, 245.00667), 205.03167 $[\text{M}-\text{H}]^-$ (calcd. for $\text{C}_8\text{H}_{13}\text{O}_2\text{S}_2$, 205.03624).

- Preparation of (R)-1,2,4-Butanetriol (**13b**):



Procedure: To a stirred solution of 2 M BMS-THF complex (61 mL, 121.19 mmol) and trimethylborate (12.5 mL, 111.87 mmol) at 0°C was added dropwise (R)-malic acid (5.0 g, 37.29 mmol) in THF (25 mL). After stirring the homogeneous solution for an additional 5 min at 0°C, the cooling bath was removed. A white precipitate appeared and re-dissolved within 20 min. After stirring overnight, methanol (30 mL) was carefully added dropwise over 1h and the resulting solution evaporated to dryness. A further three co-evaporations with methanol (25 mL) afforded 9.98 g of (R)-1,2,4-butanetriol containing residual boron by-products. Flash chromatography (DCM-MeOH; 9: 1) of the crude triol yielded pure (R)-1,2,4-butanetriol **13b** (4.0 g) as a colorless oil.

Molecular Formula: C₄H₁₀O₃

Yield: quantitative

Rf: 0.35 (dichloromethane/methanol 9:1).

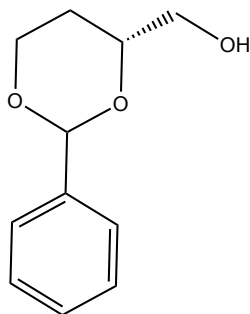
IR v_{max}, (neat, cm⁻¹): 3295, 2950, 2850.

¹H NMR (400 MHz, Deuterium Oxide): δ 3.80 – 3.67 (m, 1H), 3.70 – 3.55 (m, 2H), 3.55 – 3.46 (m, 1H), 3.39 (dd, J = 11.8, 6.8 Hz, 1H), 1.71 – 1.44 (m, 2H).

¹³C NMR (101 MHz, Deuterium Oxide): δ 68.88, 65.49, 58.30, 34.64.

HRESIMS *m/z*: 107.07080 [M+H]⁺ (calcd. for C₄H₁₁O₃, 107.07026), 129.05281 [M+Na]⁺ (calcd. for C₄H₁₀NaO₃, 129.05220).

- Preparation of (2R,4R)-4-(Hydroxymethyl)-2-phenyl-1,3-dioxane (**12b**):



Procedure: (R)-1,2,4-Butanetriol **13b** (3.91 g, 36.84 mmol) and benzaldehyde dimethylacetal (6.64 mL, 44.21 mmol) in dry dichloromethane (120 mL) were stirred at room temperature in the presence of camphorsulfonic acid (427.94 mg, 1.84 mmol). After the mixture had been stirred for 16 h, triethylamine (513.91 mL, 3.68 mmol) was added and the solvents were removed under reduced pressure. The product **12b** (5.62 g) was obtained after column chromatography on silica gel (n-hexane/ethyl acetate 2:1 to 1:1) as a colorless oil.

Molecular Formula: C₁₁H₁₄O₃

Yield: 79%

Rf: 0.41 (n-hexane/ethyl acetate 4:6).

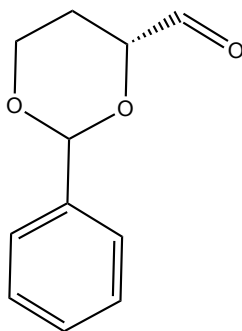
IR v_{max}, (neat, cm⁻¹): 3393, 3030, 2954, 2855, 1700, 750.

¹H NMR (400 MHz, Chloroform-*d*): δ 7.56 – 7.33 (m, 5H), 5.58 (s, 1H), 4.33 (dd, *J* = 11.3 Hz, 1H), 4.10 – 3.95 (m, 2H), 3.78 – 3.64 (m, 2H), 2.17 (s, 1H), 2.04 – 1.88 (m, 1H), 1.48 (d, *J* = 13.3 Hz, 1H).

¹³C NMR (101 MHz, Chloroform-*d*): δ 138.36, 129.00, 128.31, 126.13, 101.31, 77.55, 66.64, 65.73, 26.83.

HRESIMS *m/z*: 195.10105 [M+H]⁺ (calcd. for C₁₁H₁₅O₃, 195.10156), 217.08308 [M+Na]⁺ (calcd. for C₁₁H₁₄NaO₃, 217.08350), 411.17747 [2M+Na]⁺ (calcd. for C₂₂H₂₈NaO₆, 411.17779).

- Preparation of (2R,4R)-4-Formyl-2-phenyl-1,3-dioxane (**11b**):



Procedure: A solution of dry DMSO (4.63 mL, 5.10 g, 65.22 mmol) in dichloromethane (33 mL) was added dropwise at -78 °C under argon to oxalyl chloride (2.60 mL, 3.85 g, 30.36 mmol). After the mixture had been stirred for 12 min, a solution of alcohol **12b** (5.46 g, 28.11 mmol) in dichloromethane (33 mL) was added dropwise. The mixture was stirred at -78 °C for 30 minutes and was then treated with triethylamine (18.49 mL, 132.68 mmol). After a further 5 minutes the cooling bath was removed, water (70 mL) was added, and the mixture was allowed to warm up to room temperature. The phases were separated, the aqueous phase was extracted with dichloromethane (3x70 mL), and the combined organic extracts were washed with saturated ammonium chloride solution (180 mL) and dried over anhydrous Na₂SO₄. Evaporation of the solvents afforded crude aldehyde **11b** (5.17 g) as a colorless oil. The product was used in the next step without purification. An aliquot was purified and ¹H NMR was recorded.

Molecular Formula: C₁₁H₁₂O₃

Yield: 96%

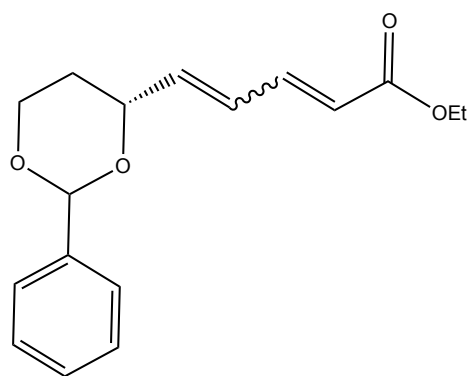
Rf: 0.58 (n-hexane/ethyl acetate 7:3).

IR v_{max}, (neat, cm⁻¹): 2900, 2875, 1710, 750.

¹H NMR (400 MHz, Chloroform-d): δ 9.76 (s, 1H), 7.56 – 7.25 (m, 5H), 5.63 (s, 1H), 4.38 (dt, $J = 11.7, 4.1$ Hz, 2H), 4.04 (td, $J = 11.9, 2.6$ Hz, 1H), 2.08 – 1.91 (m, 1H), 1.83 (dtd, $J = 13.5, 2.8, 1.5$ Hz, 1H).

HRESIMS m/z : 193.08628 [M+H]⁺ (calcd. for C₁₁H₁₃O₃, 193.08591), 215.06155 [M+Na]⁺ (calcd. for C₁₁H₁₂NaO₃, 215.06785), 407.14058 [2M+Na]⁺ (calcd. for C₂₂H₂₄NaO₆, 407.14649).

- Preparation of ethyl (2E,4E)-5-((2R,4R)-2-phenyl-1,3-dioxan-4-yl) penta-2,4-dienoate (**10b**):



Procedure: Lithium bis(trimethylsilyl) amide (1.0 M in THF, 26.80 mL, 26.79 mmol) was added slowly to a solution of Triethyl 4-phosphonocrotonate (5.94 mL, 26.79 mmol) in THF (12 mL) at 0 °C. The resulting dark orange solution was stirred at 0 °C for an additional 30 minutes before the dropwise addition of **11b** (5.15 g, 26.79 mmol). The mixture was stirred at 0 °C for 2 h and then left to warm at room temperature. The reaction was quenched with saturated aqueous ammonium chloride (60 mL) and extracted with EtoAc (3 x 80 mL). The combined organic layers were washed with water (2 x 70 mL) and with brine (70 mL), dried with anhydrous Na₂SO₄, filtered, and concentrated in vacuum. Evaporation of the solvents afforded crude olefins **10b** (7.27 g) as a yellow oil. The product was used in the next step without purification. An aliquot was purified for analytical purposes.

Molecular Formula: C₁₇H₂₀O₄

Rf: for major isomer= 0.33 and for major isomer= 0.44 (n-hexane/ethyl acetate 8:2).

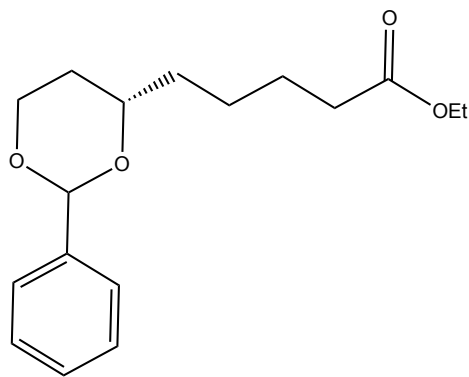
IR v_{max}, (neat, cm⁻¹): 2987, 2845, 1700, 1655, 1615, 698, 745.

¹H NMR (400 MHz, Chloroform-*d*): δ 7.59 – 7.33 (m, 5H), 7.30 (ddd, J = 15.4, 11.1, 0.8 Hz, 1H), 6.48 (dddd, J = 15.4, 11.1, 1.6, 0.8 Hz, 1H), 6.17 (ddt, J = 15.4, 5.2, 0.8 Hz, 1H), 5.94 (dd, J = 15.3, 0.8 Hz, 1H), 5.61 (s, 1H), 4.58 – 4.48 (m, 1H), 4.38 – 4.28 (m, 1H), 4.23 (q, J = 7.1 Hz, 2H), 4.12 – 3.96 (m, 1H), 2.09 – 1.88 (m, 1H), 1.72 – 1.62 (m, 1H), 1.32 (t, J = 7.1 Hz, 3H).

¹³C NMR (101 MHz, Chloroform-*d*): δ 166.85, 143.61, 140.76, 138.34, 128.93, 128.28, 127.93, 126.13, 122.13, 101.26, 76.37, 66.81, 60.37, 31.13, 14.28.

HRESIMS *m/z*: 289.14147 [M+H]⁺ (calcd. for C₁₇H₂₁O₄, 289.14343), 311.12506 [M+Na]⁺ (calcd. for C₁₇H₂₀NaO₄, 311.12537).

- Preparation of ethyl 5-((2R,4S)-2-phenyl-1,3-dioxan-4-yl) pentanoate (**9b**):



Procedure: To a stirred solution of **10b** (7.25 g, 25.14 mmol) in ethyl acetate (100 mL) was added a catalytic amount of 10% Pd/C and stirred under an H₂ atmosphere at room temperature for 24 h. The progress of the reaction was monitored by TLC. After completion, the reaction was stopped and filtered over celite bed and the celite bed was washed with ethyl acetate. All the organic layers were combined and concentrated on a rotavaporator to give a crude residue. Purification of the

crude residue was carried out by silica gel column chromatography using (n-hexane/ethyl acetate 80:20) to give **9b** (2 g) as a yellow oil.

Molecular Formula: C₁₇H₂₄O₄

Yield: 20% (based on **12b**)

Rf: 0.51 (n-hexane/ethyl acetate 8:2).

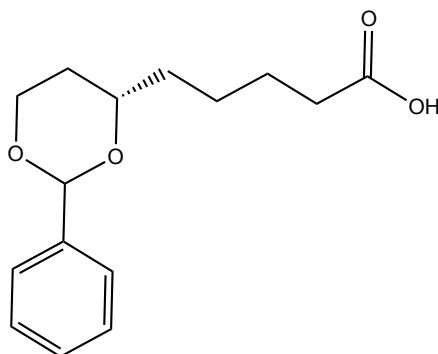
IR v_{max}, (neat, cm⁻¹): 2935, 2877, 1735, 746, 699.

¹H NMR (500 MHz, Chloroform-*d*): δ 7.48 – 7.12 (m, 5H), 5.37 (s, 1H), 4.13 (dd, *J* = 11.4, 5.0 Hz, 1H), 3.99 (q, *J* = 7.2 Hz, 2H), 3.83 (td, *J* = 12.9, 11.7, 3.8 Hz, 1H), 3.74 – 3.65 (m, 1H), 2.19 (t, *J* = 7.5 Hz, 2H), 1.73 – 1.61 (m, 1H), 1.59 – 1.47 (m, 3H), 1.44 – 1.26 (m, 4H), 1.12 (t, *J* = 7.1 Hz, 3H).

¹³C NMR (126 MHz, Chloroform-*d*): δ 173.62, 138.72, 128.55, 128.10, 125.91, 101.00, 76.85, 66.97, 60.15, 35.55, 34.17, 31.21, 24.78, 24.46, 14.18.

HRESIMS *m/z*: 293.17372 [M+H]⁺ (calcd. for C₁₇H₂₅O₄, 293.17473), 315.15613 [M+Na]⁺ (calcd. for C₁₇H₂₄NaO₄, 315.15667).

- Preparation of 5-((2R,4S)-2-phenyl-1,3-dioxan-4-yl) pentanoic acid (**8b**):



Procedure: LiOH (0.67 g) dissolved in 7mL H₂O (4M) was added to a solution of **9b** (2 g) in THF (7 mL). The reaction mixture was stirred at rt for 24 h. The mixture was concentrated and the

resulting aqueous solution was slowly acidified with 3M HCl under ice bath. The mixture was extracted with EtOAc (3 x 15 mL), dried over anhydrous Na₂SO₄, and concentrated. Purification of the crude residue was carried out by silica gel column chromatography using (n-hexane/ethyl acetate 8:2) to give the acid **8b** as a white oil (962 mg).

Molecular Formula: C₁₅H₂₀O₄

Yield: 53%

Rf: 0.20 (n-hexane/ethyl acetate 8:2).

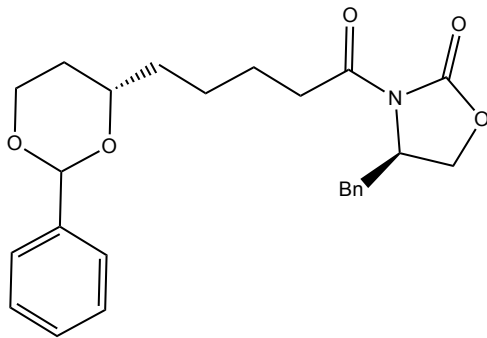
IR v_{max}, (neat, cm⁻¹): 3300-2500, 2921, 1705, 1608, 850, 739.

¹H NMR (400 MHz, Chloroform-*d*): δ 9.86 (s, 1H), 7.57 – 7.47 (m, 2H), 7.47 – 7.31 (m, 3H), 5.54 (s, 1H), 4.30 (ddd, J = 11.4, 5.0, 1.4 Hz, 1H), 3.98 (ddd, J = 12.4, 11.4, 2.6 Hz, 1H), 3.92 – 3.80 (m, 1H), 2.40 (t, J = 7.4 Hz, 2H), 1.94 – 1.82 (m, 1H), 1.84 – 1.76 (m, 1H), 1.79 – 1.65 (m, 2H), 1.65 – 1.53 (m, 3H), 1.53 – 1.41 (m, 1H).

¹³C NMR (101 MHz, Chloroform-*d*): δ 180.00, 138.81, 128.69, 128.22, 126.06, 101.17, 76.96, 67.07, 35.61, 34.03, 31.33, 24.60, 24.52.

HRESIMS *m/z*: 265.14212 [M+H]⁺ (calcd. for C₁₅H₂₁O₄, 265.14343), 287.12546 [M+Na]⁺ (calcd. for C₁₅H₂₀NaO₄, 287.12537), 263.12683 [M-H]⁻ (calcd. for C₁₅H₁₉O₄, 263.12888).

- Preparation of (R)-4-benzyl-3-(5-((2R,4S)-2-phenyl-1,3-dioxan-4yl) pentanoyl) oxazolidin-2-one (**7b**):



Procedure: To a stirred solution of **8b** (962 mg, 3.64 mmol) in THF (40 mL) was added TEA (1.15 mL, 8.27 mmol) followed by pivaloyl chloride (0.62 mL, 4.96 mmol) at -20 °C. After being stirred for 2 h, LiCl (182.33 mg, 4.30 mmol) and (4R)-benzyloxazolidin-2-one (586.30 mg, 3.31 mmol) were added. The mixture was allowed to warm to 0 °C and then to room temperature slowly and was stirred for an additional 4 h. The mixture was concentrated, and residue was partitioned between 5% aqueous KHSO₄ (20 mL) and ethyl acetate (50 mL). The organic layer was washed with 1 M sodium bicarbonate (2 × 10 mL) and brine (10 mL) and then dried over anhydrous magnesium sulfate and concentrated. Purification of the crude residue was carried out by silica gel column chromatography using (n-hexane/ethyl acetate 8:2) to give **7b** (1.4 g) as a colorless oil.

Molecular Formula: C₂₅H₂₉NO₅

Yield: quantitative

Rf: 0.33 (n-hexane/ethyl acetate 8:2).

IR v_{max}, (neat, cm⁻¹): 2927, 2873, 1778, 1694, 724, 695.

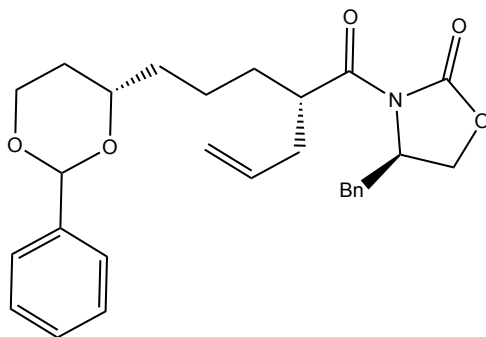
¹H NMR (400 MHz, Chloroform-d): δ 7.56 – 7.50 (m, 2H), 7.40 – 7.33 (m, 5H), 7.31 – 7.27 (m, 1H), 7.23 (d, J = 6.7 Hz, 2H), 5.53 (s, 1H), 4.69 (ddt, J = 10.2, 6.8, 3.3 Hz, 1H), 4.34 – 4.23 (m, 1H), 4.23 – 4.14 (m, 2H), 4.05 – 3.96 (m, 1H), 3.89 (d, J = 12.5 Hz, 1H), 3.32 (dd, J = 13.4, 3.3

Hz, 1H), 3.07 – 2.88 (m, 2H), 2.85 – 2.72 (m, 1H), 1.86 (td, $J = 12.5, 5.1$ Hz, 1H), 1.78 (d, $J = 7.5$ Hz, 2H), 1.64 (td, $J = 8.7, 7.8, 4.3$ Hz, 2H), 1.61 – 1.55 (m, 1H), 1.53 (d, $J = 5.9$ Hz, 2H).

^{13}C NMR (101 MHz, Chloroform-*d*): δ 173.20, 153.46, 138.86, 135.30, 129.42, 128.96, 128.63, 128.20, 127.35, 126.03, 101.15, 76.99, 67.10, 66.19, 55.16, 37.94, 35.74, 35.49, 31.36, 24.56, 24.16.

HRESIMS m/z : 424.21190 $[\text{M}+\text{H}]^+$ (calcd. for $\text{C}_{25}\text{H}_{30}\text{NO}_5$, 424.21184), 446.19493 $[\text{M}+\text{Na}]^+$ (calcd. for $\text{C}_{25}\text{H}_{29}\text{NNaO}_5$, 446.19378), 462.19174 $[\text{M}+\text{K}]^+$ (calcd. for $\text{C}_{25}\text{H}_{29}\text{KNO}_5$, 462.16772), 460.15360 $[\text{M}+\text{K}-2\text{H}]^-$ (calcd. for $\text{C}_{25}\text{H}_{27}\text{KNO}_5$, 460.15317).

- Preparation of (R)-4-benzyl-3-((S)-2-(3-((2R,4S)-2-phenyl-1,3-dioxan-4-yl)propyl) pent-4-enoyl) oxazolidin-2-one (**6b**):



Procedure: 20 mL THF was added to **7b** (1.35 g, 3.19 mmol) under argon at 0 °C. Lithium bis(trimethylsilyl) amide (1.0 M in THF, 7.97 mL, 7.97 mmol) was then added dropwise and the mixture was left for 1 h. Then, freshly distilled allyl bromide (1.38 mL, 15.94 mmol) was added and reaction was monitored via TLC. Once the starting material is totally converted to product, 20 mL NH_4Cl was added and mixture was allowed to warm up to rt. Then mixture was extracted by EtOAc (2x 30 mL), organic layer was washed with 30 mL brine, dried over anhydrous Na_2SO_4

and concentrated in vacuum. Purification of the crude residue was carried out by silica gel column chromatography using (n-hexane/ethyl acetate 9.5:0.5) to give **6b** (895 mg) as a colorless oil.

Molecular Formula: C₂₈H₃₃NO₅

Yield: 61%

Rf: 0.40 (n-hexane/ethyl acetate 8:2).

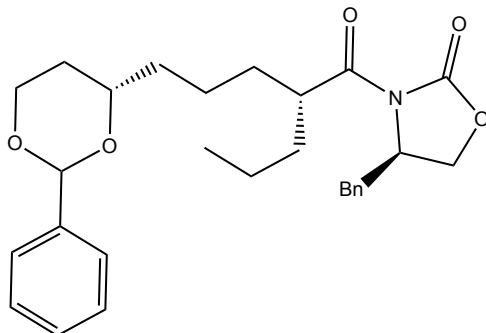
IR v_{max}, (neat, cm⁻¹): 2920, 2857, 1774, 1694, 749, 698.

¹H NMR (400 MHz, Chloroform-*d*): δ 7.52 – 7.22 (m, 10H), 5.93 – 5.78 (m, 1H), 5.52 (s, 1H), 5.17 – 5.04 (m, 2H), 4.72 – 4.60 (m, 1H), 4.28 (ddd, J = 11.3, 5.0, 1.3 Hz, 1H), 4.16 – 4.05 (m, 2H), 4.03 – 3.90 (m, 2H), 3.90 – 3.78 (m, 1H), 3.31 (dd, J = 13.3, 3.3 Hz, 1H), 2.68 (dd, J = 13.3, 10.0 Hz, 1H), 2.57 – 2.44 (m, 1H), 2.42 – 2.30 (m, 1H), 1.90 – 1.75 (m, 2H), 1.75 – 1.55 (m, 3H), 1.55 – 1.38 (m, 3H).

¹³C NMR (101 MHz, Chloroform-*d*): δ 175.91, 153.17, 138.89, 135.45, 135.20, 129.41, 128.94, 128.62, 128.17, 127.32, 126.02, 117.25, 101.09, 76.94, 67.07, 65.93, 55.55, 42.24, 38.10, 36.88, 35.92, 31.43, 31.29, 22.77.

HRESIMS *m/z*: 464.24335 [M+H]⁺ (calcd. for C₂₈H₃₄NO₅, 464.24314), 486.22955 [M+Na]⁺ (calcd. for C₂₈H₃₃NNaO₅, 486.22508).

- Preparation of (R)-4-benzyl-3-((R)-5-((2R,4S)-2-phenyl-1,3-dioxan-4-yl)-2-propyl pentanoyl) oxazolidin-2-one (**5b**)



Procedure: To a solution of **6b** (880 mg) in EtOAc (40 mL) was added a catalytic amount of 10% Pd/C and stirred under H₂ atmosphere at room temperature for 24 h. The mixture was filtered through a pad of celite and the pad was washed with EtOAc (50 mLx2). The filtrate was concentrated to provide a clean crude of **5b** (878 mg) as a colorless oil.

Molecular Formula: C₂₈H₃₅NO₅

Yield: quantitative

Rf: 0.42 (n-hexane/ethyl acetate 8:2).

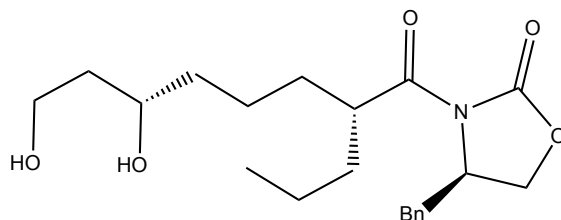
IR v_{max}, (neat, cm⁻¹): 2927, 2865, 1778, 1698, 721, 700.

¹H NMR (400 MHz, Chloroform-d): δ 7.56 – 7.21 (m, 10H), 5.51 (s, 1H), 4.69 (ddt, J = 10.3, 7.5, 3.2 Hz, 1H), 4.28 (ddd, J = 11.4, 5.0, 1.3 Hz, 1H), 4.16 – 4.07 (m, 2H), 3.97 (td, J = 12.3, 11.4, 2.6 Hz, 1H), 3.91 – 3.79 (m, 2H), 3.33 (dd, J = 13.3, 3.3 Hz, 1H), 2.73 (dd, 1H), 1.88 – 1.75 (m, 2H), 1.75 – 1.63 (m, 1H), 1.66 – 1.54 (m, 2H), 1.62 – 1.45 (m, 3H), 1.52 – 1.44 (m, 1H), 1.49 – 1.28 (m, 3H), 0.96 (t, J = 7.3 Hz, 3H).

¹³C NMR (101 MHz, Chloroform-d): δ 176.84, 153.19, 138.88, 135.41, 129.41, 128.94, 128.65, 128.18, 127.32, 126.06, 101.16, 76.87, 67.10, 65.89, 55.49, 42.55, 38.07, 35.89, 34.65, 31.79, 31.24, 22.67, 20.36, 14.24.

HRESIMS m/z: 466.25995 [M+H]⁺ (calcd. for C₂₈H₃₆NO₅, 466.25879), 488.24592 [M+Na]⁺ (calcd. for C₂₈H₃₅NNaO₅, 488.24073), 483.28578 [M+NH₄]⁺ (calcd. for C₂₈H₃₉N₂O₅, 483.28534).

- Preparation of (R)-4-benzyl-3-((2R,6S)-6,8-dihydroxy-2-propyloctanoyl) oxazolidin-2-one
(4b):



Procedure: To a solution of **5b** (850 mg) in EtOAc (40 mL) was added a catalytic amount of 10% Pd/C and stirred under H₂ atmosphere at room temperature for 24 h. The mixture was filtered through a pad of celite and the pad was washed with EtOAc (50 mLx2). The filtrate was concentrated to provide a clean crude of **4b** (646 mg) as a colorless oil.

Molecular Formula: C₂₁H₃₁NO₅

Yield: (93% based on **6b**)

Rf: 0.22 (n-hexane/ethyl acetate 2:8).

IR v_{max}, (neat, cm⁻¹): 3600-3100, 2939, 2873, 1776, 1700, 701.

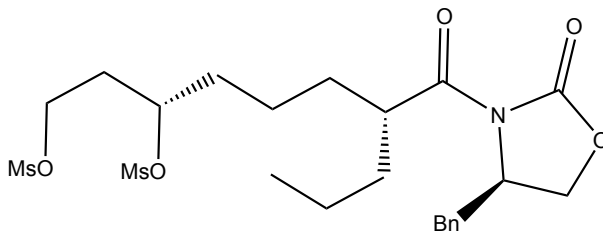
¹H NMR (400 MHz, Chloroform-d): δ 7.39 – 7.16 (m, 5H), 4.77 – 4.61 (m, 1H), 4.26 – 4.09 (m, 2H), 3.93 – 3.71 (m, 4H), 3.31 (dd, J = 13.4, 3.1 Hz, 1H), 3.08 (d, J = 12.7 Hz, 2H), 2.72 (dd, J = 13.3, 9.8 Hz, 1H), 1.79 – 1.59 (m, 3H), 1.58 – 1.47 (m, 3H), 1.47 – 1.45 (m, 3H), 1.45 – 1.28 (m, 3H), 0.93 (t, J = 7.3 Hz, 3H).

¹³C NMR (101 MHz, Chloroform-d): δ 176.93, 153.31, 135.35, 129.40, 128.93, 127.32, 71.59, 65.99, 61.48, 55.46, 42.57, 38.29, 38.04, 37.59, 34.69, 31.80, 23.27, 20.36, 14.21.

HRESIMS m/z: 378.22993 [M+H]⁺ (calcd. for C₂₁H₃₂NO₅, 378.22749), 400.21340 [M+Na]⁺ (calcd. for C₂₁H₃₁NNaO₅, 400.20943), 416.18840 [M+K]⁺ (calcd. for C₂₁H₃₁KNO₅, 416.18337),

777.43137 [2M+Na]⁺ (calcd. for C₄₂H₆₂N₂NaO₁₀, 777.42965), 412.18222 [M+Cl]⁻ (calcd. for C₂₁ClH₃₁NO₅, 412.18962).

- Preparation of (3*S*,7*R*)-7-((*R*)-4-benzyl-2-oxooxazolidine-3-carbonyl) decane-1,3-diyl dimethanesulfonate (**3b**):



Procedure: To a stirred solution of **4b** (620 mg, 1.64 mmol) in anhydrous dichloromethane (30 mL) were added Et₃N (1.14 mL, 8.21 mmol) and MsCl (0.29237 mL, 3.78 mmol) at 0 °C. The progress of the reaction was monitored by TLC. After completion, the reaction mixture was poured into aqueous NaHCO₃ (2%, 30 mL) and extracted with DCM (2x30 mL). The combined organic extracts were washed with brine, dried over anhydrous Na₂SO₄, filtered, and concentrated under reduced pressure to give a clean crude **3b** in an excellent yield (864 mg) as a yellow oil. The crude was utilized directly in the next reaction.

Molecular Formula: C₂₃H₃₅NO₉S₂

Rf: 0.66 (n-hexane/ethyl acetate 2:8).

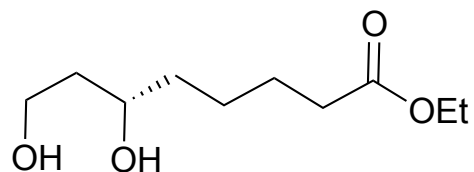
IR v_{max}, (neat, cm⁻¹): 2943, 2852, 1784, 1697.

¹H NMR (400 MHz, Chloroform-d): δ 7.37 – 7.22 (m, 5H), 4.91 – 4.83 (m, 1H), 4.77 – 4.66 (m, 1H), 4.38 – 4.28 (m, 2H), 4.28 – 4.09 (m, 2H), 3.88 – 3.79 (m, 1H), 3.31 (dd, J = 13.3, 3.3 Hz, 1H), 3.05 (d, J = 1.1 Hz, 6H), 2.73 (dd, J = 13.3, 9.8 Hz, 1H), 2.17 – 2.01 (m, 2H), 1.81 – 1.23 (m, 10H), 0.94 (t, J = 7.2 Hz, 3H).

¹³C NMR (101 MHz, Chloroform-*d*): δ 176.44, 153.33, 135.39, 129.40, 128.93, 127.31, 78.61, 66.05, 65.65, 55.43, 42.19, 38.63, 38.05, 37.40, 34.67, 34.64, 34.00, 31.30, 22.32, 20.36, 14.18.

HRESIMS *m/z*: 534.18780 [M+H]⁺ (calcd. for C₂₃H₃₆NO₉S₂, 534.18259), 556.16582[M+Na]⁺ (calcd. for C₂₃H₃₅NNaO₉S₂, 556.16453), 572.13821 [M+K]⁺ (calcd. for C₂₃H₃₅KNO₉S₂, 572.13847), 551.20968 [M+NH₄]⁺ (calcd. for C₂₃H₃₉N₂O₉S₂, 551.20914).

- Preparation of ethyl (S)-6,8-dihydroxyoctanoate (**16b**):



Procedure: To a stirred solution of **9b** (290 mg, 991.88 μmol) in ethyl acetate (10 mL) was added a catalytic amount of 10% Pd (70 mg) and stirred under an H₂ atmosphere at room temperature for 24 h. The progress of the reaction was monitored by TLC. After completion, the reaction was stopped and filtered over celite bed, and the celite bed was washed with ethyl acetate. All the organic layers were combined and concentrated on a rotavaporator to give a crude residue. Purification of the crude residue was carried out by silica gel column chromatography using (n-hexane/ethyl acetate 1:1) to give **16b** (200 mg) as a colorless oil.

Molecular Formula: C₁₀H₂₀O₄

Yield: quantitative

R_f: 0.30 (n-hexane/ethyl acetate 2:8).

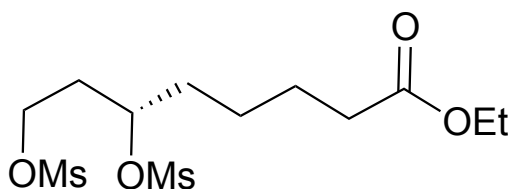
IR v_{max}, (neat, cm⁻¹): 3395, 2946, 2885, 1711.

¹H NMR (400 MHz, Chloroform-*d*): δ 4.14 (q, *J* = 7.1 Hz, 2H), 3.95 – 3.76 (m, 3H), 2.88 (s, 1H), 2.77 (s, 1H), 2.33 (t, *J* = 7.4 Hz, 2H), 1.77 – 1.58 (m, 4H), 1.56 – 1.43 (m, 3H), 1.43 – 1.32 (m, 1H), 1.27 (t, *J* = 7.1 Hz, 3H).

¹³C NMR (101 MHz, Chloroform-*d*): δ 173.98, 71.02, 61.04, 60.29, 38.34, 37.18, 34.19, 24.98, 24.76, 14.15.

HRESIMS *m/z*: 205.14378 [M+H]⁺ (calcd. for C₁₀H₂₁O₄, 205.14343), 227.12778 [M+Na]⁺ (calcd. for C₁₀H₂₀NaO₄, 227.12537).

- Preparation of ethyl (S)-6,8-dimesyloxy octanoate (**17b**):



Procedure: To a solution of the diol **16b** (180 mg, 881.20 μ mol) in anhydrous dichloromethane (8 mL) were added triethylamine (0.614 mL, 4.41 mmol) and methanesulfonyl chloride (0.157 mL, 2.03 mmol) at 0 °C and stirred for 1 h at the same temperature. The reaction mixture was poured into aqueous sodium hydrogen carbonate and extracted with dichloromethane (2x10 mL). The combined organic extracts were washed with brine, dried over anhydrous Na₂SO₄, filtered and concentrated under reduced pressure. The crude oily compound was purified by silica gel column chromatography using (n-hexane/ethyl acetate 1:1) as an eluent to afford 6, 8 dimesylate **17b** (312 mg) as a colorless oil.

Molecular Formula: C₁₂H₂₄O₈S₂

Yield: 98%

Rf: 0.62 (n-hexane/ethyl acetate 2:8).

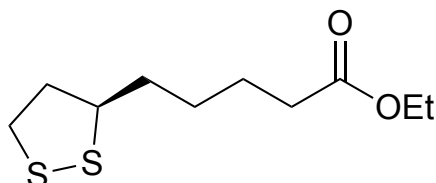
IR v_{max}, (neat, cm⁻¹): 3027, 2947, 1711, 1175.

¹H NMR (400 MHz, Chloroform-*d*): δ 4.96 – 4.85 (m, 1H), 4.43 – 4.31 (m, 2H), 4.14 (q, J = 7.1 Hz, 2H), 3.07 (d, 6H), 2.34 (t, J = 7.3 Hz, 2H), 2.26 – 1.98 (m, 2H), 1.94 – 1.73 (m, 2H), 1.73 – 1.53 (m, 2H), 1.51 – 1.40 (m, 2H), 1.27 (t, J = 7.1 Hz, 3H).

¹³C NMR (101 MHz, Chloroform-*d*): δ 173.31, 78.54, 65.58, 60.37, 38.67, 37.43, 34.61, 34.01, 33.90, 24.49, 24.23, 14.24.

HRESIMS *m/z*: 383.08804 [M+Na]⁺ (calcd. for C₁₂H₂₄NaO₈S₂, 383.08047), 378.12868 [M+NH₄]⁺ (calcd. for C₁₂H₂₈NO₈S₂, 378.12508), 399.05676 [M+K]⁺ (calcd. for C₁₂H₂₄KO₈S₂, 399.05441), 395.06972 [M+Cl]⁻ (calcd. for C₁₂ClH₂₄O₈S₂, 395.06066).

- Preparation of ethyl R-(+)-lipoate or [ethyl (5S)-5-(1,2-dithiolan-3yl) pentanoate] (**18b**):



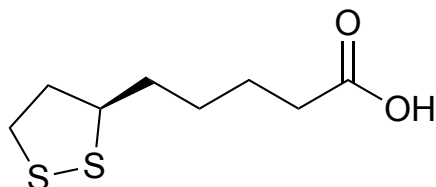
Procedure: A mixture of dimesylate **17b** (290 mg, 804.58 μmol), finely powdered sodium sulfide (72 mg, 917.22 μmol) and sulfur (30 mg, 917.22 μmol) in anhydrous dimethylformamide (5 mL) were heated at 85-90 °C for 24 h. The reaction mixture was diluted with cold water, extracted with EtOAc (2x10 mL) and the combined organic fractions were washed with brine, dried over anhydrous Na₂SO₄, filtered and concentrated under reduced pressure. The residue was purified by silica gel column chromatography using (n-hexane/ethyl acetate 1:1) as an eluent to afford **18b** (135 mg) as a light-yellow oil.

Molecular Formula: C₁₀H₁₈O₂S₂

Yield: 71%

Rf: 0.81 (n-hexane/ethyl acetate 6:4).

- Preparation of (R)-5-(1,2-dithiolan-3-yl)-pentanoic acid or **(R)-lipoic acid**:



Procedure: To a stirred solution of **18b** (120 mg, 512.01 μmol) in THF (2 mL) was added aqueous LiOH (3 M, 2 mL) and stirred at rt for 24 h. THF was evaporated on a rotavaporator and the aqueous layer was acidified carefully with 6 M HCl to pH 2. The product was extracted with dichloromethane (2x10 mL) and the combined organic phases were dried over anhydrous Na_2SO_4 , filtered, and concentrated on a rotavaporator to afford a crude residue. The resulting residue was purified by flash column chromatography (silica gel) using n-hexane/ethyl acetate 85:15 as an eluent, to afford **(R)-lipoic acid** (75 mg) as a yellow solid.

Molecular Formula: $\text{C}_8\text{H}_{14}\text{O}_2\text{S}_2$

Yield: 71%

Rf: 0.22 (n-hexane/ethyl acetate 8:2).

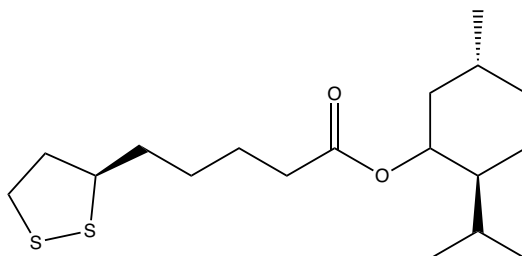
IR ν_{max} , (neat, cm^{-1}): 3021, 2920, 1698, 725.

^1H NMR (400 MHz, Chloroform-*d*): δ 10.40 (s, 1H), 3.64 – 3.52 (m, 1H), 3.25 – 3.07 (m, 2H), 2.53 – 2.47 (m, 1H), 2.41 (t, $J = 7.4$ Hz, 2H), 1.99 – 1.86 (m, 1H), 1.81 – 1.61 (m, 4H), 1.61 – 1.40 (m, 2H).

^{13}C NMR (101 MHz, Chloroform-*d*): δ 179.62, 56.26, 40.20, 38.48, 34.55, 33.80, 28.60, 24.39.

HRESIMS m/z : 229.03317 $[\text{M}+\text{Na}]^+$ (calcd. for $\text{C}_8\text{H}_{14}\text{NaO}_2\text{S}_2$, 229.03273), 245.02795 $[\text{M}+\text{K}]^+$ (calcd. for $\text{C}_8\text{H}_{14}\text{KO}_2\text{S}_2$, 245.00667), 205.03197 $[\text{M}-\text{H}]^-$ (calcd. for $\text{C}_8\text{H}_{13}\text{O}_2\text{S}_2$, 205.03624).

- Preparation of (1R,2S,5R)-2-isopropyl-5-methylcyclohexyl 5-((R)-1,2-dithiolan-3-yl)pentanoate (**19**):



Procedure: To a mixture of R-lipoic acid (1 g, 4.85 mmol) and L-menthol (0.757 g, 4.85 mmol) in pyridine (10 mL) was added diethyl chlorophosphate (0.773 mL, 5.33 mmol) slowly at rt under argon atmosphere, and the reaction mixture was stirred at rt for about 30 min. The heterogeneous mixture was heated at 70 °C under argon atmosphere for 20 h, during which the reaction mixture became homogeneous. Pyridine was removed in vacuo, and the residue partitioned between ethyl acetate (50 mL) and saturated sodium bicarbonate (20 mL). After 10 min of stirring, the organic layer was separated, dried over anhydrous Na₂SO₄ and the solvent evaporated in vacuum to yield the crude product. The crude was then purified via a column chromatography using normal phase silica gel (n-hexane/ethyl acetate 9:1) to give **19** (536 mg) as a yellow oil.

Molecular Formula: C₁₈H₃₂O₂S₂

Yield: 32%

Rf: 0.37 (n-hexane/ethyl acetate 9:1).

IR v_{max}, (neat, cm⁻¹): 2952, 2926, 2868, 1727, 1455, 1369.

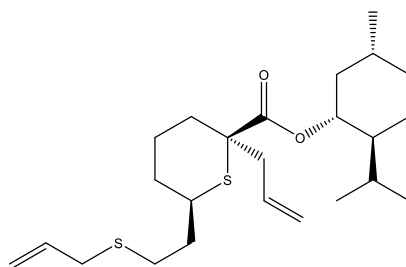
¹H NMR (400 MHz, Chloroform-d): δ 4.76 – 4.64 (m, 1H), 3.64 – 3.53 (m, 1H), 3.26 – 3.08 (m, 2H), 2.54 – 2.42 (m, 1H), 2.31 (t, J = 7.2 Hz, 2H), 2.05 – 1.79 (m, 3H), 1.81 – 1.60 (m, 7H), 1.59

– 1.45 (m, 2H), 1.50 – 1.32 (m, 2H), 1.15 – 0.94 (m, 2H), 0.98 – 0.87 (m, 7H), 0.91 – 0.72 (m, 3H).

¹³C NMR (101 MHz, Chloroform-*d*): δ 173.07, 74.05, 56.37, 47.01, 40.97, 40.21, 38.49, 34.63, 34.49, 34.27, 31.39, 28.77, 26.30, 24.86, 23.42, 22.04, 20.79, 16.32.

HRESIMS *m/z*: 345.19190 [M+H]⁺ (calcd. for C₁₈H₃₃O₂S₂, 345.19164), 367.17990 [M+Na]⁺ (calcd. for C₁₈H₃₂NaO₂S₂, 367.17358), 383.16999 [M+K]⁺ (calcd. for C₁₈H₃₃KO₂S₂, 383.14752), 711.35919 [2M+Na]⁺ (calcd. for C₃₆H₆₄NaO₄S₄, 711.35795).

- Preparation of (1R,2S,5R)-2-isopropyl-5-methylcyclohexyl (2R,6R)-2-allyl-6-(2-(allylthio) ethyl) tetrahydro-2H-thiopyran-2-carboxylate (**20**):



Procedure: 4 mL THF was added to **19** (200 mg, 580.43 μ mol) under argon at 0 °C. Lithium bis(trimethylsilyl) amide (1.0 M in THF, 1.45 mL, 1.45 mmol) was then added dropwise, mixture was left for 30 minutes. Allyl iodide (265.38 μ L, 2.90 mmol) was added and reaction was monitored via TLC. Once the starting material is totally converted to product after 1 h, 4 mL NH₄Cl was added and mixture was allowed to warm up to rt. THF was removed by rotavaporator, then 20 mL water was added to the residue. The mixture was extracted by EtOAc (3x 20 mL), organic layer was washed with 60 mL brine, dried over anhydrous Na₂SO₄, and concentrated in vacuum. Purification of crude extract was performed using a column chromatography via a reverse-phase

C18 silica gel and eluted with methanol/water in composition of 90:10 to give **20** (115 mg) as a colorless oil.

Molecular Formula: $C_{24}H_{40}O_2S_2$

Yield: 52%

Rf: 0.44 (n-hexane/ethyl acetate 95:5).

IR v_{max}, (neat, cm⁻¹): 2952, 2926, 2868, 1714, 1436, 985, 915.

¹H NMR (500 MHz, Chloroform-*d*): δ 5.85 – 5.68 (m, 2H), 5.17 – 5.06 (m, 4H), 4.73 – 4.65 (m, 1H), 3.16 – 3.05 (m, 3H), 2.64 – 2.41 (m, 4H), 2.39 – 2.26 (m, 1H), 2.08 – 1.90 (m, 3H), 1.87 – 1.62 (m, 5H), 1.63 – 1.42 (m, 3H), 1.38 – 1.24 (m, 1H), 1.12 – 0.96 (m, 2H), 0.96 – 0.82 (m, 8H), 0.76 (d, $J = 7.0$ Hz, 3H).

¹³C NMR (126 MHz, Chloroform-*d*): δ 172.85, 134.33, 132.21, 118.86, 117.00, 75.56, 53.68, 46.90, 44.98, 40.70, 40.67, 36.46, 35.68, 34.62, 34.25, 33.78, 31.43, 27.66, 25.93, 23.40, 22.96, 22.07, 20.91, 15.82.

HRESIMS *m/z*: 447.23547 [M+Na]⁺ (calcd. for $C_{24}H_{40}NaO_2S_2$, 447.23618), 463.21605 [M+K]⁺ (calcd. for $C_{24}H_{40}KO_2S_2$, 463.21012), 887.45929 [2M+K] (calcd. for $C_{48}H_{80}KO_4S_4$, 887.45709).

CHAPTER IV

LATE-STAGE DIVERSIFICATION OF MENTHONE HOMOLOG AS JUVENILE HORMONE ANALOG AND ITS GROWTH INHIBITING EFFECT AGAINST BED BUGS

1. Introduction

1.1. Bed Bugs

Cimex lectularius (L.) are blood-feeding insects that are synanthropic⁵⁷. Although their biting behavior causes discomfort to individuals who are bitten, they are not recognized as disease carriers and transmitters^{52,57}. Following World War II, the public was spared from pests, partially for the extensive applications of DDT (dichloro-diphenyl-trichloroethane)¹³⁹. Multiple variables, including less effective insecticides, international travel, and a lack of care exhibited in earlier periods, are inclined to blame for the recent resurgence¹³⁹. Many hypotheses have been postulated to explain the rebound, however there is growing evidence of resistance to frequently used insecticides¹³⁹. As a result, researchers are seeking for alternative insecticides that may be used in combination with or rather than the commonly used one.

Adult bed bugs have oval, flattened bodies and are about 3/16-inch long and reddish-brown in color⁵⁶. The common bed bug prefers to feed on humans, although it will bite other warm-blooded creatures such as dogs, cats, birds, and rodents⁵².

Insects go through larval or nymphal stages during their development from egg to adult and acquire biomass through feeding ⁵⁷. This process is regulated by juvenile hormones (JHs). Furthermore, as the insect develops, a new exoskeleton must be created inside the old one and the old one subsequently must shed ⁵⁷. The new exoskeleton will then expand to its full size and hardens, a process known as molting ⁵⁷, (**Figure 4.1**).

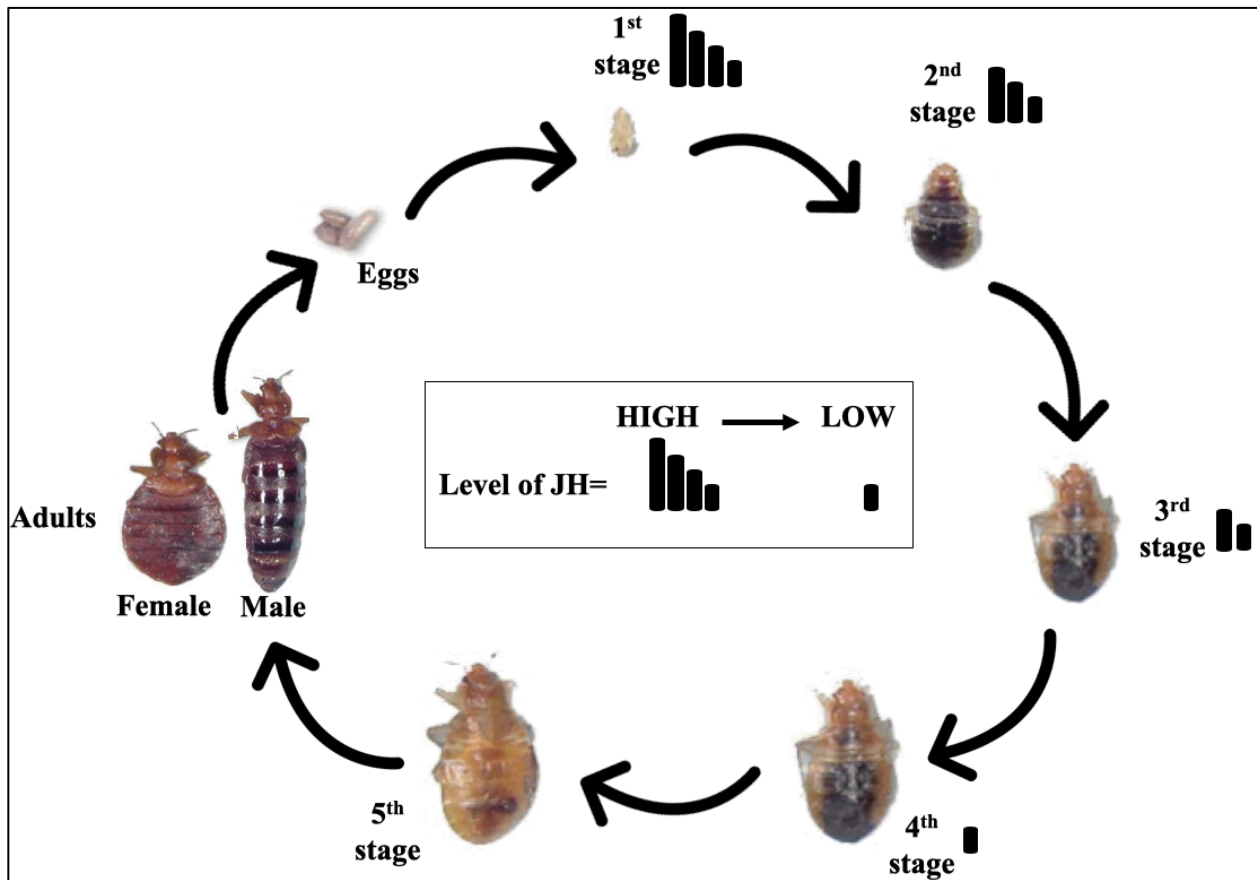


Figure 4. 1. The life cycle of a bed bug.

1.2. Juvenile Hormone Analogues (JHAs)

JHAs are a class of insect growth regulators (IGRs) that act by mimicking insect juvenile hormone, a pivotal developmental hormone that plays a critical role in regulating insect's life-cycle, keeping insects in immature stages, and preventing their reproduction ¹⁴⁰. They are synthetically made analogues of juvenile hormones. Williams and Slama were the first to discover JH analogues in 1966 ¹⁴⁰. They observed that rearing a *Pyrrhocoris* bug in a glass container with a paper towel led the bug to die before reaching mature stage. As a result, the incident was called 'paper factor' or 'juvabione' by the two scientists. They later discovered that the paper was made from balsam fir tree (*Abies balsamea*), specifically the wood pulp part, which contained the JH mimic ¹⁴⁰.

Thus far, there are two commercially available JHAs, namely methoprene and hydroxyphenoxypyrene, (**Figure 4.2**), which have been reported to be effective against a variety of pests in stored products and both have been used successfully to manage urban pests ⁵¹. They exert their effects from causing any physical internal damage, incomplete body parts, and disruption of the cycle ¹⁴⁰. These JHAs are economical because they are effective in minute quantities and target specific. Additionally, they have a favorable safety profile, including minimal mammalian toxicity and rapid environmental degradation ^{51, 141}. However, they have a slow mode of action and only kill at specific stages of pests ^{140, 141}. Also, these JHAs are sensitive under light and could be subjected to hydrolysis when dissolved in water ^{51, 141}. Furthermore, findings such as developing resistance and consequently, human and aquatic overexposure are additional disadvantages of these JHAs that need to be overcome and addressed ⁵⁶.

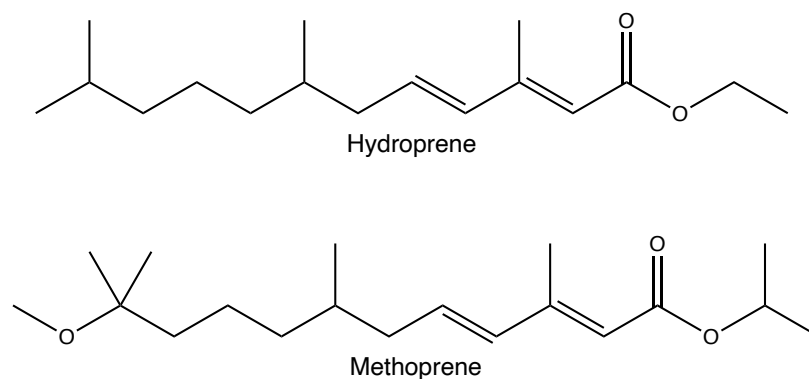


Figure 4. 2. Chemical structures of currently used JHAs.

2. Significance

Cimex lectularius (L.) are reported the most in urban areas and have raised many concerns regarding the public and environmental health ^{51, 142}. The bugs survive solely on the blood of humans and animals causing skin rashes, bleeding, inflammation, as well as psychological impacts including sleep difficulties, anxiety, and stress as a result of the continuous and overwhelming infestations ^{52, 53}. Recent details on the efficacy of insecticides against bed bugs are limited, and there is even less on the efficacy of insect growth regulators. Although JHAs are considered optimal for their proven effectiveness and relatively low toxicity to non-arthropods, their efficacy for bed bug management remains, nevertheless, inconsistent ¹⁴³. Because some strains of bed bugs developed resistance to common insecticides, JHAs have shown insecticidal activity when used at higher application rates than the labeled rate ^{56, 57}. Accordingly, it has been reported that certain strains of bed bugs and mosquitoes have developed cross-resistance to other classes of insecticides ⁵⁶. Based on that, observations such as aquatic toxicity and human overexposure to insecticides through inhalation or dermal contact have been recorded ⁵⁸. Hence, this study aims on developing a novel natural product-derived analog as an IGR for managing bed bugs with preferable safety profile compared to other available IGRs.

3. Innovation

The novel natural product-derived IGR was attained in one step synthesis with feasible and cost-effective material, compared to those commercially available IGRs that are purely synthetic and achieved in multiple steps.

4. Approach

For the synthesis of the new IGR, the natural monoterpene, menthone (or (2S,5R)-trans-2-isopropyl-5-methylcyclohexanone) will be transformed via Horner–Wadsworth–Emmons reaction into its C4 elongated conjugate ester, **AJM-IGR-100**, (**Figure 4.3**). Furthermore, the impact on development and reproduction of bed bugs will be tested by residual bioassay experiment, a method that is developed by our entomologist in NCNPR.

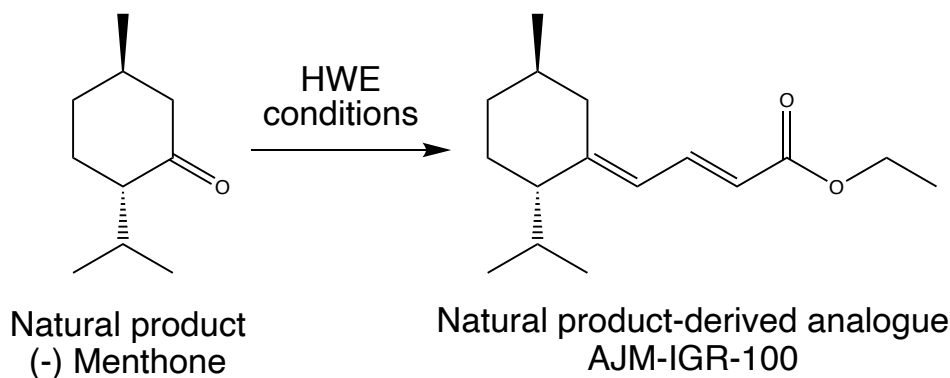


Figure 4. 3. Olefination of menthone via HWE reaction.

5. Results and Discussion

5.1. Synthesis of (AJM-IGR-100)

Initially, the reaction conditions were monitored by screening several parameters, such as different bases, temperatures, and reaction duration, (**Table 4.1-4.3**). Deprotonation of the phosphonate by the base gives a phosphonate carbanion that undergoes a nucleophilic addition onto the carbonyl group of menthone, leading to the formation of a four-membered ring

(oxaphosphetane). Next, the final product is released through the decomposition of oxaphosphetane by ring opening process (cycloreversion) to produce the E alkene predominantly, releasing a phosphate anion as a byproduct that is water soluble and easily removed by aqueous extraction. The initial nucleophilic addition and the equilibrium of the oxaphosphetane intermediate can determine the overall rate of the reaction. Giving the steric crowding caused by the two bulky groups (the 2-isopropyl-5-methyl cyclohexanolate and the phosphonate carbanion), the rate of elimination to give the trans diastereoisomer with the two bulky groups on opposite sides of the ring is significantly faster than the rate of elimination to give the cis diastereoisomer.

Accordingly, Triethyl 4-phosphonocrotonate (HWE reagent) was slowly added to a solution of LiHMDS in anhydrous THF at rt. The resulting dark orange was stirred for 30 minutes before the dropwise addition of *l*-Menthone. After the reaction went to completion, pure compound **AJM-IGR-100** was obtained with a gradient elution of methanol–water mobile phases in composition from 50:50 to 70:30 in 45% yield as dark orange viscous liquid, (**Figure 4.4**).

Table 4. 1. Optimization conditions for HWE reaction using NaHMDS.

Entry	Base (equiv)		Temperature	Duration	Comments
1	NaHMDS	1	-78 °C	4 h	SM
2			-20 °C		SM
3			0 °C		SM
4			rt		SM
5		SM			
6		2		6 h	SM
7		3		4 h	SM
8			6 h	SM	

Table 4. 2. Optimization conditions for HWE reaction using KHMDS.

Entry	Base (equiv)		Temperature	Duration	Comments
1	KHMDS	1	-78 °C	4 h	SM
2			-20 °C		SM
3			0 °C		SM
4			rt		SM
5		SM			
6		2		6 h	SM
7		3		4 h	SM
8			6 h	SM	

Table 4. 3. Table 4. 2. Optimization conditions for HWE reaction using LiHMDS.

Entry	Base (equiv)		Temperature	Duration	Comments
1	LiHMDS	1	-78 °C	4 h	SM
2			-20 °C		SM
3			0 °C		SM
4			rt		trace
5		2.5	0 °C		trace
6			rt	45% ^a	
7				6 h	34% ^a
8				4 h	25% ^a
9			3	6 h	20% ^a

^a = yields reported for isolated compounds.

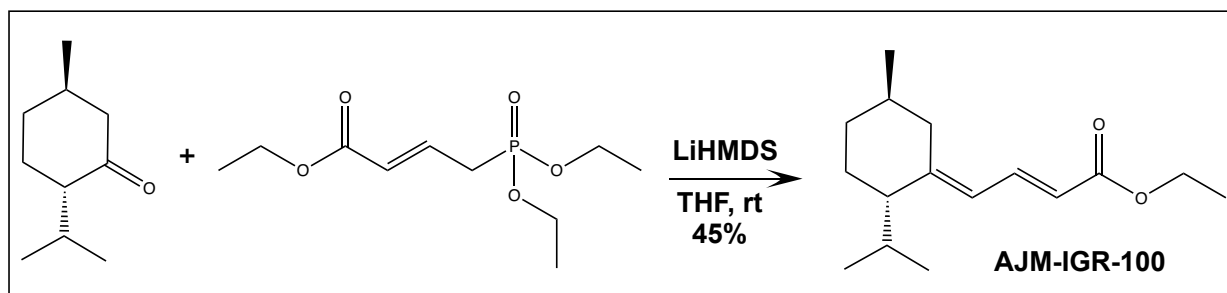


Figure 4. 4. HWE reaction conditions of menthone.

5.2. IGR Activity

To observe any possible IGR activity in **AJM-IGR-100**, the material diluted in acetone were directly delivered topically to ensure the direct contact of the test compounds. We looked for various parameters for possible IGR activity, e.g., indigestion of the blood, incomplete molting,

any deformity in limbs, any mortality or failing to feed. Bed bug will molt to next instar after each blood meal. The unfed bed bugs indirectly point at the possible disruption in life cycle. Any disruption, delay or deformity will delay the molting process, leading to desiccation of partially molted or complete mortality. Hence, in screening studies, 7 days after treatment (**Figure 4.5**), **AJM-IGR-100** induced 21.9% mortality and only 17.4% could feed on blood. While the positive control, methoprene, induced 19.9% mortality with 14.8% bed bug fed on the blood. It was followed by menthone with 9.5% mortality and 14.2% feeding success. The impact of the treatment was more pronounced in the 2nd week after treatment where higher mortality was observed in **AJM-IGR-100** and methoprene (**Figure 4.6**) 33.7% & 30.9 %, respectively. While only 9% of bed bugs died in menthone. The structural deformities were very prominent in **AJM-IGR-100** and methoprene.

On the basis of preliminary screening profile, we ran a dose response of new compound only. We observed the similar mortality time curve/pattern in the dose response of new compound in comparison to standard methoprene. Based on data in (**Figure 4.5 and 4.6**), the new compound, **AJM-IGR-100**, has almost similar mortality and feeding profiles as the positive control, methoprene, after two weeks of exposure to treatment groups of 1000 and 2000 ppm. Additionally, in the treatment group with 1000 ppm of **AJM-IGR-100**, the remaining 20% of bed bugs exhibited several exoskeleton structural deformities along with their inability to consume a meal. Taken together, **AJM-IGR-100** has the potential to disrupt the life-cycle of bed bugs and might serve as a novel insect growth regulator.

The study we presented here is forced feeding to further explore the potential of the new compound. In actual scenarios, the successive feeding possibility of bed bugs exposed to treatment is very narrow, as being weakened due to treatment, may not be able to reach to blood source. Although, in 20mL vial they are few centimeter close to blood feeder but in actual scenario the bugs might be couple of feet away from the targeted human on bed/furniture.

Figure 4. 5. Mortality and feeding behavior of 1st instar bed bugs with a novel insect growth regulator.

Screening section: *levels not connected by same lowercase letter are significantly different; Dose response section: levels not connected by same uppercase letter are significantly different, replicate =3 /treatment with 20 1st instar bed bug/replicate (One Way ANOVA, P < 0.05, mean separated by Tukey’s HSD Test).

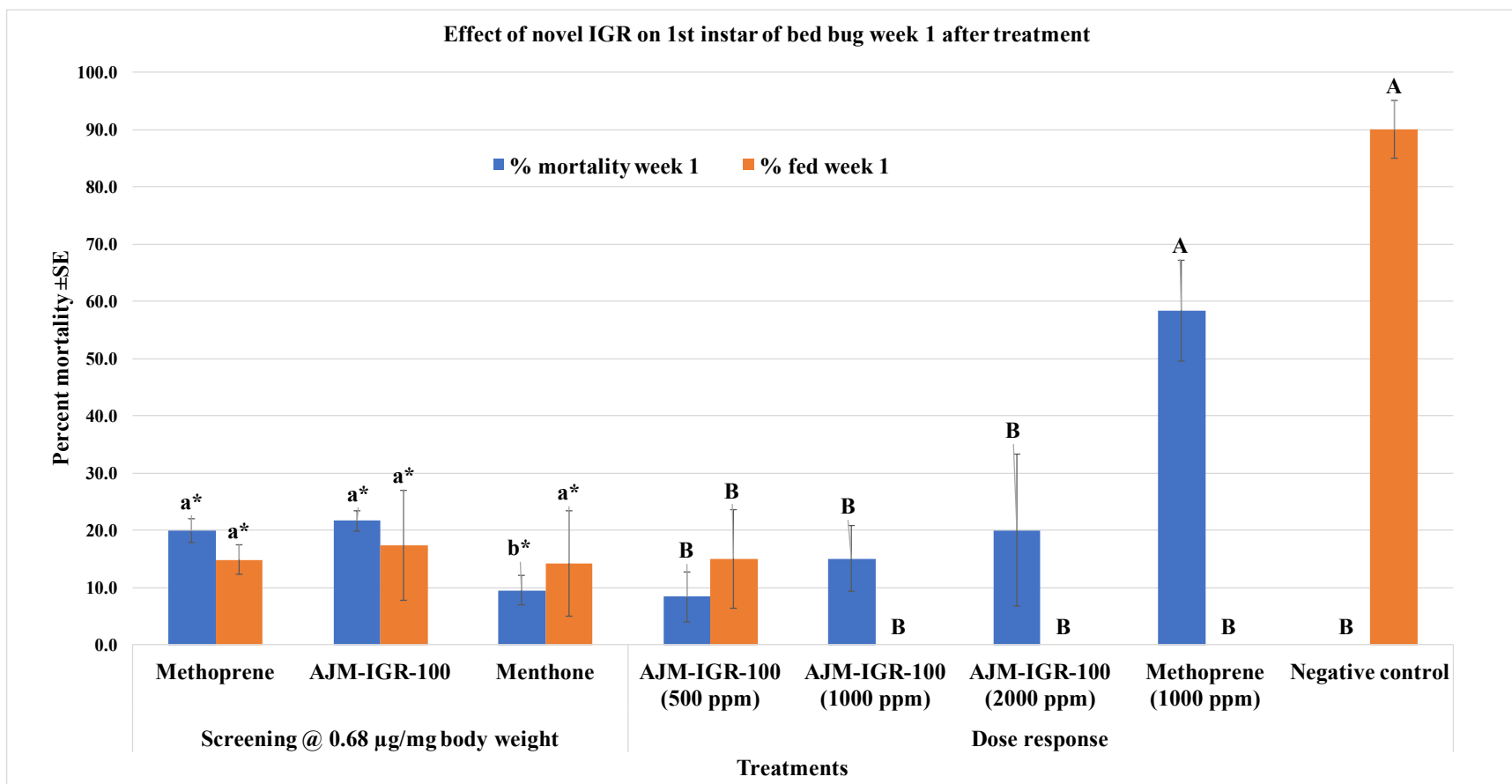
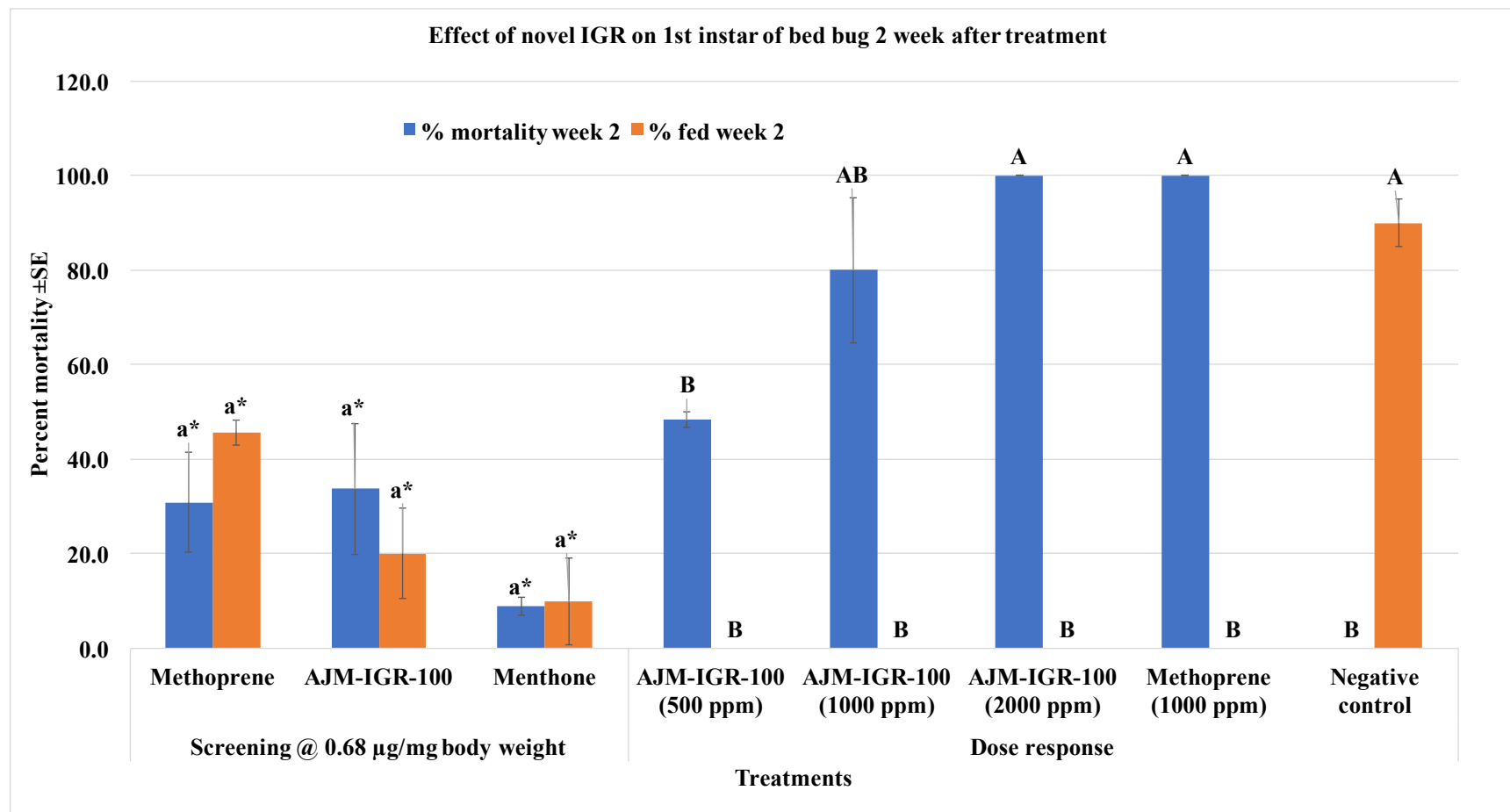


Figure 4. 6. Mortality and feeding behavior of 1st instar bed bugs with a novel insect growth regulator.

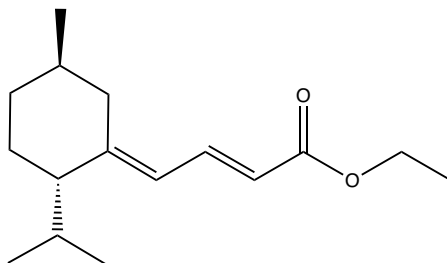
Screening section: *levels not connected by same lowercase letter are significantly different; Dose response section: levels not connected by same uppercase letter are significantly different, replicate =3 /treatment with 20 1st instar bed bug/replicate (One Way ANOVA, P < 0.05, mean separated by Tukey’s HSD Test).



6. Experimental Procedures

6.1. Synthesis of (AJM-IGR-100):

- Preparation of ethyl (2E,4E)-4-((2S,5R)-2-isopropyl-5-methylcyclohexylidene) but-2-enoate:



Procedure: Triethyl 4-phosphonocrotonate (1.44 mL, 6.48 mmol) was slowly added to a solution of Lithium bis(trimethylsilyl)amide (6.48 mL, 6.48 mmol) in 10 mL anhydrous THF at rt. The resulting dark orange was stirred for 30 minutes before the dropwise addition of *l*-Menthone ((2*S*,5*R*)-*trans*-2-isopropyl-5-methylcyclohexanone) (1 g, 6.48 mmol). The mixture was then stirred and the progress of the reaction was monitored by TLC. After the reaction went to completion, the mixture was quenched with saturated aqueous ammonium chloride and extracted with EtOAc (3x 20 mL) The organic layer was then washed with 60 mL brine, dried over anhydrous Na₂SO₄, and concentrated in vacuum. Purification of crude extract was performed using a column chromatography via a reverse-phase C18 silica gel and eluted with methanol/water in composition from 50:50 to 70:30 to give (AJM-IGR-100) (725 mg) as a colorless oil.

Molecular Formula: C₁₆H₂₆O₂

Yield: 45%

Rf: 0.16 (n-hexane/ethyl acetate 99:1).

IR v_{max}, (neat, cm⁻¹): 2953, 2926, 1746, 1712, 1630, 1271.

¹H NMR (400 MHz, Chloroform-d): δ 7.67 (dd, J = 15.1, 11.6 Hz, 1H), 6.00 (d, J = 11.6 Hz, 1H), 5.83 (d, J = 15.1 Hz, 1H), 4.22 (q, 2H), 2.68 – 2.59 (m, 1H), 2.09 – 1.92 (m, 2H), 1.92 – 1.74 (m, 4H), 1.47 – 1.33 (m, 1H), 1.29 (t, 3H), 1.23 – 1.14 (m, 1H), 1.04 – 0.85 (m, 9H).

¹³C NMR (101 MHz, Chloroform-d): δ 167.72, 155.24, 140.44, 120.94, 119.17, 59.96, 52.25, 36.23, 33.12, 31.54, 27.08, 26.83, 21.83, 20.38, 19.66, 14.32;

HRESIMS *m/z*: 251.20158 [M+H]⁺ (calcd. for C₁₆H₂₇O₂, 251.20055).

6.2. IGR Activity

- **Preliminary Screening: Topically Delivered Test Compound to 1st Instar Bed Bugs for IGR Activity**

To observe any possible IGR, the test compounds (new IGR, methoprene and menthone) were topically delivered to 1st instars of the bed bug. Before treatment, twenty 1st instars of freshly-fed bed bugs (strain Bayonne ‘Insecticide’) were weighed and placed on a small piece of paper in a Petri dish. Three, 1 μ L drops of treatment solution (concentration= 2 μ g/ μ l) diluted in acetone were delivered topically. Five minutes after the treatment, bed bugs were transferred to 20mL scintillation vial and placed in the growth chamber. Each treatment had 3 replicates with 20 1st instars bed bug per replicate. Menthone and methoprene were used as parallel controls with the IGR. Bed bugs were fed after 7 days after the treatment and the data for mortality, fed and unfed was recorded.

- **Residual Bioassay: Exposing 1st Instar Bed Bugs to Filter Paper Treated With IGR**

In a 20 mL scintillation vial with 20 1st instars of freshly-fed bed bugs (strain Bayonne ‘Insecticide-resistant’), [AJM-IGR-100, methoprene, or acetone] treated on a filter paper (30x20

mm) was introduced. The new IGR was tested with three different concentrations (500, 1000 and 2000 ppm). For controls, methoprene was used as a positive control at 1000 ppm and pure acetone treated filter paper was used as a negative control. Each treatment had three replicates with twenty 1st instars per replicate. All bed bugs were manually inspected for their feeding behavior, deformation to their exoskeleton, and mortality on a weekly basis. Mortality and feeding behavior (as % of bugs were able to consume defibrillated rabbit blood) was recorded for week 1 and week 2, (Figure 4.7 and Figure 4.8).

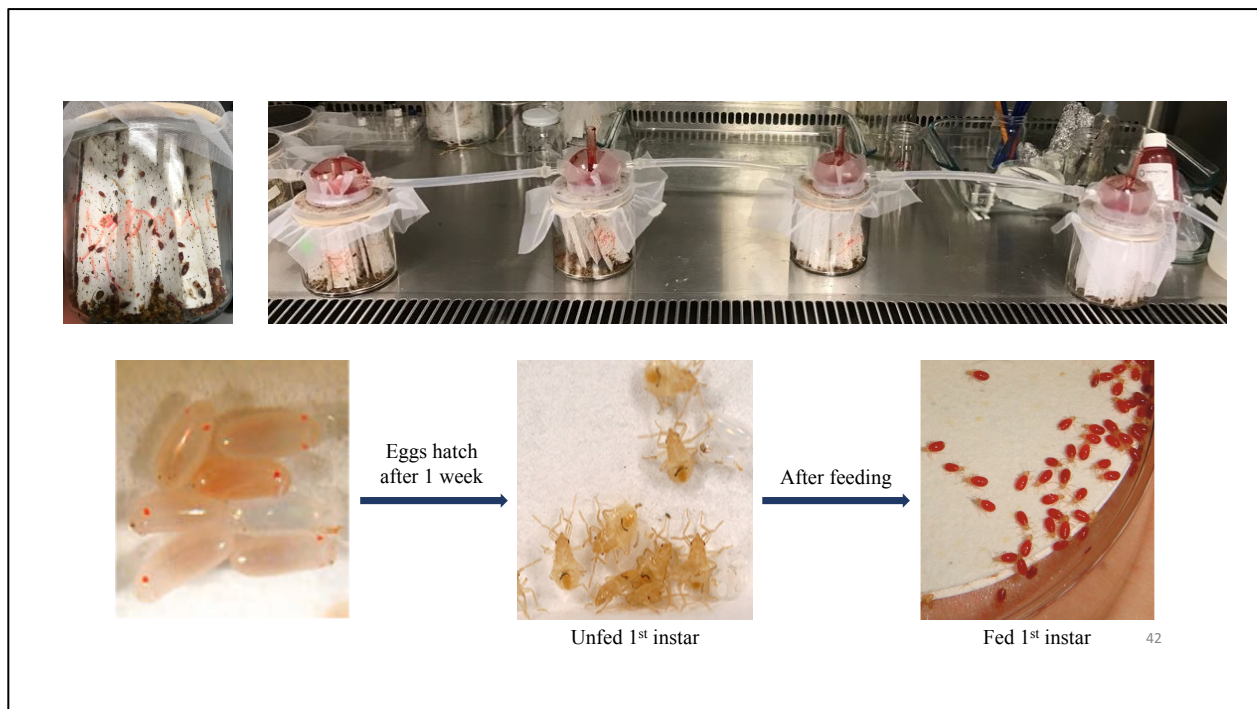


Figure 4. 7. *In vivo* residual bioassay: Feeding of bed bugs.

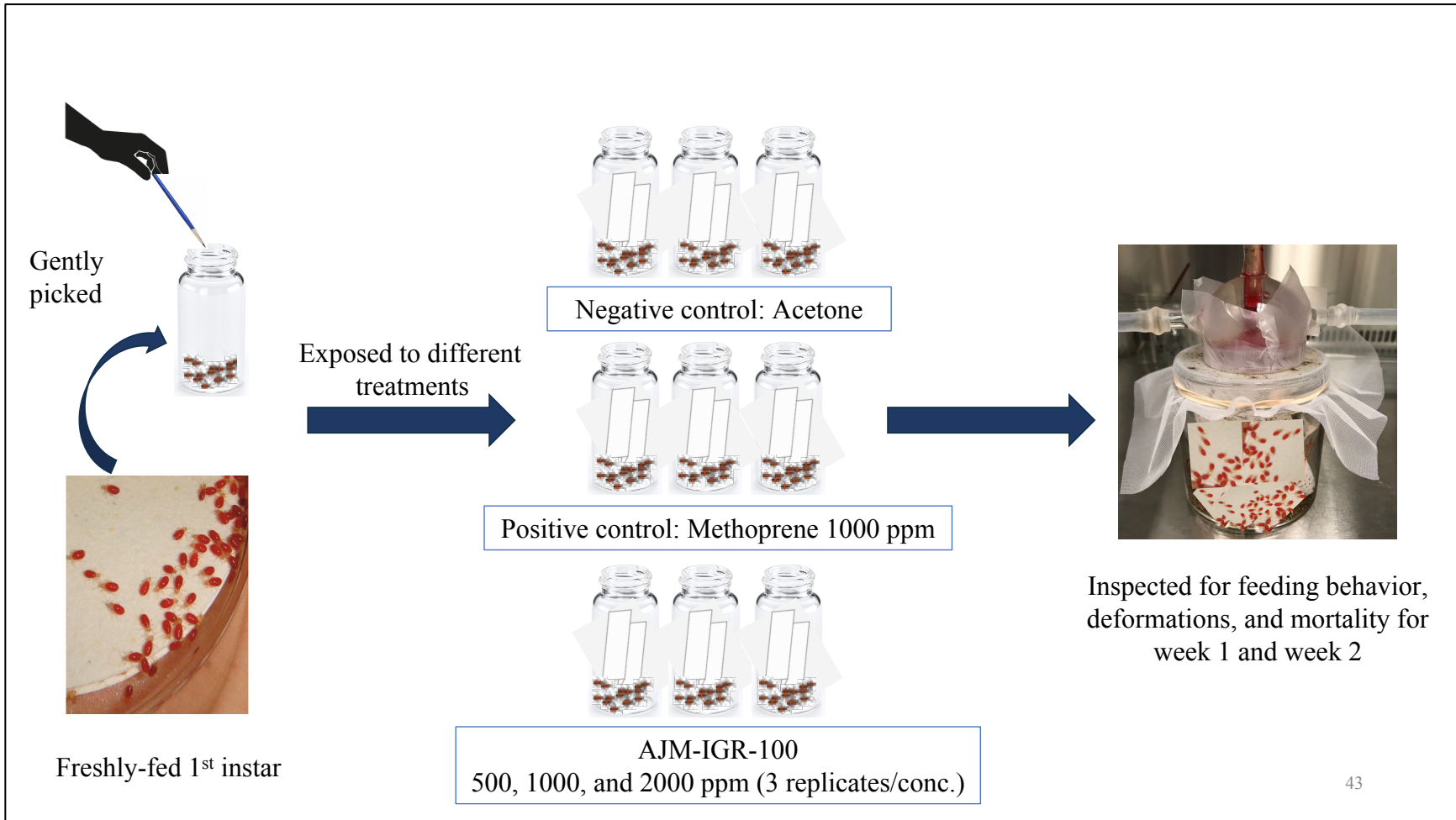


Figure 4. 8. *In vivo* residual bioassay: Exposing 1st instar bed bugs to filter paper treated with IGR

- **Statistical Analysis**

Mortality data from the bioassays were subjected to analysis of variance (ANOVA) using SAS® 9.3 and JMP® 10.0 (SAS Institute 2005) $P < 0.05$, and means were separated by Tukey's honest significant difference (HSD).

BIBLIOGRAPHY

1. Cragg, G. M.; Newman, D. J., Natural products: a continuing source of novel drug leads. *Biochim Biophys Acta* **2013**, 1830, (6), 3670-95.
2. Butler, M. S.; Robertson, A. A.; Cooper, M. A., Natural product and natural product derived drugs in clinical trials. *Nat Prod Rep* **2014**, 31, (11), 1612-61.
3. Guo, Z., The modification of natural products for medical use. *Acta Pharm Sin B* **2017**, 7, (2), 119-136.
4. Crane, E. A.; Gademann, K., Capturing Biological Activity in Natural Product Fragments by Chemical Synthesis. *Angewandte Chemie International Edition* **2016**, 55, (12), 3882-3902.
5. Xiao, Z.; Morris-Natschke, S. L.; Lee, K. H., Strategies for the Optimization of Natural Leads to Anticancer Drugs or Drug Candidates. *Med Res Rev* **2016**, 36, (1), 32-91.
6. Newman, D. J.; Cragg, G. M., Natural Products as Sources of New Drugs over the Nearly Four Decades from 01/1981 to 09/2019. *J Nat Prod* **2020**, 83, (3), 770-803.
7. Jiménez, C., Marine Natural Products in Medicinal Chemistry. *ACS Med Chem Lett* **2018**, 9, (10), 959-961.
8. Li, J. W.; Vederas, J. C., [Drug discovery and natural products: end of era or an endless frontier?]. *Biomed Khim* **2011**, 57, (2), 148-60.
9. Sparks, T. C.; Duke, S. O., Structure Simplification of Natural Products as a Lead Generation Approach in Agrochemical Discovery. *Journal of agricultural and food chemistry* **2021**.
10. Yao, H.; Liu, J.; Xu, S.; Zhu, Z.; Xu, J., The structural modification of natural products for novel drug discovery. *Expert Opin Drug Discov* **2017**, 12, (2), 121-140.
11. Chen, J.; Li, W.; Yao, H.; Xu, J., Insights into drug discovery from natural products through structural modification. *Fitoterapia* **2015**, 103, 231-41.
12. Maier, M. E., Design and synthesis of analogues of natural products. *Organic & biomolecular chemistry* **2015**, 13 19, 5302-43.
13. Wang, S.; Dong, G.; Sheng, C., Structural Simplification of Natural Products. *Chem Rev* **2019**, 119, (6), 4180-4220.
14. Fodstad, O.; Breistøl, K.; Pettit, G. R.; Shoemaker, R. H.; Boyd, M. R., Comparative antitumor activities of halichondrins and vinblastine against human tumor xenografts. *J Exp Ther Oncol* **1996**, 1, (2), 119-25.
15. Hamel, E., Natural products which interact with tubulin in the vinca domain: maytansine, rhizoxin, phomopsin A, dolastatins 10 and 15 and halichondrin B. *Pharmacol Ther* **1992**, 55, (1), 31-51.
16. Aicher, T. D.; Buszek, K. R.; Fang, F. G.; Forsyth, C. J.; Jung, S. H.; Kishi, Y.; Matelich, M. C.; Scola, P. M.; Spero, D. M.; Yoon, S. K., Total synthesis of halichondrin B and norhalichondrin B. *Journal of the American Chemical Society* **1992**, 114, (8), 3162-3164.
17. Towle, M. J.; Salvato, K. A.; Budrow, J.; Wels, B. F.; Kuznetsov, G.; Aalfs, K. K.; Welsh, S.; Zheng, W.; Seletsky, B. M.; Palme, M. H.; Habgood, G. J.; Singer, L. A.; Dipietro, L. V.; Wang, Y.; Chen, J. J.; Quincy, D. A.; Davis, A.; Yoshimatsu, K.; Kishi, Y.; Yu, M. J.; Littlefield, B. A., In vitro and in vivo anticancer activities of synthetic macrocyclic ketone analogues of halichondrin B. *Cancer Res* **2001**, 61, (3), 1013-21.

18. Doherty, M. K.; Morris, P. G., Eribulin for the treatment of metastatic breast cancer: an update on its safety and efficacy. *Int J Womens Health* **2015**, *7*, 47-58.
19. Eguchi, M., Recent advances in selective opioid receptor agonists and antagonists. *Med Res Rev* **2004**, *24*, (2), 182-212.
20. Blakemore, P. R.; White, J. D., Morphine, the Proteus of organic molecules. *Chem Commun (Camb)* **2002**, (11), 1159-68.
21. Van Bever, W. F. M.; Niemegeers, C. J. E.; Janssen, P. A. J., Synthetic analgesics. Synthesis and pharmacology of the diastereoisomers of N-[3-methyl-1-(2-phenylethyl)-4-piperidyl]-N-phenylpropanamide and N-[3-methyl-1-(1-methyl-2-phenylethyl)-4-piperidyl]-N-phenylpropanamide. *Journal of Medicinal Chemistry* **1974**, *17*, (10), 1047-1051.
22. Donner, B.; Zenz, M.; Strumpf, M.; Raber, M., Long-term treatment of cancer pain with transdermal fentanyl. *J Pain Symptom Manage* **1998**, *15*, (3), 168-75.
23. Barna, J. C.; Williams, D. H., The structure and mode of action of glycopeptide antibiotics of the vancomycin group. *Annu Rev Microbiol* **1984**, *38*, 339-57.
24. Hubbard, B. K.; Walsh, C. T., Vancomycin Assembly: Nature's Way. *Angewandte Chemie International Edition* **2003**, *42*, (7), 730-765.
25. Williams, D. H.; Bardsley, B., The Vancomycin Group of Antibiotics and the Fight against Resistant Bacteria. *Angewandte Chemie International Edition* **1999**, *38*, (9), 1172-1193.
26. Perkins, H. R., Vancomycin and related antibiotics. *Pharmacol Ther* **1982**, *16*, (2), 181-97.
27. Walsh, C. T., Vancomycin resistance: decoding the molecular logic. *Science* **1993**, *261*, (5119), 308-9.
28. Healy, V. L.; Lessard, I. A.; Roper, D. I.; Knox, J. R.; Walsh, C. T., Vancomycin resistance in enterococci: reprogramming of the D-ala-D-Ala ligases in bacterial peptidoglycan biosynthesis. *Chem Biol* **2000**, *7*, (5), R109-19.
29. McComas, C. C.; Crowley, B. M.; Boger, D. L., Partitioning the Loss in Vancomycin Binding Affinity for d-Ala-d-Lac into Lost H-Bond and Repulsive Lone Pair Contributions. *Journal of the American Chemical Society* **2003**, *125*, (31), 9314-9315.
30. Higgins, D. L.; Chang, R.; Debabov, D. V.; Leung, J.; Wu, T.; Krause, K. M.; Sandvik, E.; Hubbard, J. M.; Kaniga, K.; Schmidt, D. E., Jr.; Gao, Q.; Cass, R. T.; Karr, D. E.; Benton, B. M.; Humphrey, P. P., Telavancin, a multifunctional lipoglycopeptide, disrupts both cell wall synthesis and cell membrane integrity in methicillin-resistant *Staphylococcus aureus*. *Antimicrob Agents Chemother* **2005**, *49*, (3), 1127-34.
31. Damodaran, S. E.; Madhan, S., Telavancin: A novel lipoglycopeptide antibiotic. *J Pharmacol Pharmacother* **2011**, *2*, (2), 135-7.
32. Yun, B.-W.; Yan, Z.; Amir, R.; Hong, S.; Jin, Y.-W.; Lee, E.-K.; Loake, G. J., Plant natural products: history, limitations and the potential of cambial meristematic cells. *Biotechnology and Genetic Engineering Reviews* **2012**, *28*, (1), 47-60.
33. Li, J.; Zhao, F., Anti-inflammatory functions of *Houttuynia cordata* Thunb. and its compounds: A perspective on its potential role in rheumatoid arthritis (Review). *Exp Ther Med* **2015**, *10*, (1), 3-6.
34. Wang, Q.; Li, Z.; Feng, X.; Wang, A.; Li, X.; Wang, D.; Fan, L., Mercury accumulation in vegetable *Houttuynia cordata* Thunb. from two different geological areas in southwest China and implications for human consumption. *Scientific Reports* **2021**, *11*, (1), 52.
35. Wu, Z.; Deng, X.; Hu, Q.; Xiao, X.; Jiang, J.; Ma, X.; Wu, M., *Houttuynia cordata* Thunb: An Ethnopharmacological Review. *Front Pharmacol* **2021**, *12*, 714694.

36. Zhao, Y.; Mei, L.; Si, Y.; Wu, J.; Shao, J.; Wang, T.; Yan, G.; Wang, C.; Wu, D., Sodium New Houttuynonate Affects Transcriptome and Virulence Factors of *Pseudomonas aeruginosa* Controlled by Quorum Sensing. *Frontiers in Pharmacology* **2020**, 11.
37. Breslin, H. J.; Miskowski, T. A.; Rafferty, B. M.; Coutinho, S. V.; Palmer, J. M.; Wallace, N. H.; Schneider, C. R.; Kimball, E. S.; Zhang, S. P.; Li, J.; Colburn, R. W.; Stone, D. J.; Martinez, R. P.; He, W., Rationale, design, and synthesis of novel phenyl imidazoles as opioid receptor agonists for gastrointestinal disorders. *J Med Chem* **2004**, 47, (21), 5009-20.
38. Li, Y.; Yu, P. L.; Chen, Y. X.; Li, L. Q.; Gai, Y. Z.; Wang, D. S.; Zheng, Y. P., [Studies on analogs of artemisinin. I. The synthesis of ethers, carboxylic esters and carbonates of dihydroartemisinin (author's transl)]. *Yao Xue Xue Bao* **1981**, 16, (6), 429-39.
39. Sun, C.; Wang, Q.; Brubaker, J. D.; Wright, P. M.; Lerner, C. D.; Noson, K.; Charest, M.; Siegel, D. R.; Wang, Y.-M.; Myers, A. G., A Robust Platform for the Synthesis of New Tetracycline Antibiotics. *Journal of the American Chemical Society* **2008**, 130, (52), 17913-17927.
40. Zhang, X.; Zhang, S.; Zhao, S.; Wang, X.; Liu, B.; Xu, H., Click Chemistry in Natural Product Modification. *Frontiers in Chemistry* **2021**, 9.
41. Hou, W.; Liu, B.; Xu, H., Triptolide: Medicinal chemistry, chemical biology and clinical progress. *Eur J Med Chem* **2019**, 176, 378-392.
42. Nelson, P. T.; Braak, H.; Markesbery, W. R., Neuropathology and cognitive impairment in Alzheimer disease: a complex but coherent relationship. *J Neuropathol Exp Neurol* **2009**, 68, (1), 1-14.
43. Yiannopoulou, K. G.; Papageorgiou, S. G., Current and future treatments for Alzheimer's disease. *Ther Adv Neurol Disord* **2013**, 6, (1), 19-33.
44. Liu, P.-P.; Xie, Y.; Meng, X.-Y.; Kang, J.-S., History and progress of hypotheses and clinical trials for Alzheimer's disease. *Signal Transduct Target Ther* **2019**, 4, (1), 29.
45. Gray, S. C.; Kinghorn, K. J.; Woodling, N. S., Shifting equilibriums in Alzheimer's disease: the complex roles of microglia in neuroinflammation, neuronal survival and neurogenesis. *Neural Regen Res* **2020**, 15, (7), 1208-1219.
46. Huang, W. J.; Zhang, X.; Chen, W. W., Role of oxidative stress in Alzheimer's disease. *Biomed Rep* **2016**, 4, (5), 519-522.
47. Teixeira, J. P.; de Castro, A. A.; Soares, F. V.; da Cunha, E. F. F.; Ramalho, T. C., Future Therapeutic Perspectives into the Alzheimer's Disease Targeting the Oxidative Stress Hypothesis. *Molecules* **2019**, 24, (23).
48. Cheng, X.; Zhang, L.; Lian, Y. J., Molecular Targets in Alzheimer's Disease: From Pathogenesis to Therapeutics. *Biomed Res Int* **2015**, 2015, 760758.
49. Rehman, J. U.; Wang, M.; Yang, Y.; Liu, Y.; Li, B.; Qin, Y.; Wang, W.; Chittiboyina, A. G.; Khan, I. A., Toxicity of *Kadsura coccinea* (Lem.) A. C. Sm. Essential Oil to the Bed Bug, *Cimex lectularius* L. (Hemiptera: Cimicidae). *Insects* **2019**, 10, (6).
50. Delaunay, P.; Blanc, V.; Del Giudice, P.; Levy-Bencheton, A.; Chosidow, O.; Marty, P.; Brouqui, P., Bedbugs and Infectious Diseases. *Clinical Infectious Diseases* **2011**, 52, (2), 200-210.
51. Goodman, M. H.; Potter, M. F.; Haynes, K. F., Effects of juvenile hormone analog formulations on development and reproduction in the bed bug *Cimex lectularius* (Hemiptera: Cimicidae). *Pest Manag Sci* **2013**, 69, (2), 240-4.
52. Goddard, J.; deShazo, R., Bed bugs (*Cimex lectularius*) and clinical consequences of their bites. *Jama* **2009**, 301, (13), 1358-66.

53. Goddard, J.; de Shazo, R., Psychological effects of bed bug attacks (*Cimex lectularius* L.). *Am J Med* **2012**, 125, (1), 101-3.
54. Naylor, R.; Bajomi, D.; Boase, C.; Robinson, W. H. In *Efficacy of (S)-methoprene against Cimex lectularius (Hemiptera: Cimicidae)*, 2008; 2008.
55. Sierras, A.; Schal, C., Lethal and Sublethal Effects of Ingested Hydroprene and Methoprene on Development and Fecundity of the Common Bed Bug (Hemiptera: Cimicidae). *Journal of Medical Entomology* **2020**, 57, (4), 1199-1206.
56. Dang, K.; Doggett, S. L.; Veera Singham, G.; Lee, C.-Y., Insecticide resistance and resistance mechanisms in bed bugs, *Cimex* spp. (Hemiptera: Cimicidae). *Parasites & Vectors* **2017**, 10, (1), 318.
57. Zhu, F.; Gujar, H.; Gordon, J. R.; Haynes, K. F.; Potter, M. F.; Palli, S. R., Bed bugs evolved unique adaptive strategy to resist pyrethroid insecticides. *Scientific Reports* **2013**, 3, (1), 1456.
58. La Clair, J. J.; Bantle, J. A.; Dumont, J., Photoproducts and Metabolites of a Common Insect Growth Regulator Produce Developmental Deformities in *Xenopus*. *Environmental Science & Technology* **1998**, 32, (10), 1453-1461.
59. Rajan, K. B.; Weuve, J.; Barnes, L. L.; McAninch, E. A.; Wilson, R. S.; Evans, D. A., Population estimate of people with clinical Alzheimer's disease and mild cognitive impairment in the United States (2020-2060). *Alzheimers Dement* **2021**, 17, (12), 1966-1975.
60. Kumar, A.; Sidhu, J.; Goyal, A.; Tsao, J. W., Alzheimer Disease. In *StatPearls*, StatPearls Publishing
Copyright © 2022, StatPearls Publishing LLC.: Treasure Island (FL), 2022.
61. Selkoe, D. J., Alzheimer's disease: genes, proteins, and therapy. *Physiol Rev* **2001**, 81, (2), 741-66.
62. Herrup, K., The case for rejecting the amyloid cascade hypothesis. *Nature Neuroscience* **2015**, 18, (6), 794-799.
63. Villemagne, V. L.; Burnham, S.; Bourgeat, P.; Brown, B.; Ellis, K. A.; Salvado, O.; Szoek, C.; Macaulay, S. L.; Martins, R.; Maruff, P.; Ames, D.; Rowe, C. C.; Masters, C. L., Amyloid β deposition, neurodegeneration, and cognitive decline in sporadic Alzheimer's disease: a prospective cohort study. *Lancet Neurol* **2013**, 12, (4), 357-67.
64. Fratiglioni, L.; Viitanen, M.; von Strauss, E.; Tontodonati, V.; Herlitz, A.; Winblad, B., Very old women at highest risk of dementia and Alzheimer's disease: incidence data from the Kungsholmen Project, Stockholm. *Neurology* **1997**, 48, (1), 132-8.
65. Lippa, C. F.; Saunders, A. M.; Smith, T. W.; Swearer, J. M.; Drachman, D. A.; Ghetti, B.; Nee, L.; Pulaski-Salo, D.; Dickson, D.; Robitaille, Y.; Bergeron, C.; Crain, B.; Benson, M. D.; Farlow, M.; Hyman, B. T.; George-Hyslop, S. P.; Roses, A. D.; Pollen, D. A., Familial and sporadic Alzheimer's disease: neuropathology cannot exclude a final common pathway. *Neurology* **1996**, 46, (2), 406-12.
66. Saunders, A. M.; Strittmatter, W. J.; Schmechel, D.; George-Hyslop, P. H.; Pericak-Vance, M. A.; Joo, S. H.; Rosi, B. L.; Gusella, J. F.; Crapper-MacLachlan, D. R.; Alberts, M. J.; et al., Association of apolipoprotein E allele epsilon 4 with late-onset familial and sporadic Alzheimer's disease. *Neurology* **1993**, 43, (8), 1467-72.
67. Rajan, K. B.; Barnes, L. L.; Wilson, R. S.; McAninch, E. A.; Weuve, J.; Sighoko, D.; Evans, D. A., Racial Differences in the Association Between Apolipoprotein E Risk Alleles and Overall and Total Cardiovascular Mortality Over 18 Years. *J Am Geriatr Soc* **2017**, 65, (11), 2425-2430.

68. Evans, D. A.; Bennett, D. A.; Wilson, R. S.; Bienias, J. L.; Morris, M. C.; Scherr, P. A.; Hebert, L. E.; Aggarwal, N.; Beckett, L. A.; Joglekar, R.; Berry-Kravis, E.; Schneider, J., Incidence of Alzheimer disease in a biracial urban community: relation to apolipoprotein E allele status. *Arch Neurol* **2003**, 60, (2), 185-9.
69. Tang, M. X.; Stern, Y.; Marder, K.; Bell, K.; Gurland, B.; Lantigua, R.; Andrews, H.; Feng, L.; Tycko, B.; Mayeux, R., The APOE-epsilon4 allele and the risk of Alzheimer disease among African Americans, whites, and Hispanics. *Jama* **1998**, 279, (10), 751-5.
70. De Strooper, B.; Iwatsubo, T.; Wolfe, M. S., Presenilins and γ -secretase: structure, function, and role in Alzheimer Disease. *Cold Spring Harb Perspect Med* **2012**, 2, (1), a006304.
71. Hithersay, R.; Hamburg, S.; Knight, B.; Strydom, A., Cognitive decline and dementia in Down syndrome. *Curr Opin Psychiatry* **2017**, 30, (2), 102-107.
72. Van Cauwenberghe, C.; Van Broeckhoven, C.; Sleegers, K., The genetic landscape of Alzheimer disease: clinical implications and perspectives. *Genet Med* **2016**, 18, (5), 421-30.
73. Hung, S. Y.; Fu, W. M., Drug candidates in clinical trials for Alzheimer's disease. *J Biomed Sci* **2017**, 24, (1), 47.
74. Hardy, J.; Selkoe, D. J., The amyloid hypothesis of Alzheimer's disease: progress and problems on the road to therapeutics. *Science* **2002**, 297, (5580), 353-6.
75. Krassnig, S.; Schweinzer, C.; Taub, N.; Havas, D.; Auer, E.; Flunkert, S.; Schreiber, W.; Hutter-Paier, B.; Windisch, M., Influence of Lentiviral β -Synuclein Overexpression in the Hippocampus of a Transgenic Mouse Model of Alzheimer's Disease on Amyloid Precursor Protein Metabolism and Pathology. *Neurodegener Dis* **2015**, 15, (4), 243-57.
76. Zhang, Y. W.; Thompson, R.; Zhang, H.; Xu, H., APP processing in Alzheimer's disease. *Mol Brain* **2011**, 4, 3.
77. Lichtenthaler, S. F.; Haass, C.; Steiner, H., Regulated intramembrane proteolysis--lessons from amyloid precursor protein processing. *J Neurochem* **2011**, 117, (5), 779-96.
78. Thinakaran, G.; Koo, E. H., Amyloid precursor protein trafficking, processing, and function. *J Biol Chem* **2008**, 283, (44), 29615-9.
79. Rowe, C. C.; Villemagne, V. L., Amyloid imaging with PET in early Alzheimer disease diagnosis. *Med Clin North Am* **2013**, 97, (3), 377-98.
80. Villemagne, V. L.; Pike, K. E.; Chételat, G.; Ellis, K. A.; Mulligan, R. S.; Bourgeat, P.; Ackermann, U.; Jones, G.; Szoëke, C.; Salvado, O.; Martins, R.; O'Keefe, G.; Mathis, C. A.; Klunk, W. E.; Ames, D.; Masters, C. L.; Rowe, C. C., Longitudinal assessment of A β and cognition in aging and Alzheimer disease. *Ann Neurol* **2011**, 69, (1), 181-92.
81. Kim, J.; Chakrabarty, P.; Hanna, A.; March, A.; Dickson, D. W.; Borchelt, D. R.; Golde, T.; Janus, C., Normal cognition in transgenic BRI2-A β mice. *Mol Neurodegener* **2013**, 8, 15.
82. Spires-Jones, T. L.; Hyman, B. T., The intersection of amyloid beta and tau at synapses in Alzheimer's disease. *Neuron* **2014**, 82, (4), 756-71.
83. Frost, B.; Jacks, R. L.; Diamond, M. I., Propagation of tau misfolding from the outside to the inside of a cell. *J Biol Chem* **2009**, 284, (19), 12845-52.
84. Nukina, N.; Ihara, Y., One of the antigenic determinants of paired helical filaments is related to tau protein. *J Biochem* **1986**, 99, (5), 1541-4.
85. Grundke-Iqbal, I.; Iqbal, K.; Quinlan, M.; Tung, Y. C.; Zaidi, M. S.; Wisniewski, H. M., Microtubule-associated protein tau. A component of Alzheimer paired helical filaments. *J Biol Chem* **1986**, 261, (13), 6084-9.
86. DeKosky, S. T., Epidemiology and pathophysiology of Alzheimer's disease. *Clin Cornerstone* **2001**, 3, (4), 15-26.

87. Dumas, J. A.; Newhouse, P. A., The cholinergic hypothesis of cognitive aging revisited again: cholinergic functional compensation. *Pharmacol Biochem Behav* **2011**, 99, (2), 254-61.
88. Zimmer, H. G., Otto Loewi and the chemical transmission of vagus stimulation in the heart. *Clin Cardiol* **2006**, 29, (3), 135-6.
89. Francis, P. T.; Palmer, A. M.; Snape, M.; Wilcock, G. K., The cholinergic hypothesis of Alzheimer's disease: a review of progress. *J Neurol Neurosurg Psychiatry* **1999**, 66, (2), 137-47.
90. Fotiou, D.; Kaltsatou, A.; Tsiptsios, D.; Nakou, M., Evaluation of the cholinergic hypothesis in Alzheimer's disease with neuropsychological methods. *Aging Clin Exp Res* **2015**, 27, (5), 727-33.
91. Atack, J. R.; Perry, E. K.; Bonham, J. R.; Perry, R. H.; Tomlinson, B. E.; Blessed, G.; Fairbairn, A., Molecular forms of acetylcholinesterase in senile dementia of Alzheimer type: selective loss of the intermediate (10S) form. *Neurosci Lett* **1983**, 40, (2), 199-204.
92. Aupperle, P. M., Navigating patients and caregivers through the course of Alzheimer's disease. *J Clin Psychiatry* **2006**, 67 Suppl 3, 8-14; quiz 23.
93. Jones, D. P., Redefining oxidative stress. *Antioxid Redox Signal* **2006**, 8, (9-10), 1865-79.
94. Hauptmann, N.; Grimsby, J.; Shih, J. C.; Cadenas, E., The metabolism of tyramine by monoamine oxidase A/B causes oxidative damage to mitochondrial DNA. *Arch Biochem Biophys* **1996**, 335, (2), 295-304.
95. Di Meo, S.; Reed, T. T.; Venditti, P.; Victor, V. M., Role of ROS and RNS Sources in Physiological and Pathological Conditions. *Oxid Med Cell Longev* **2016**, 2016, 1245049.
96. Praticò, D., Evidence of oxidative stress in Alzheimer's disease brain and antioxidant therapy: lights and shadows. *Ann N Y Acad Sci* **2008**, 1147, 70-8.
97. Lovell, M. A.; Gabbita, S. P.; Markesbery, W. R., Increased DNA oxidation and decreased levels of repair products in Alzheimer's disease ventricular CSF. *J Neurochem* **1999**, 72, (2), 771-6.
98. Mecocci, P.; MacGarvey, U.; Beal, M. F., Oxidative damage to mitochondrial DNA is increased in Alzheimer's disease. *Ann Neurol* **1994**, 36, (5), 747-51.
99. Feng, Y.; Wang, X., Antioxidant therapies for Alzheimer's disease. *Oxid Med Cell Longev* **2012**, 2012, 472932.
100. Bagyinszky, E.; Giau, V. V.; Shim, K.; Suk, K.; An, S. S. A.; Kim, S., Role of inflammatory molecules in the Alzheimer's disease progression and diagnosis. *J Neurol Sci* **2017**, 376, 242-254.
101. Latta, C. H.; Brothers, H. M.; Wilcock, D. M., Neuroinflammation in Alzheimer's disease; A source of heterogeneity and target for personalized therapy. *Neuroscience* **2015**, 302, 103-11.
102. Phillips, E. C.; Croft, C. L.; Kurbatskaya, K.; O'Neill, M. J.; Hutton, M. L.; Hanger, D. P.; Garwood, C. J.; Noble, W., Astrocytes and neuroinflammation in Alzheimer's disease. *Biochem Soc Trans* **2014**, 42, (5), 1321-5.
103. McGeer, E. G.; McGeer, P. L., Neuroinflammation in Alzheimer's disease and mild cognitive impairment: a field in its infancy. *J Alzheimers Dis* **2010**, 19, (1), 355-61.
104. Steiner, J.; Bogerts, B.; Schroeter, M. L.; Bernstein, H. G., S100B protein in neurodegenerative disorders. *Clin Chem Lab Med* **2011**, 49, (3), 409-24.
105. Mori, T.; Asano, T.; Town, T., Targeting S100B in Cerebral Ischemia and in Alzheimer's Disease. *Cardiovasc Psychiatry Neurol* **2010**, 2010.

106. Michaud, M.; Balardy, L.; Moulis, G.; Gaudin, C.; Peyrot, C.; Vellas, B.; Cesari, M.; Nourhashemi, F., Proinflammatory cytokines, aging, and age-related diseases. *J Am Med Dir Assoc* **2013**, 14, (12), 877-82.
107. Liu, P. P.; Xie, Y.; Meng, X. Y.; Kang, J. S., History and progress of hypotheses and clinical trials for Alzheimer's disease. *Signal Transduct Target Ther* **2019**, 4, 29.
108. Cummings, J., Disease modification and Neuroprotection in neurodegenerative disorders. *Transl Neurodegener* **2017**, 6, 25.
109. Galimberti, D.; Scarpini, E., Disease-modifying treatments for Alzheimer's disease. *Ther Adv Neurol Disord* **2011**, 4, (4), 203-16.
110. Cummings, J.; Fox, N., Defining Disease Modifying Therapy for Alzheimer's Disease. *J Prev Alzheimers Dis* **2017**, 4, (2), 109-115.
111. Alfirevic, A.; Mills, T.; Carr, D.; Barratt, B. J.; Jawaid, A.; Sherwood, J.; Smith, J. C.; Tugwood, J.; Hartkoorn, R.; Owen, A.; Park, K. B.; Pirmohamed, M., Tacrine-induced liver damage: an analysis of 19 candidate genes. *Pharmacogenet Genomics* **2007**, 17, (12), 1091-100.
112. Cummings, J.; Lee, G.; Ritter, A.; Sabbagh, M.; Zhong, K., Alzheimer's disease drug development pipeline: 2020. *Alzheimers Dement (N Y)* **2020**, 6, (1), e12050.
113. Karran, E.; Mercken, M.; De Strooper, B., The amyloid cascade hypothesis for Alzheimer's disease: an appraisal for the development of therapeutics. *Nat Rev Drug Discov* **2011**, 10, (9), 698-712.
114. Tomita, T., Secretase inhibitors and modulators for Alzheimer's disease treatment. *Expert Rev Neurother* **2009**, 9, (5), 661-79.
115. Fahrenholz, F.; Postina, R., Alpha-secretase activation--an approach to Alzheimer's disease therapy. *Neurodegener Dis* **2006**, 3, (4-5), 255-61.
116. Mudher, A.; Lovestone, S., Alzheimer's disease--do taoists and baptists finally shake hands? *Trends Neurosci* **2002**, 25, (1), 22-6.
117. Blaikie, L.; Kay, G.; Kong Thoo Lin, P., Current and emerging therapeutic targets of alzheimer's disease for the design of multi-target directed ligands. *Medchemcomm* **2019**, 10, (12), 2052-2072.
118. Cummings, J.; Aisen, P.; Lemere, C.; Atri, A.; Sabbagh, M.; Salloway, S., Aducanumab produced a clinically meaningful benefit in association with amyloid lowering. *Alzheimers Res Ther* **2021**, 13, (1), 98.
119. Mangialasche, F.; Solomon, A.; Winblad, B.; Mecocci, P.; Kivipelto, M., Alzheimer's disease: clinical trials and drug development. *Lancet Neurol* **2010**, 9, (7), 702-16.
120. Salomone, S.; Caraci, F.; Leggio, G. M.; Fedotova, J.; Drago, F., New pharmacological strategies for treatment of Alzheimer's disease: focus on disease modifying drugs. *Br J Clin Pharmacol* **2012**, 73, (4), 504-17.
121. Bolognesi, M. L.; Rosini, M.; Andrisano, V.; Bartolini, M.; Minarini, A.; Tumiatti, V.; Melchiorre, C., MTDL design strategy in the context of Alzheimer's disease: from lipocrine to memoquin and beyond. *Curr Pharm Des* **2009**, 15, (6), 601-13.
122. Reed, L. J.; De, B. B.; Gunsalus, I. C.; Hornberger, C. S., Jr., Crystalline alpha-lipoic acid; a catalytic agent associated with pyruvate dehydrogenase. *Science* **1951**, 114, (2952), 93-4.
123. Smith, A. R.; Shenvi, S. V.; Widlansky, M.; Suh, J. H.; Hagen, T. M., Lipoic acid as a potential therapy for chronic diseases associated with oxidative stress. *Curr Med Chem* **2004**, 11, (9), 1135-46.

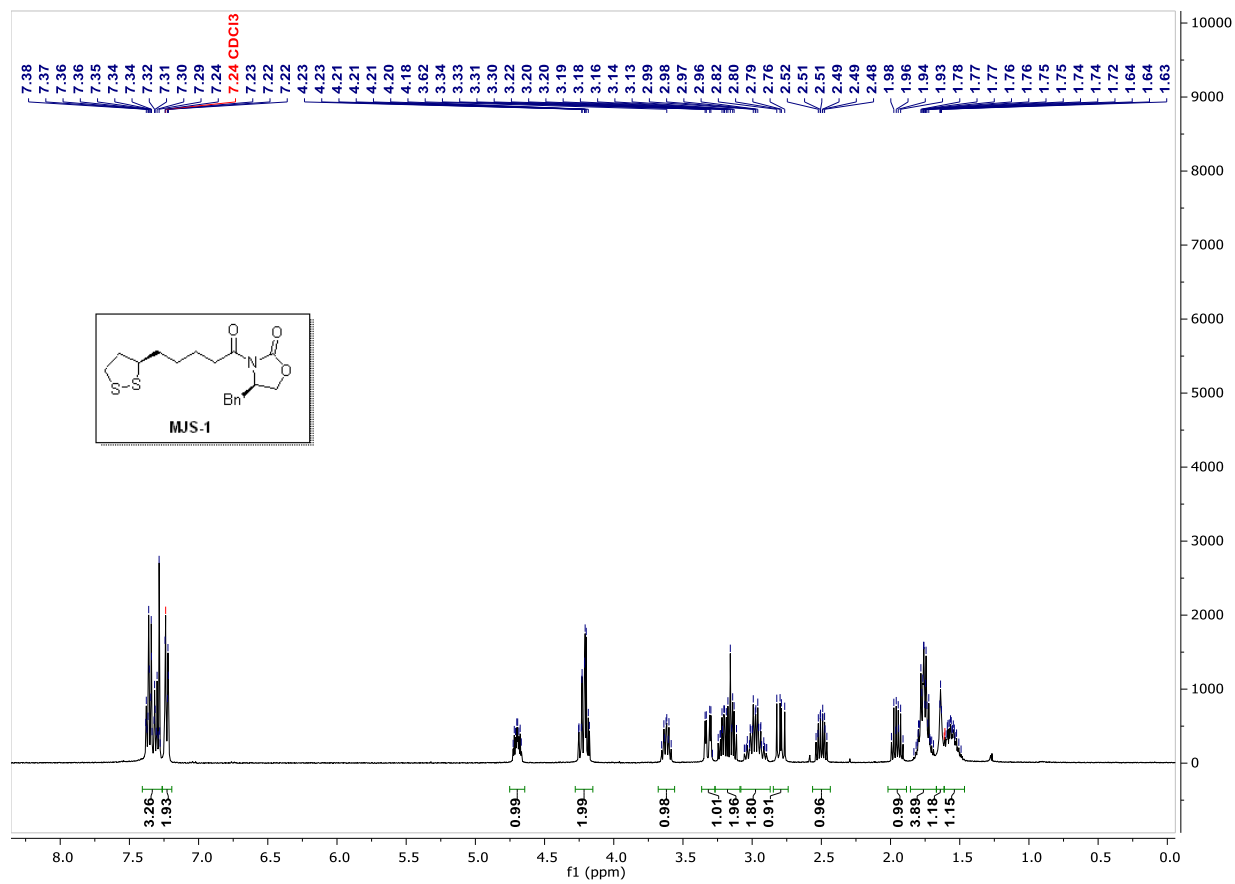
124. Maczurek, A.; Hager, K.; Kenklies, M.; Sharman, M.; Martins, R.; Engel, J.; Carlson, D. A.; Münch, G., Lipoic acid as an anti-inflammatory and neuroprotective treatment for Alzheimer's disease. *Adv Drug Deliv Rev* **2008**, 60, (13-14), 1463-70.
125. Searls, R. L.; Sanadi, D. R., alpha-Ketoglutaric dehydrogenase. 8. Isolation and some properties of a flavoprotein component. *J Biol Chem* **1960**, 235, 2485-91.
126. Chavan, S. P.; Pawar, K. P.; Praveen, C.; Patil, N. B., Chirality induction and chiron approaches to enantioselective total synthesis of α -lipoic acid. *Tetrahedron* **2015**, 71, (24), 4213-4218.
127. Molz, P.; Schröder, N., Potential Therapeutic Effects of Lipoic Acid on Memory Deficits Related to Aging and Neurodegeneration. *Frontiers in Pharmacology* **2017**, 8.
128. Huang, X.; Atwood, C. S.; Hartshorn, M. A.; Multhaup, G.; Goldstein, L. E.; Scarpa, R. C.; Cuajungco, M. P.; Gray, D. N.; Lim, J.; Moir, R. D.; Tanzi, R. E.; Bush, A. I., The A β Peptide of Alzheimer's Disease Directly Produces Hydrogen Peroxide through Metal Ion Reduction. *Biochemistry* **1999**, 38, (24), 7609-7616.
129. Watson, G. S.; Craft, S., The role of insulin resistance in the pathogenesis of Alzheimer's disease: implications for treatment. *CNS Drugs* **2003**, 17, (1), 27-45.
130. Wong, A.; Dukic-Stefanovic, S.; Gasic-Milenkovic, J.; Schinzel, R.; Wiesinger, H.; Riederer, P.; Münch, G., Anti-inflammatory antioxidants attenuate the expression of inducible nitric oxide synthase mediated by advanced glycation endproducts in murine microglia. *Eur J Neurosci* **2001**, 14, (12), 1961-7.
131. Bierhaus, A.; Chevion, S.; Chevion, M.; Hofmann, M.; Quehenberger, P.; Illmer, T.; Luther, T.; Berentshtein, E.; Tritschler, H.; Müller, M.; Wahl, P.; Ziegler, R.; Nawroth, P. P., Advanced glycation end product-induced activation of NF-kappaB is suppressed by alpha-lipoic acid in cultured endothelial cells. *Diabetes* **1997**, 46, (9), 1481-90.
132. Fonte, J.; Miklossy, J.; Atwood, C.; Martins, R., The severity of cortical Alzheimer's type changes is positively correlated with increased amyloid-beta Levels: Resolubilization of amyloid-beta with transition metal ion chelators. *J Alzheimers Dis* **2001**, 3, (2), 209-219.
133. Arivazhagan, P.; Ramanathan, K.; Panneerselvam, C., Effect of DL-alpha-lipoic acid on mitochondrial enzymes in aged rats. *Chem Biol Interact* **2001**, 138, (2), 189-98.
134. Quinn, J. F.; Bussiere, J. R.; Hammond, R. S.; Montine, T. J.; Henson, E.; Jones, R. E.; Stackman, R. W., Jr., Chronic dietary alpha-lipoic acid reduces deficits in hippocampal memory of aged Tg2576 mice. *Neurobiol Aging* **2007**, 28, (2), 213-25.
135. Tateishi, N.; Mori, T.; Kagamiishi, Y.; Satoh, S.; Katsube, N.; Morikawa, E.; Morimoto, T.; Matsui, T.; Asano, T., Astrocytic activation and delayed infarct expansion after permanent focal ischemia in rats. Part II: suppression of astrocytic activation by a novel agent (R)-(-)-2-propyloctanoic acid (ONO-2506) leads to mitigation of delayed infarct expansion and early improvement of neurologic deficits. *J Cereb Blood Flow Metab* **2002**, 22, (6), 723-34.
136. Mori, T.; Town, T.; Tan, J.; Yada, N.; Horikoshi, Y.; Yamamoto, J.; Shimoda, T.; Kamanaka, Y.; Tateishi, N.; Asano, T., Arundic Acid ameliorates cerebral amyloidosis and gliosis in Alzheimer transgenic mice. *J Pharmacol Exp Ther* **2006**, 318, (2), 571-8.
137. Mori, T.; Koyama, N.; Arendash, G. W.; Horikoshi-Sakuraba, Y.; Tan, J.; Town, T., Overexpression of human S100B exacerbates cerebral amyloidosis and gliosis in the Tg2576 mouse model of Alzheimer's disease. *Glia* **2010**, 58, (3), 300-14.
138. Fernandes, R. A.; Ingle, A. B., Arundic acid a potential neuroprotective agent: biological development and syntheses. *Curr Med Chem* **2013**, 20, (18), 2315-29.

139. van den Berg, H., Global status of DDT and its alternatives for use in vector control to prevent disease. *Environ Health Perspect* **2009**, 117, (11), 1656-63.
140. SLÁMA, K., A new look at the nature of insect juvenile hormone with particular reference to studies carried out in the Czech Republic. *EJE* **2015**, 112, (4), 567-590.
141. Dhadialla, T.; Retnakaran, A.; Smagghe, G., Insect growth- and development-disrupting insecticides. *Comprehensive Molecular Insect Science* **2005**, 6, 55-116.
142. Delaunay, P.; Blanc, V.; Del Giudice, P.; Levy-Bencheton, A.; Chosidow, O.; Marty, P.; Brouqui, P., Bedbugs and infectious diseases. *Clin Infect Dis* **2011**, 52, (2), 200-10.
143. Sierras, A.; Schal, C., Lethal and Sublethal Effects of Ingested Hydroprene and Methoprene on Development and Fecundity of the Common Bed Bug (Hemiptera: Cimicidae). *J Med Entomol* **2020**, 57, (4), 1199-1206.

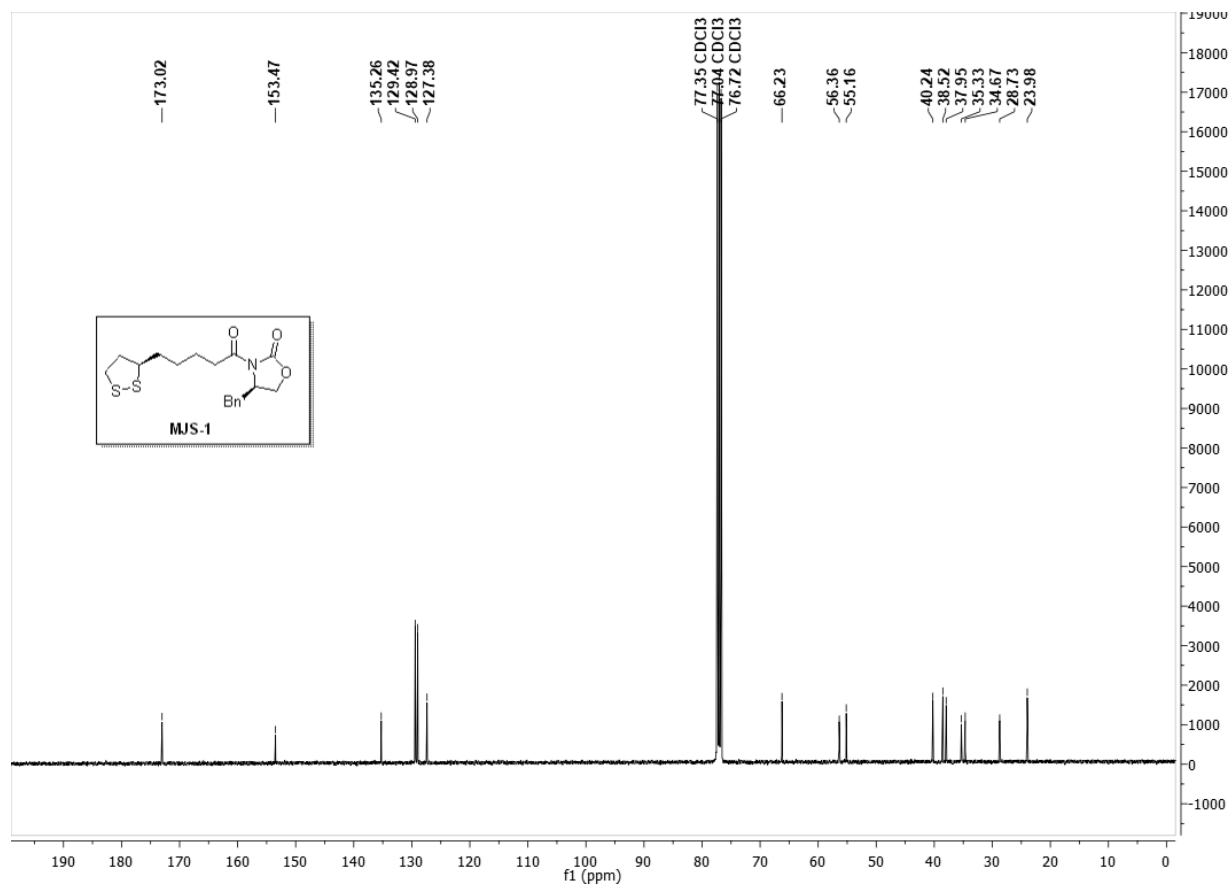
APPENDIX

APPENDIX 1. SUPPLEMENTARY DATA-CHAPTER III

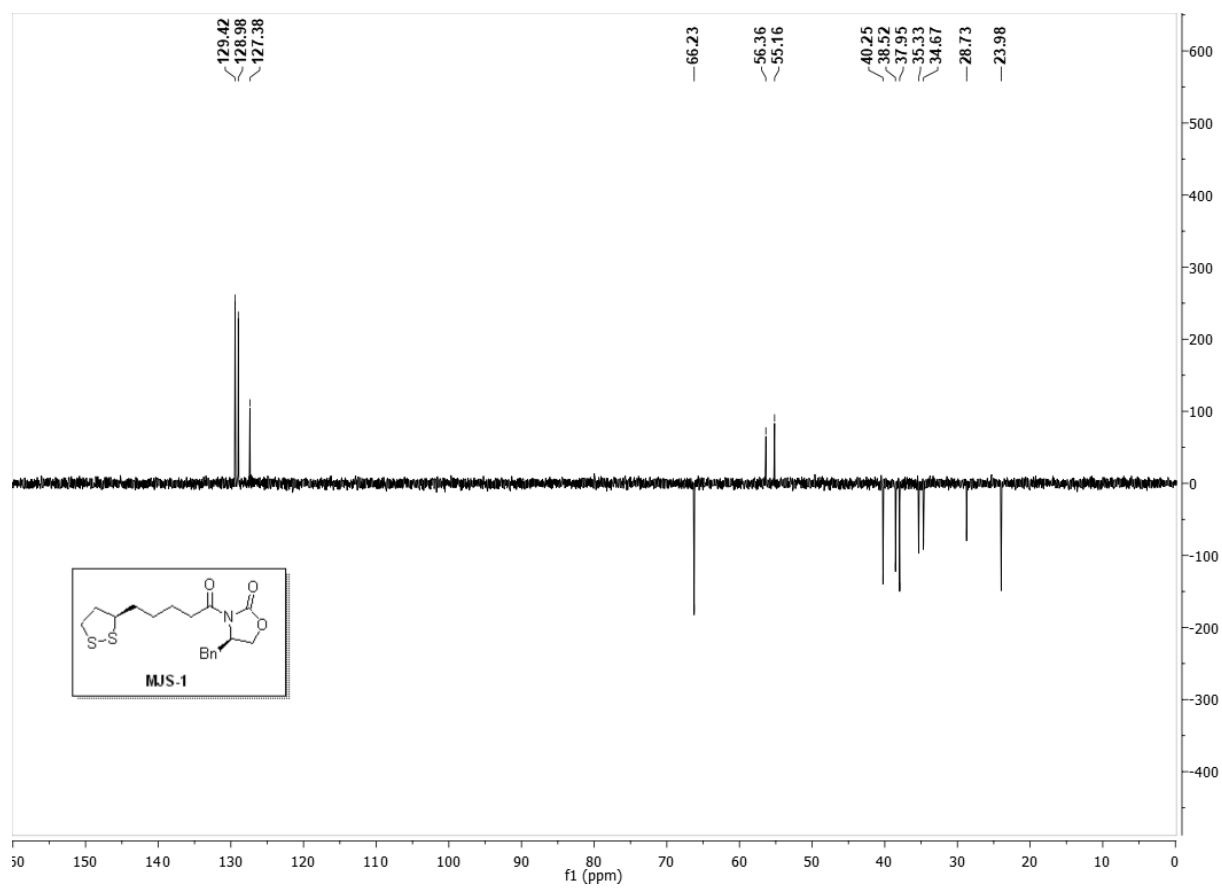
¹H NMR (400 MHz, Chloroform-d) for **MJS-1**



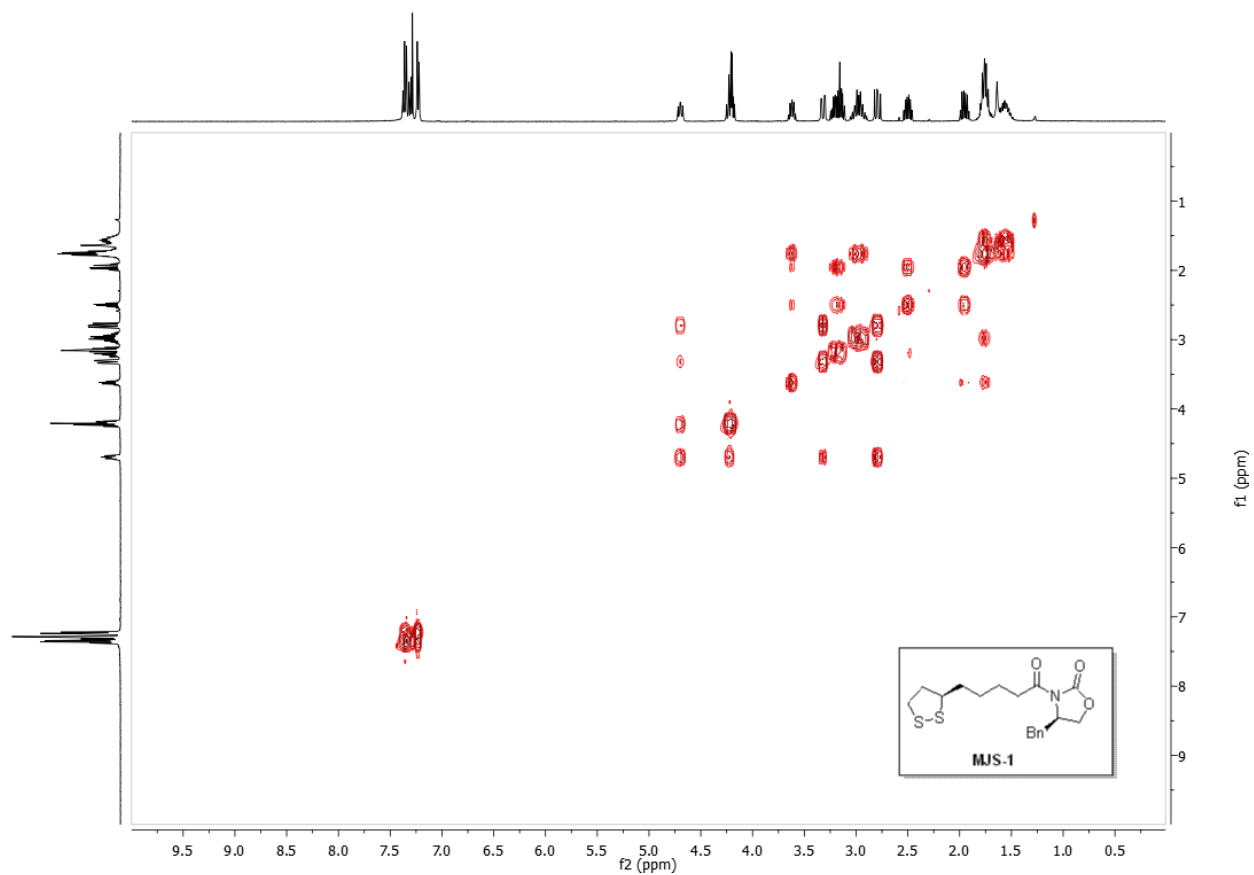
^{13}C NMR (101 MHz, Chloroform-d) for **MJS-1**



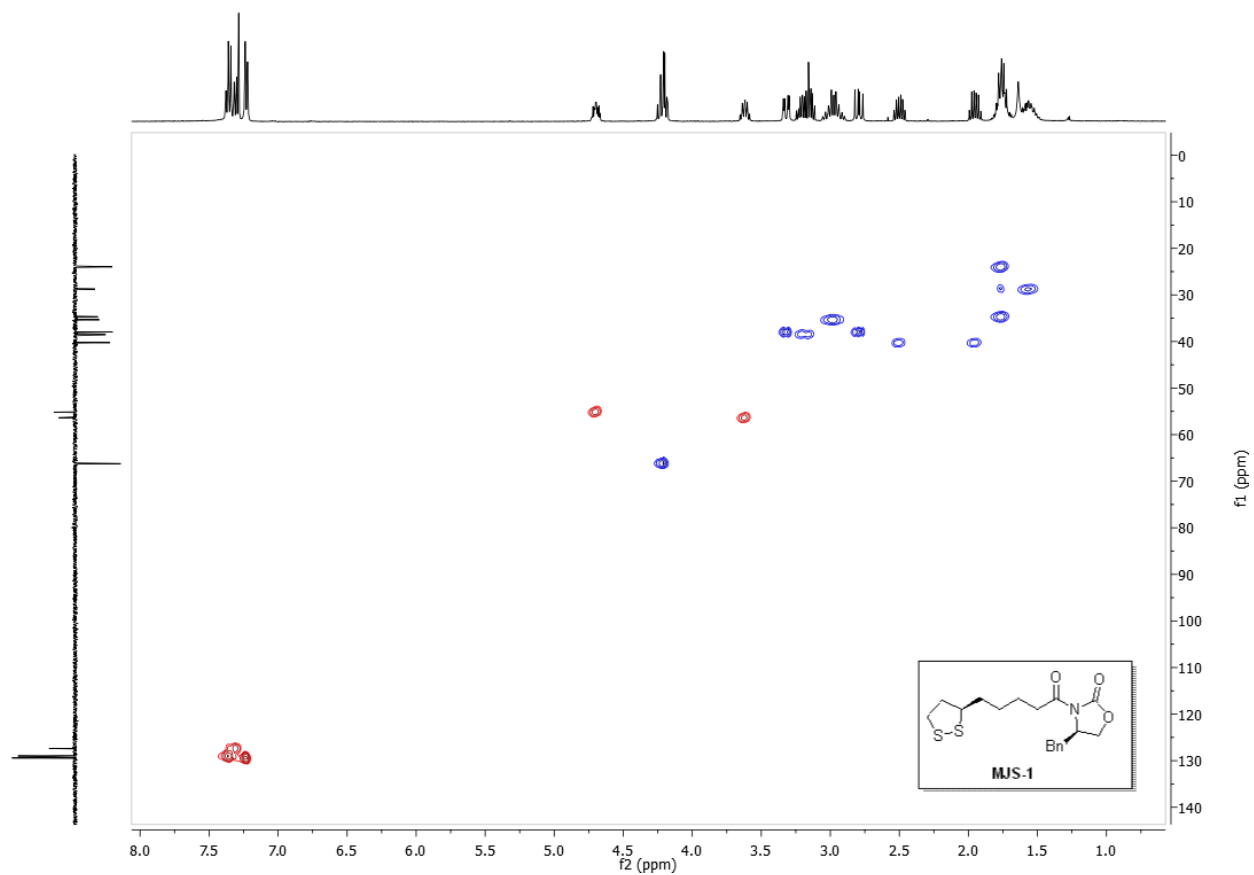
DEPT 135 (Chloroform-d) for **MJS-1**



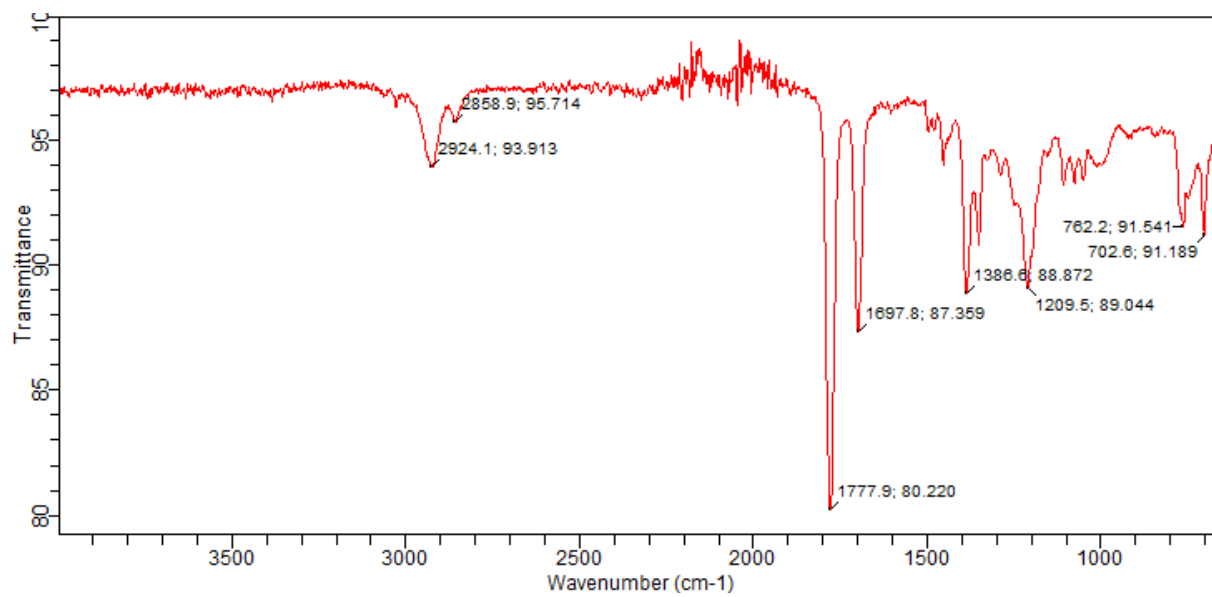
H-H COSY (Chloroform-d) for MJS-1



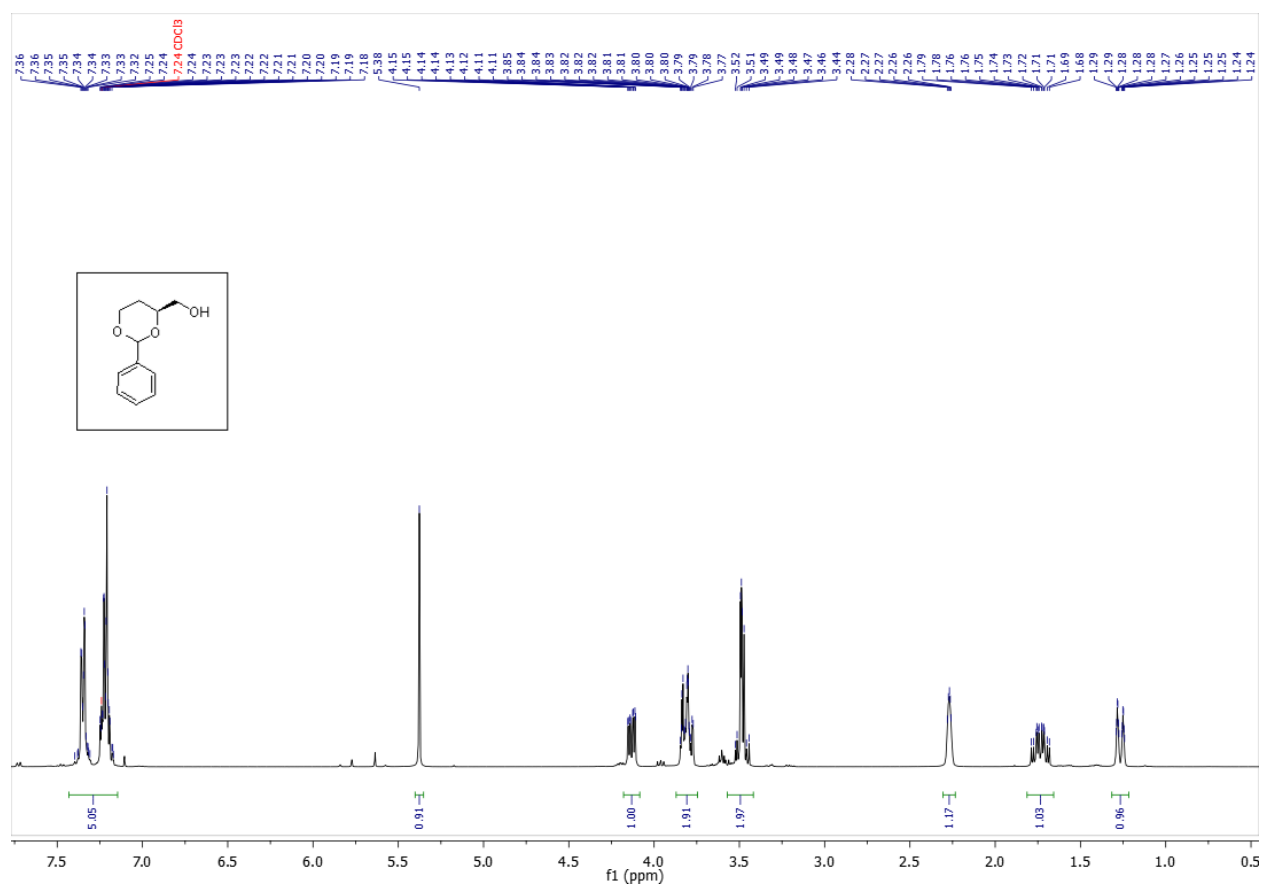
HSQC (Chloroform-d) for MJS-1



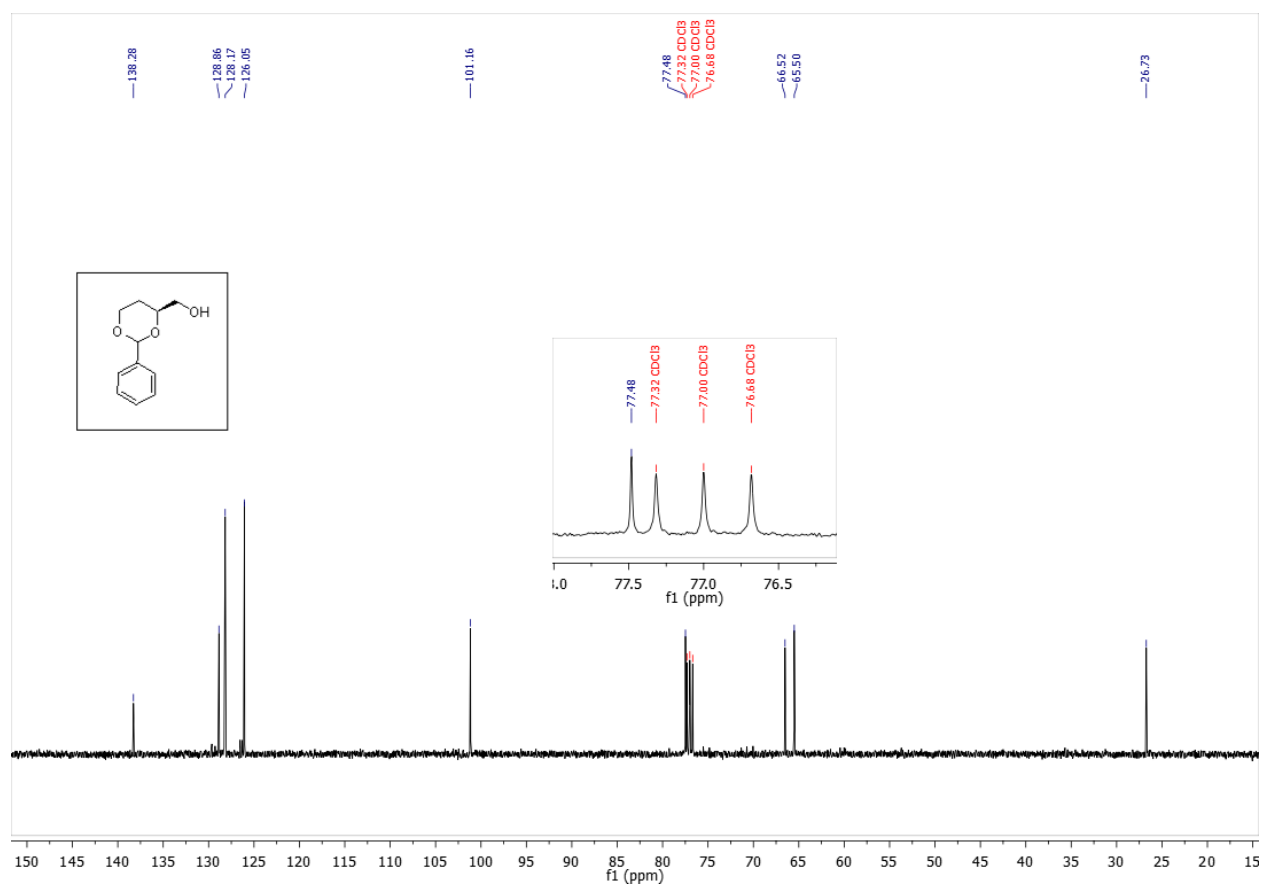
IR (KBr) for MJS-1



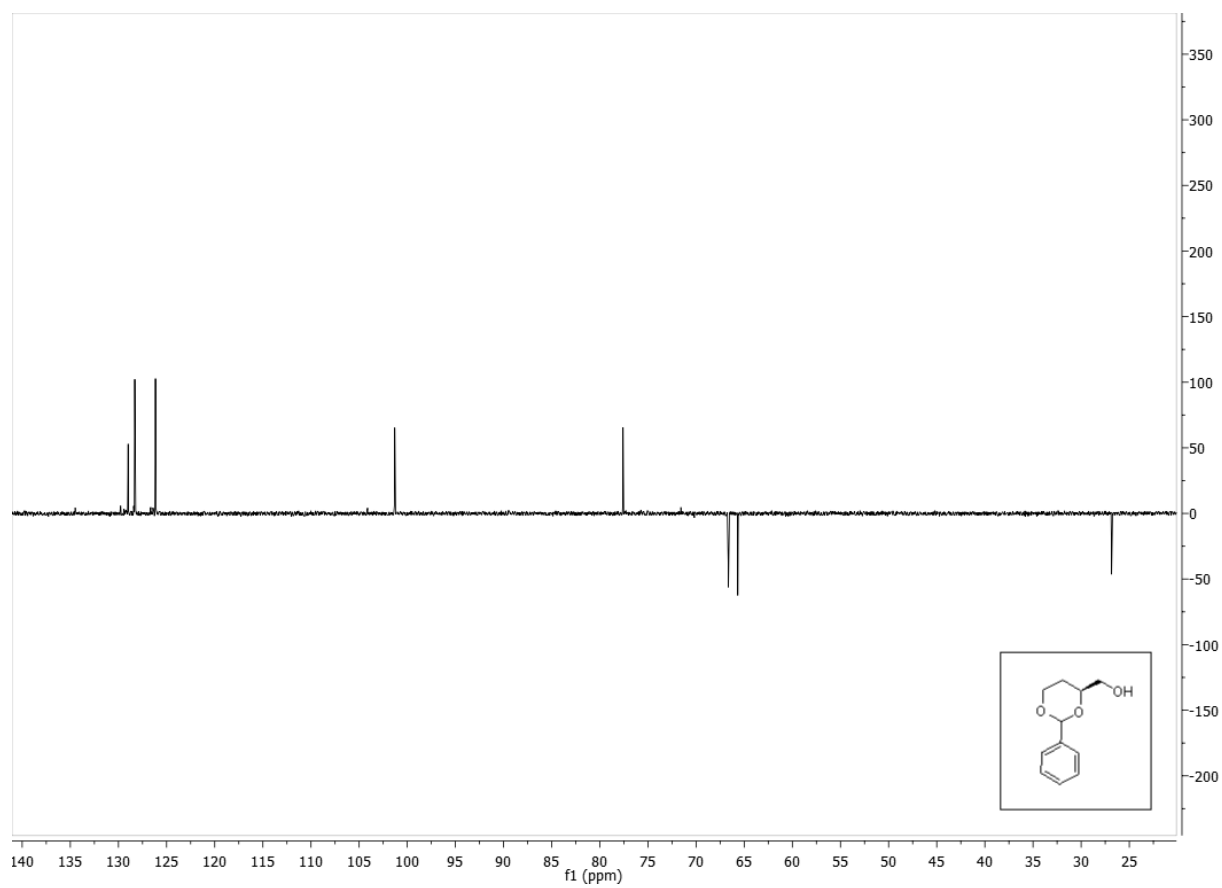
¹H NMR (400 MHz, Chloroform-d) for **12a**



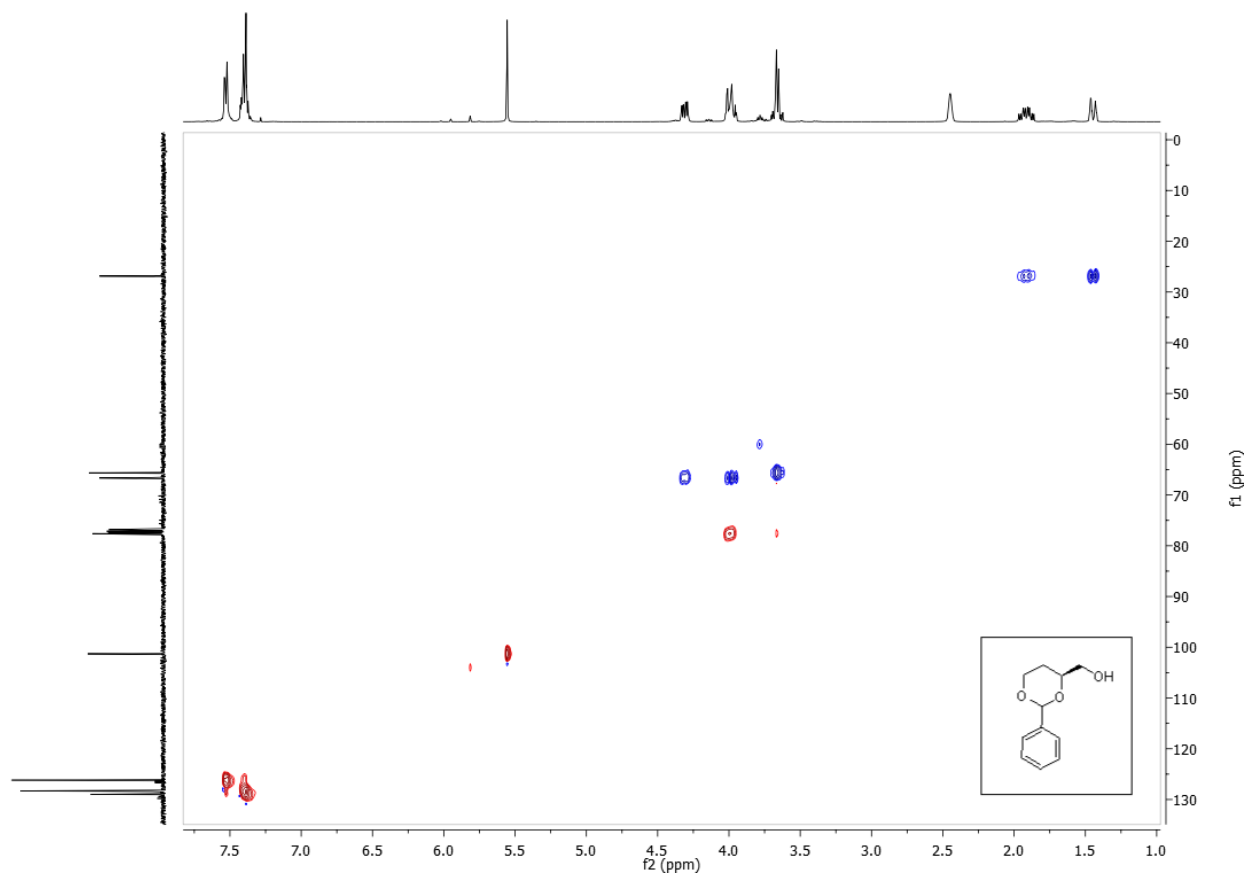
^{13}C NMR (101 MHz, Chloroform-d) for **12a**



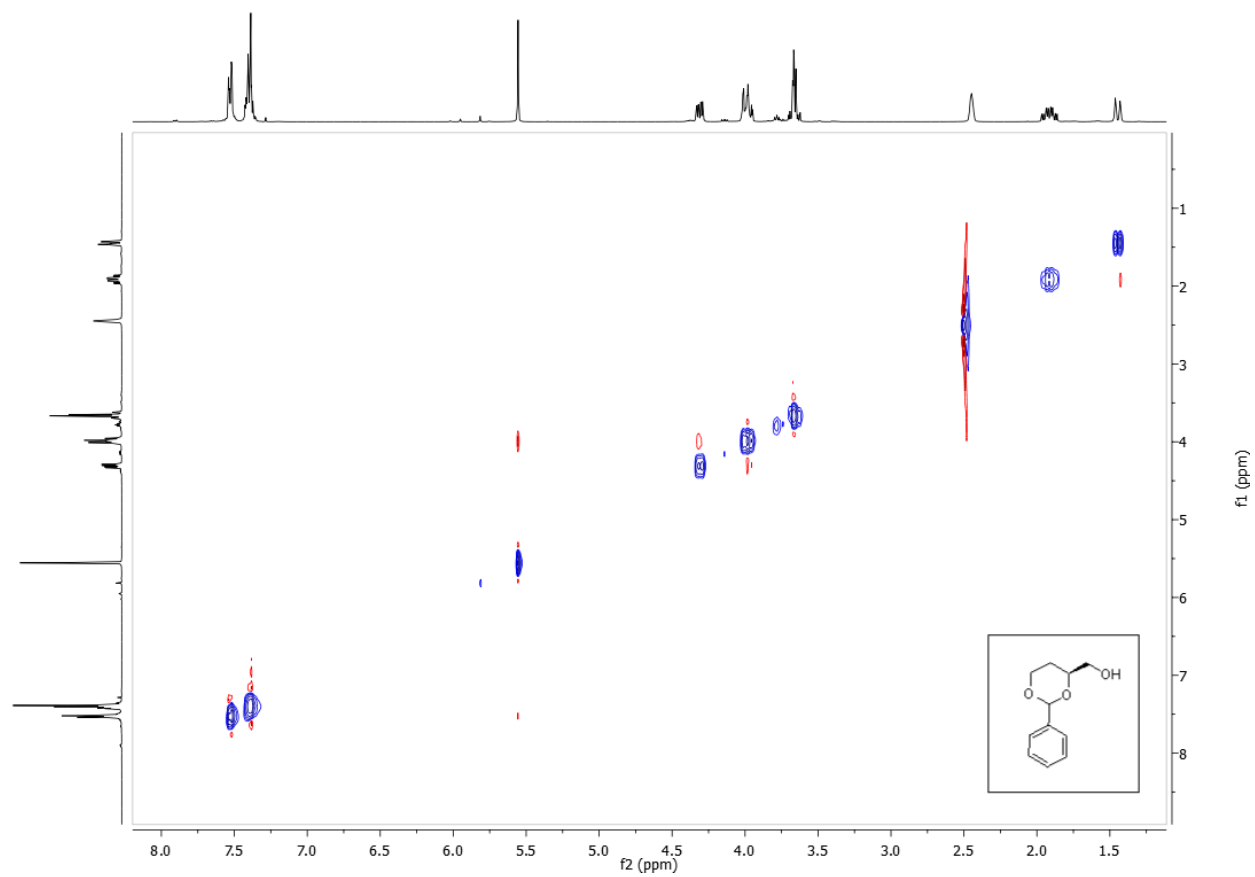
DEPT 135 (Chloroform-d) for **12a**



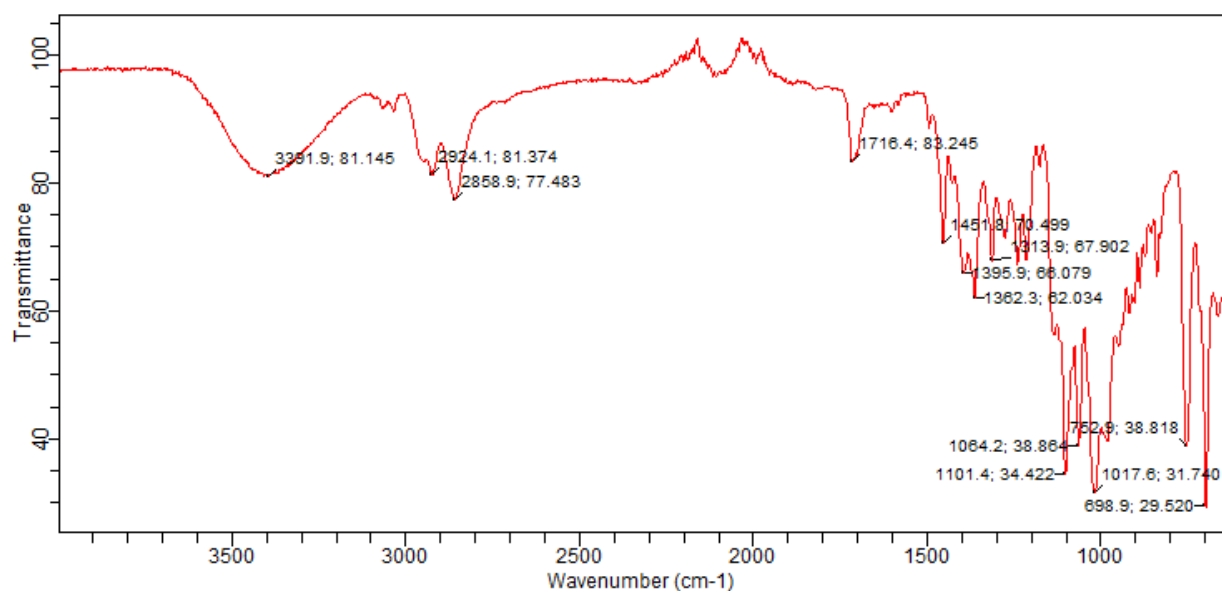
HSQC (Chloroform-d) for **12a**



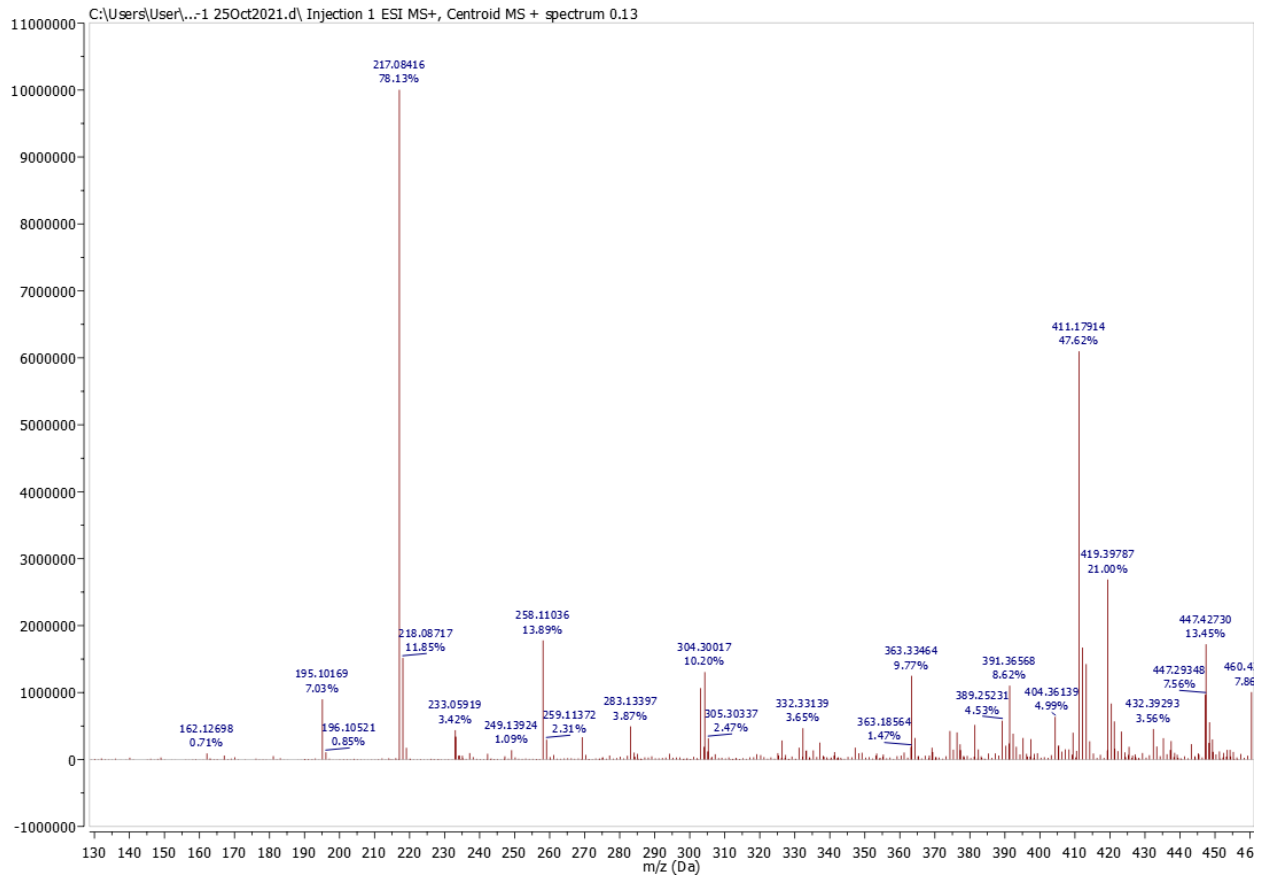
NOESY (Chloroform-d) for **12a**



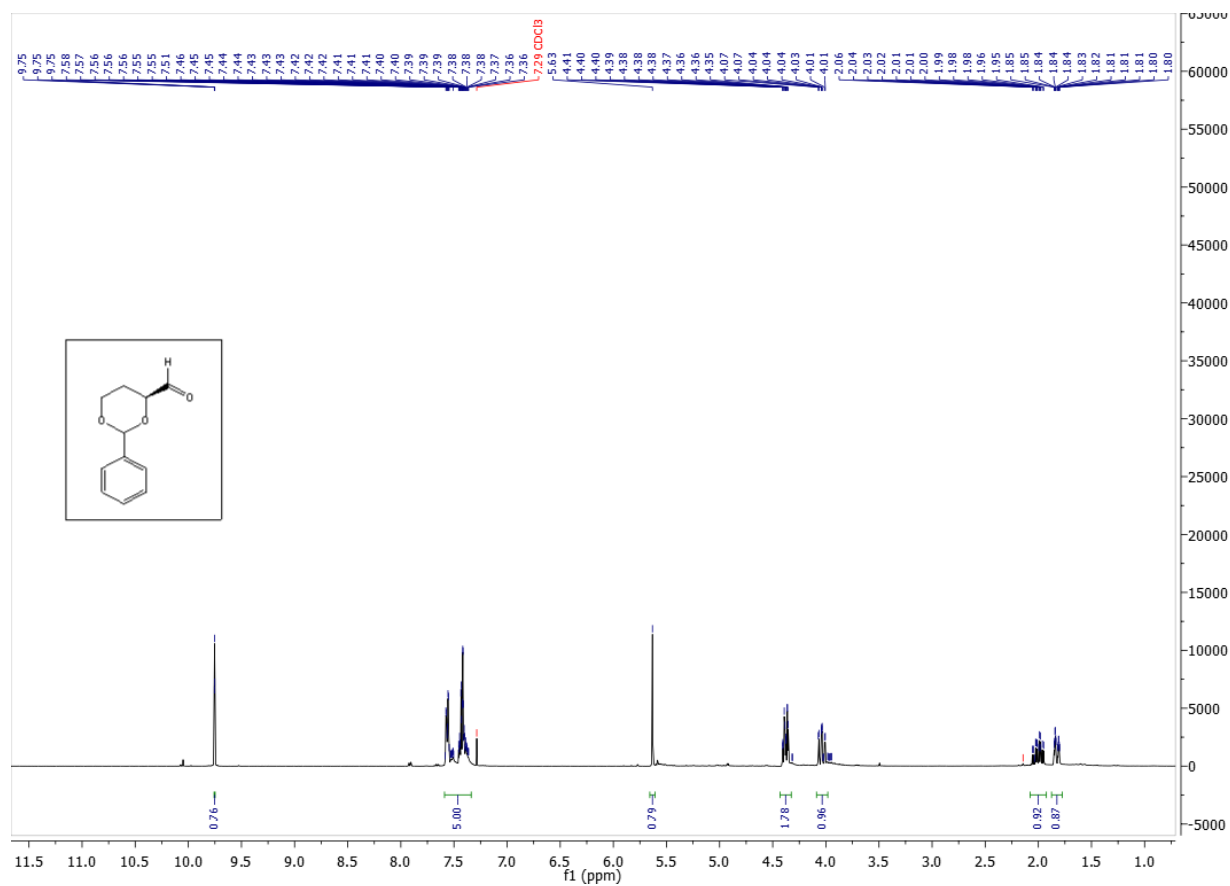
IR (KBr) for **12a**



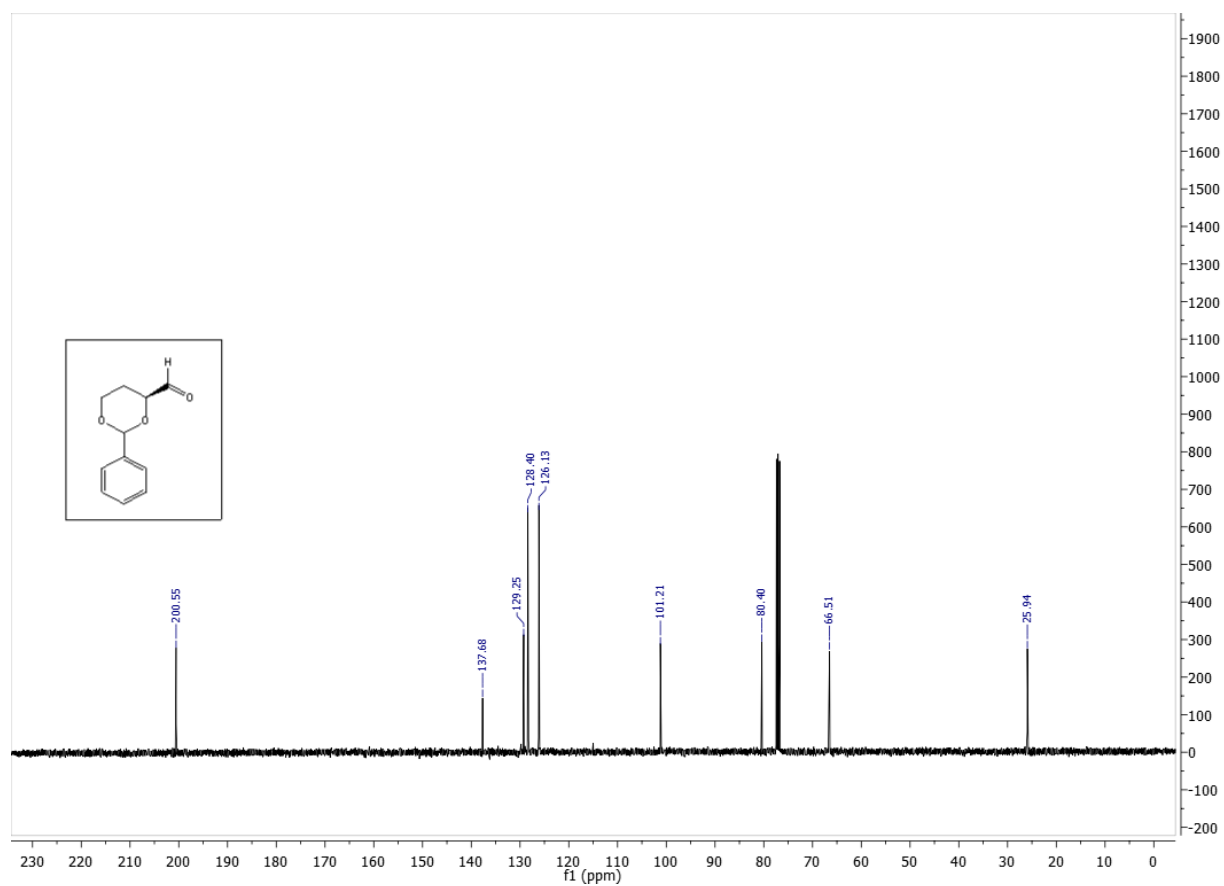
HRESIMS for 12a



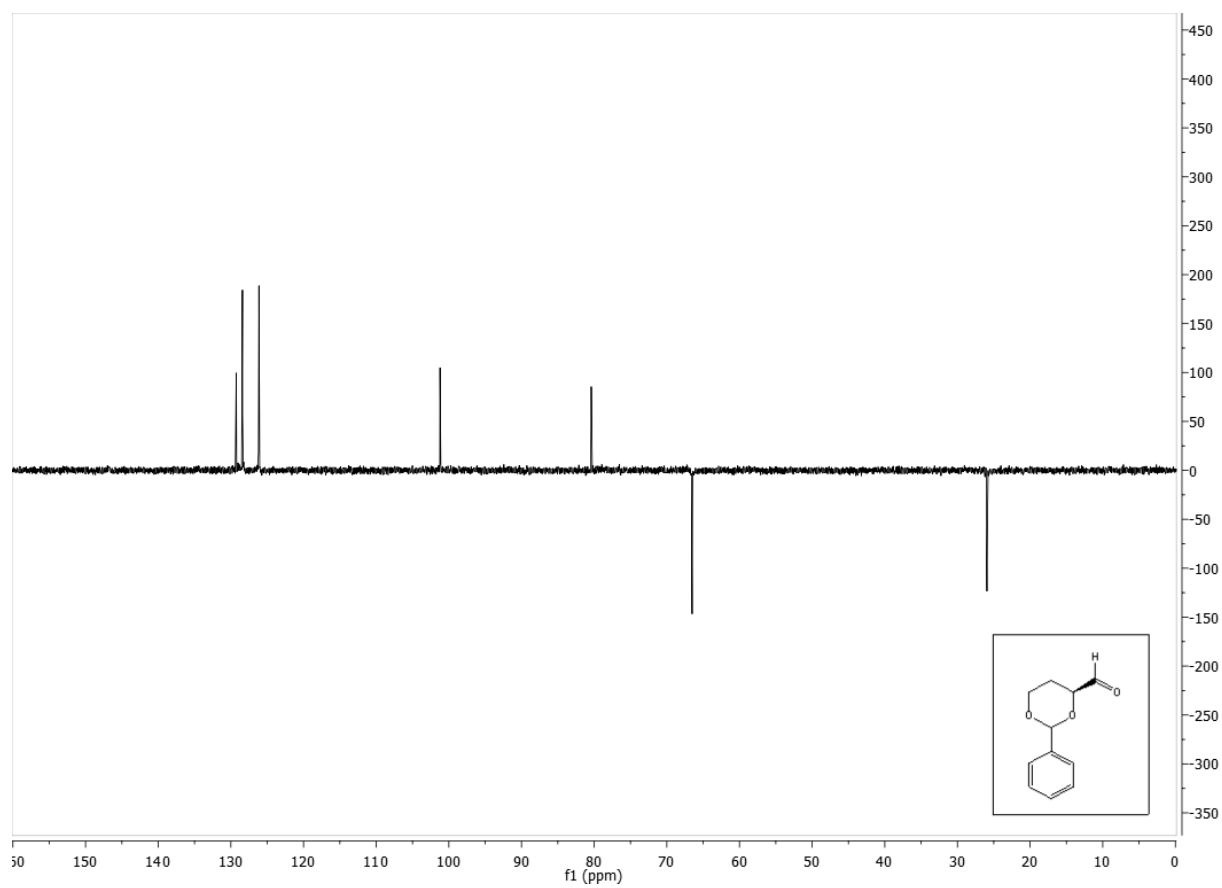
¹H NMR (400 MHz, Chloroform-d) for **11a**



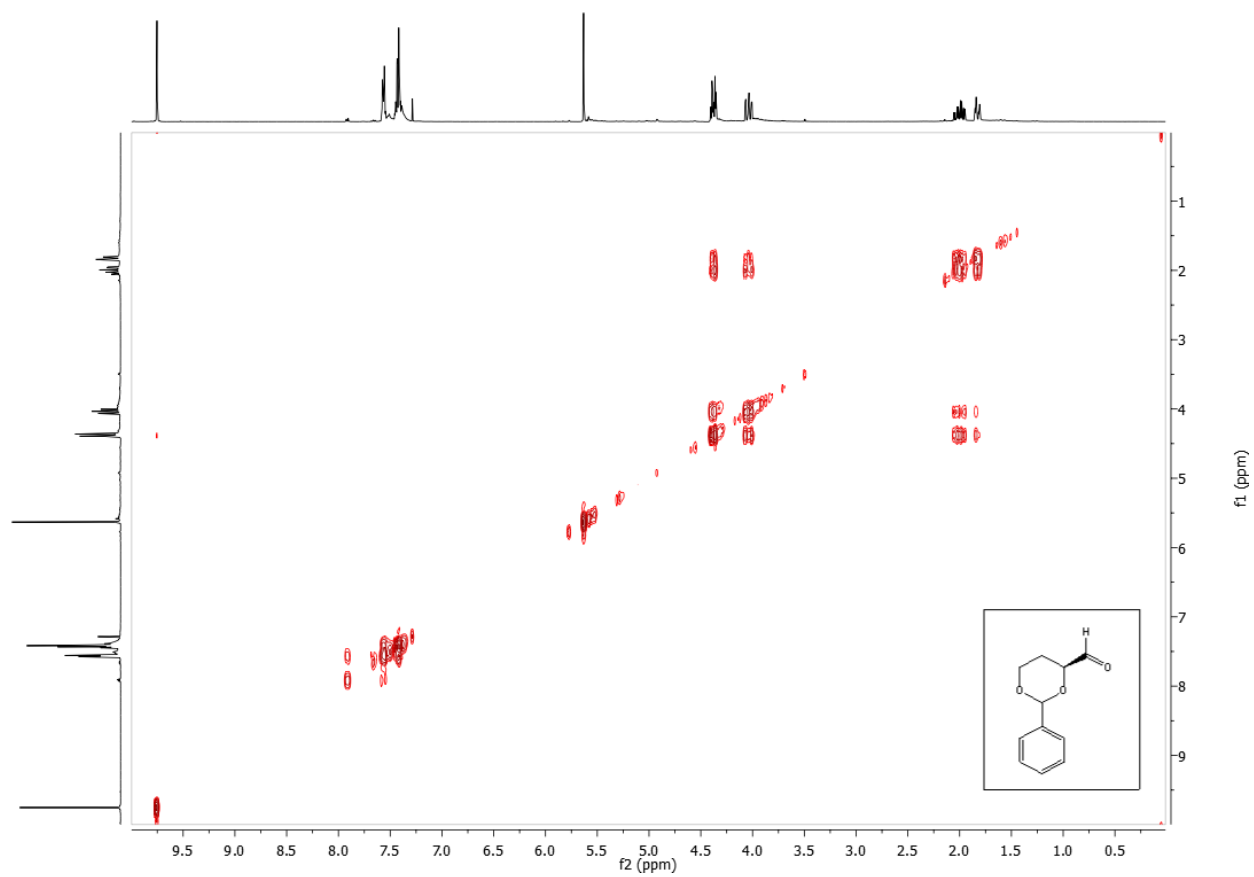
¹³C NMR (101 MHz, Chloroform-d) for **11a**



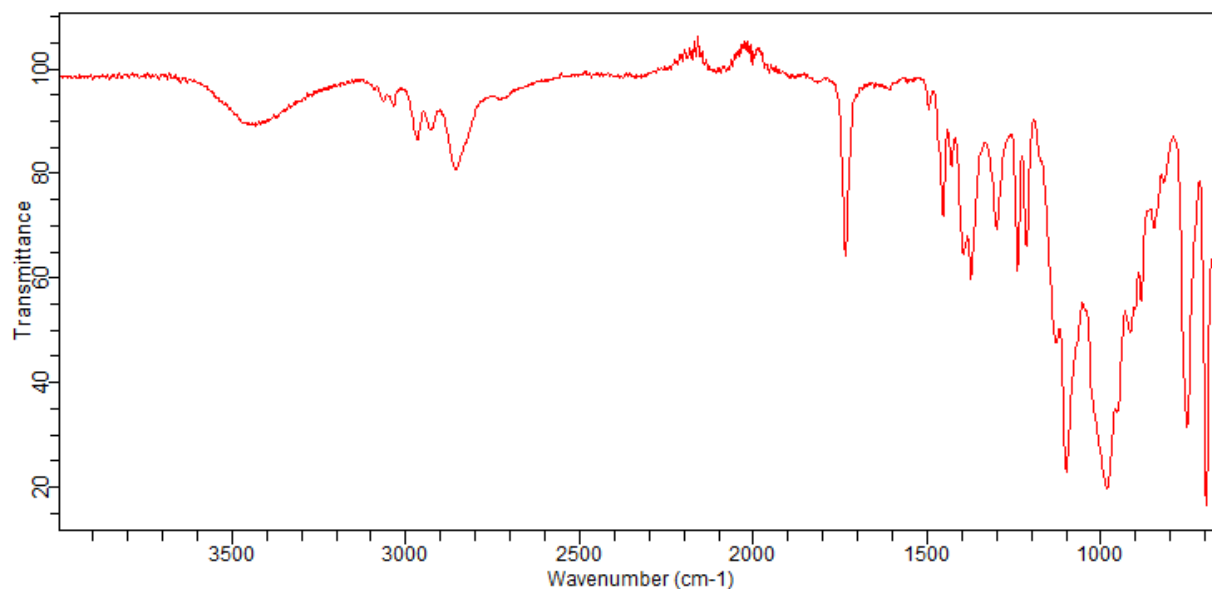
DEPT 135 (Chloroform-d) for **11a**



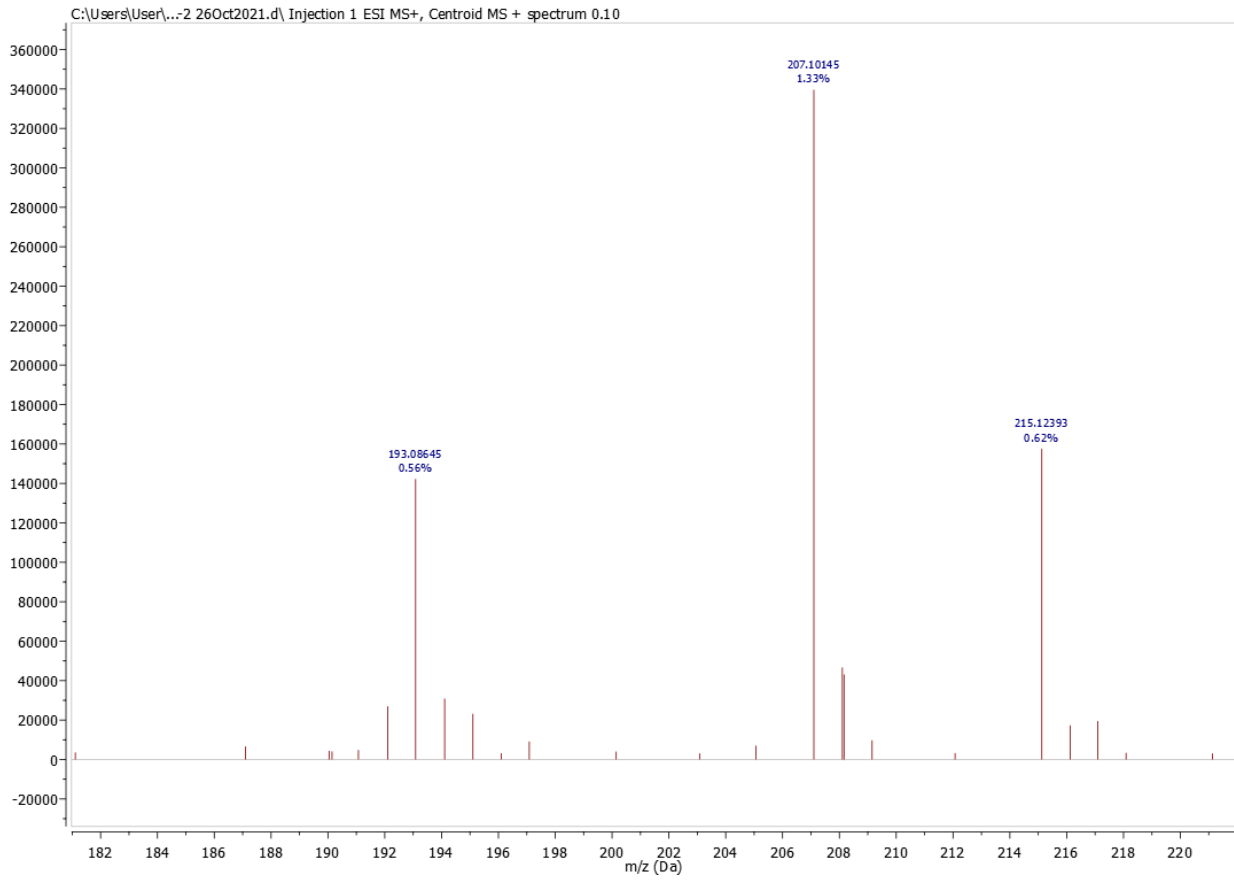
H-H COSY (Chloroform-d) for **11a**



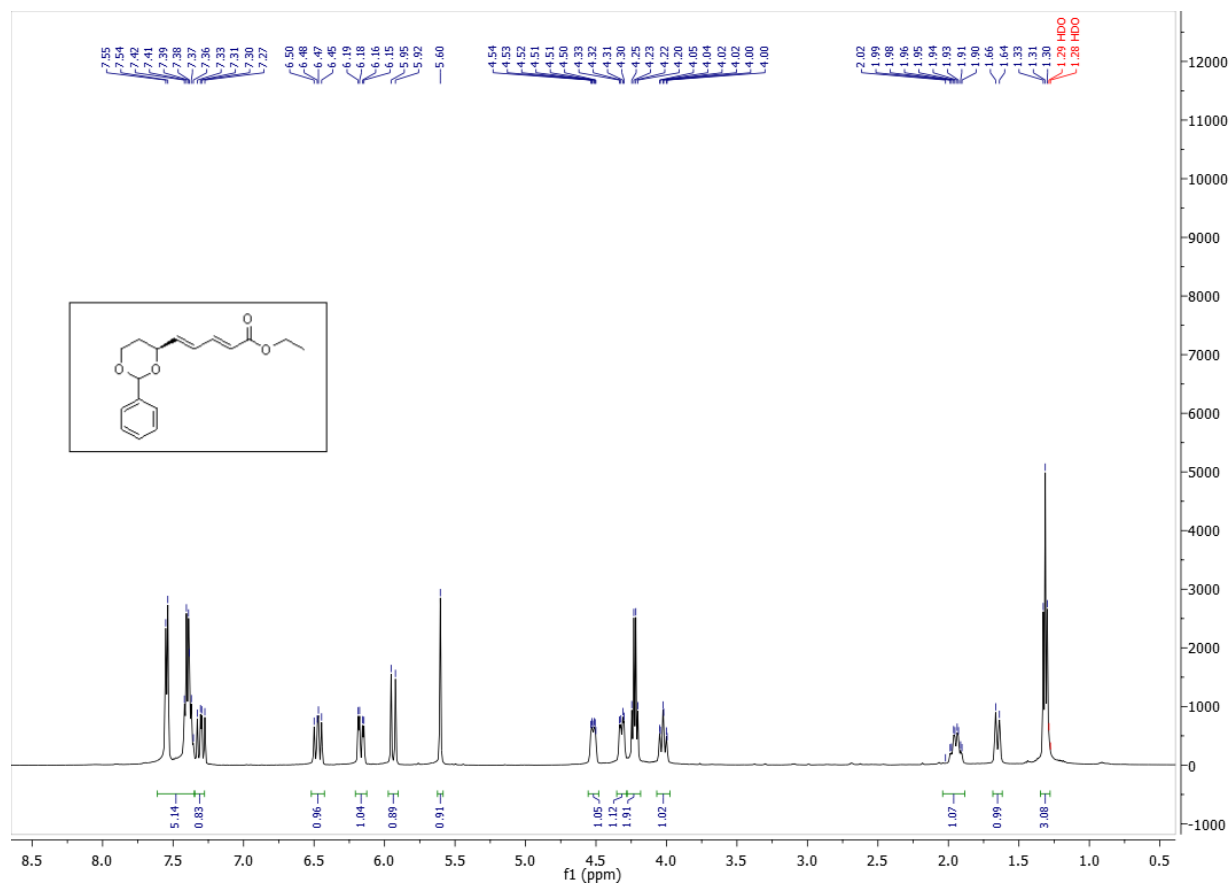
IR (KBr) for **11a**



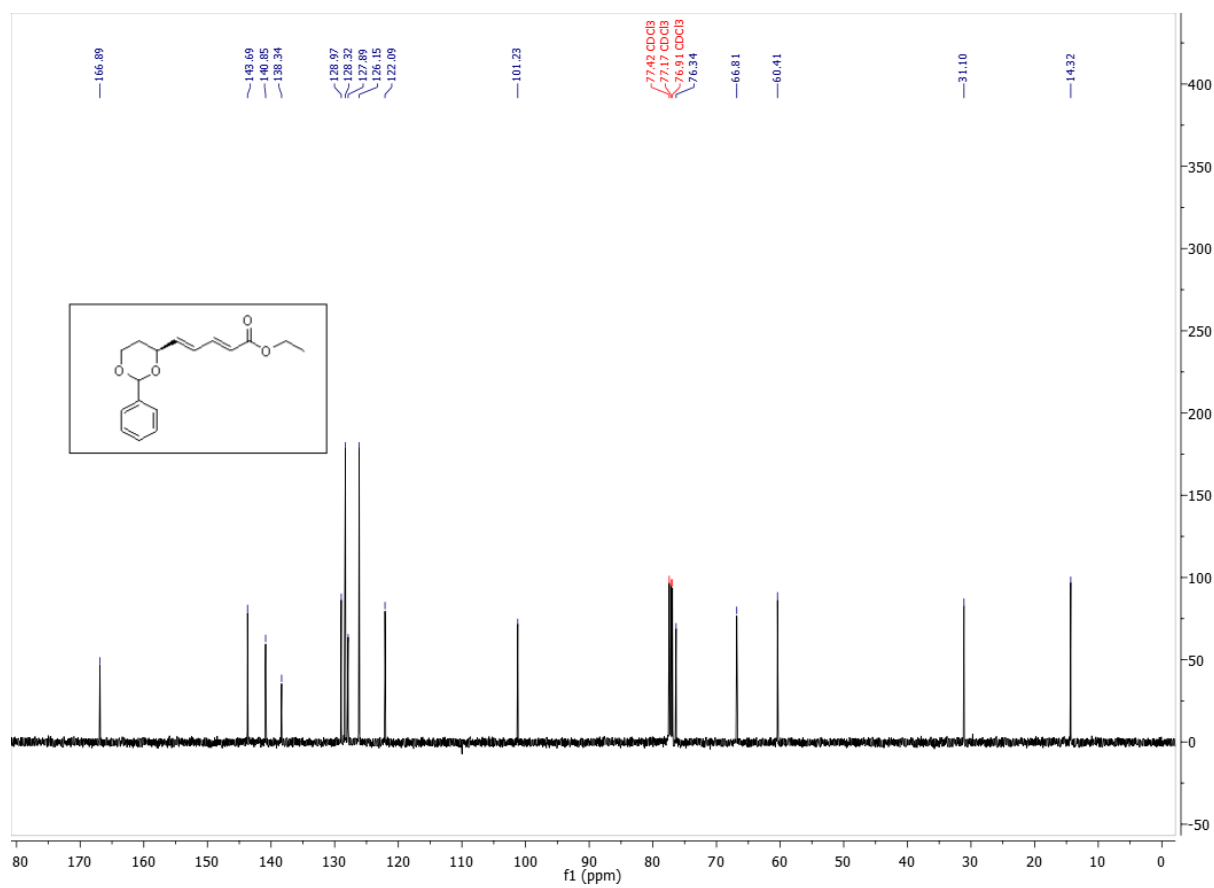
HRESIMS for 11a



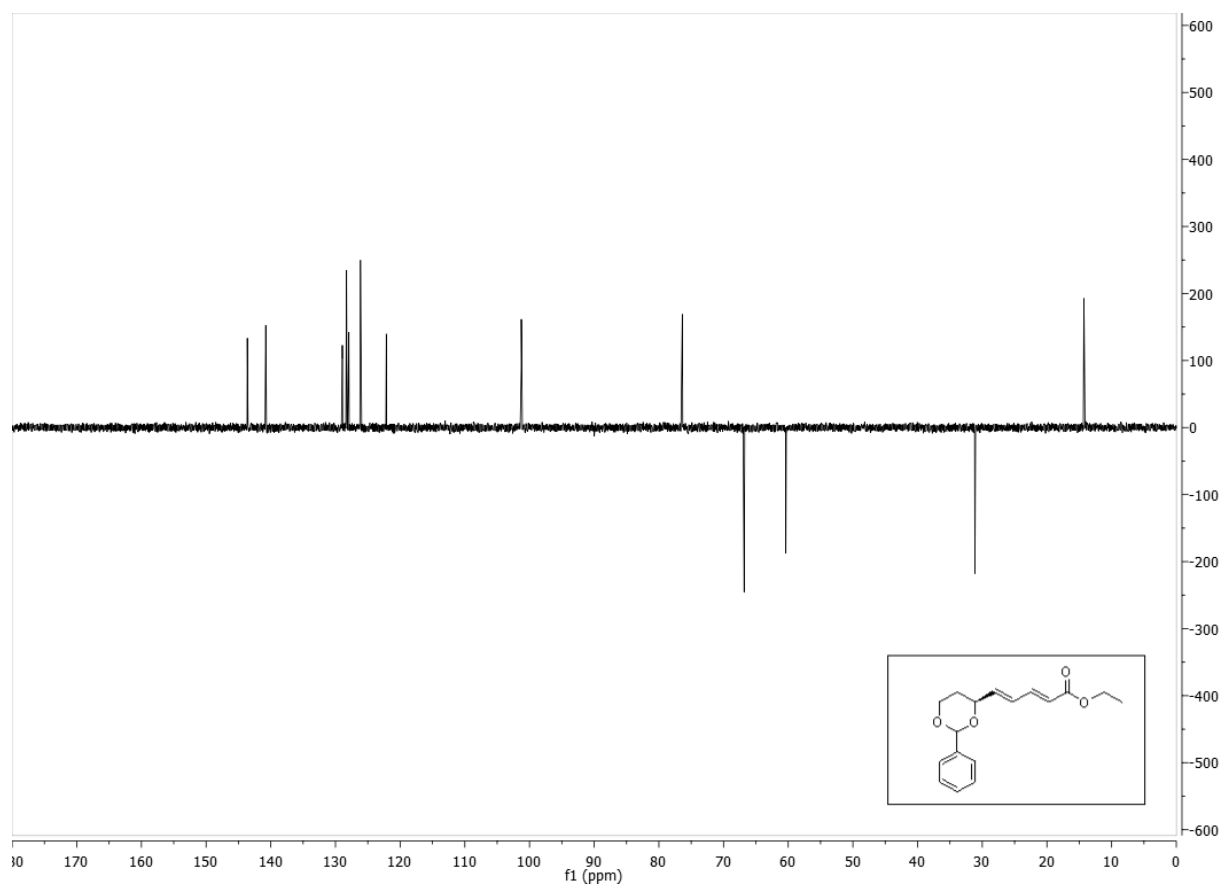
¹H NMR (500 MHz, Chloroform-d) for **10a**



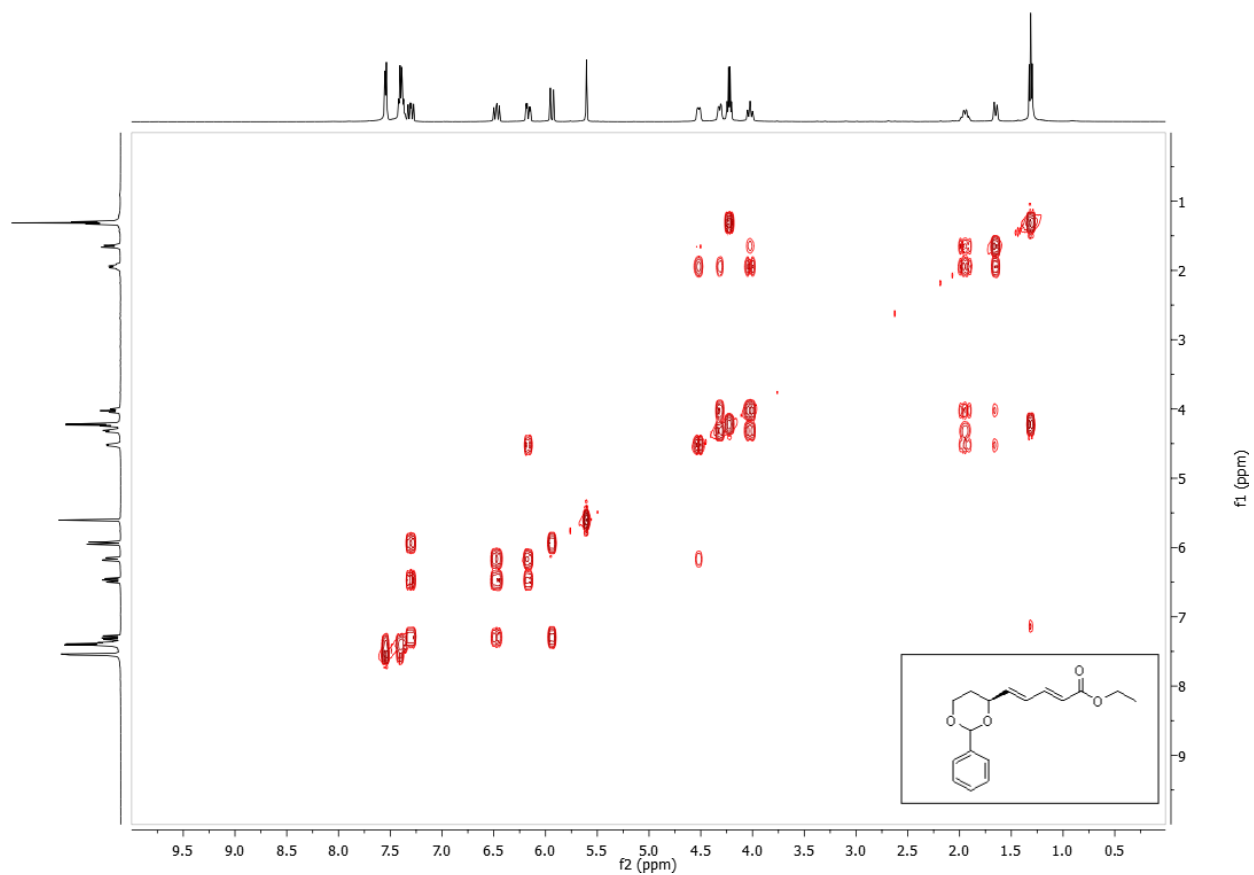
^{13}C NMR (126 MHz, Chloroform-d) for **10a**



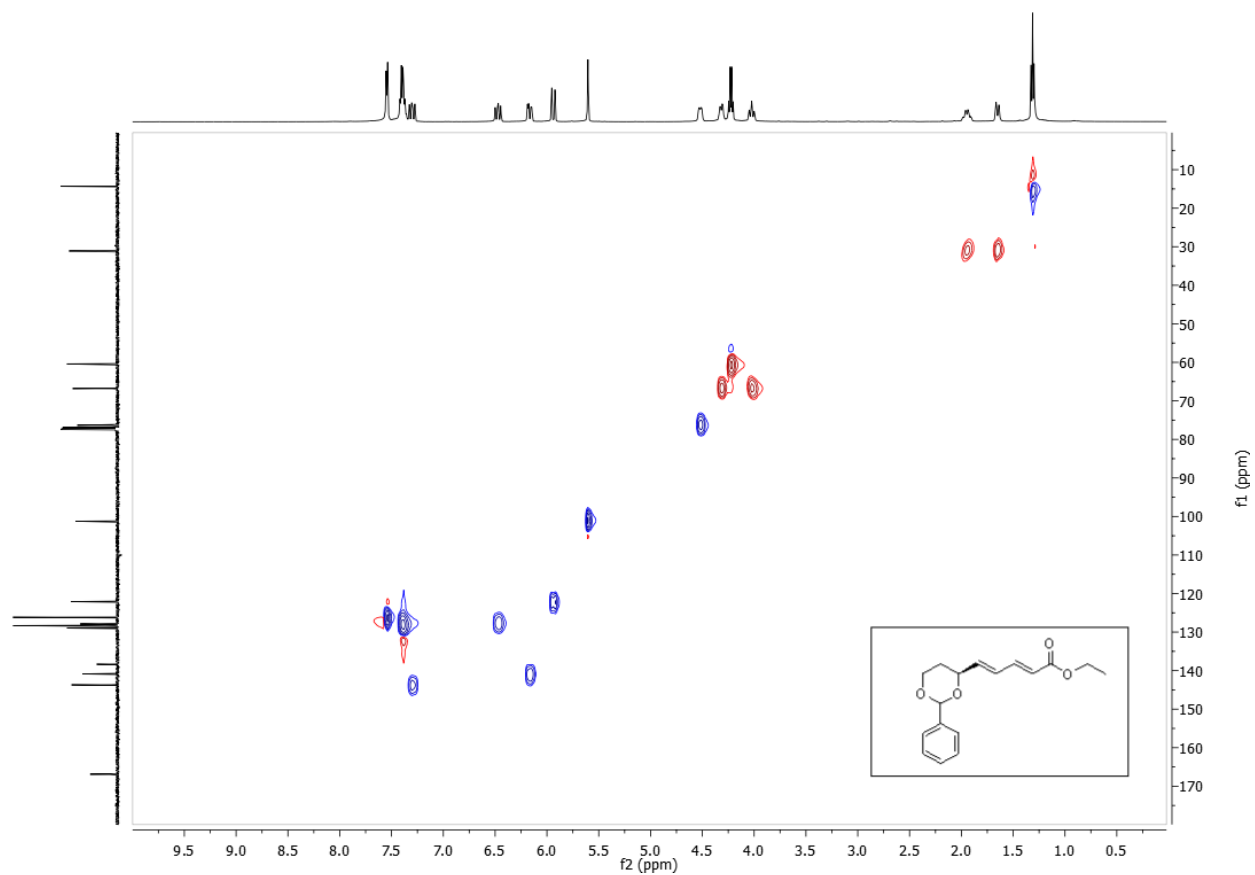
DEPT 135 (Chloroform-d) for **10a**



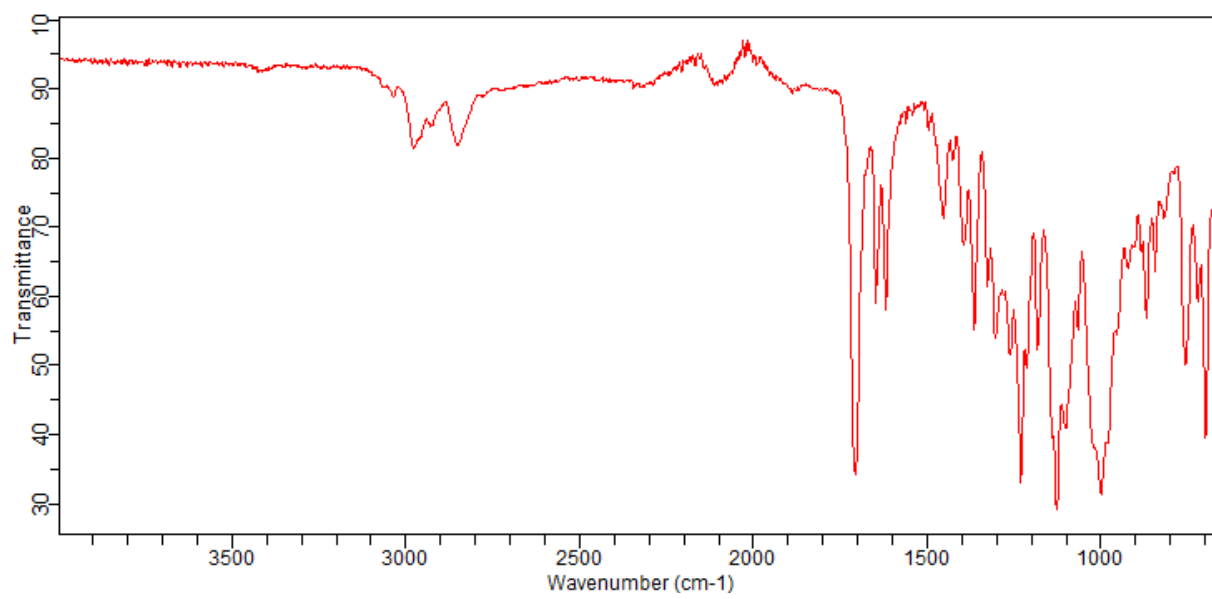
H-H COSY (Chloroform-d) for **10a**



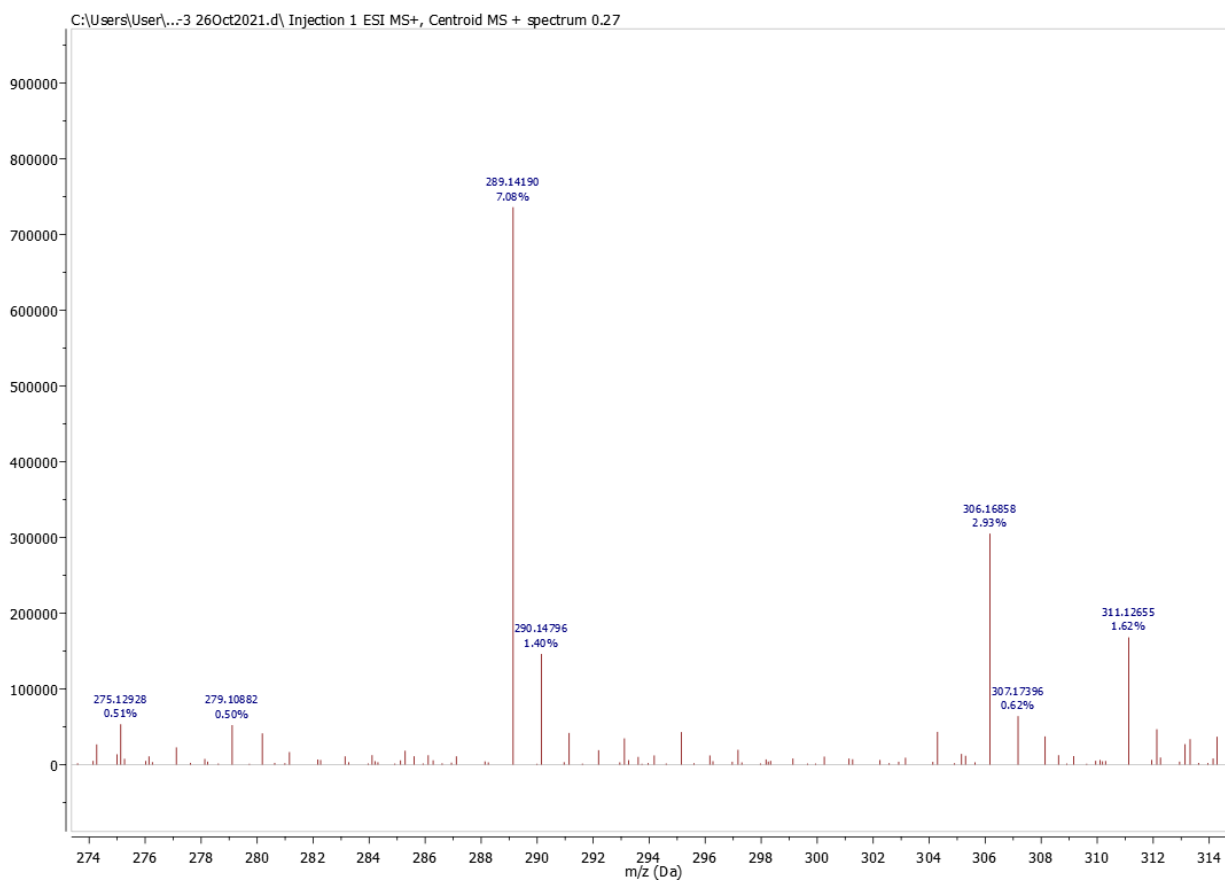
HSQC (Chloroform-d) for **10a**



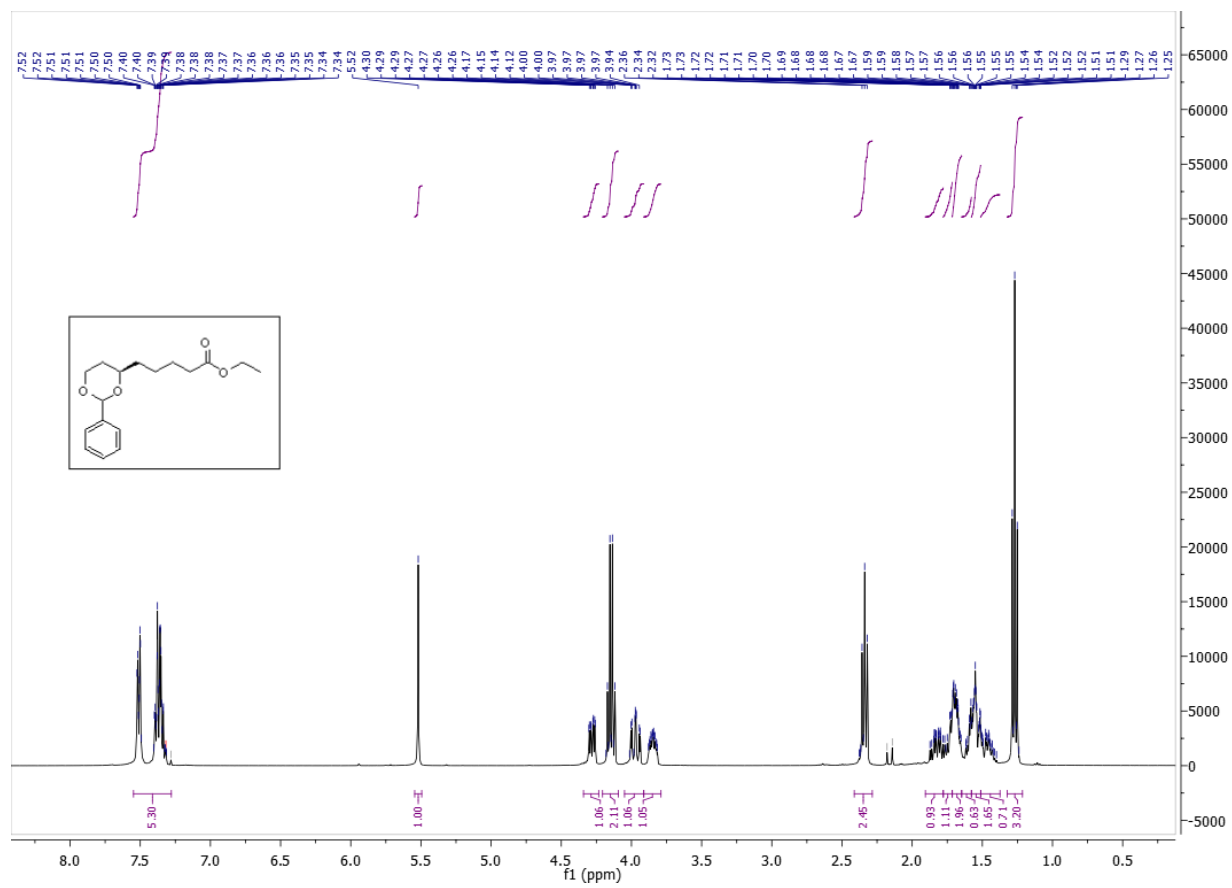
IR (KBr) for **10a**



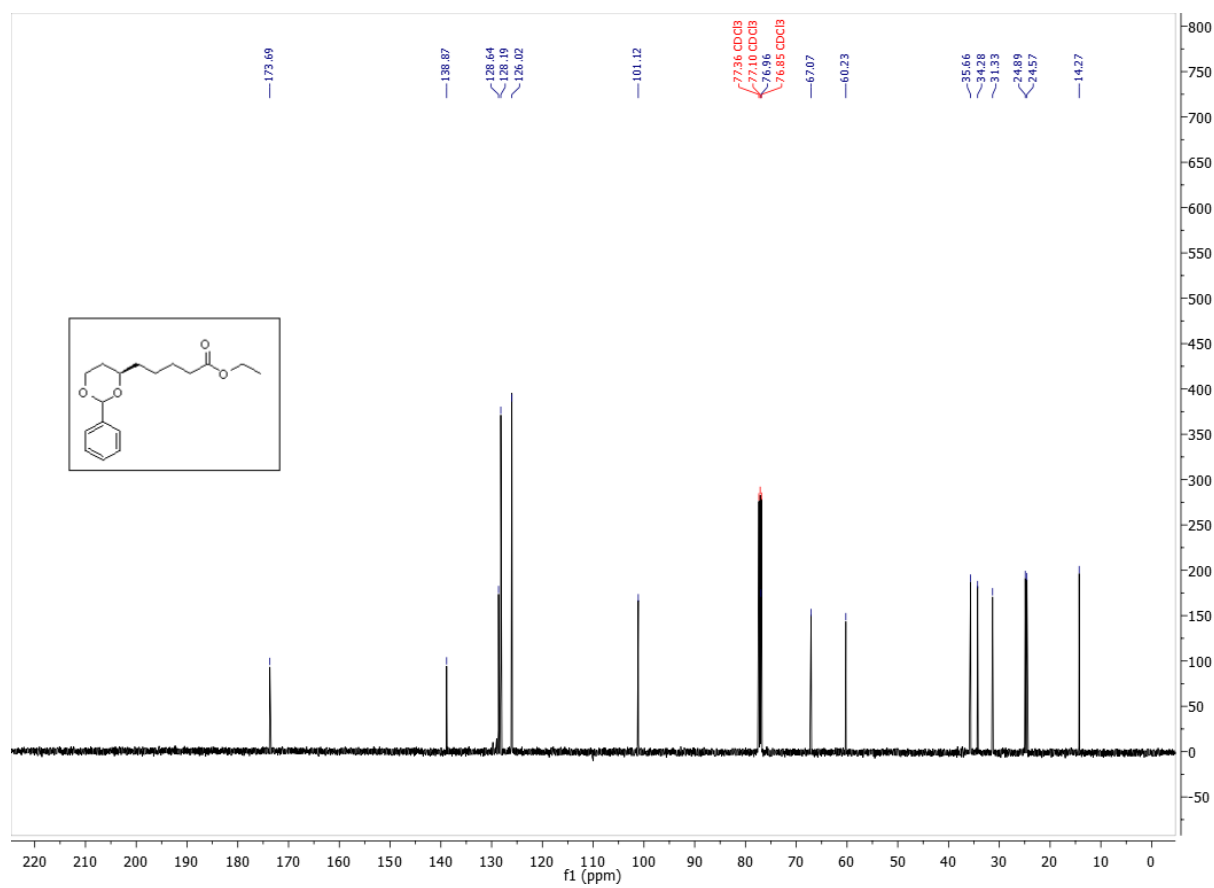
HRESIMS for 10a



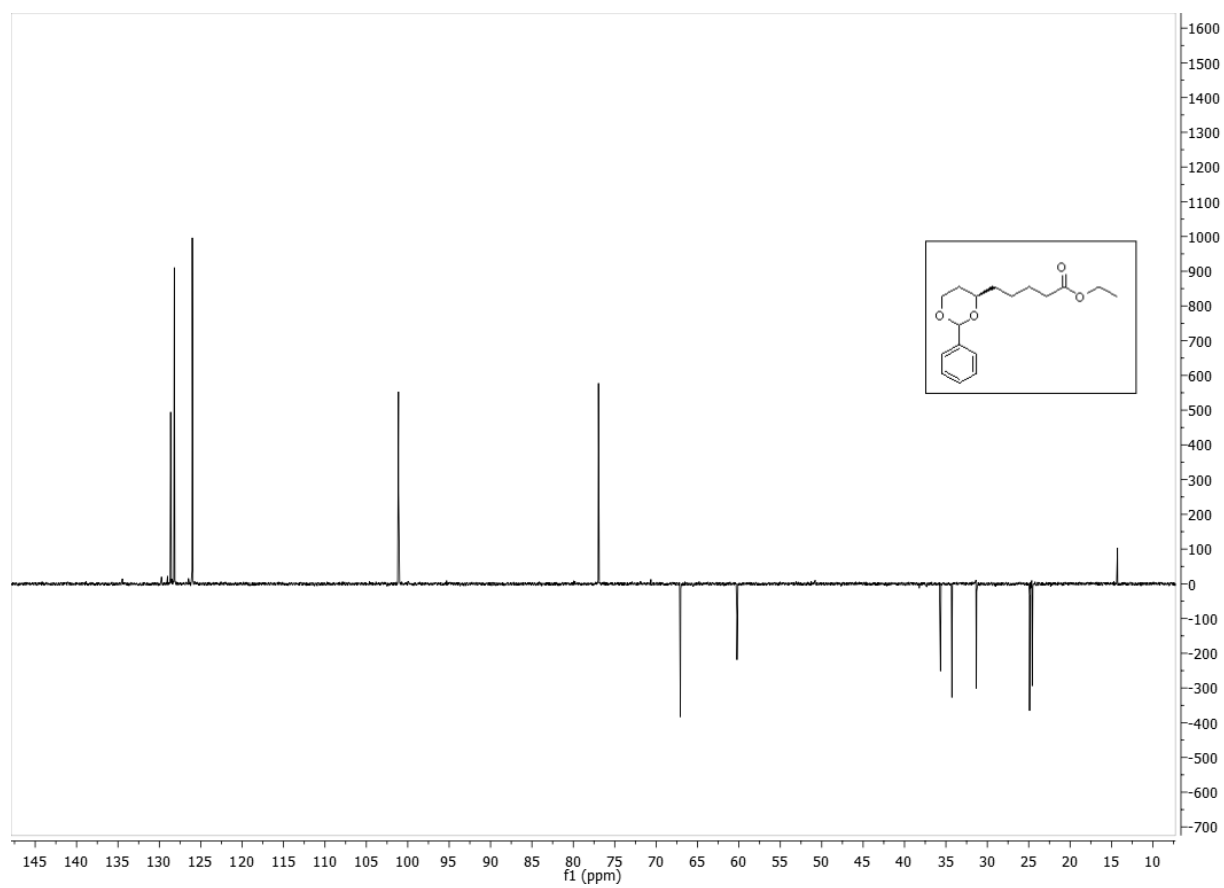
¹H NMR (400 MHz, Chloroform-d) for **9a**



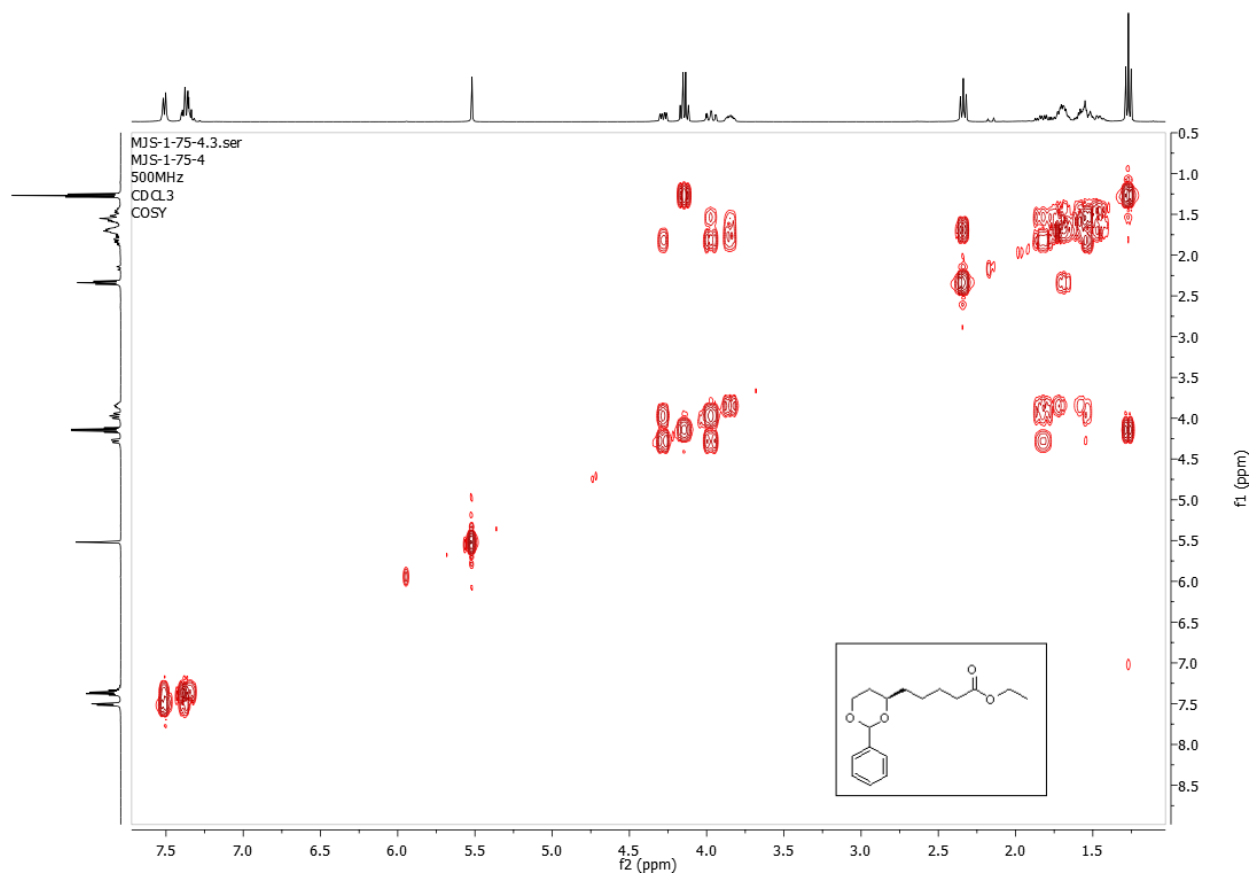
^{13}C NMR (126 MHz, Chloroform-d) for **9a**



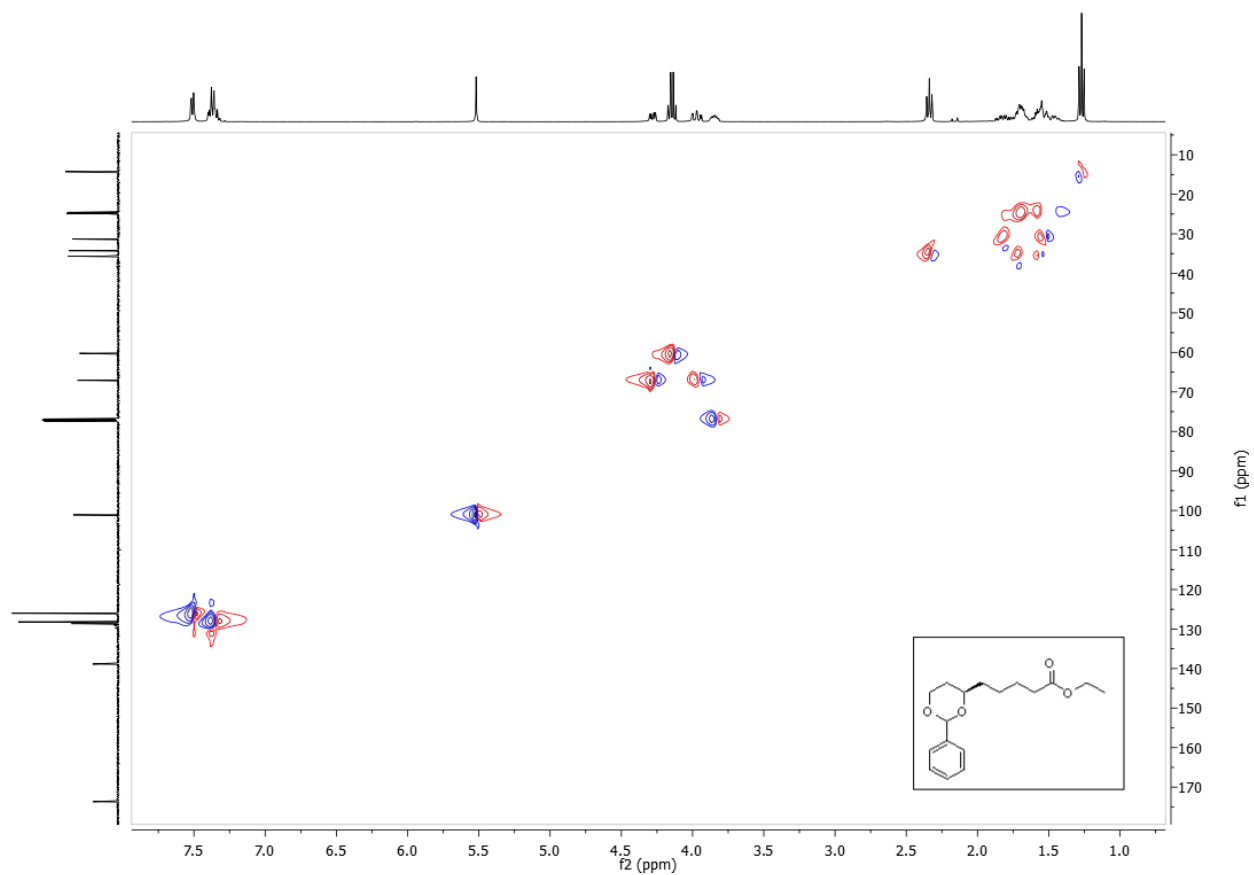
DEPT 135 (Chloroform-d) for **9a**



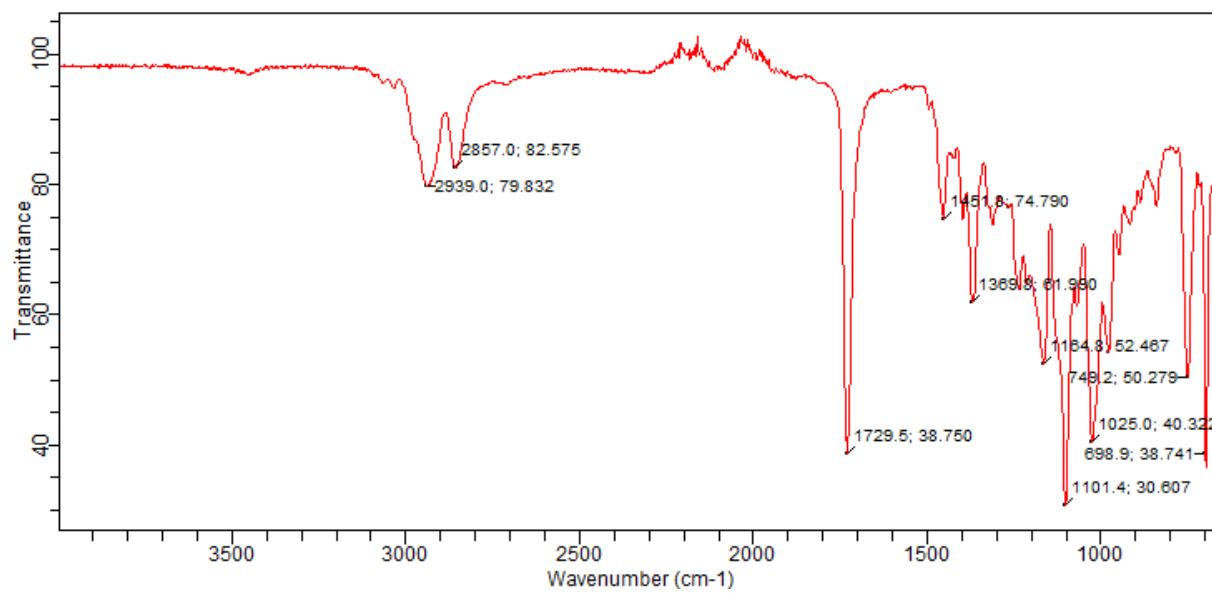
H-H COSY (Chloroform-d) for 9a



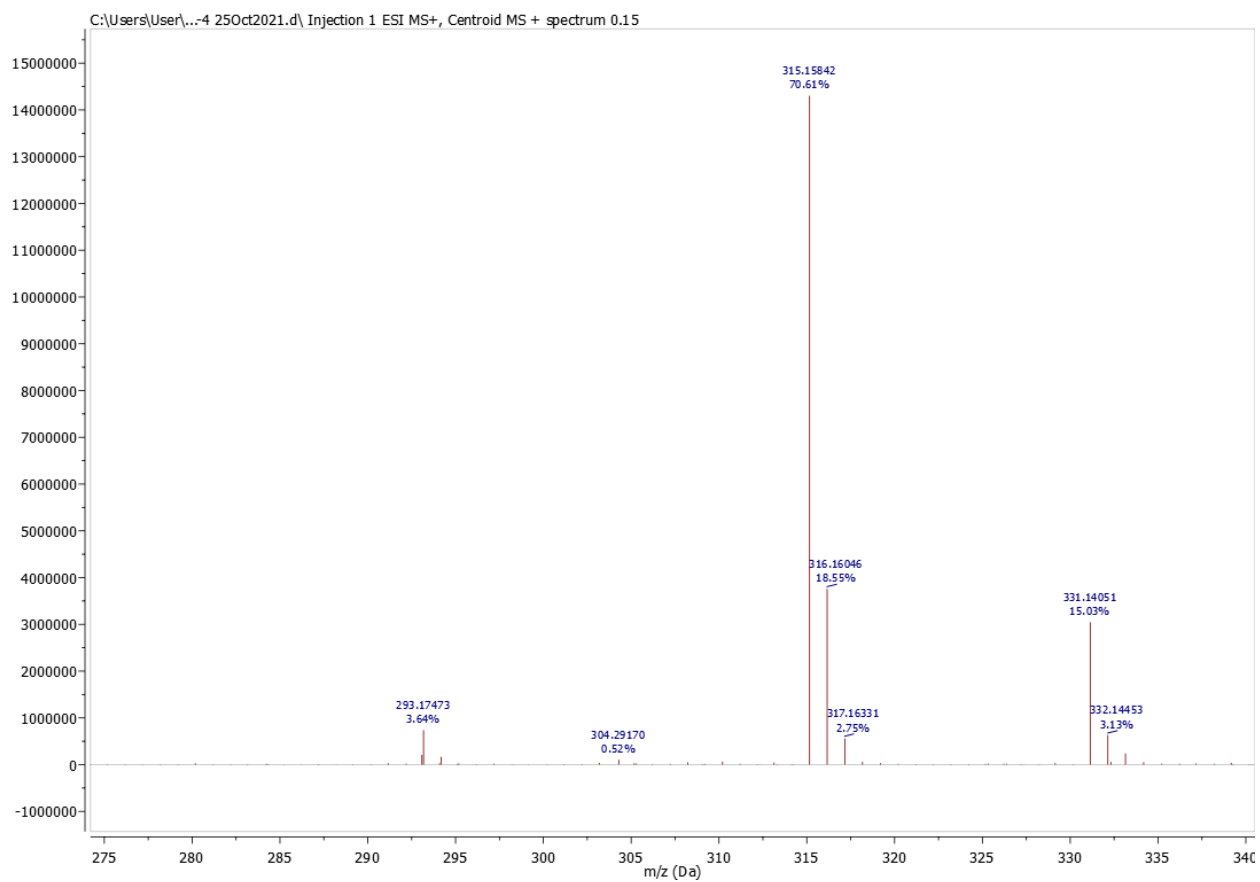
HSQC (Chloroform-d) for 9a



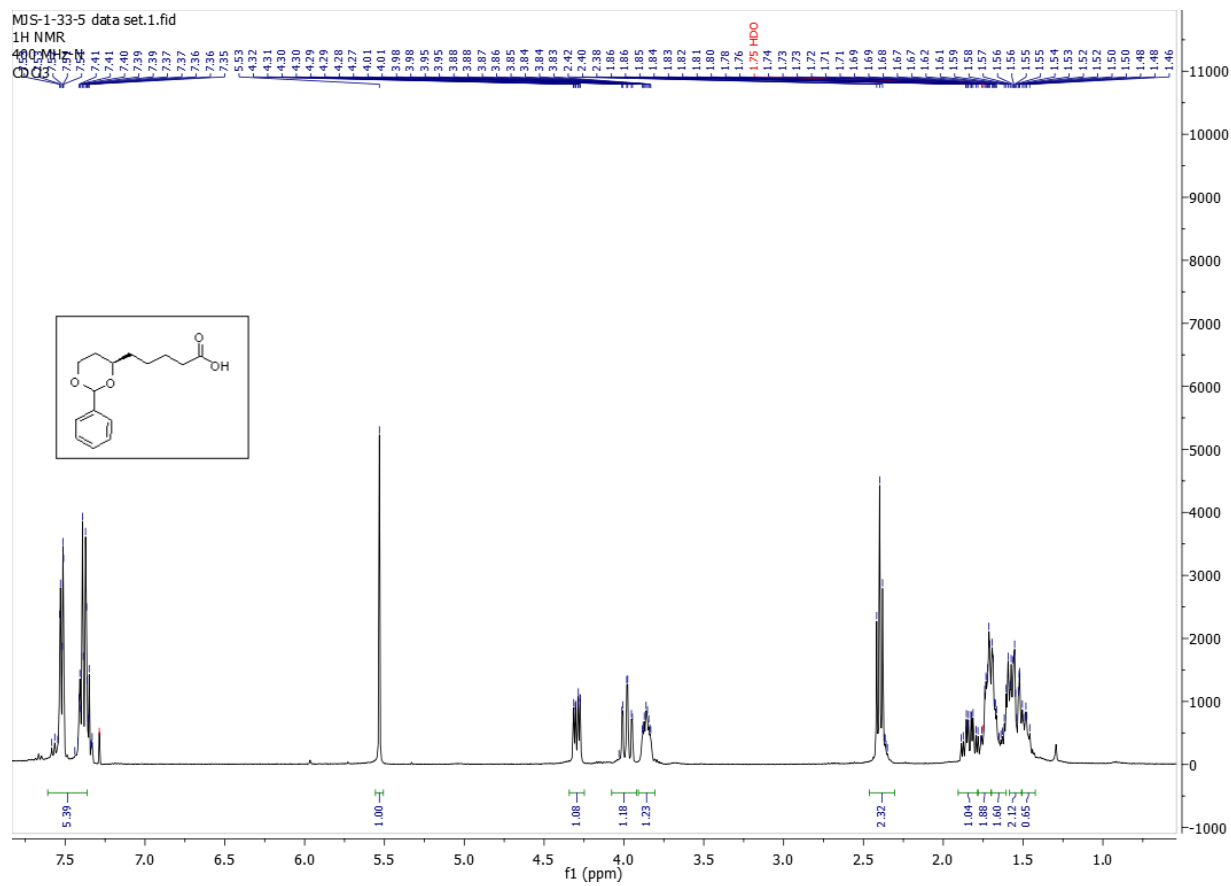
IR (KBr) for **9a**



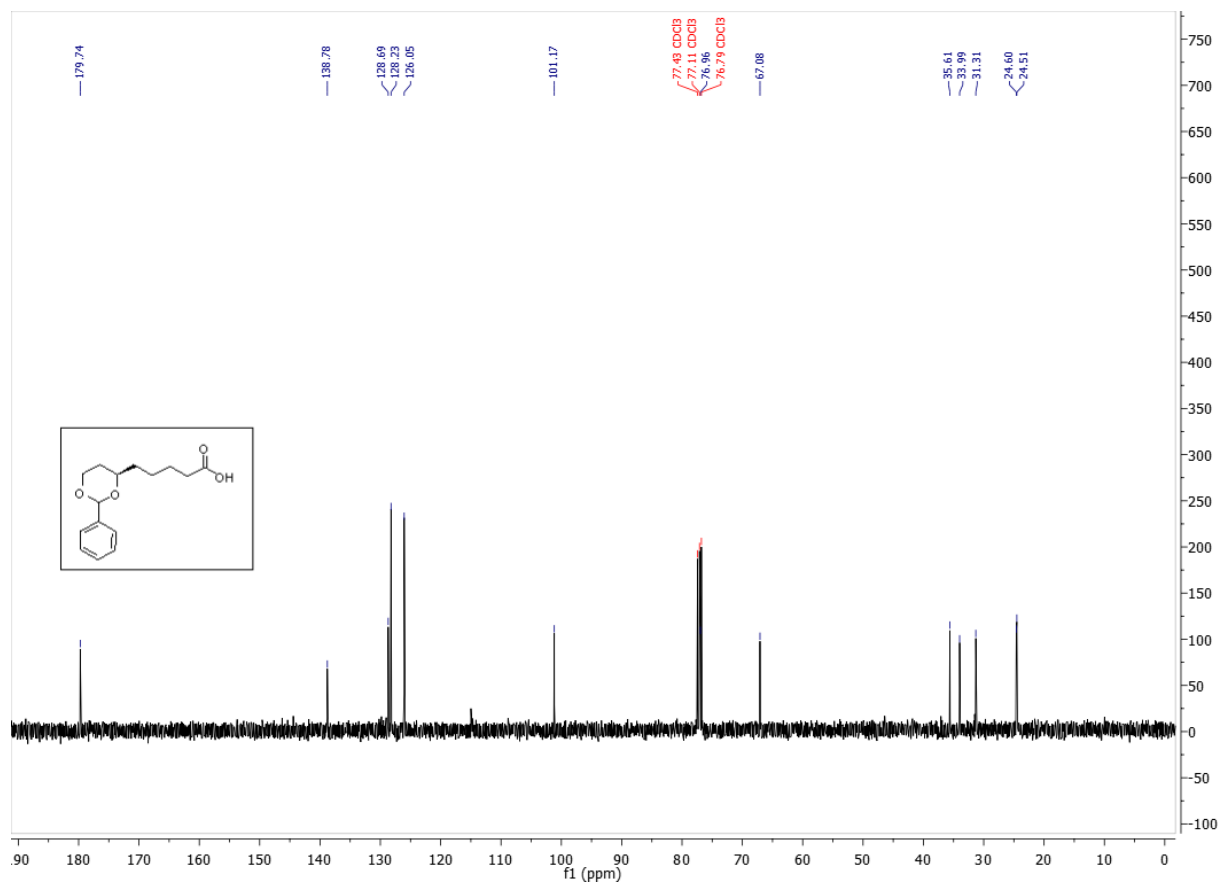
HRESIMS for 9a



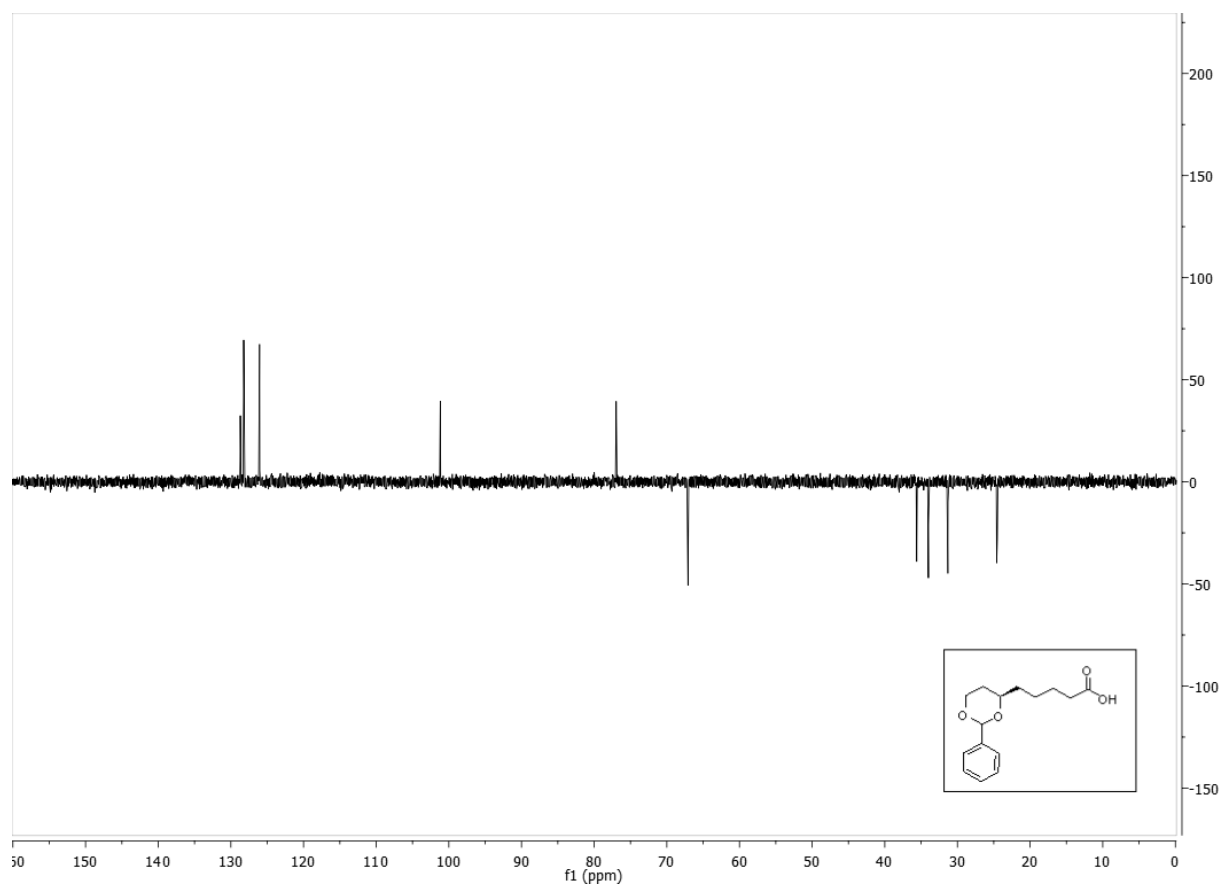
¹H NMR (400 MHz, Chloroform-d) for **8a**



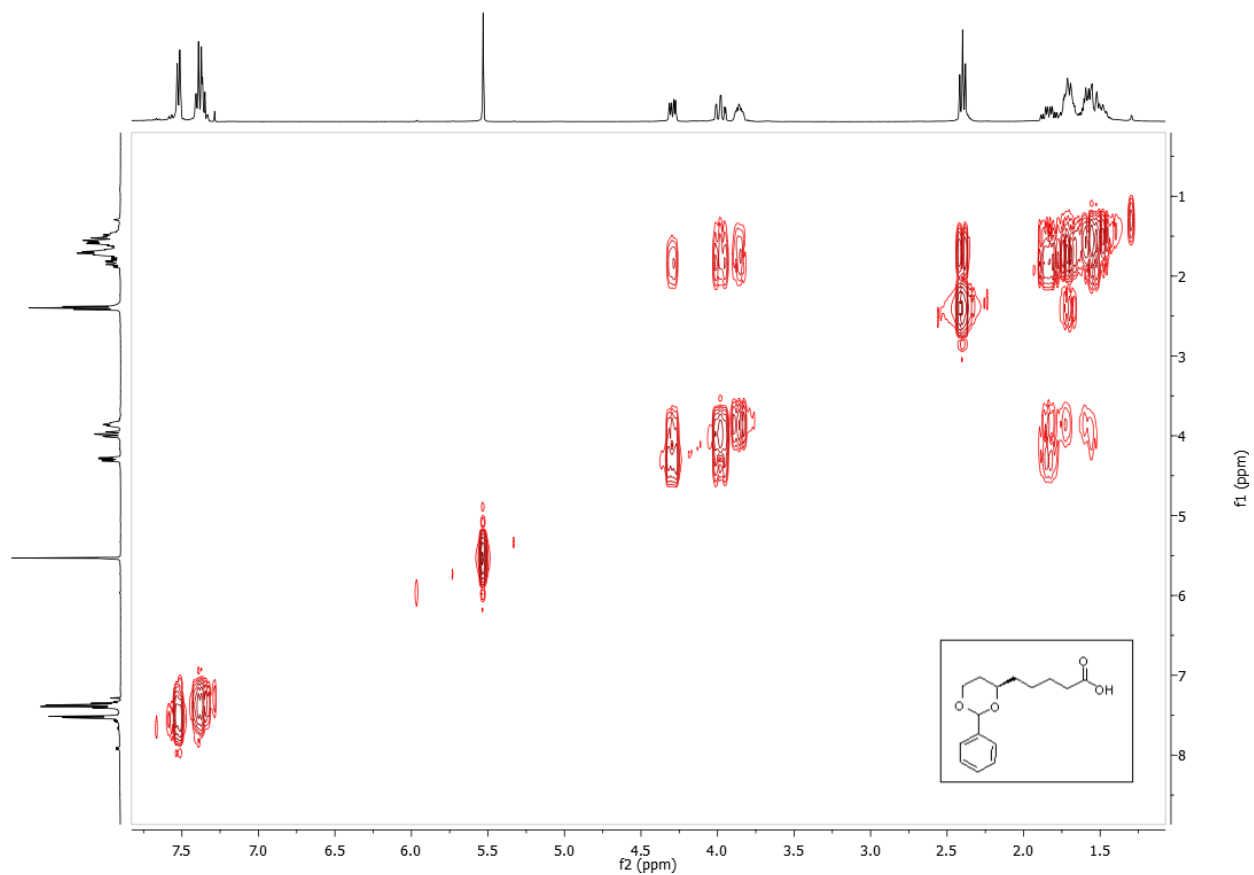
^{13}C NMR (101 MHz, Chloroform-d) for **8a**



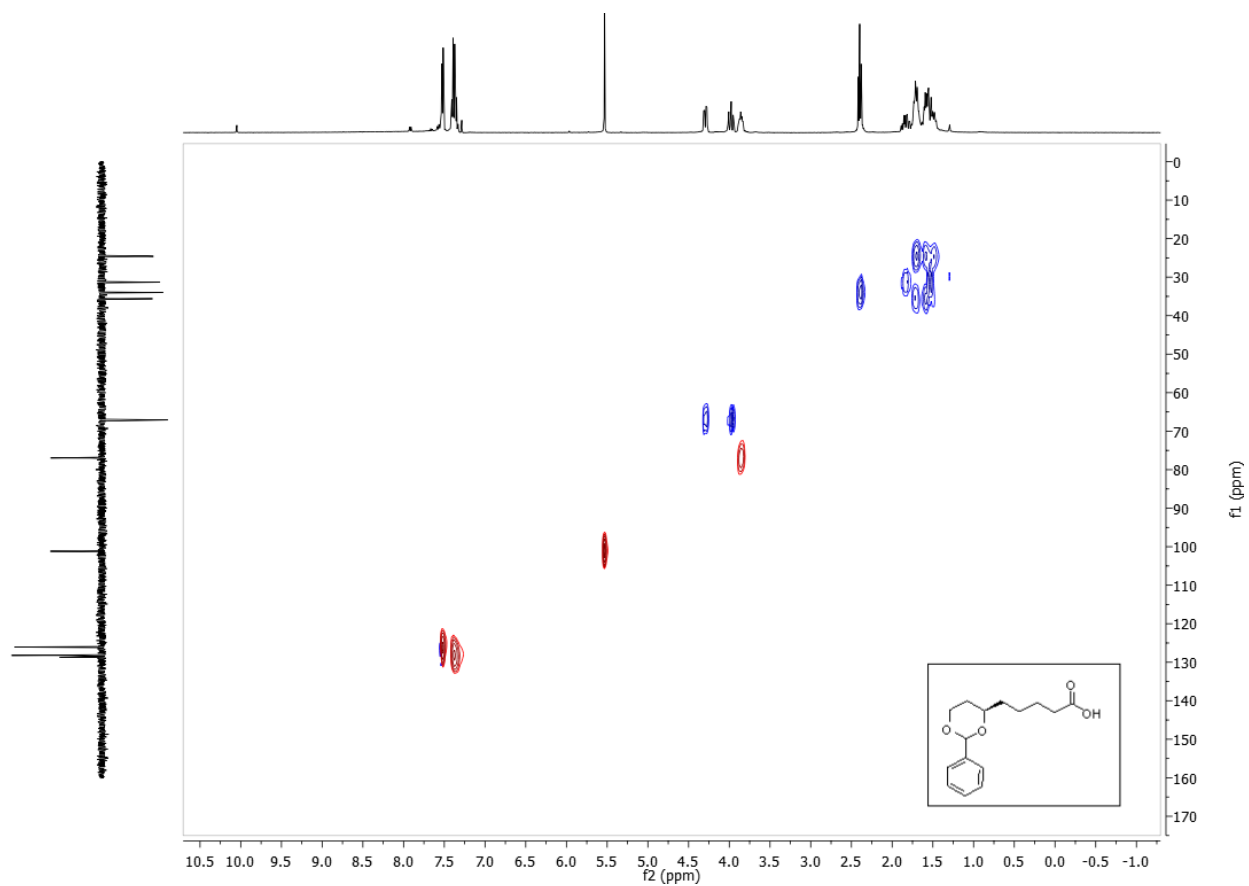
DEPT 135 (Chloroform-d) for **8a**



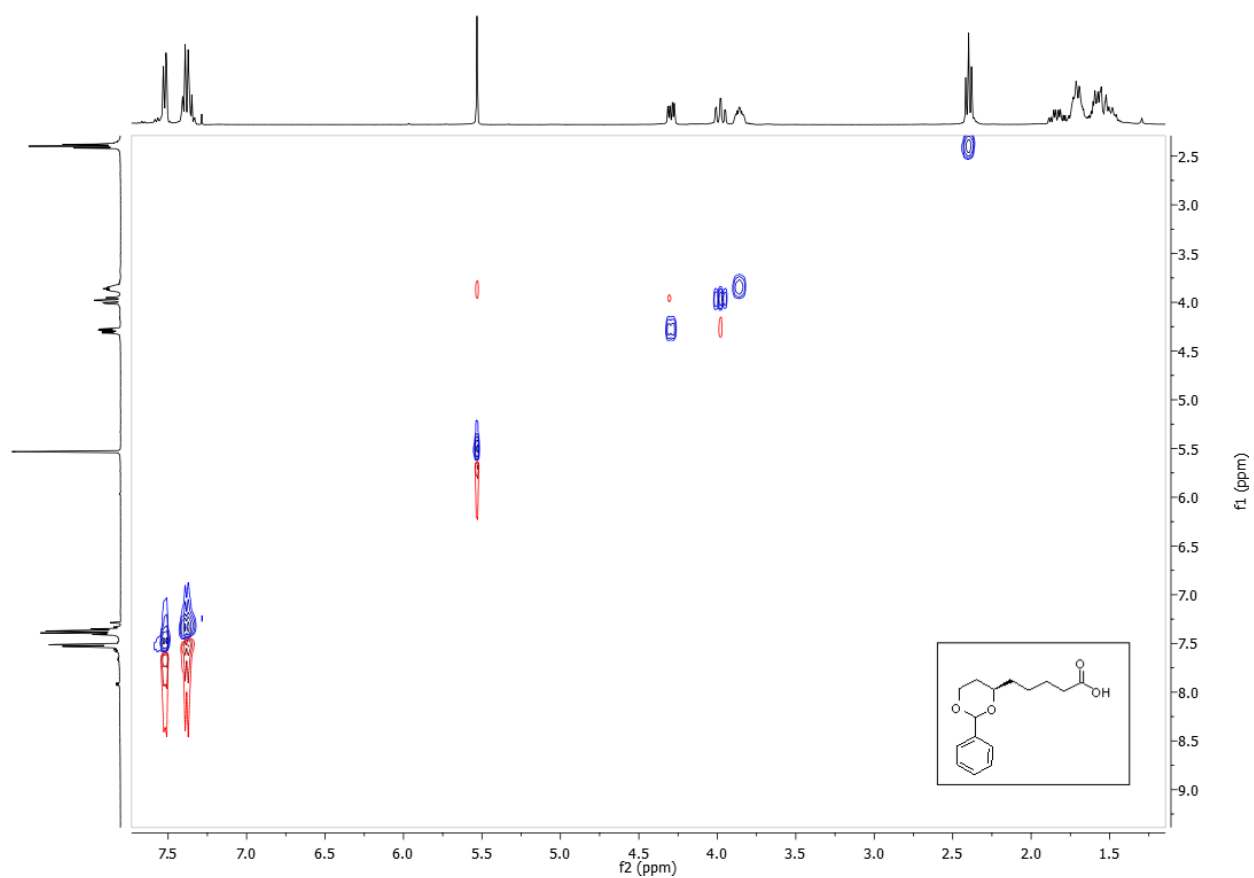
H-H COSY (Chloroform-d) for **8a**



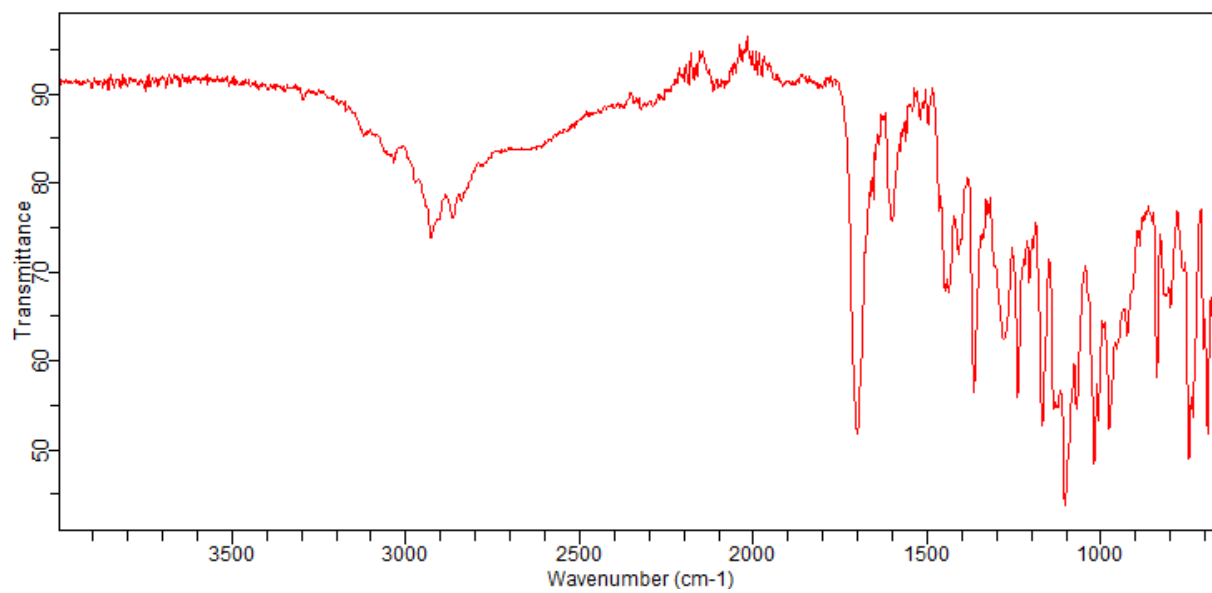
HSQC (Chloroform-d) for **8a**



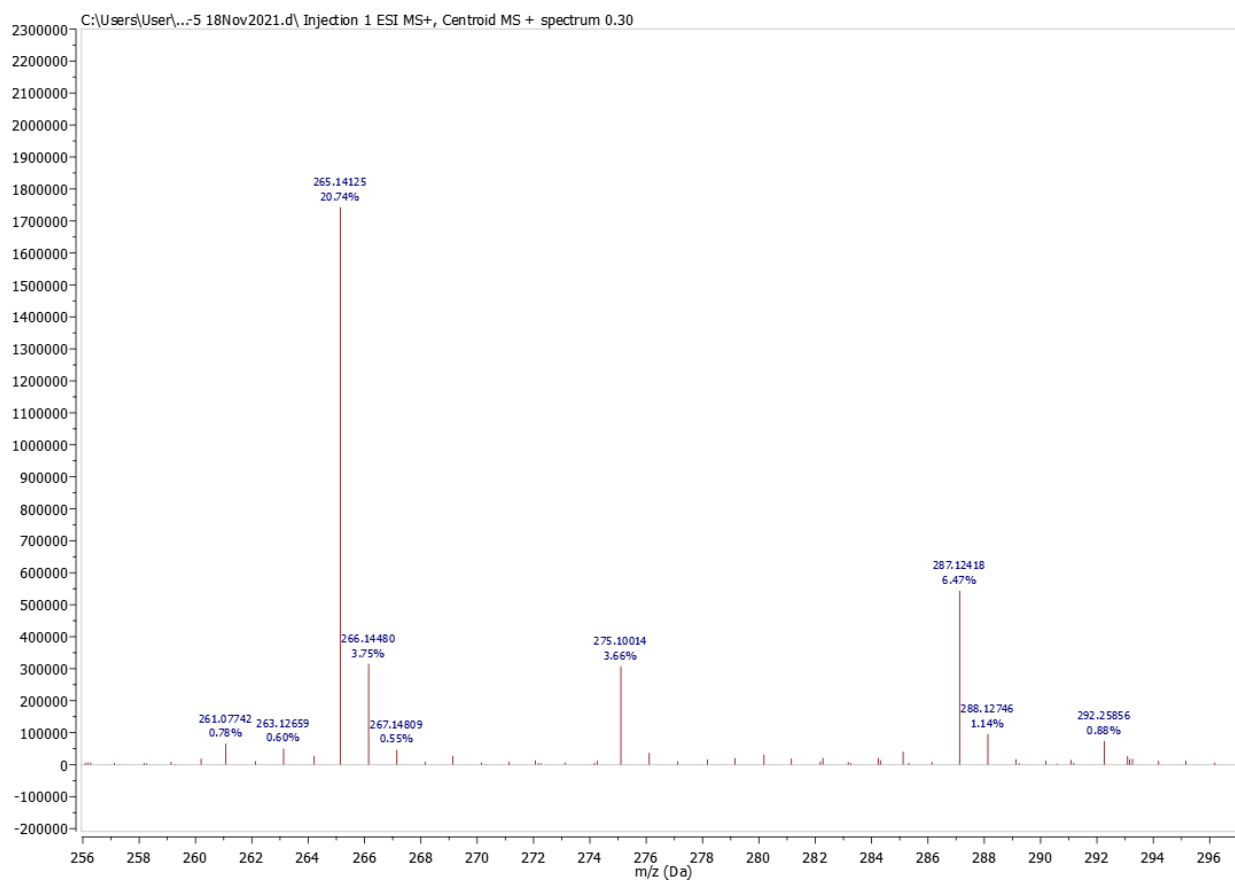
NOESY (Chloroform-d) for **8a**



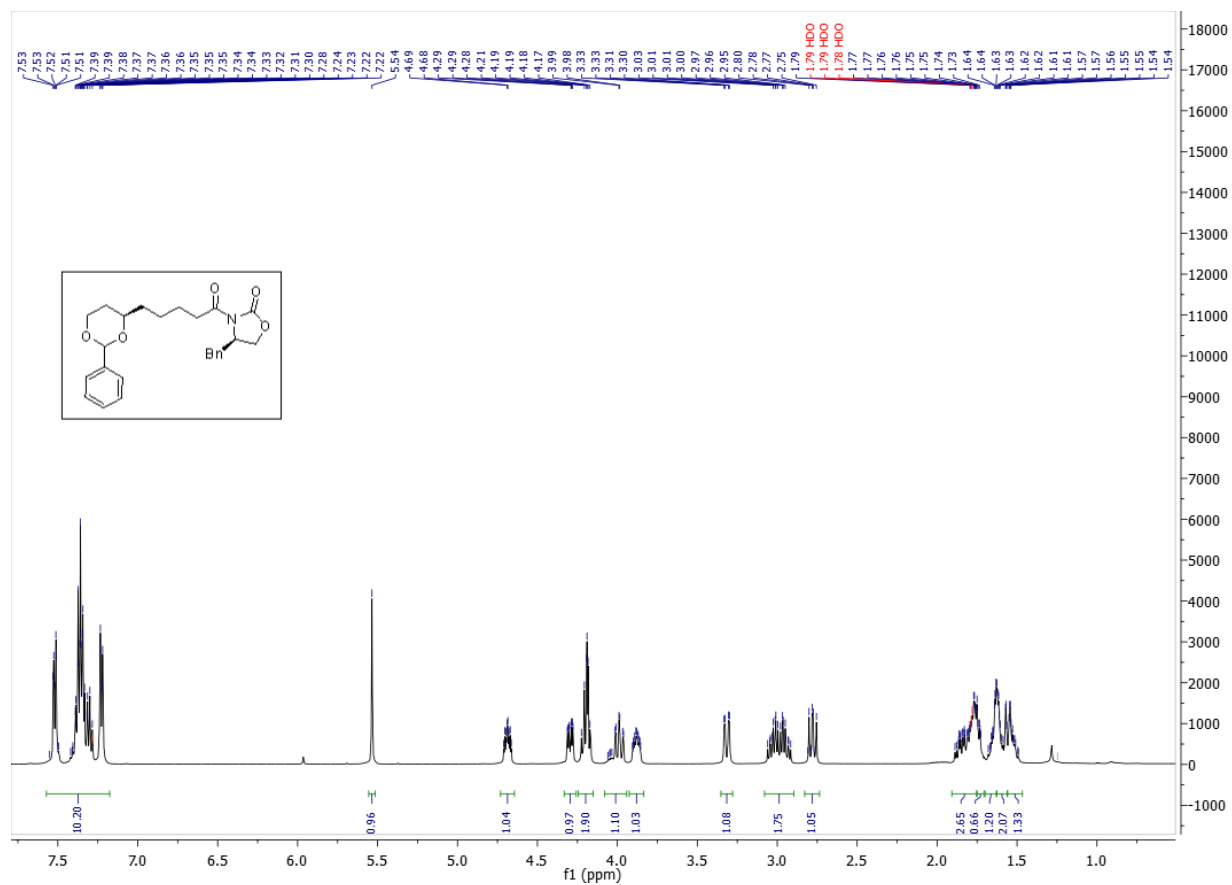
IR (KBr) for **8a**



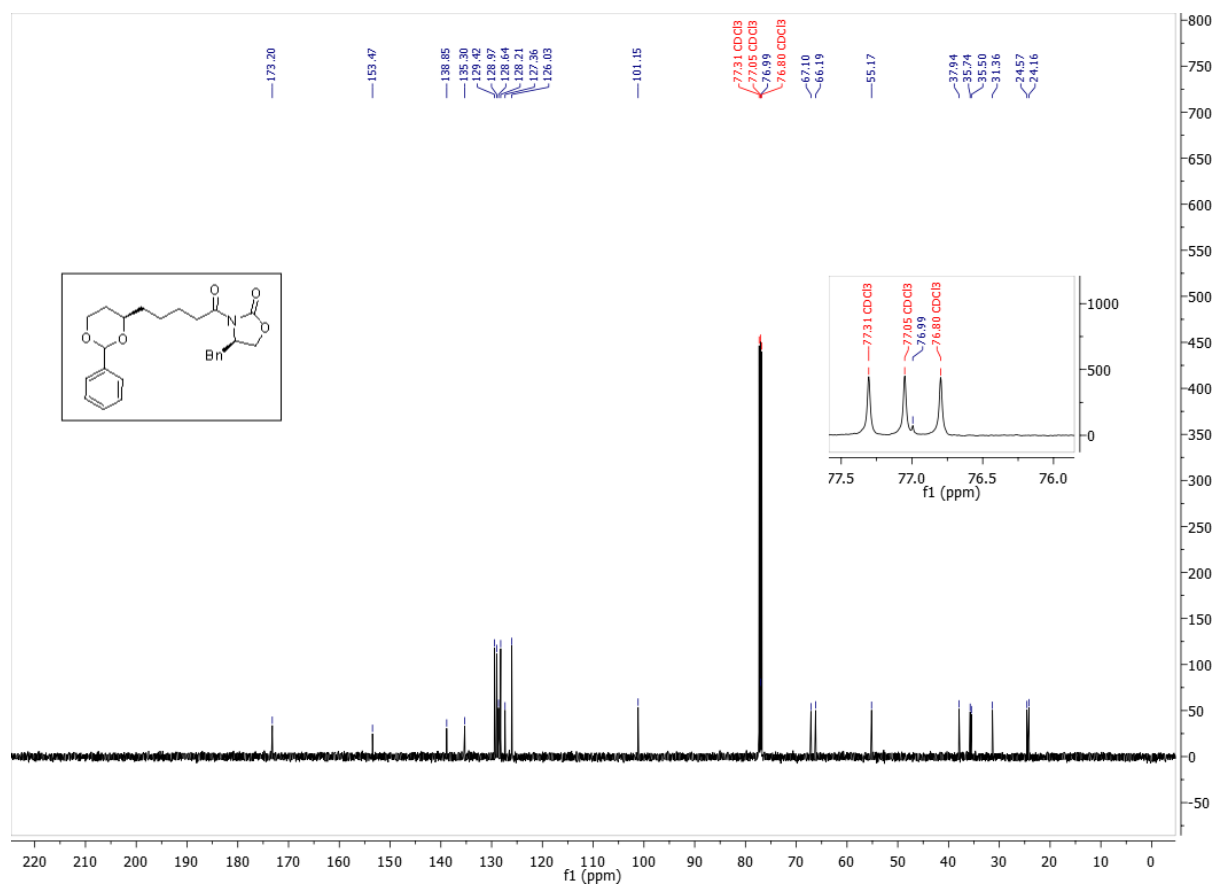
HRESIMS for 8a



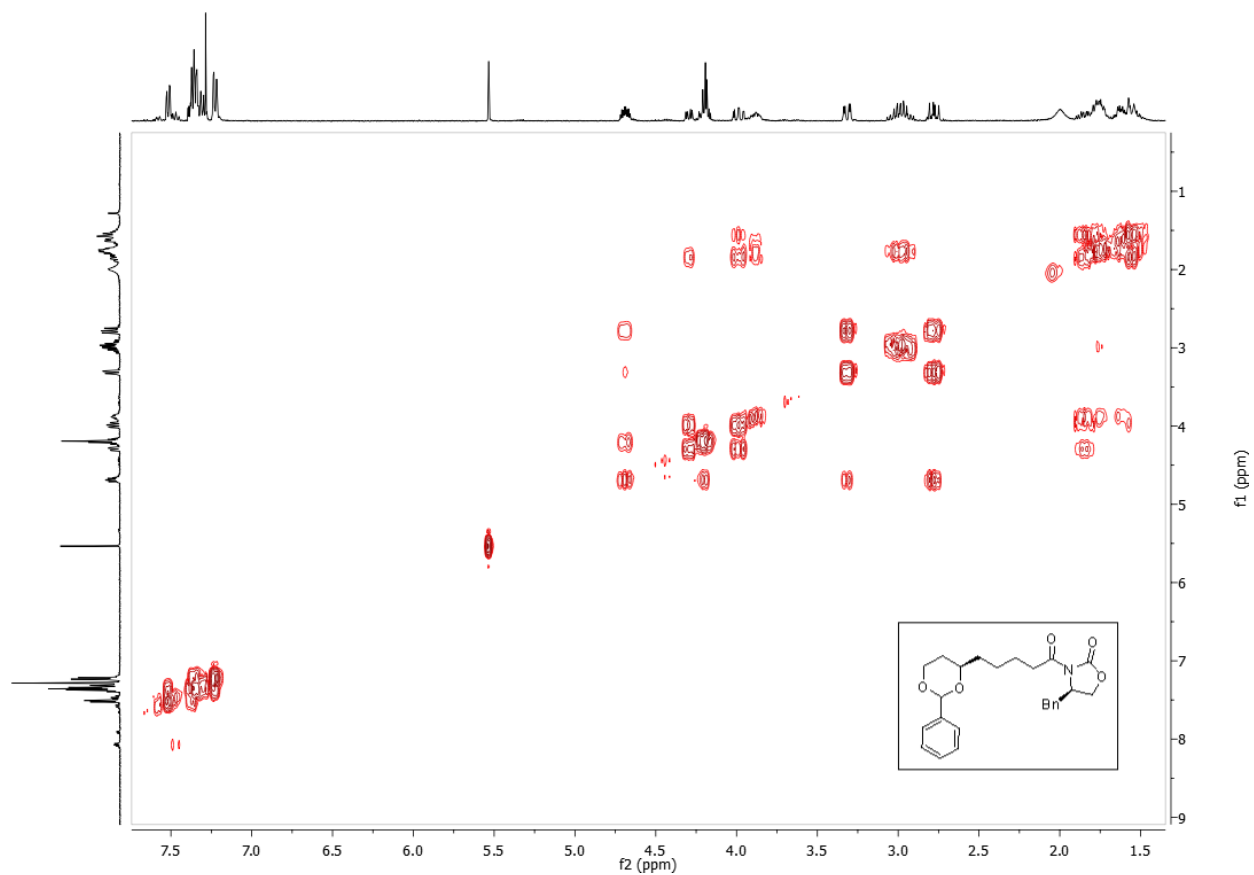
^1H NMR (500 MHz, Chloroform-d) for **7a**



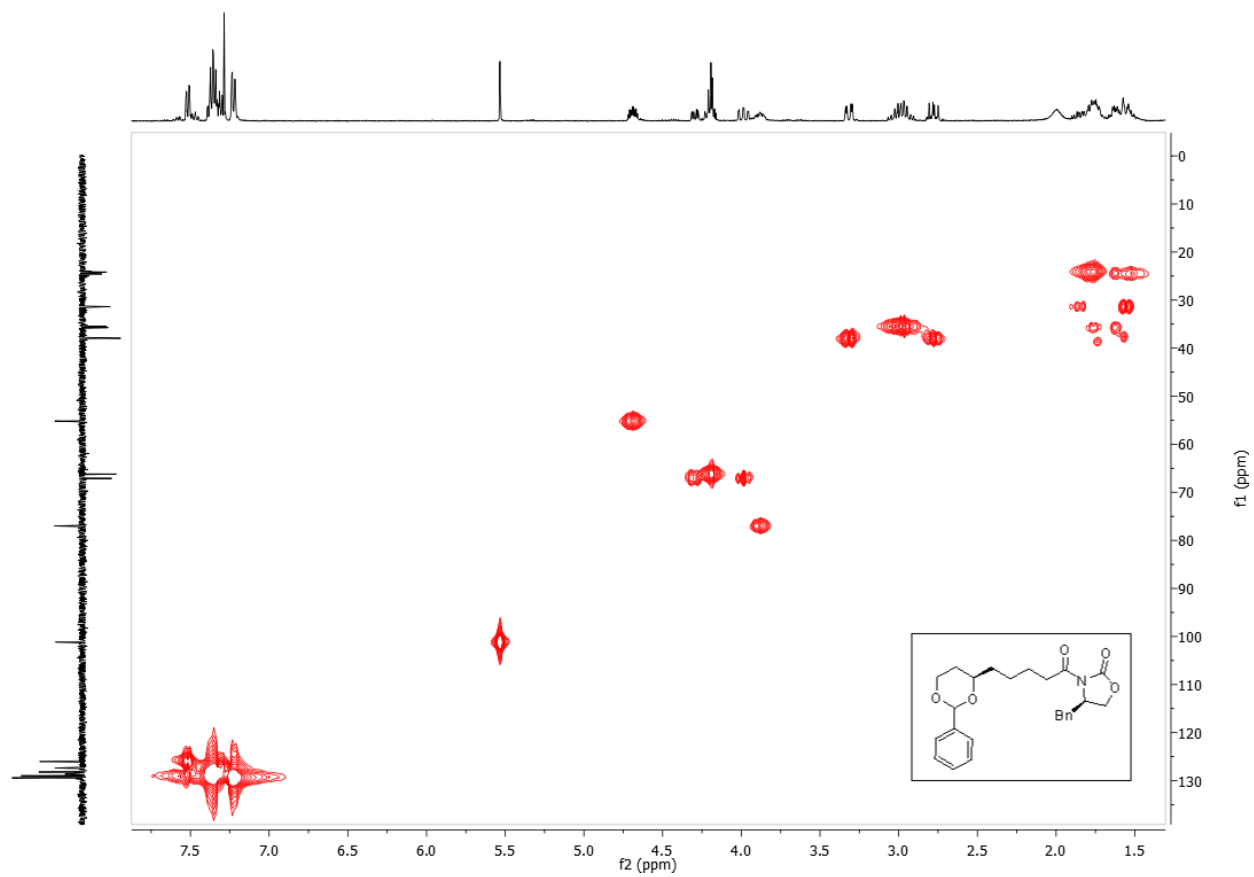
¹³C NMR (126 MHz, Chloroform-d) for **7a**



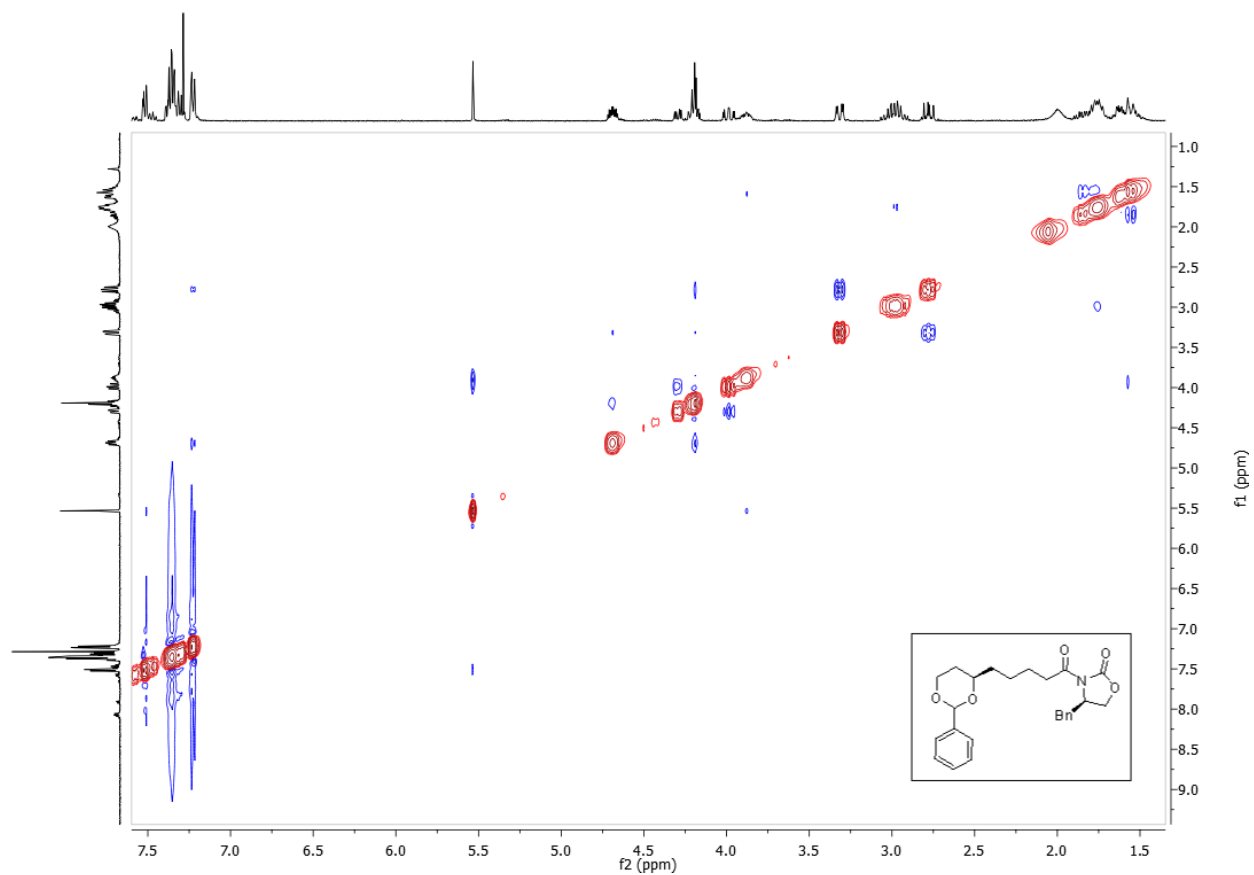
H-H COSY (Chloroform-d) for 7a



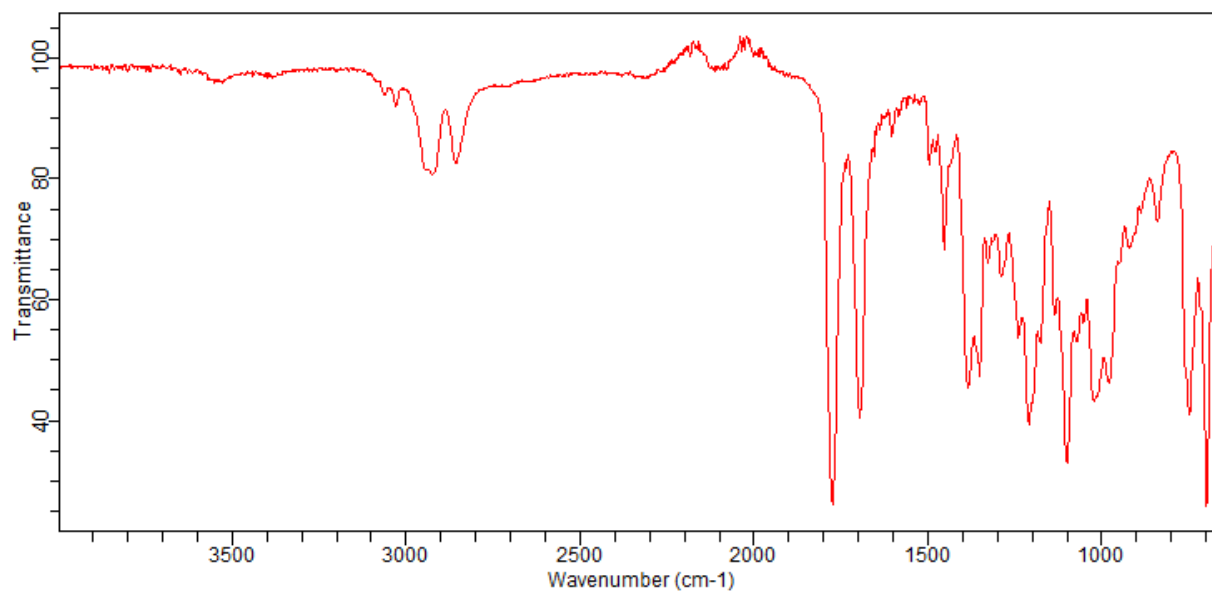
HSQC (Chloroform-d) for 7a



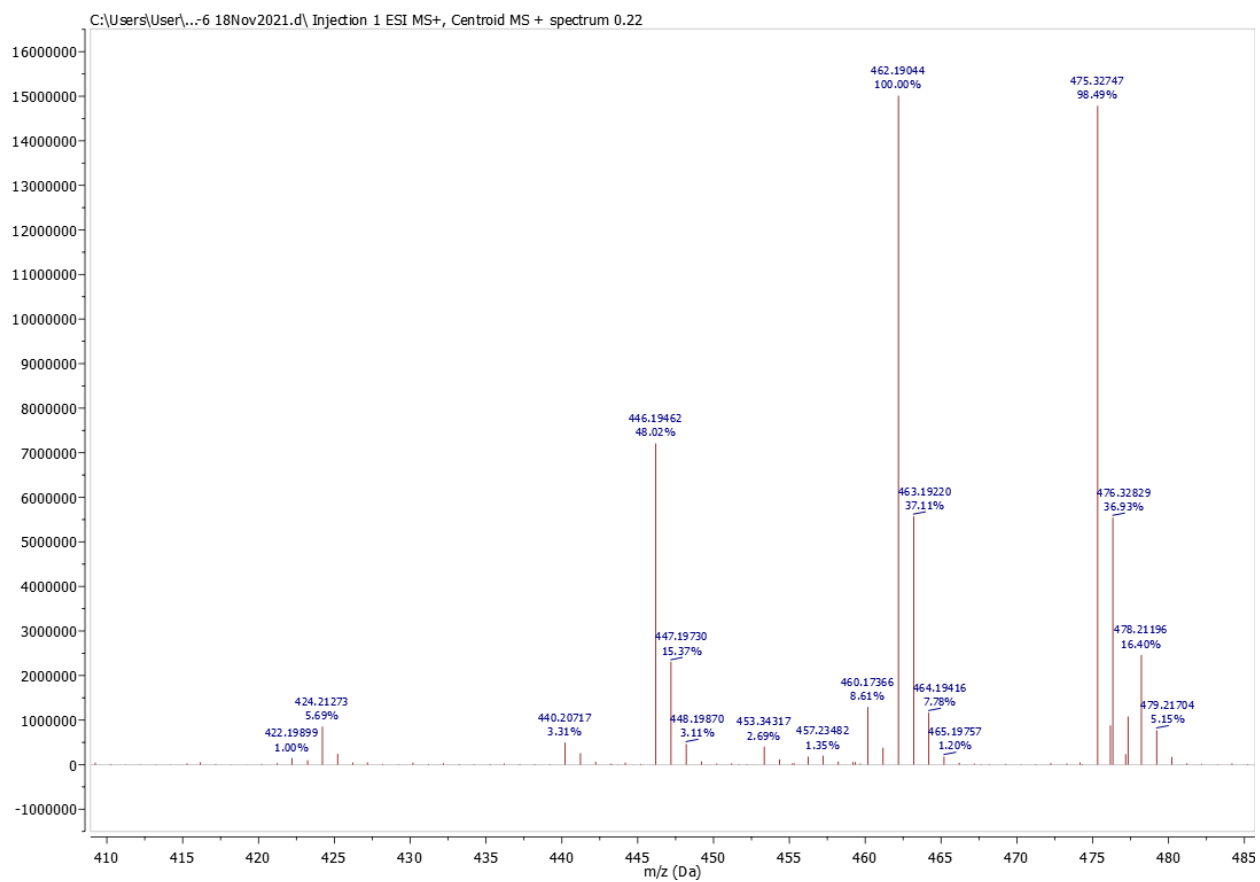
NOESY (Chloroform-d) for **7a**



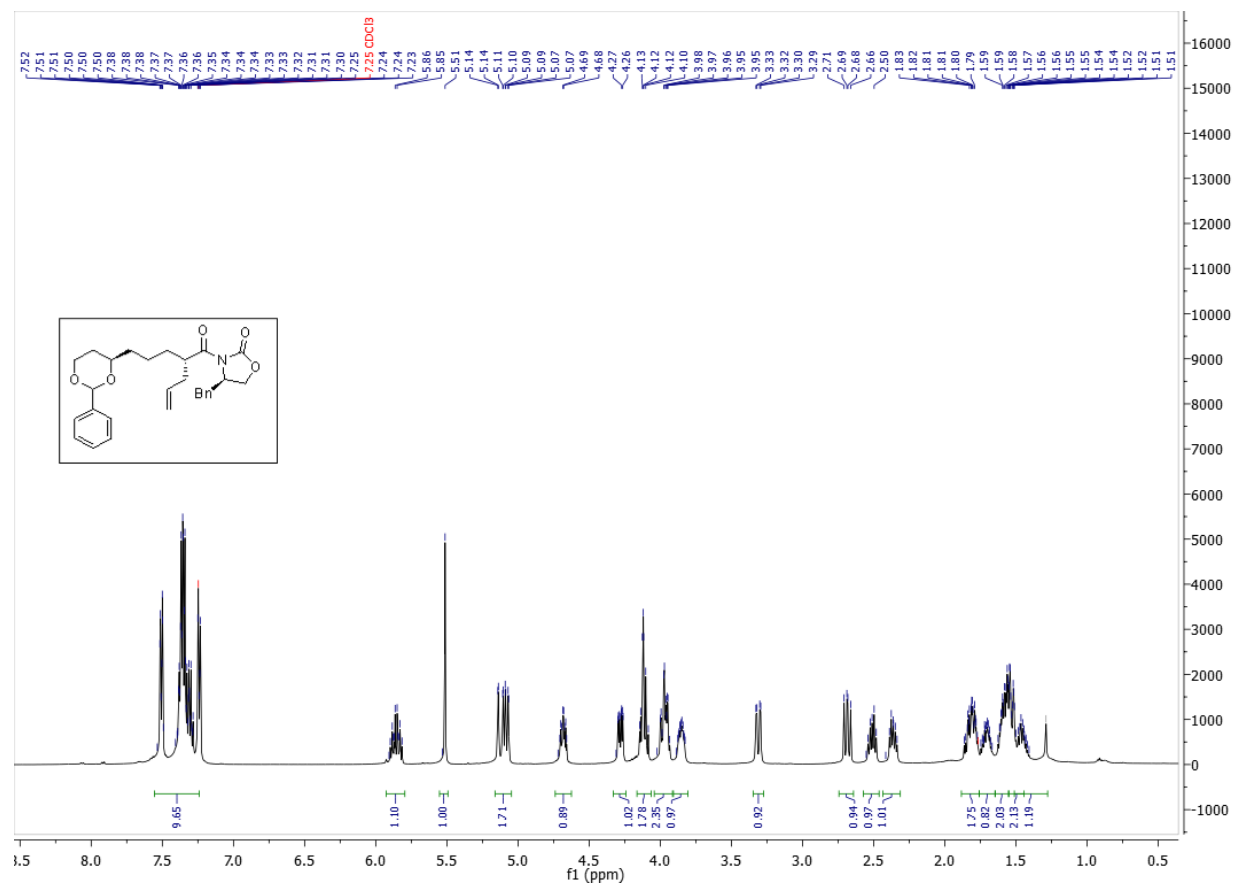
IR (KBr) for **7a**



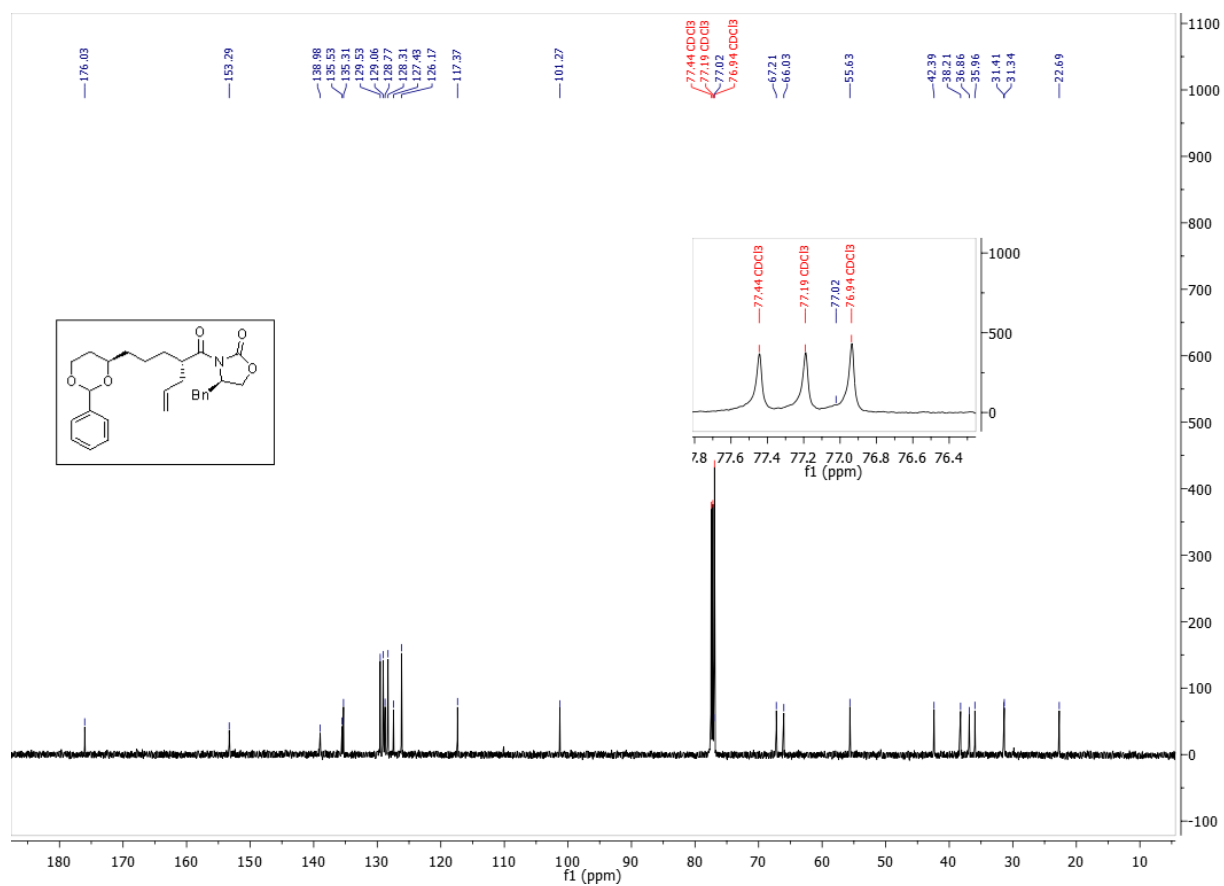
HRESIMS for 7a



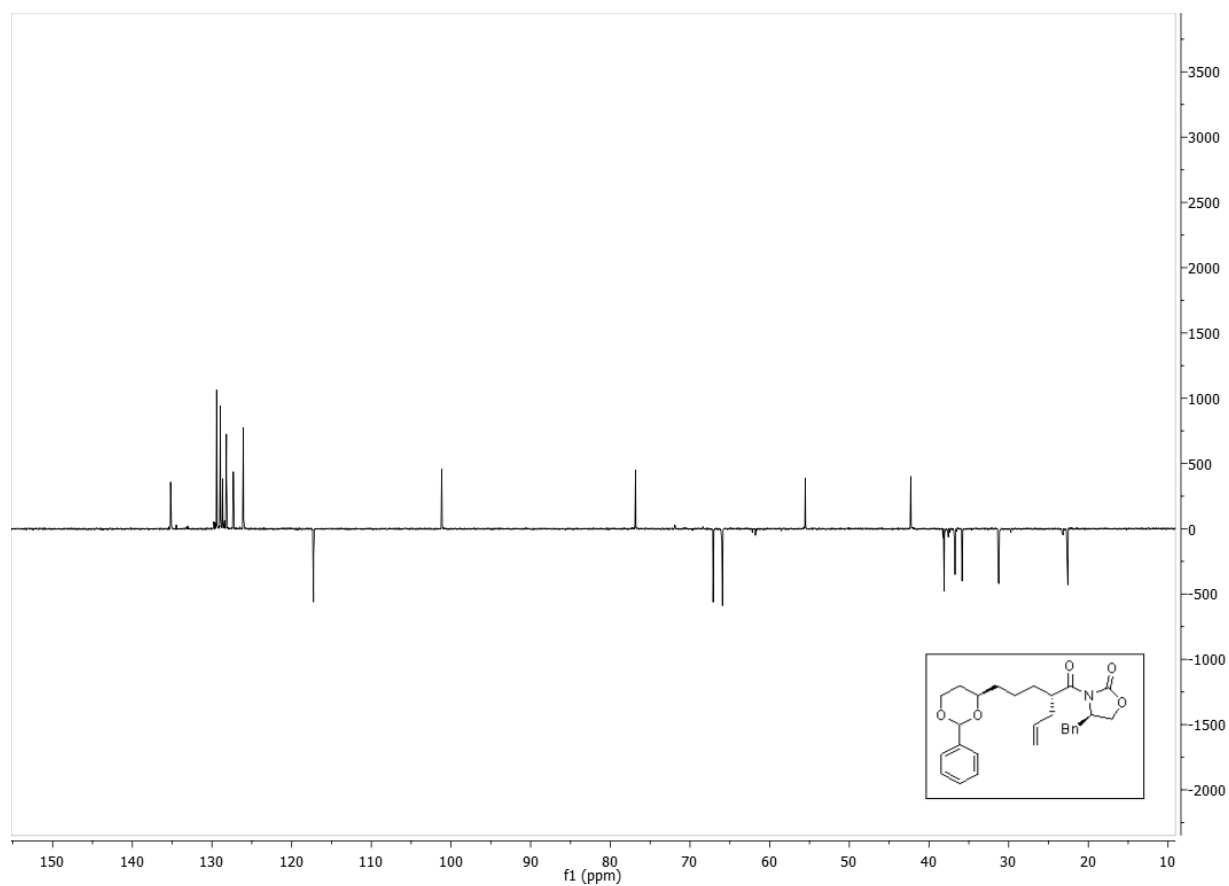
¹H NMR (500 MHz, Chloroform-d) for **6a**



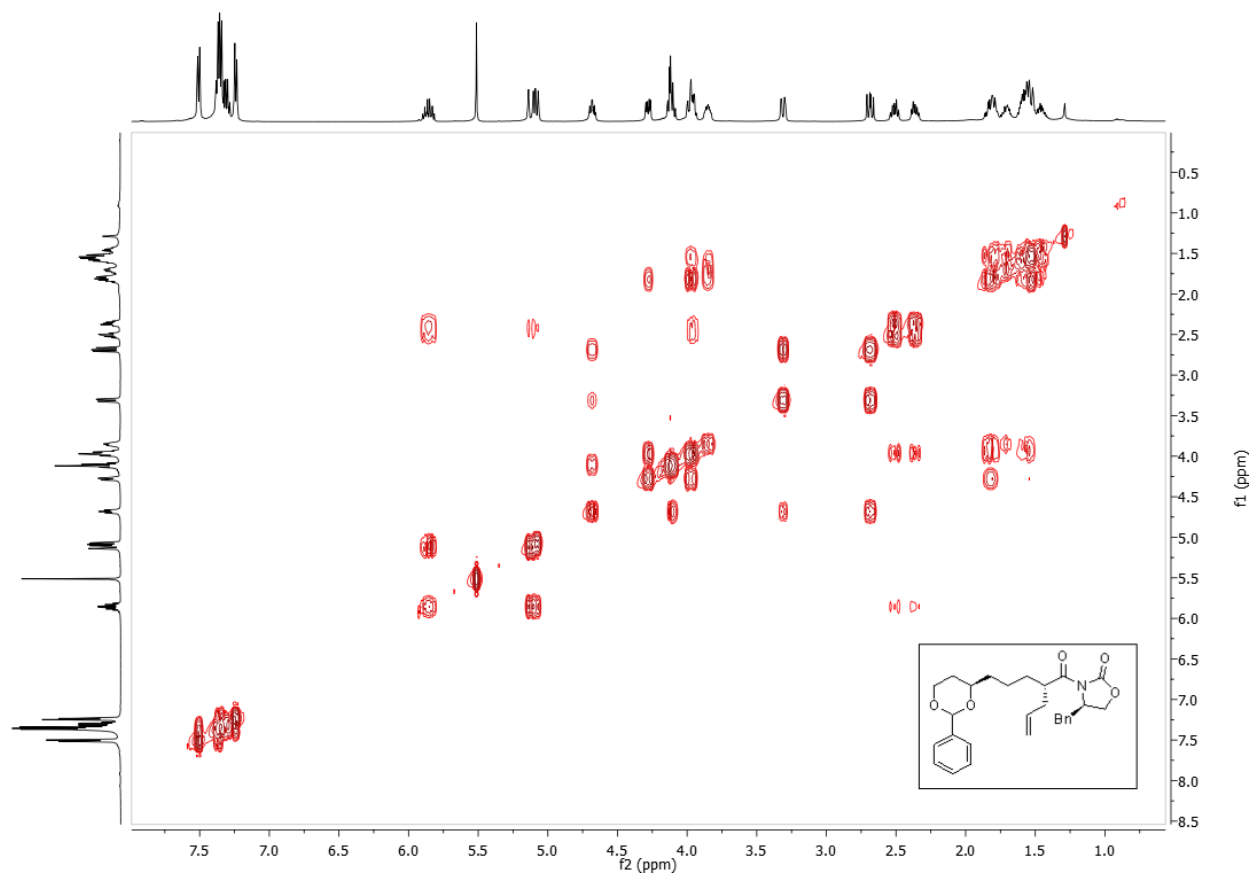
¹³C NMR (126 MHz, Chloroform-d) for **6a**



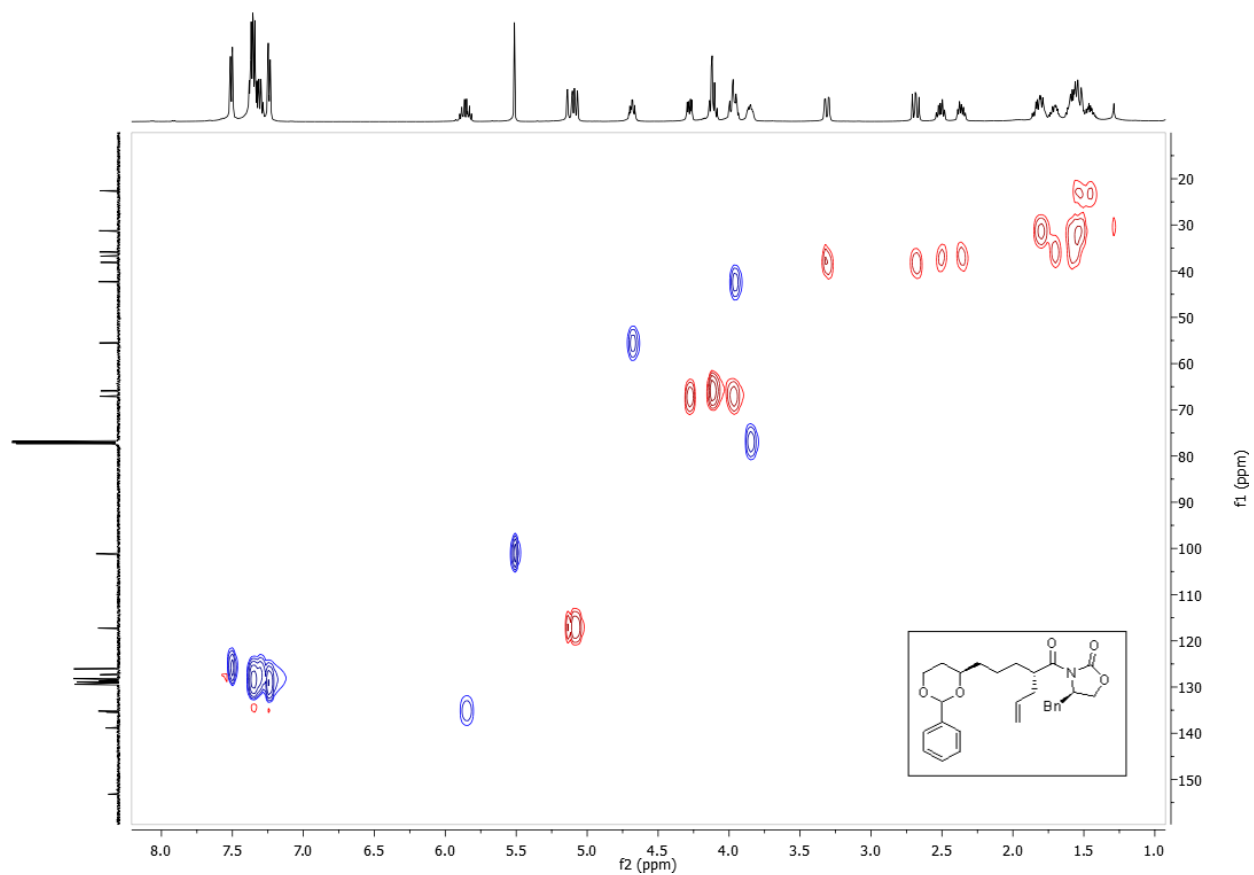
DEPT 135 (Chloroform-d) for **6a**



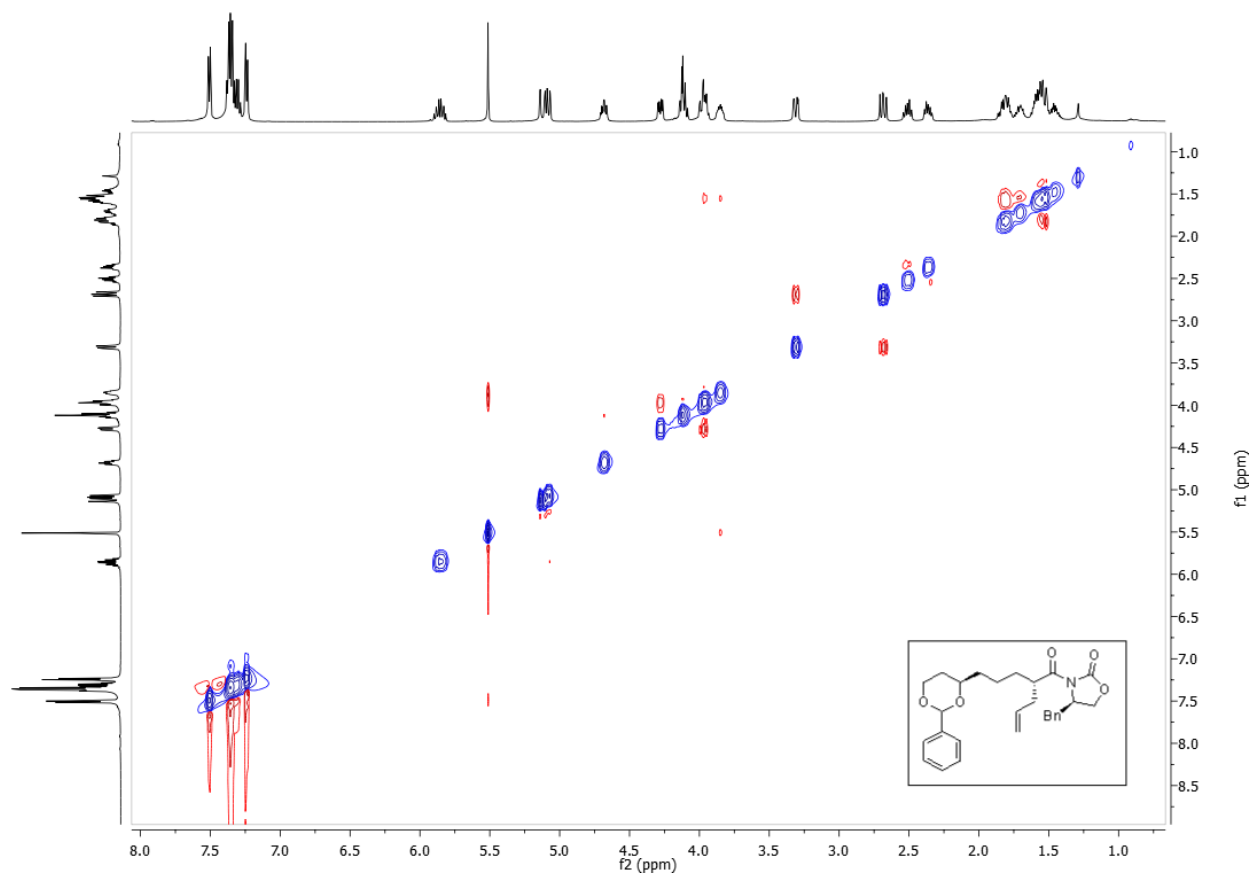
H-H COSY (Chloroform-d) for **6a**



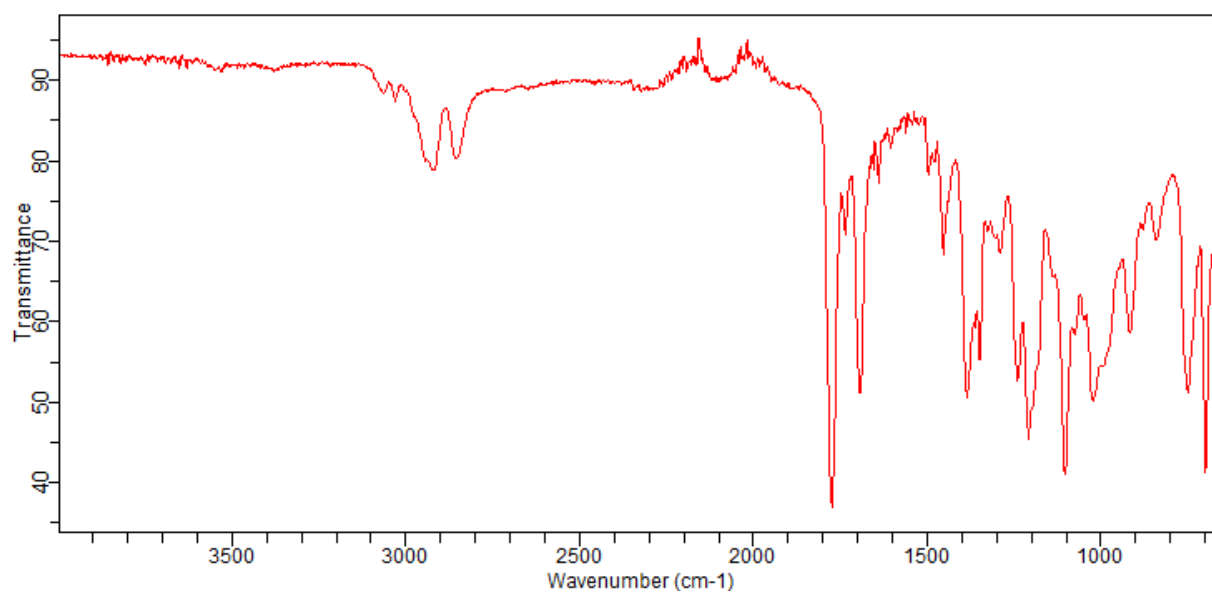
HSQC (Chloroform-d) for 6a



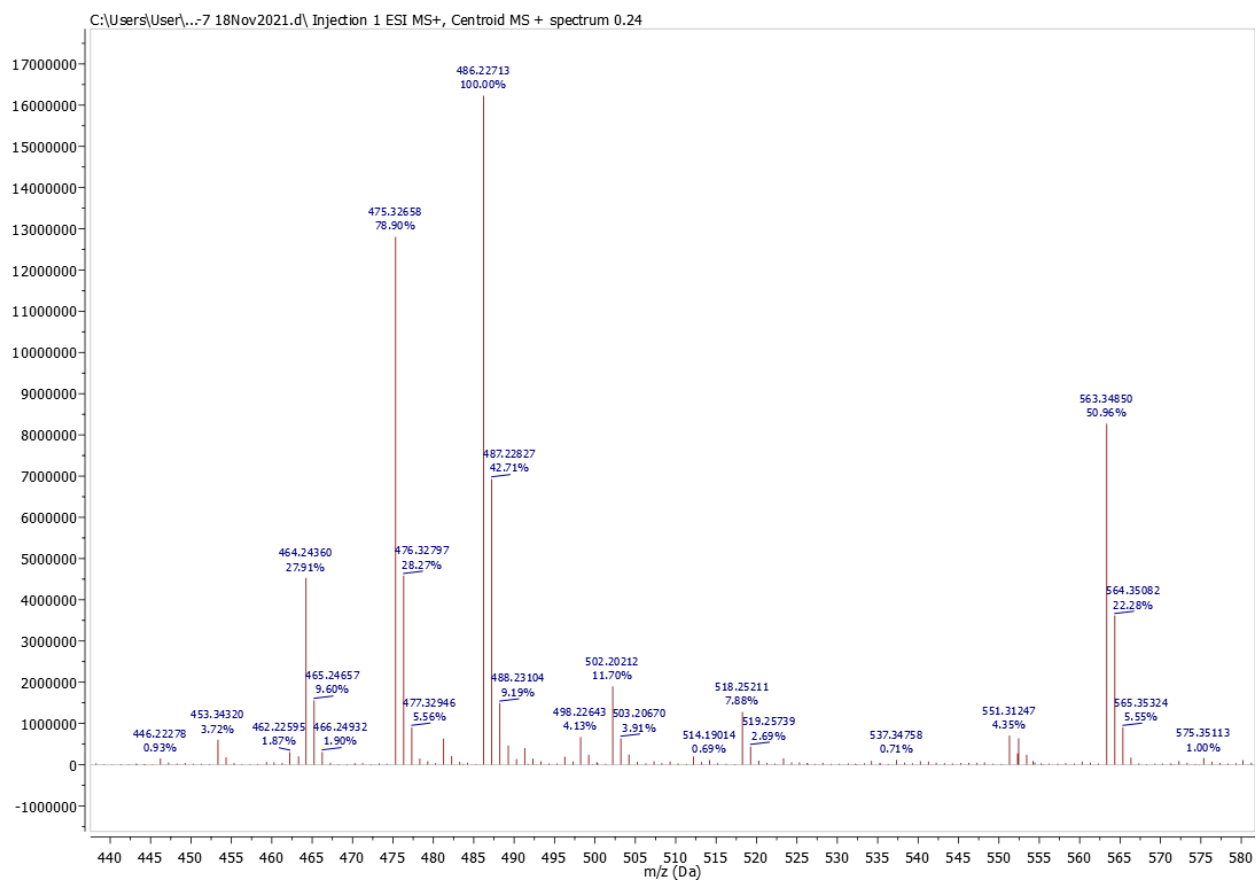
NOESY (Chloroform-d) for **6a**



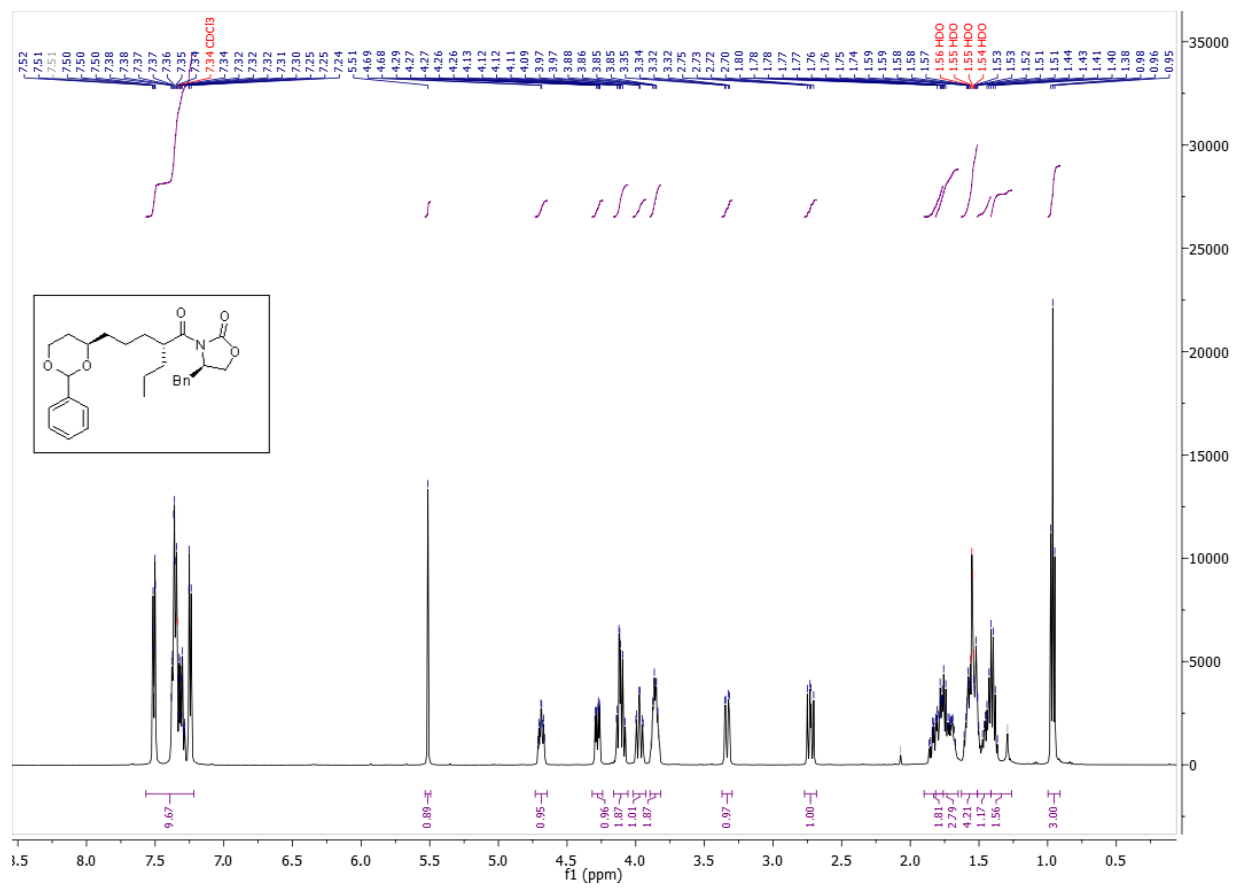
IR (KBr) for **6a**



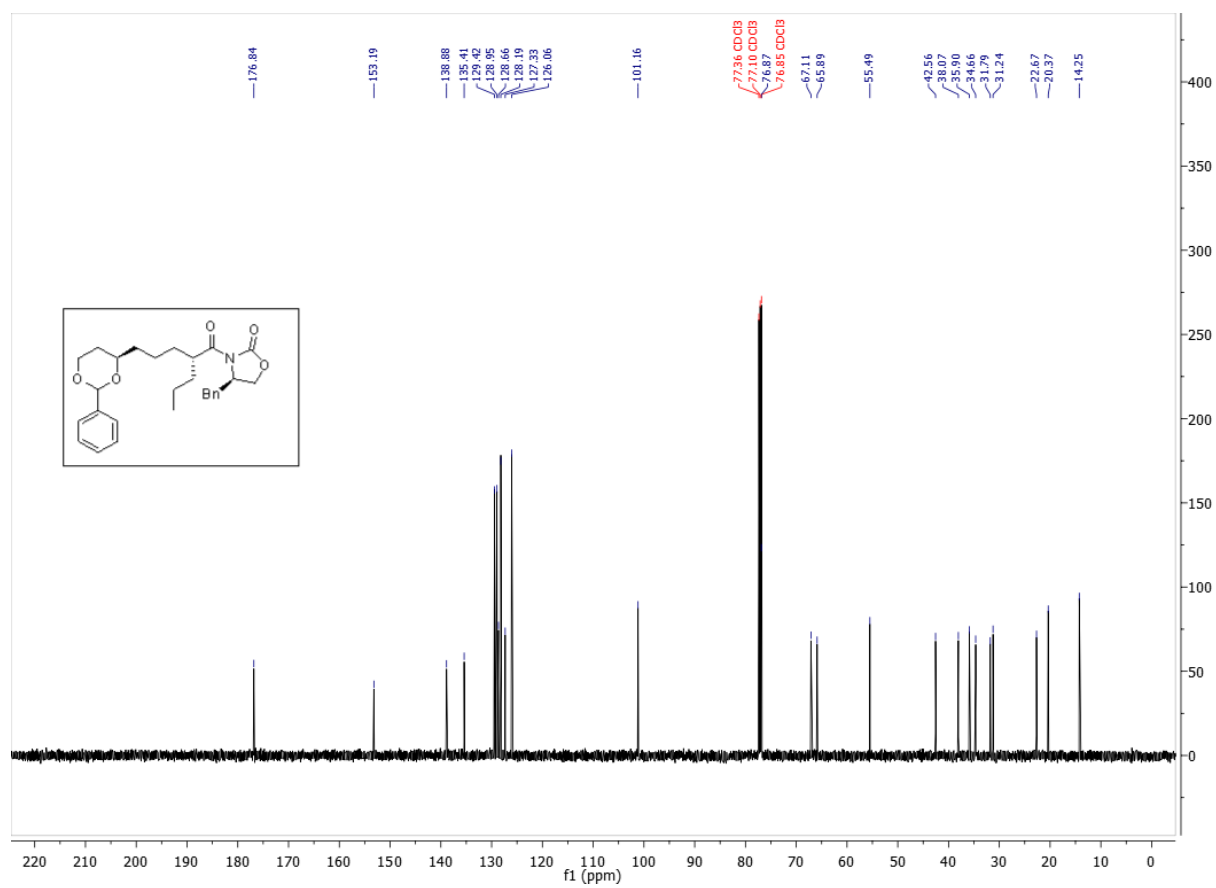
HRESIMS for 6a



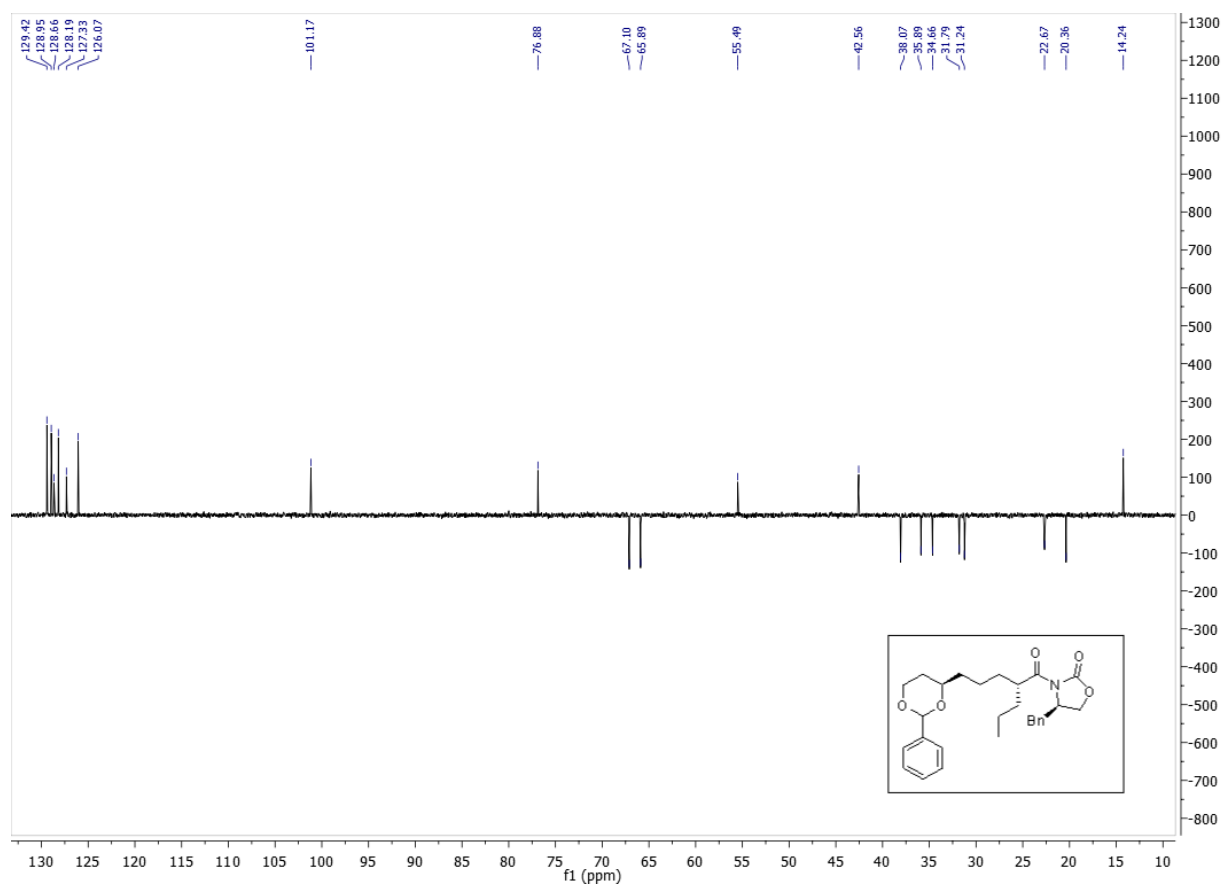
¹H NMR (500 MHz, Chloroform-d) for **5a**



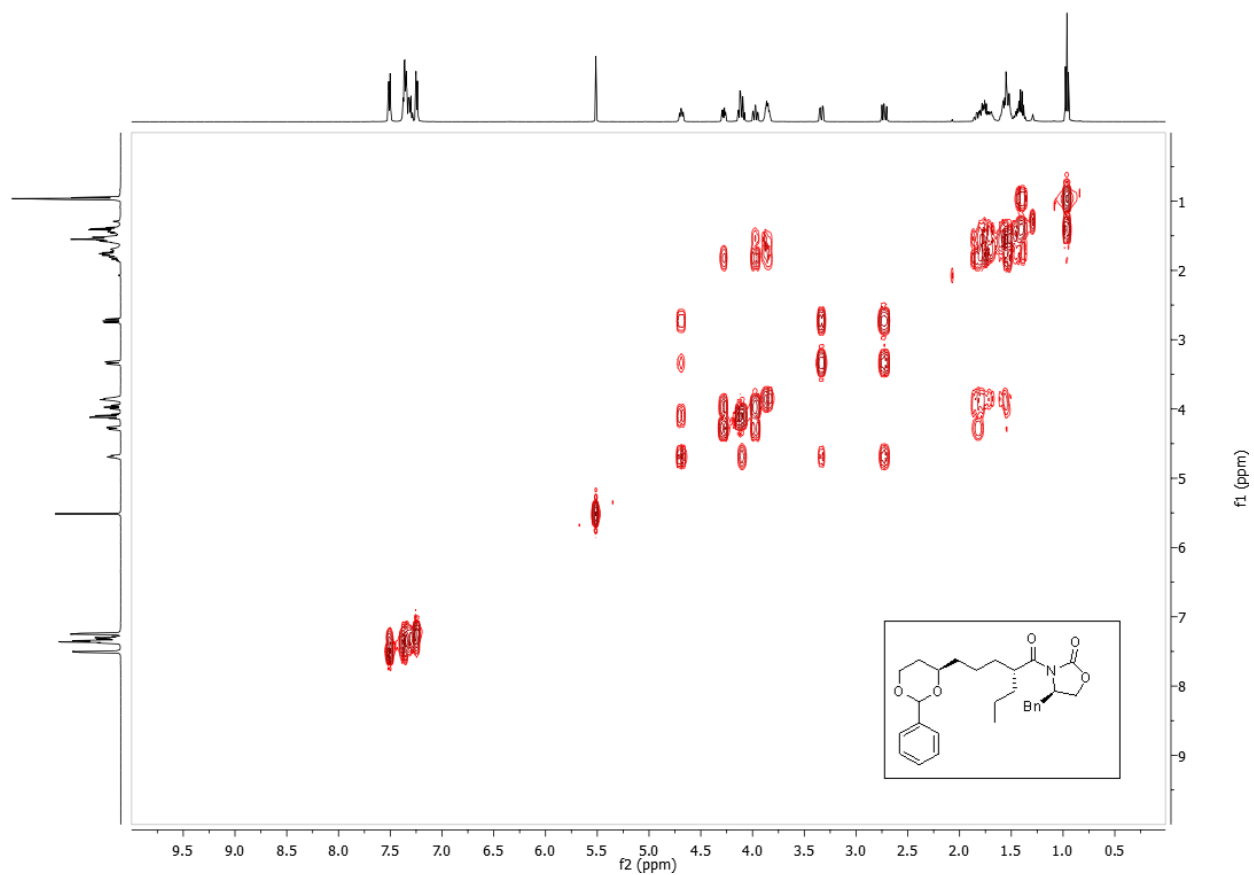
¹³C NMR (126 MHz, Chloroform-d) for **5a**



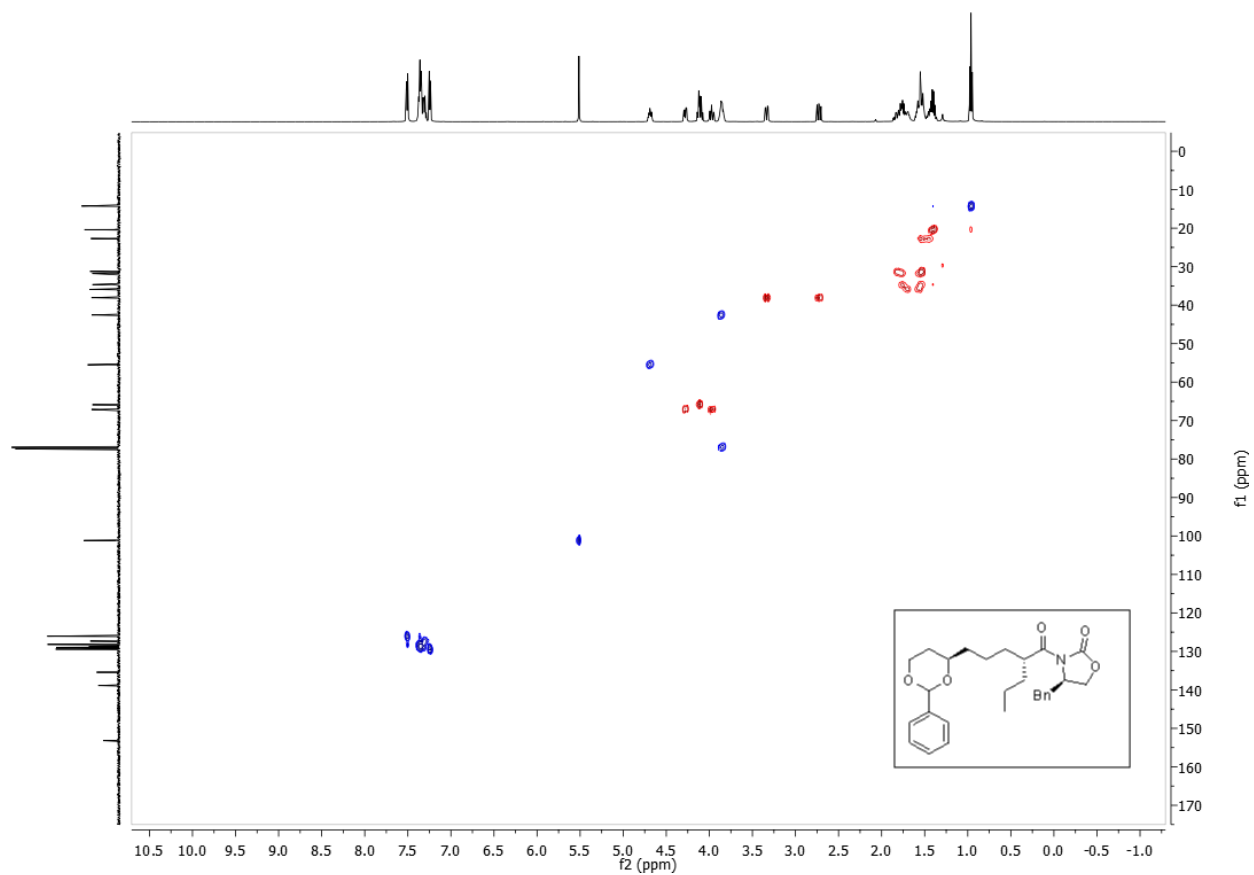
DEPT 135 (Chloroform-d) for **5a**



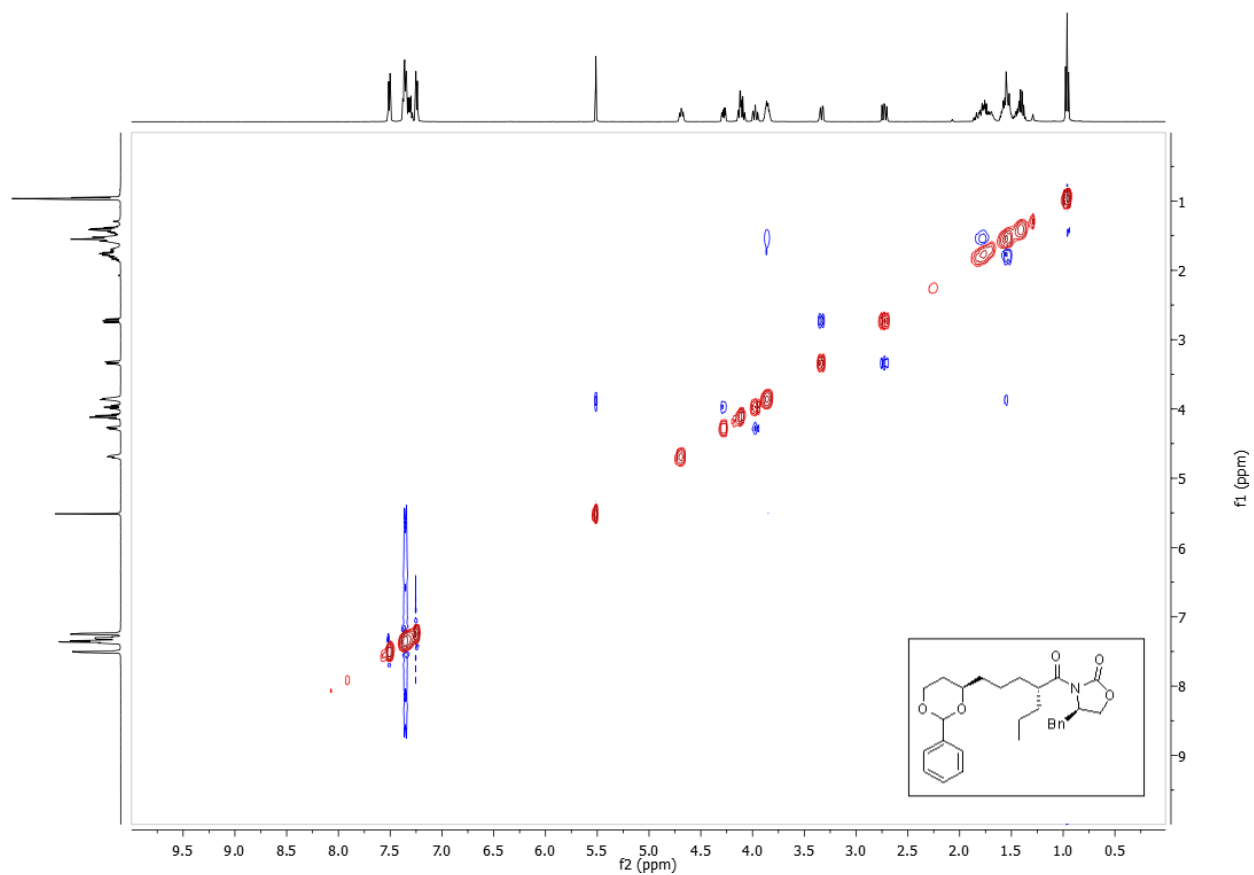
H-H COSY (Chloroform-d) for **5a**



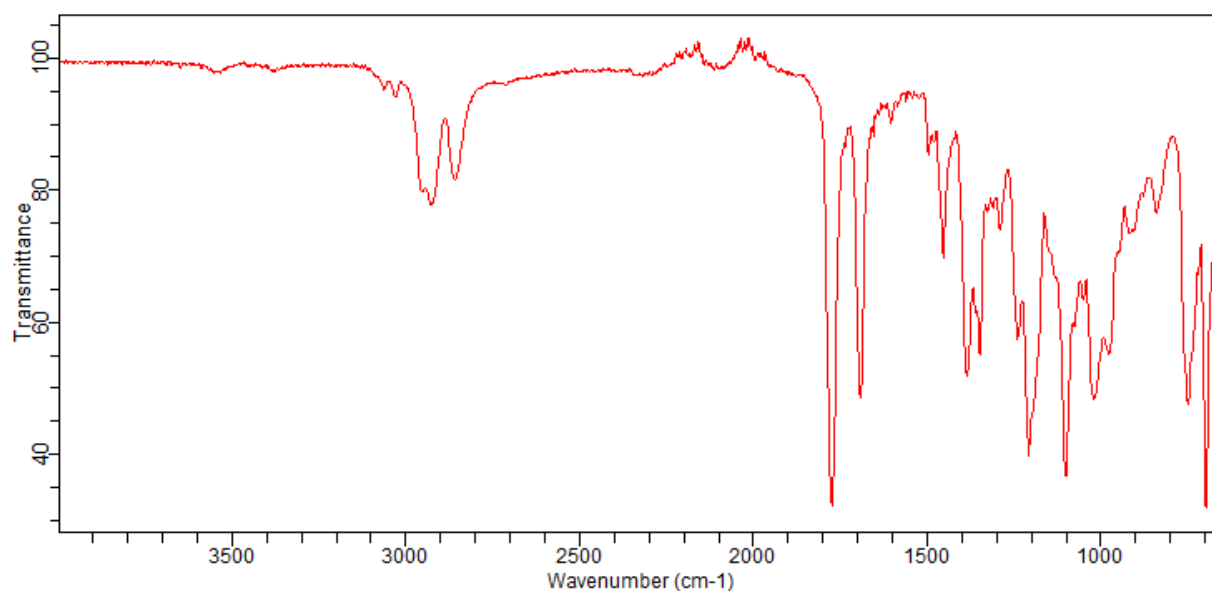
HSQC (Chloroform-d) for 5a



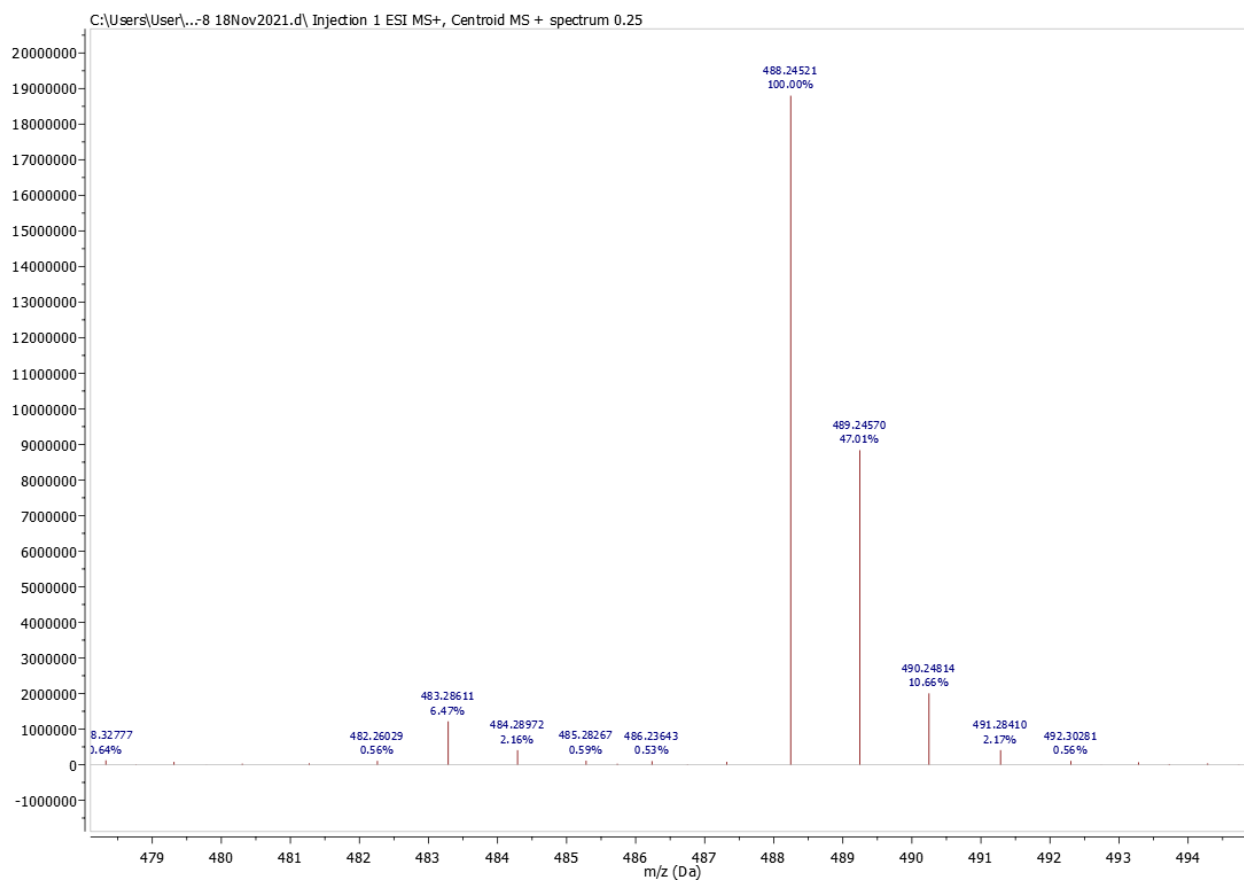
NOESY (Chloroform-d) for **5a**



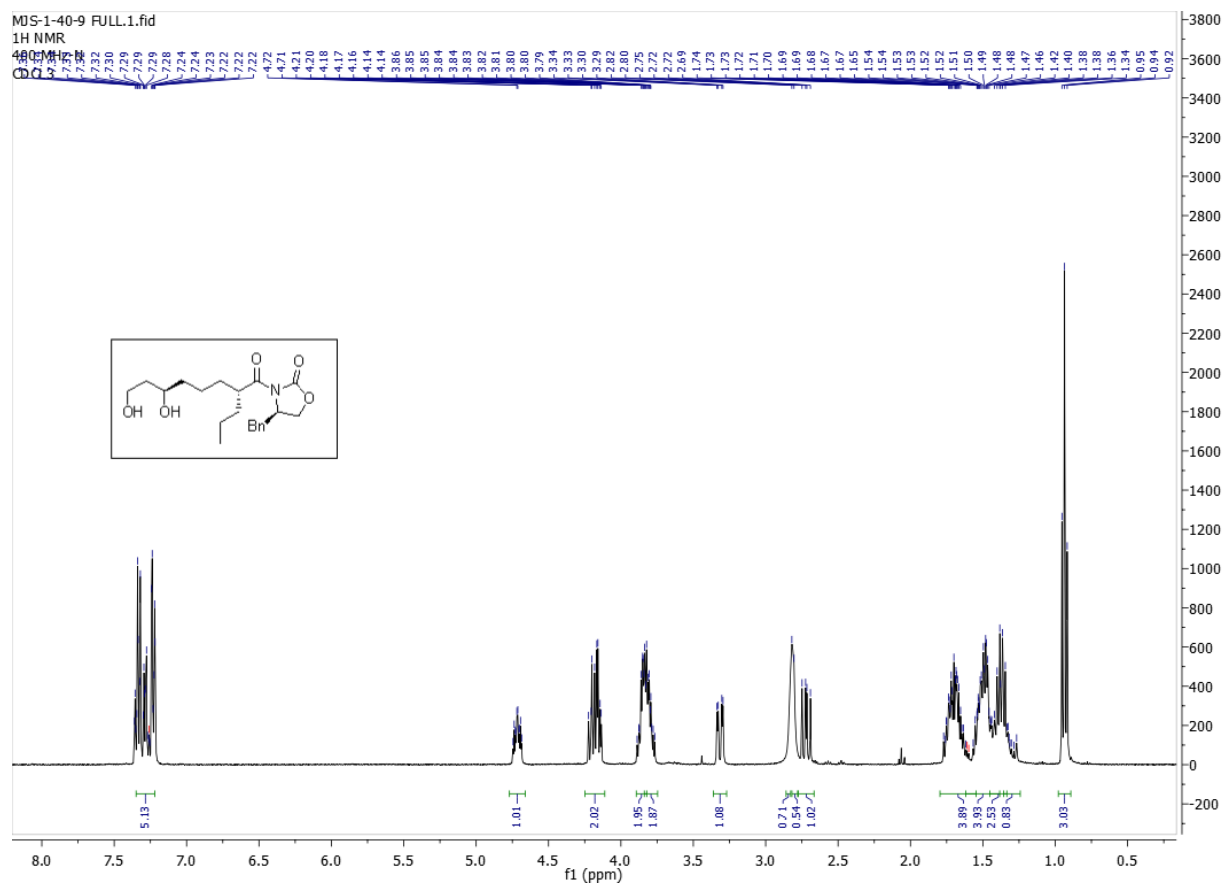
IR (KBr) for **5a**



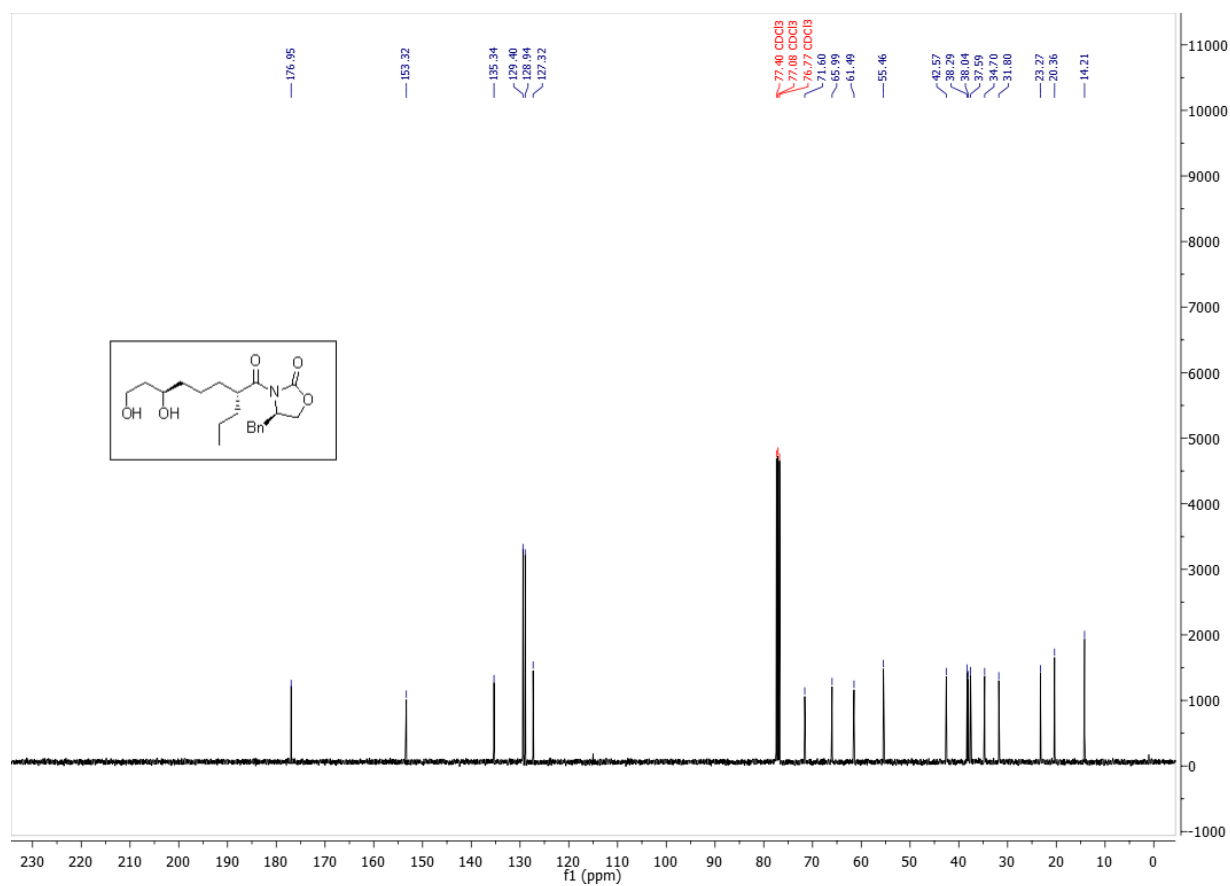
HRESIMS for 5a



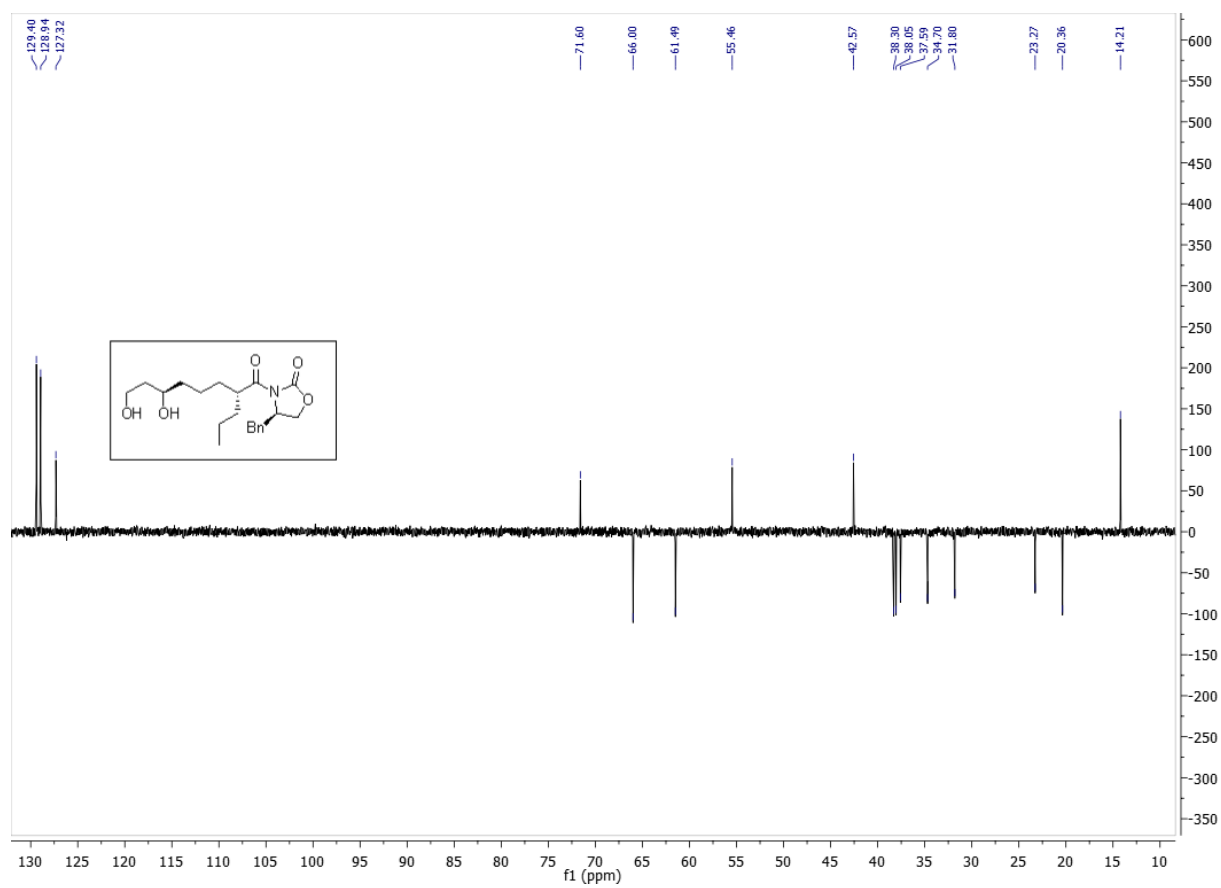
¹H NMR (400 MHz, Chloroform-d) for **4a**



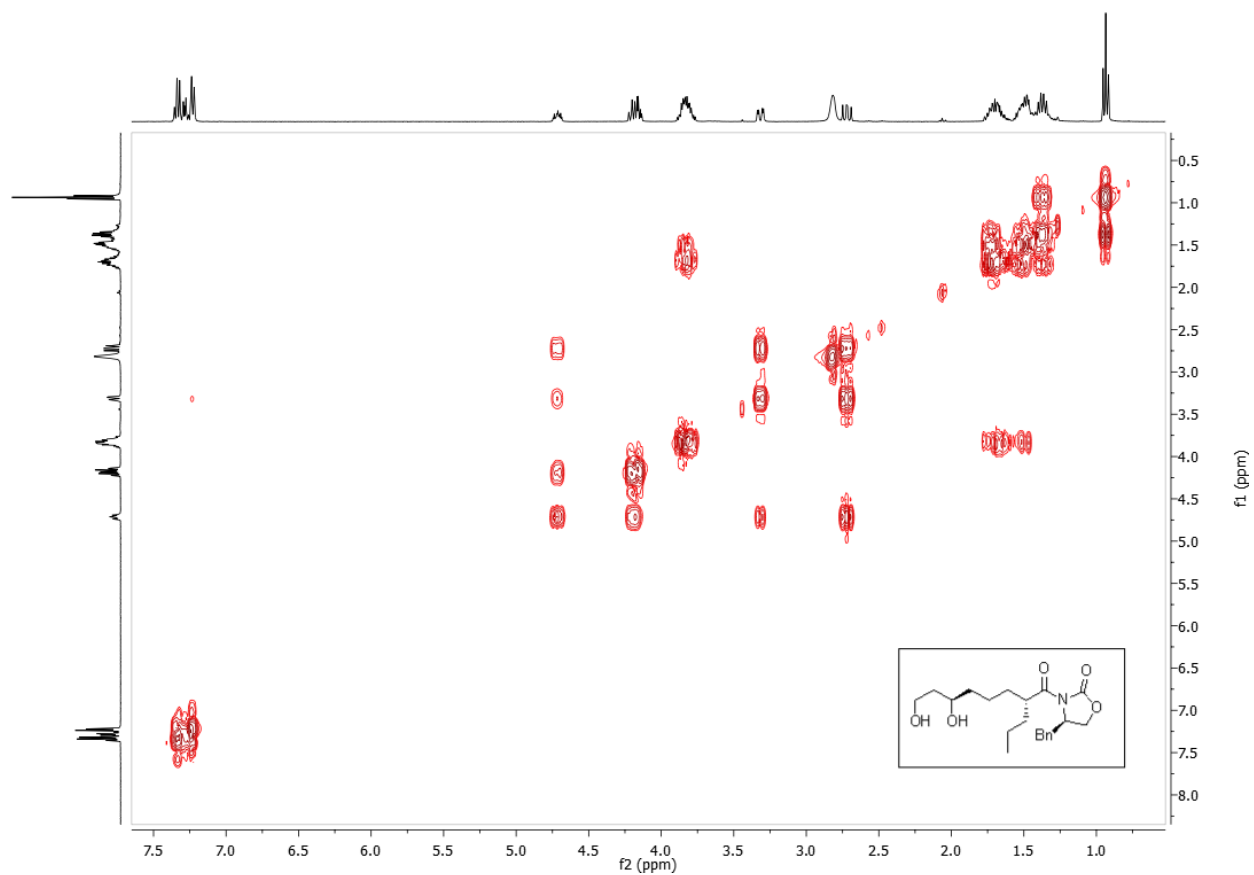
¹³C NMR (101 MHz, Chloroform-d) for **4a**



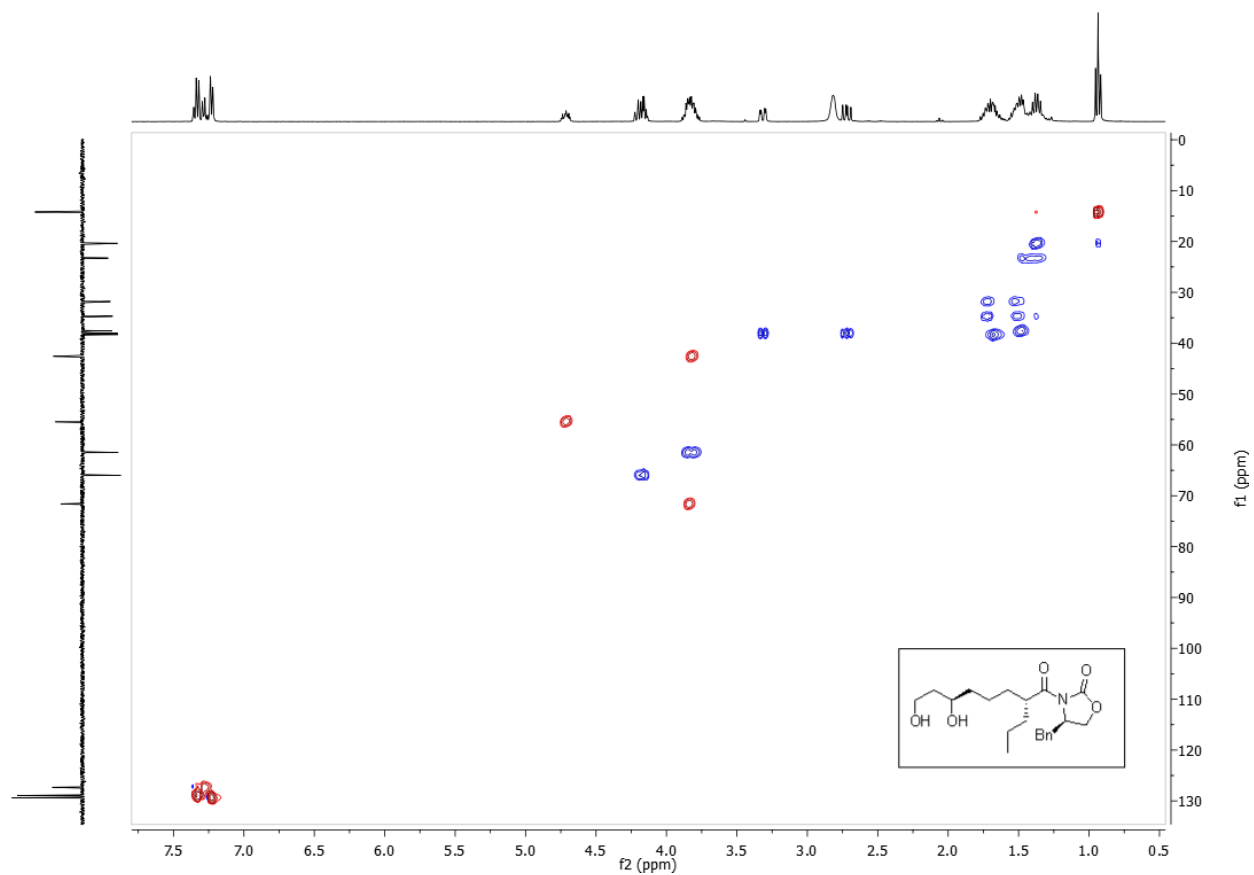
DEPT 135 (Chloroform-d) for 4a



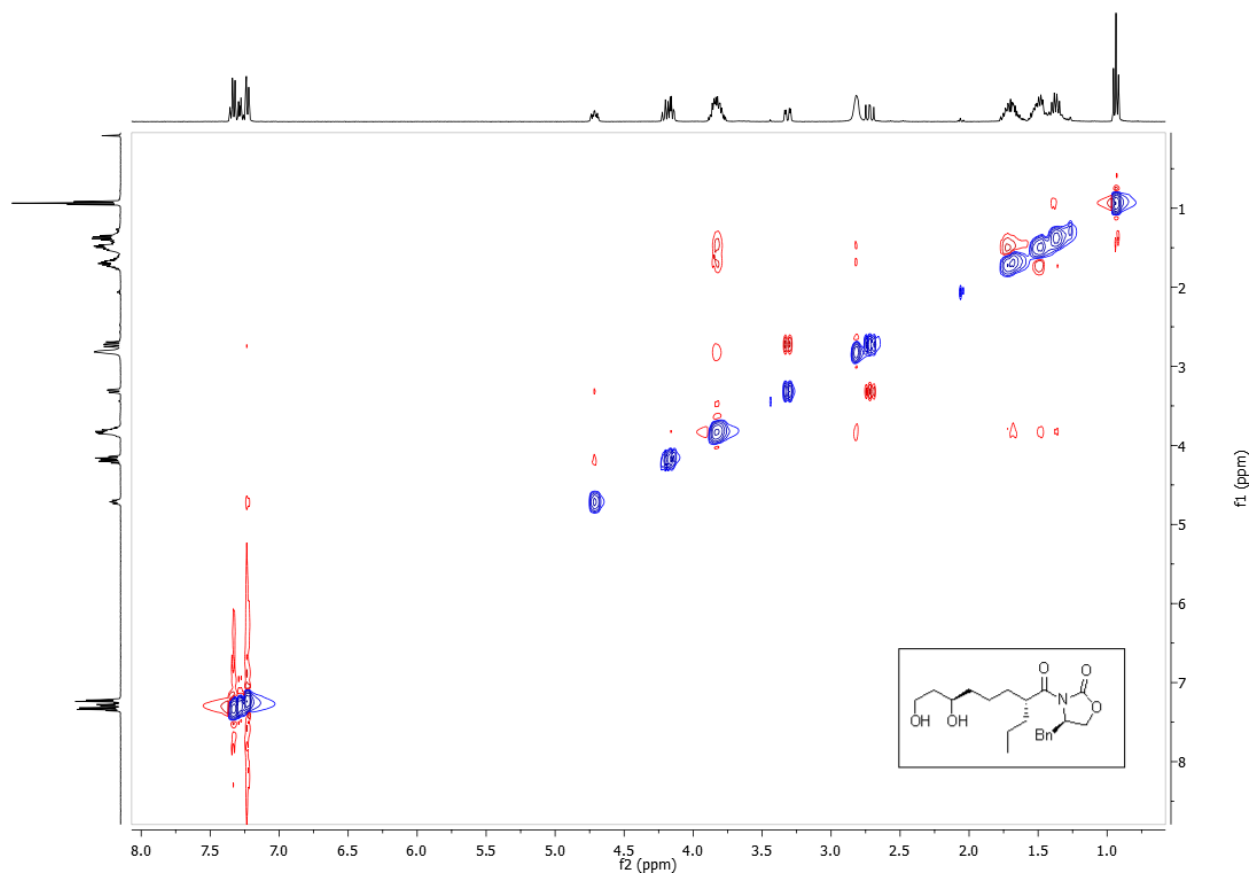
H-H COSY (Chloroform-d) for 4a



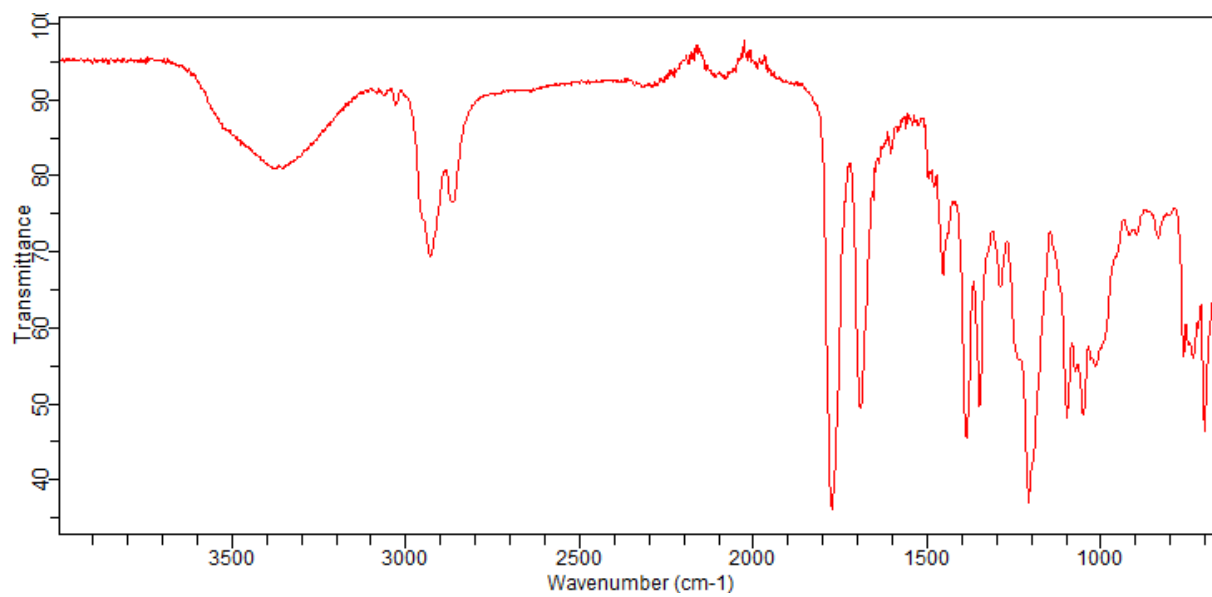
HSQC (Chloroform-d) for 4a



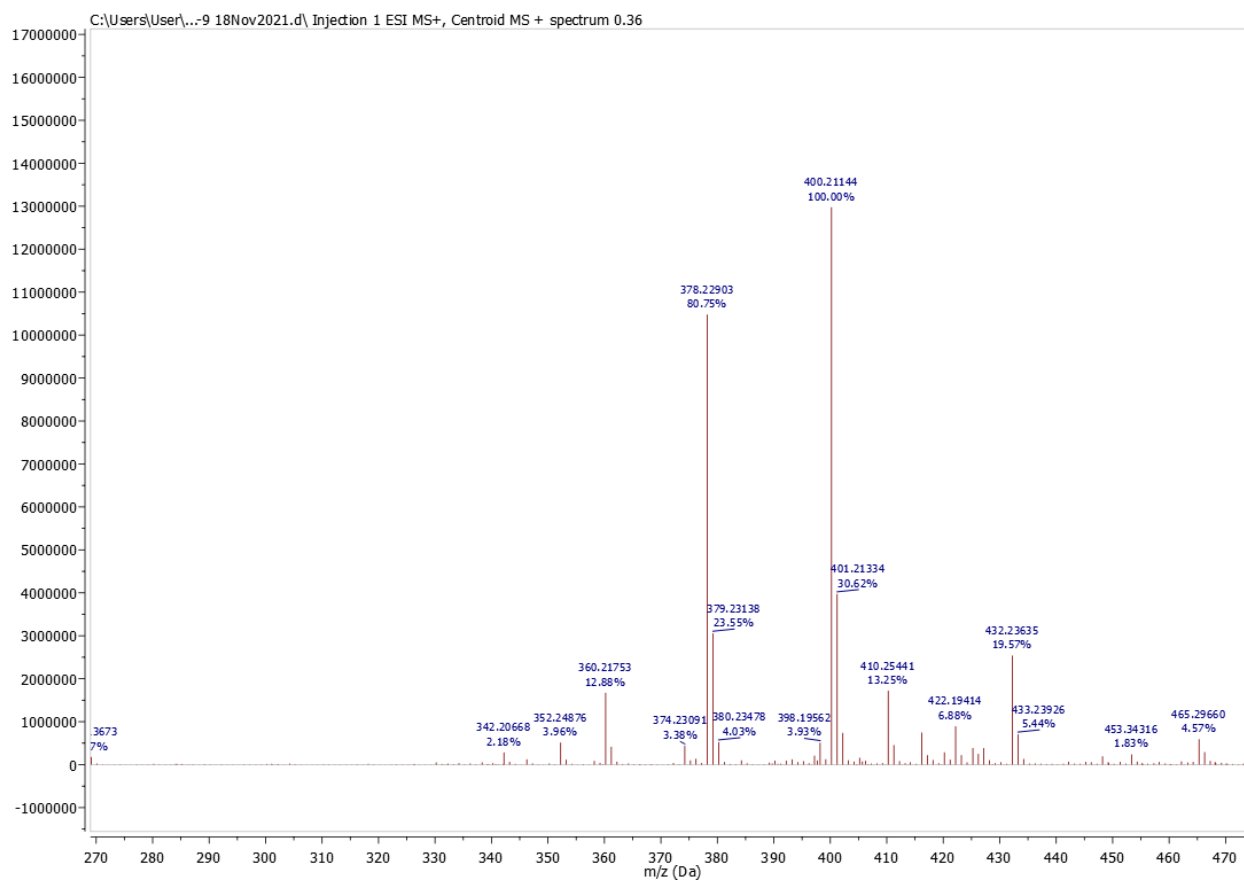
NOESY (Chloroform-d) for 4a



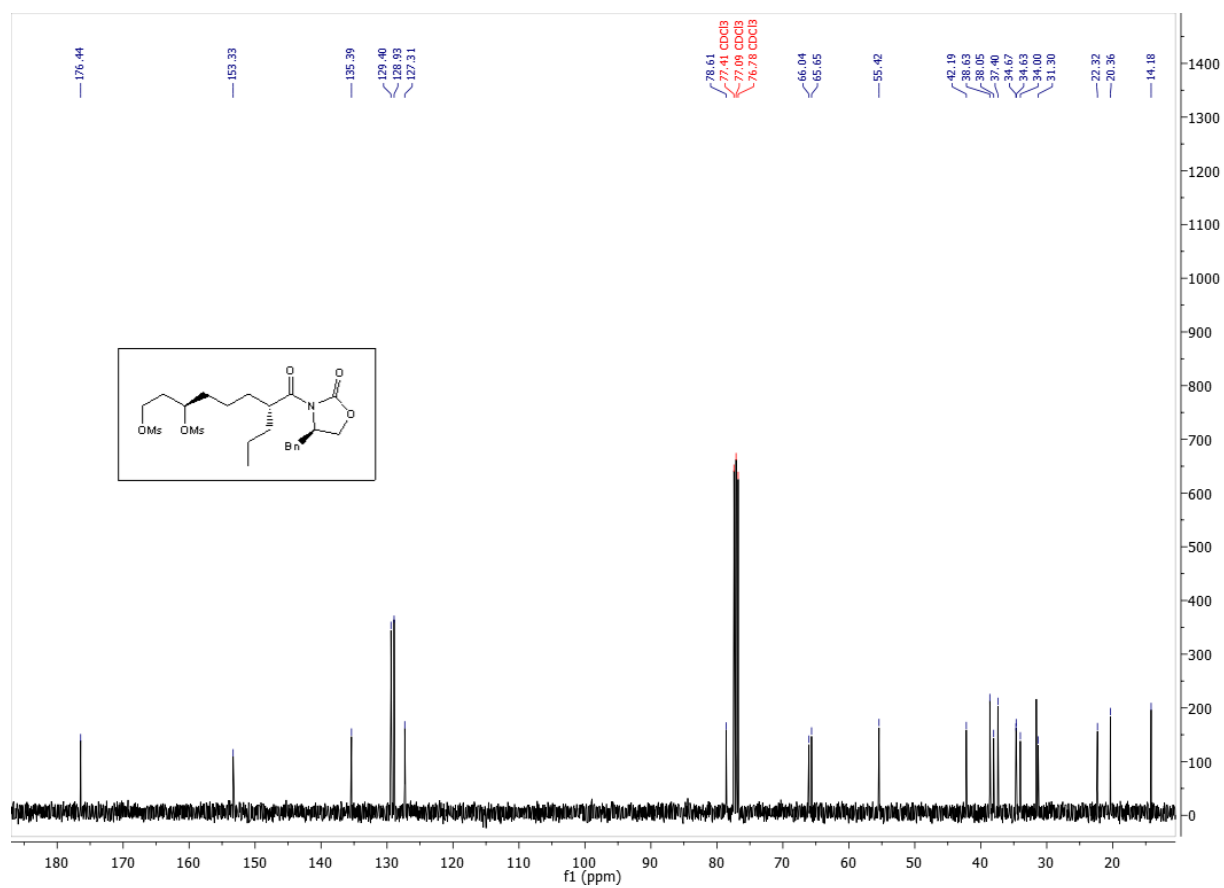
IR (KBr) for 4a



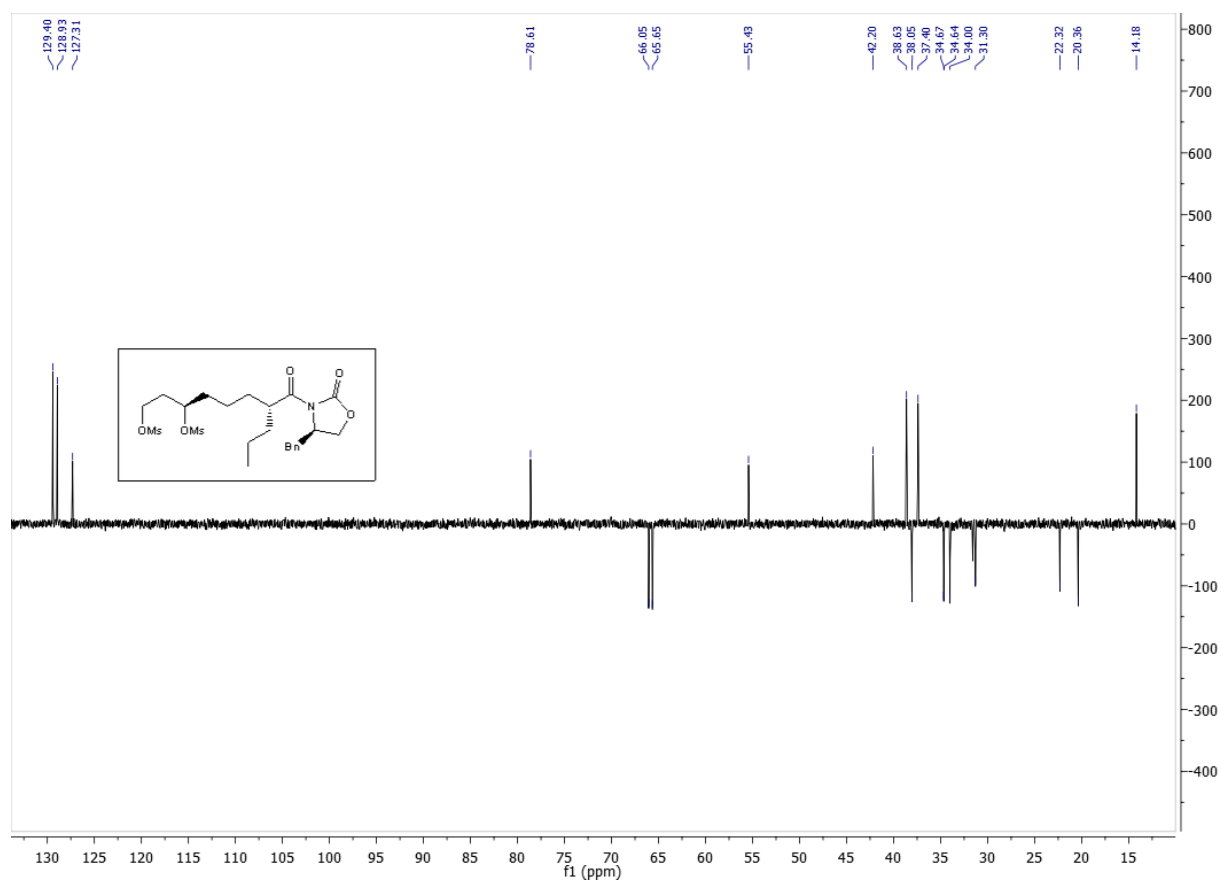
HRESIMS for 4a



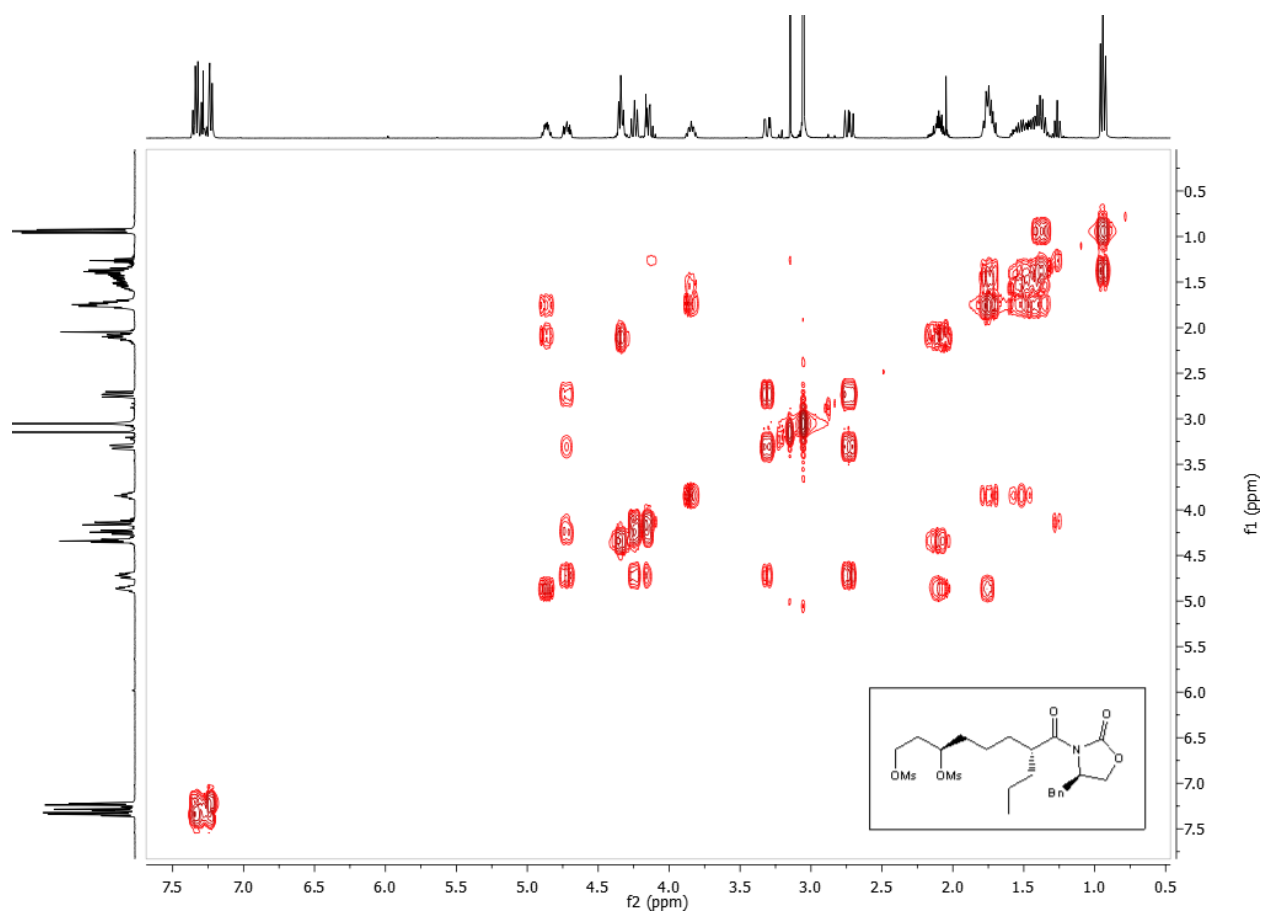
^{13}C NMR (101 MHz, Chloroform-d) for **3a**



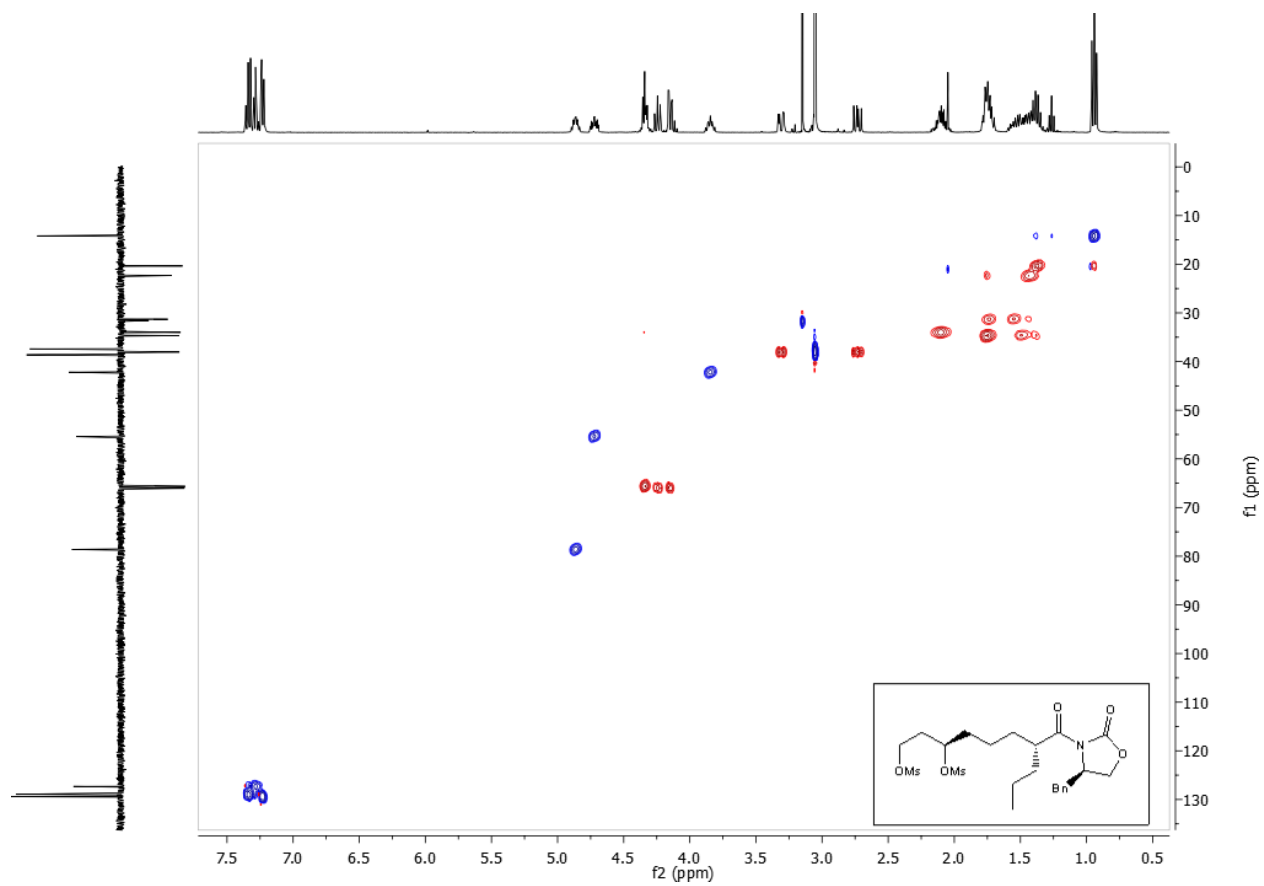
DEPT 135 (Chloroform-d) for 3a



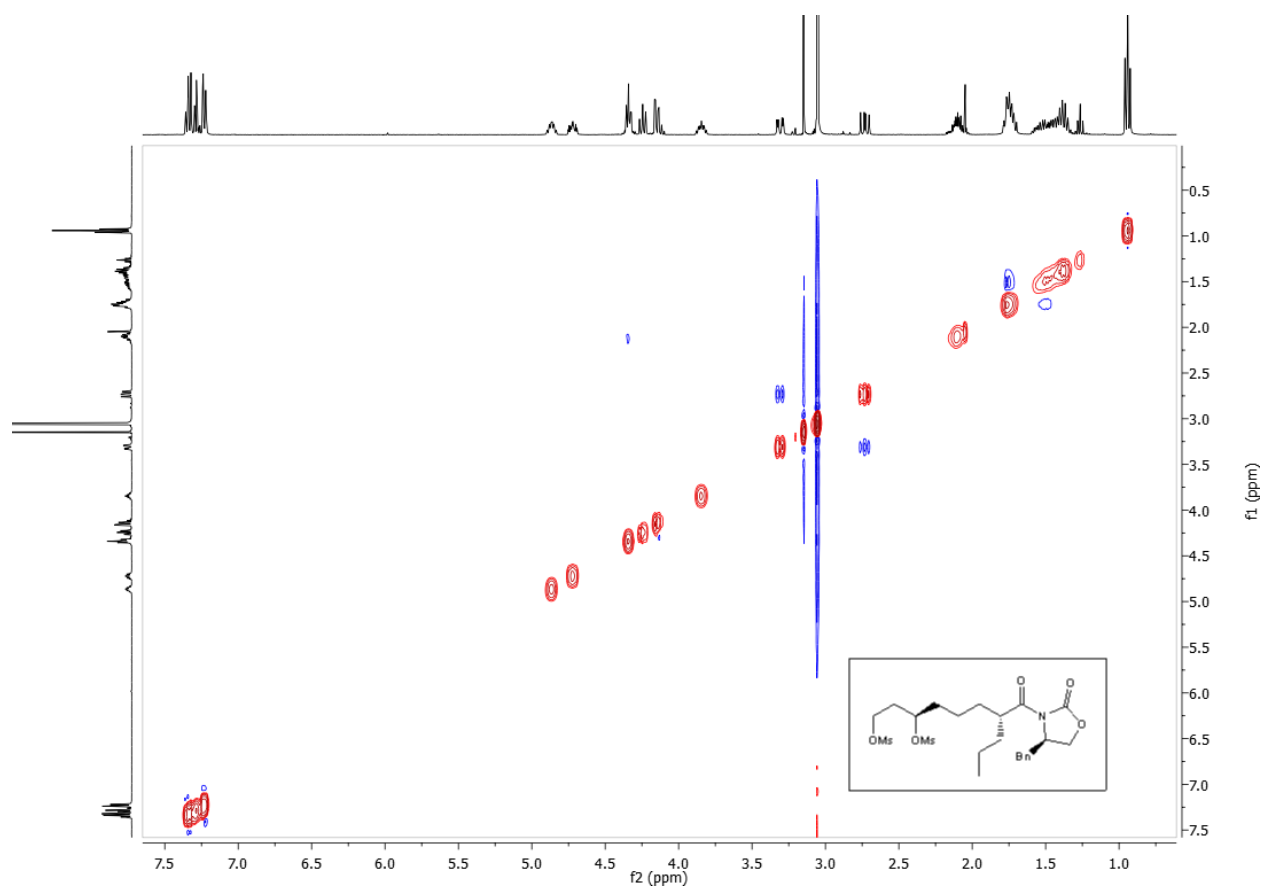
H-H COSY (Chloroform-d) for 3a



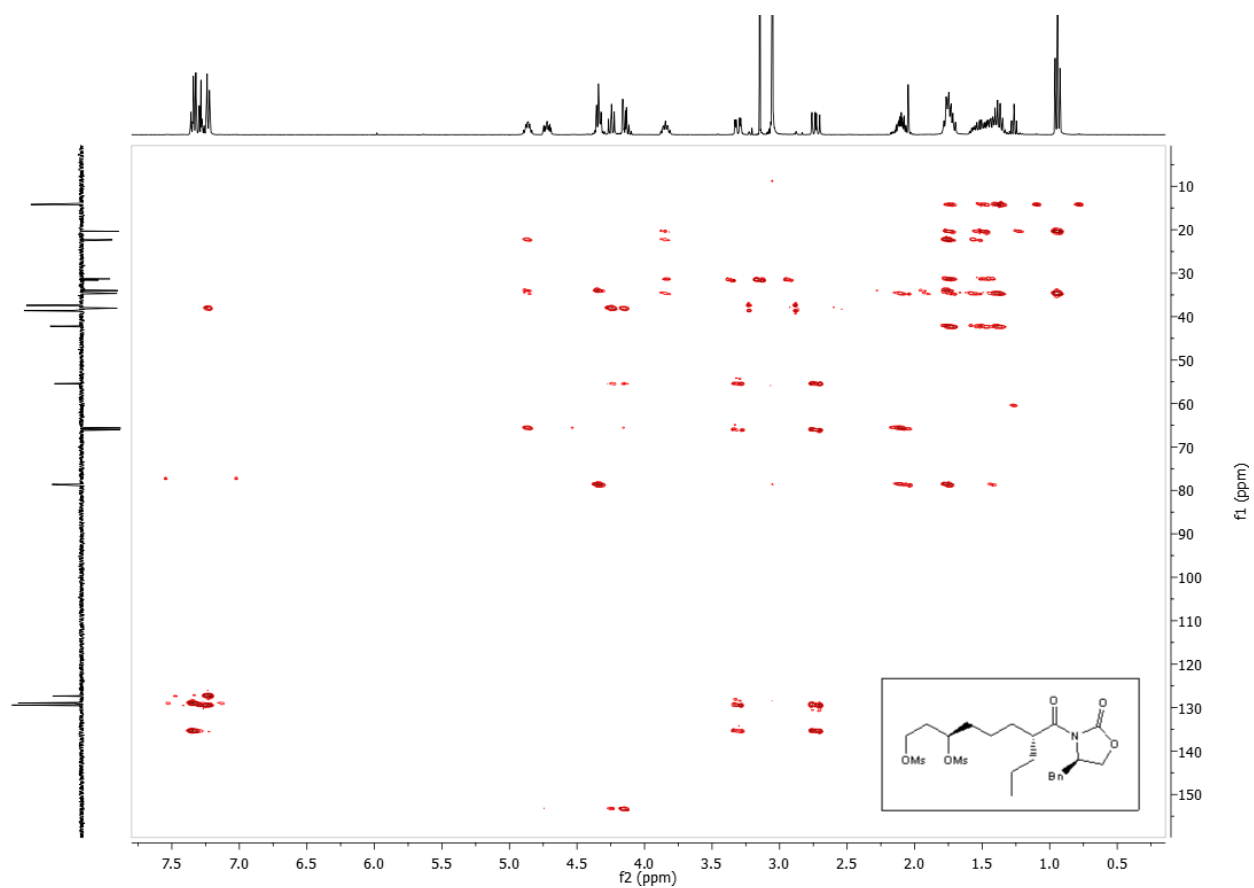
HSQC (Chloroform-d) for 3a



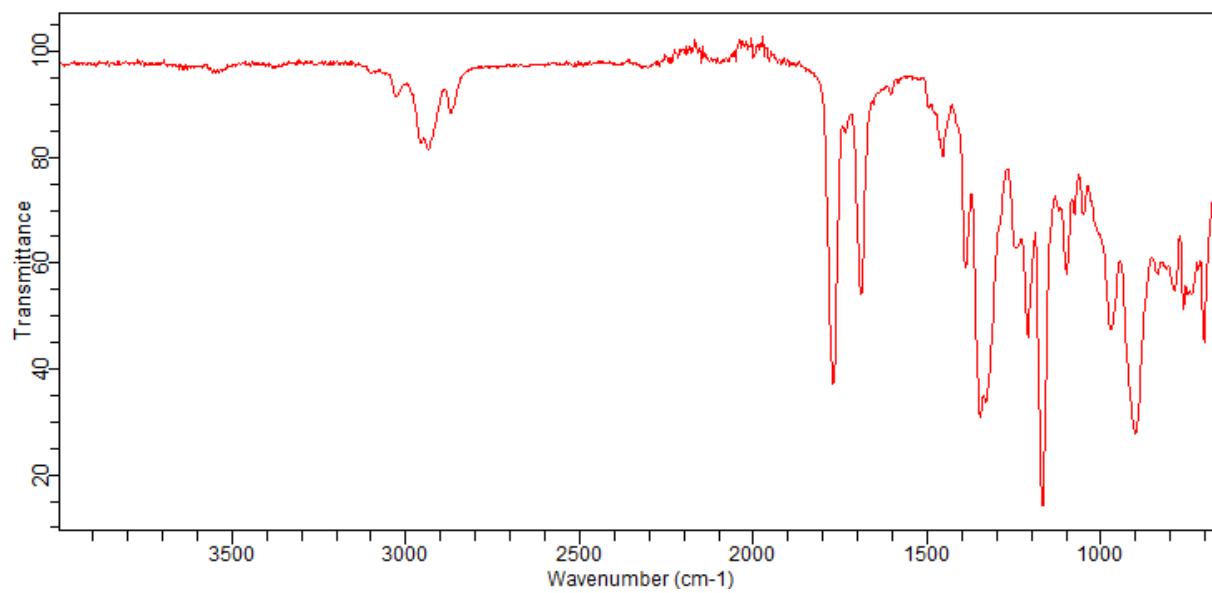
NOESY (Chloroform-d) for 3a



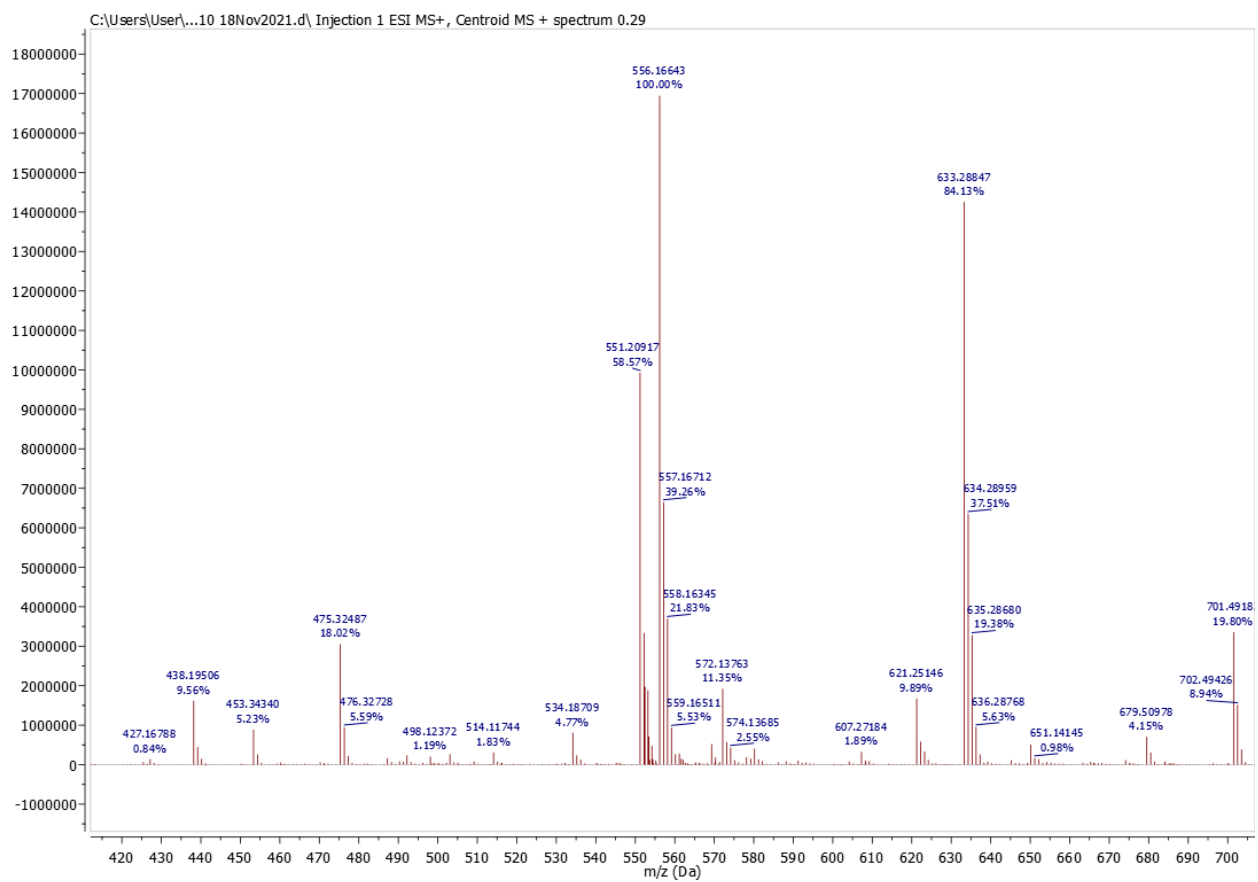
HMBC (Chloroform-d) for **3a**



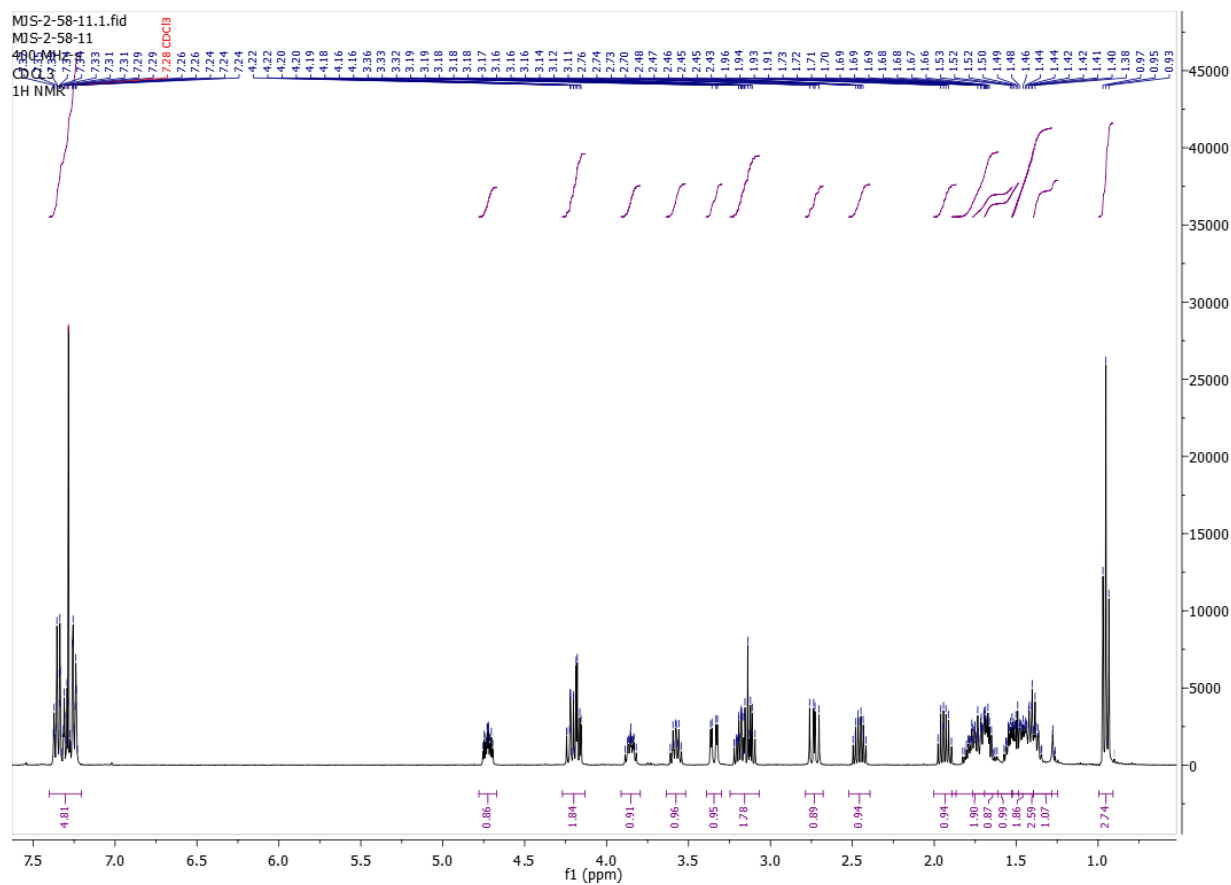
IR (KBr) for **3a**



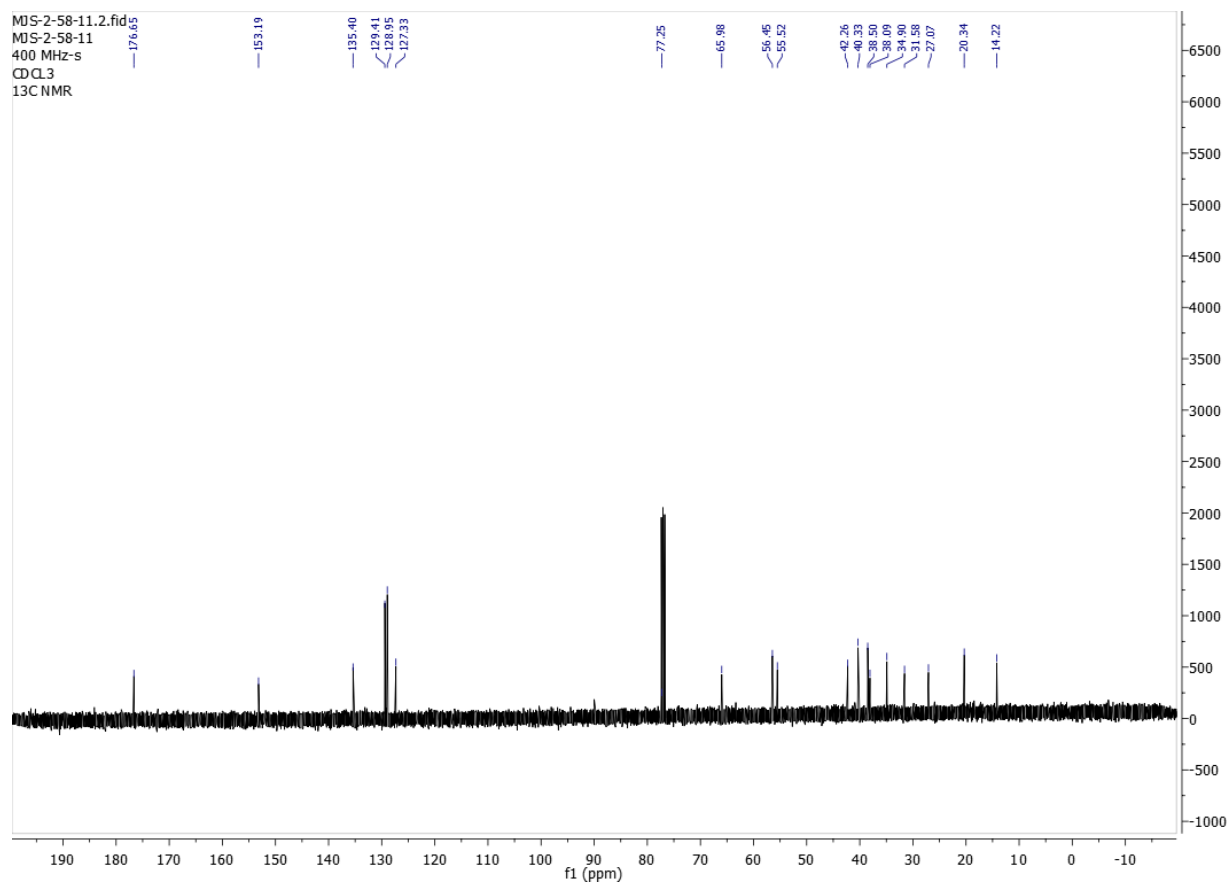
HRESIMS for 3a



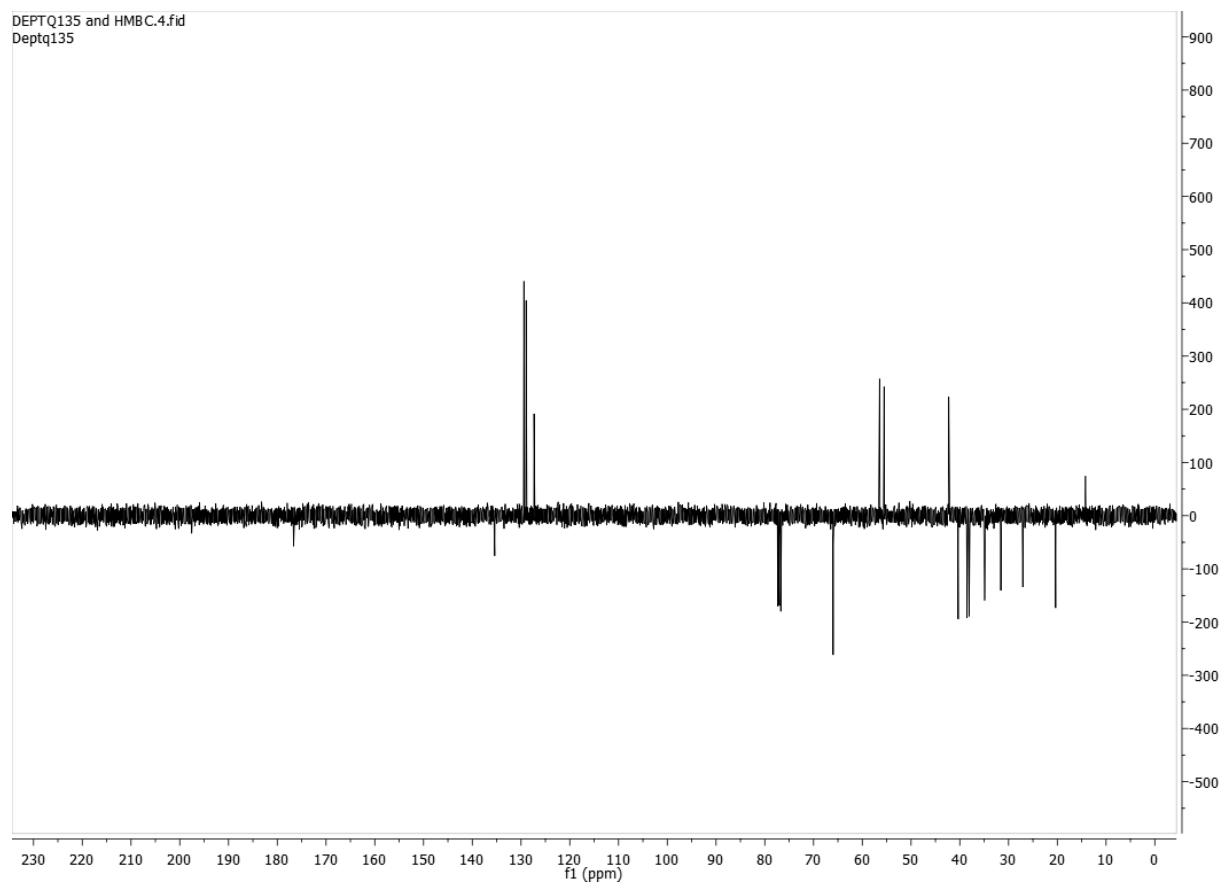
¹H NMR (400 MHz, Chloroform-d) for 15



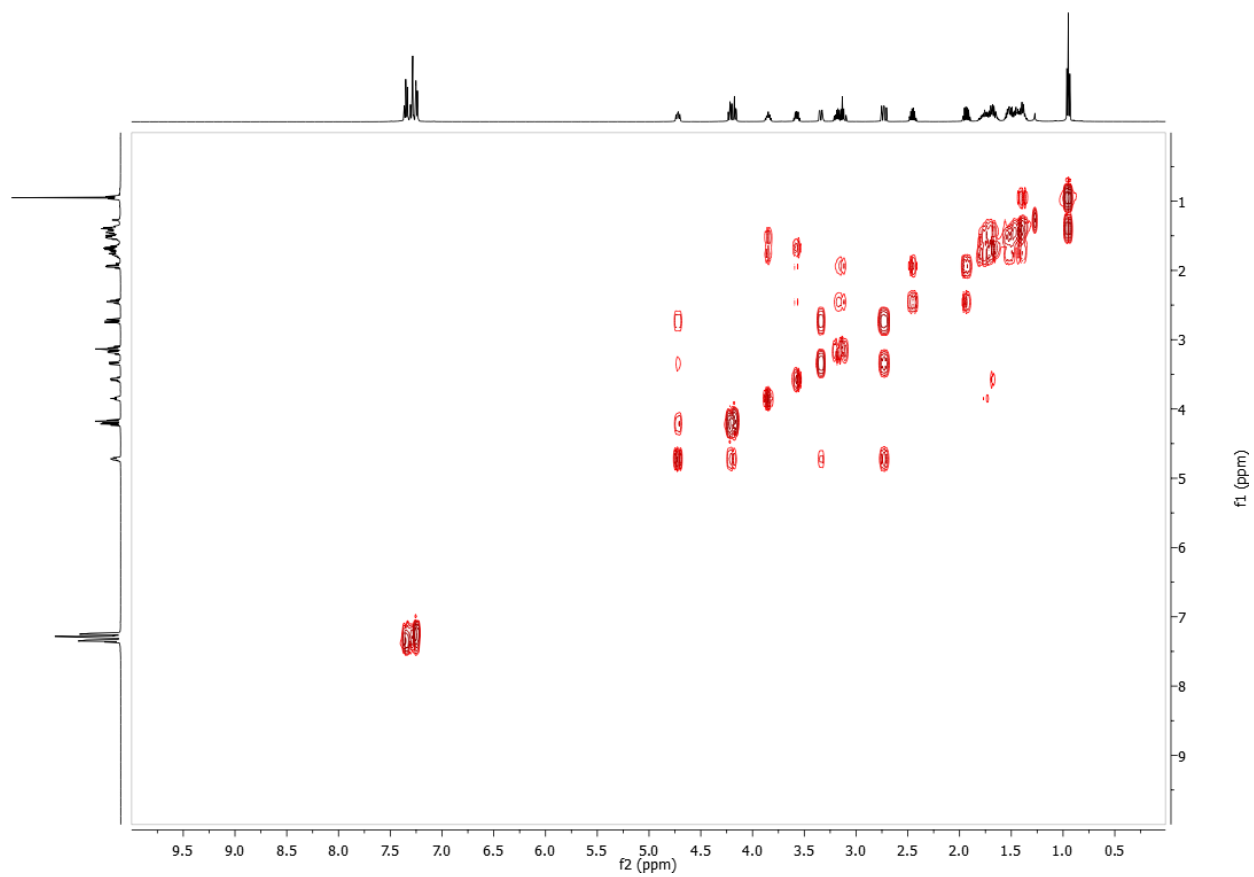
¹³C NMR (101 MHz, Chloroform-d) for **15**



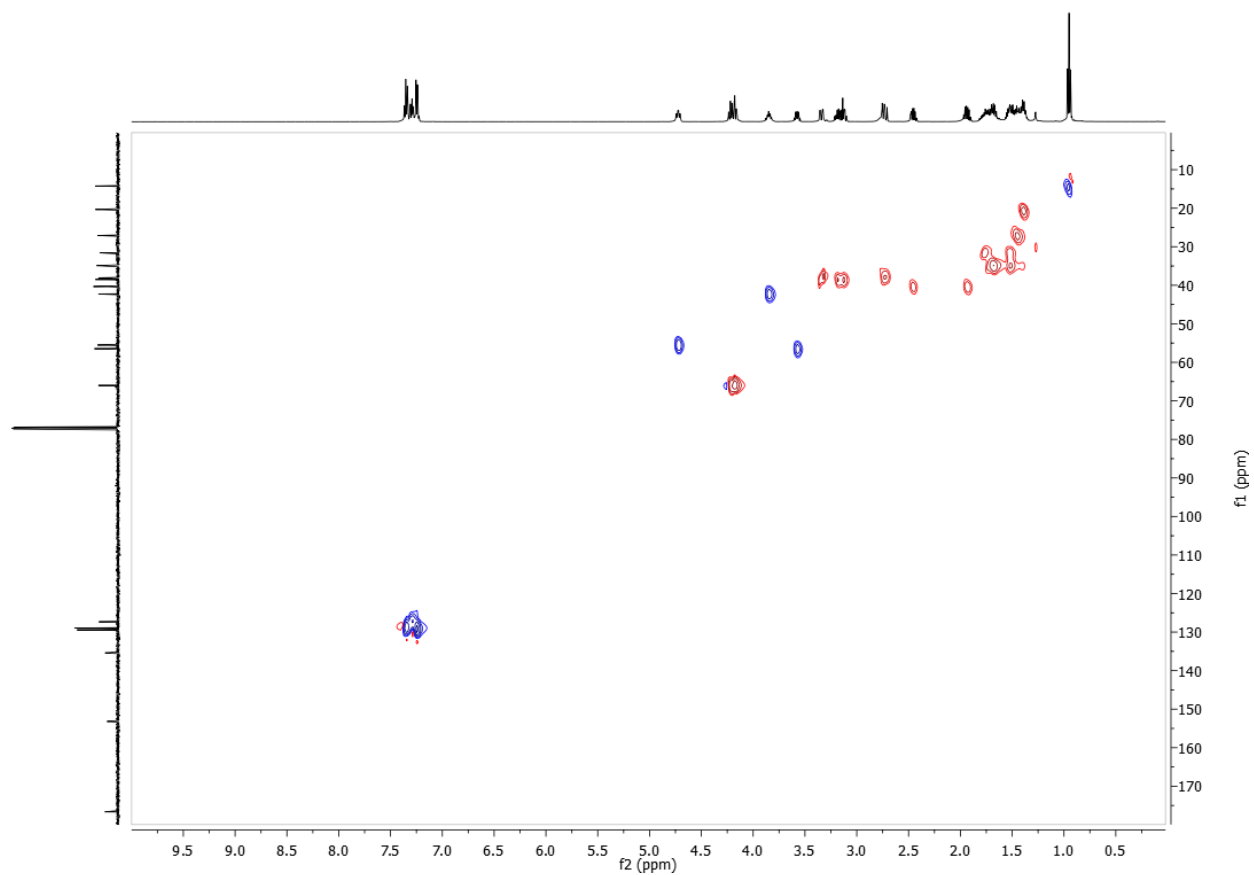
DEPT 135 (Chloroform-d) for **15**



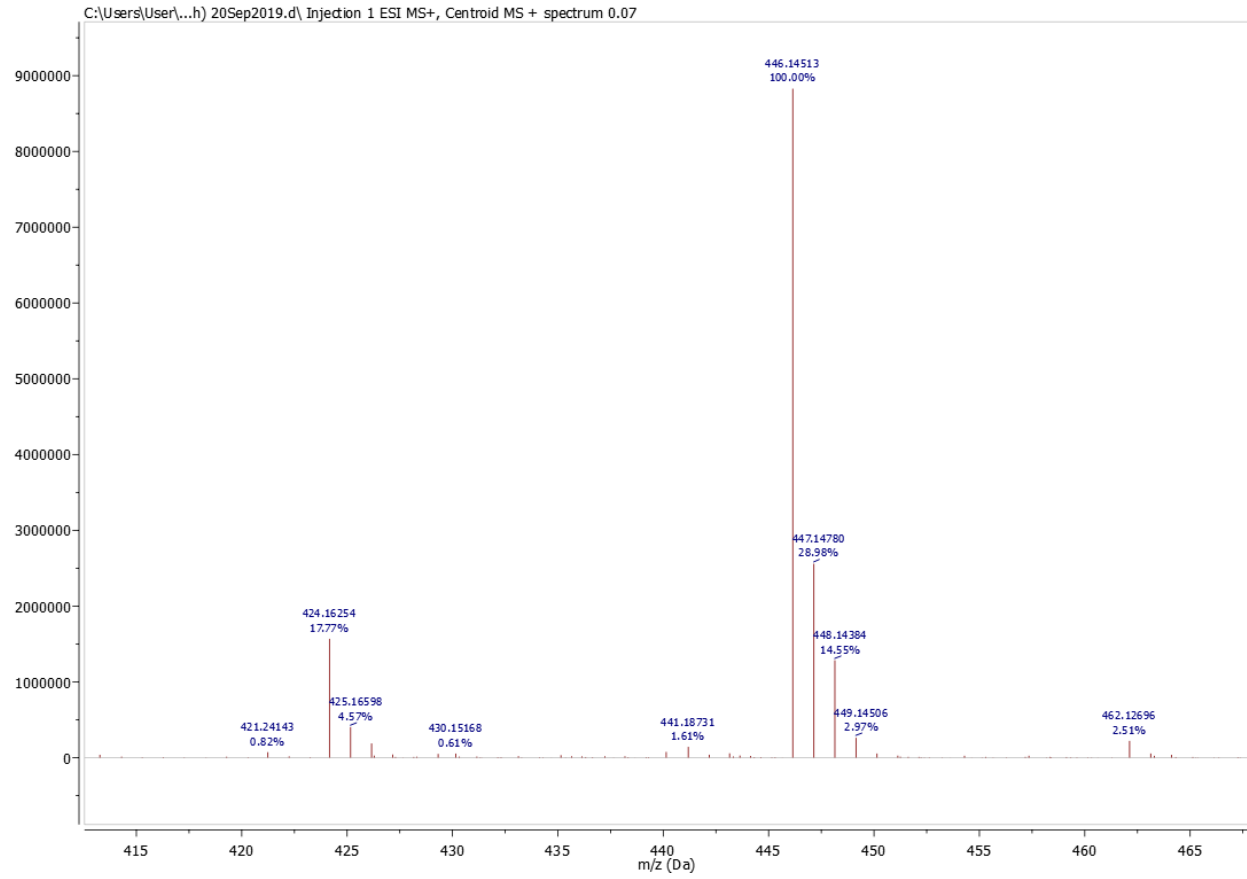
H-H COSY (Chloroform-d) for **15**



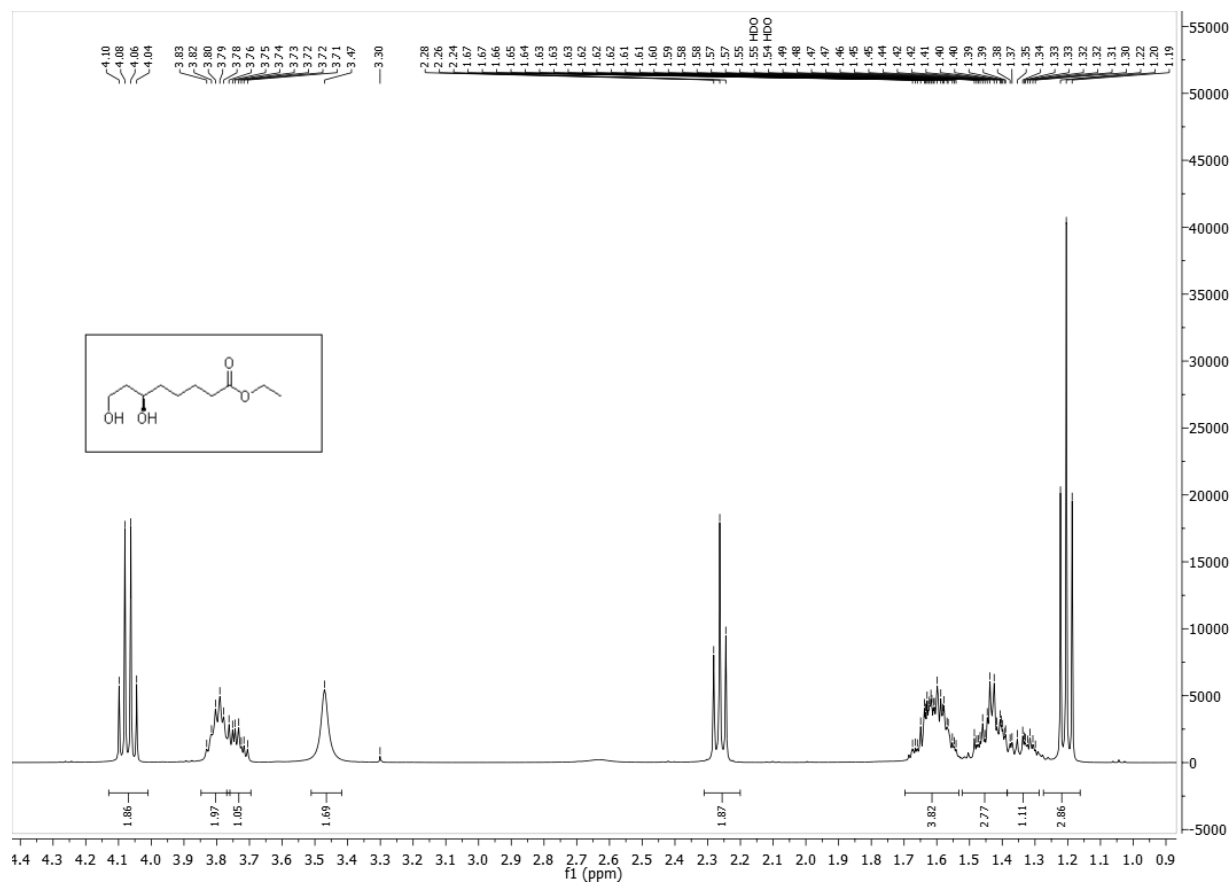
HSQC (Chloroform-d) for 15



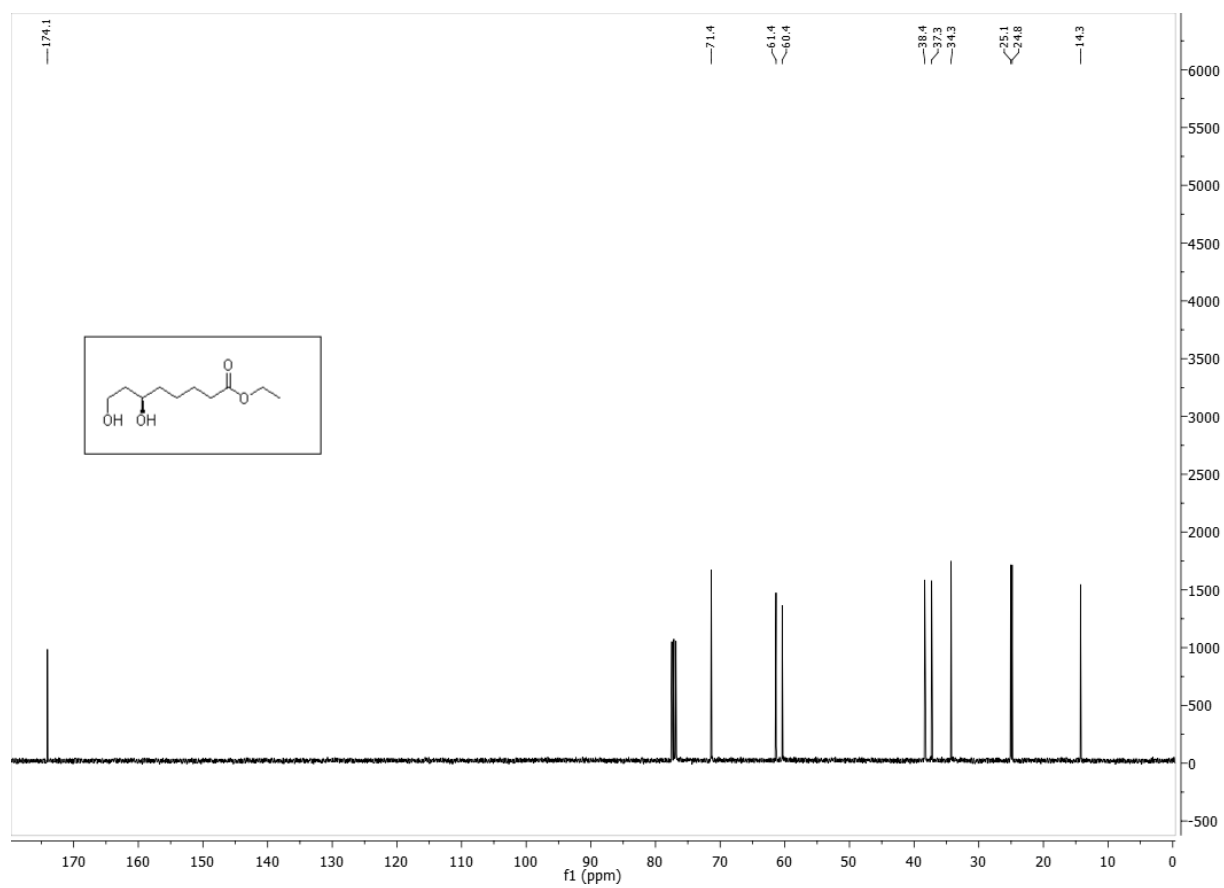
HRESI-MS for 15



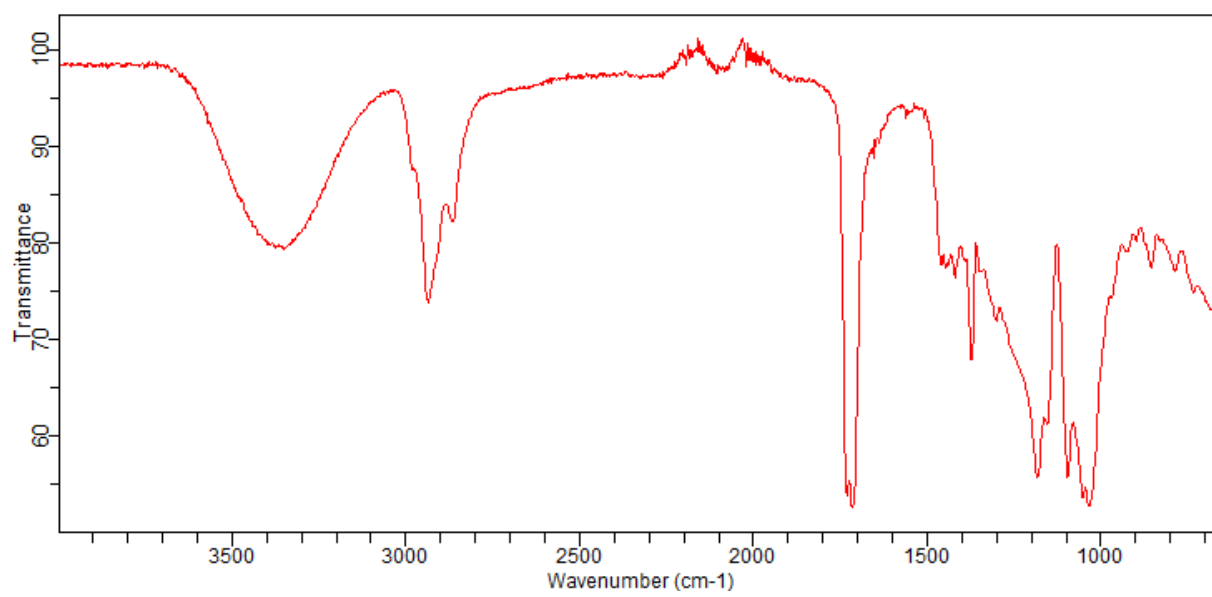
¹H NMR (400 MHz, Chloroform-d) for 16a



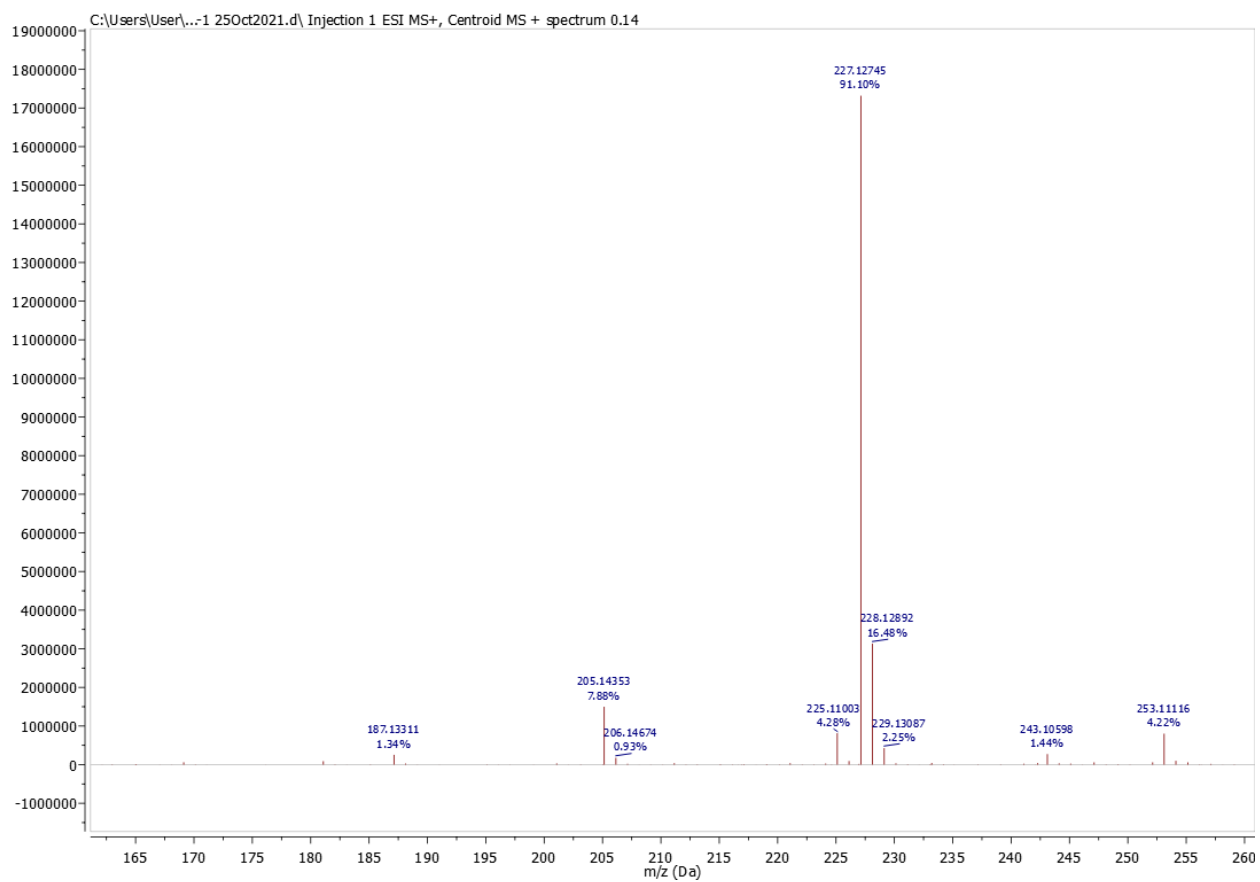
^{13}C NMR (101 MHz, Chloroform-d) for **16a**



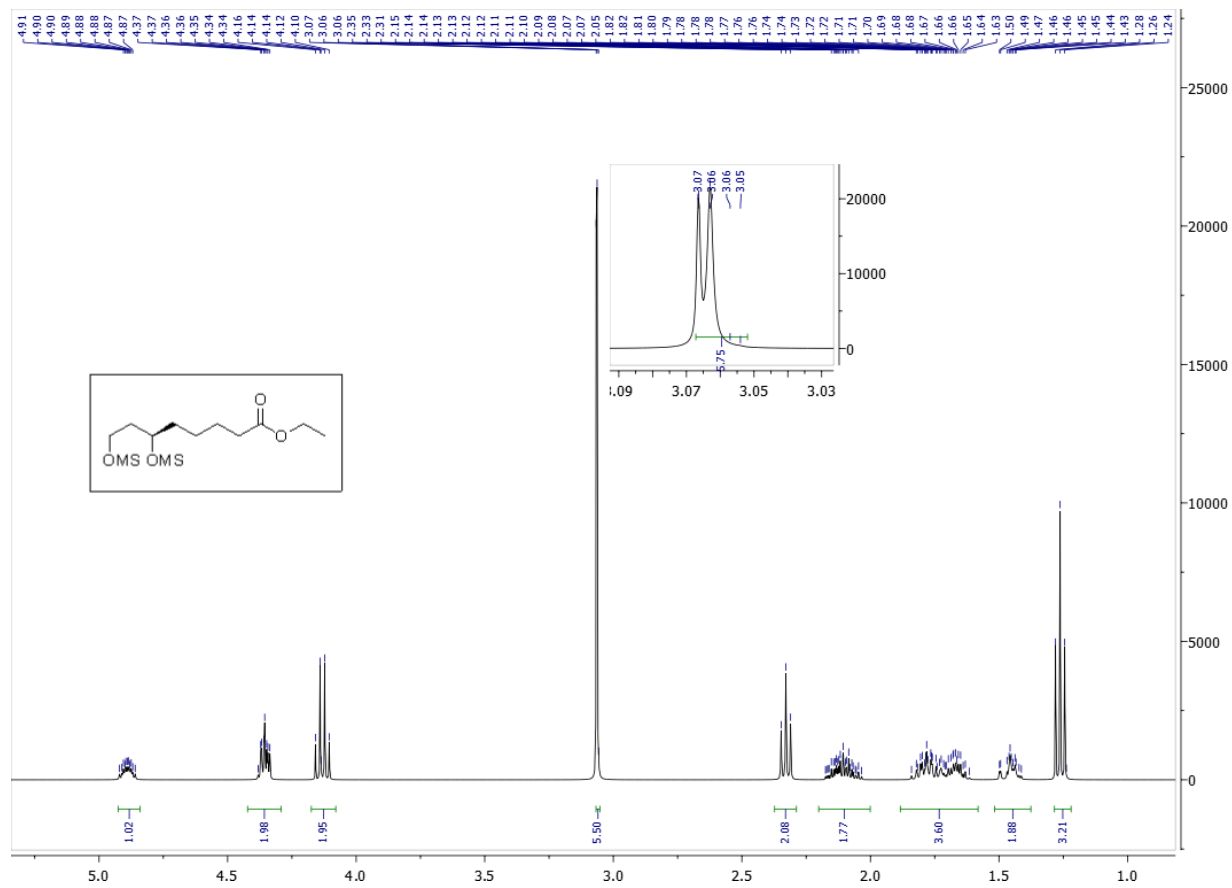
IR (KBr) for **16a**



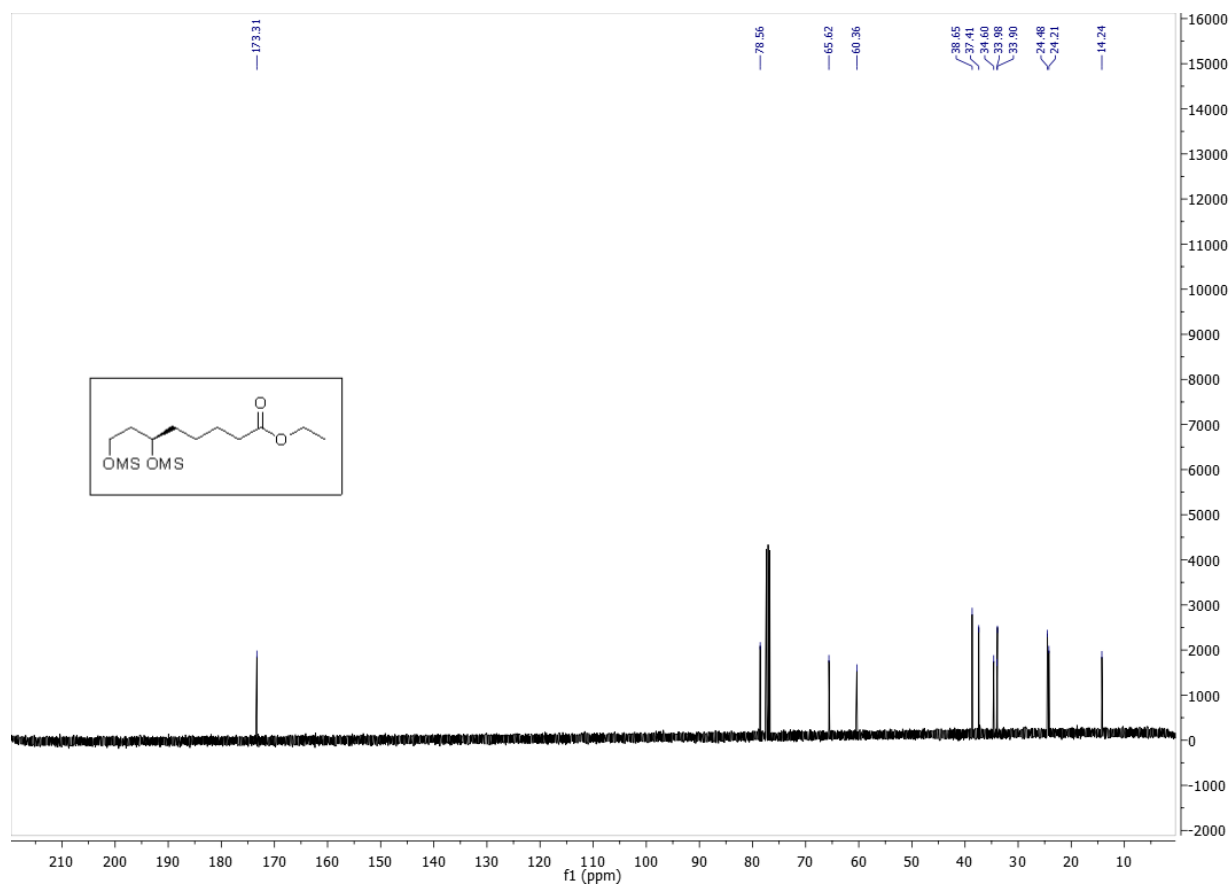
HRESIMS for 16a



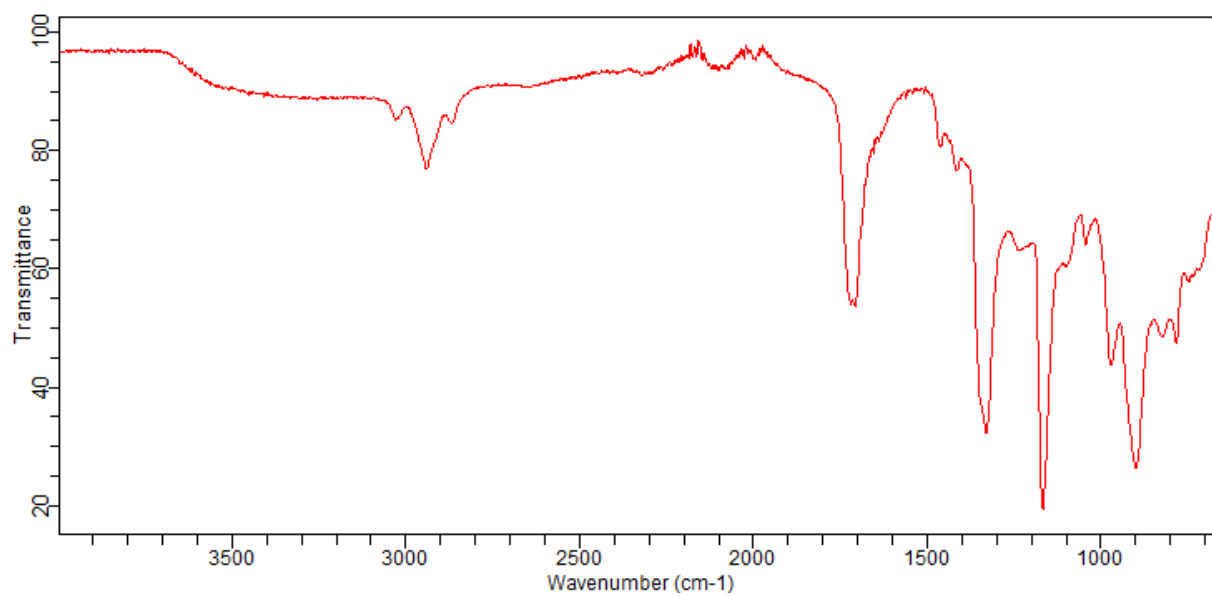
^1H NMR (400 MHz, Chloroform-d) for **17a**



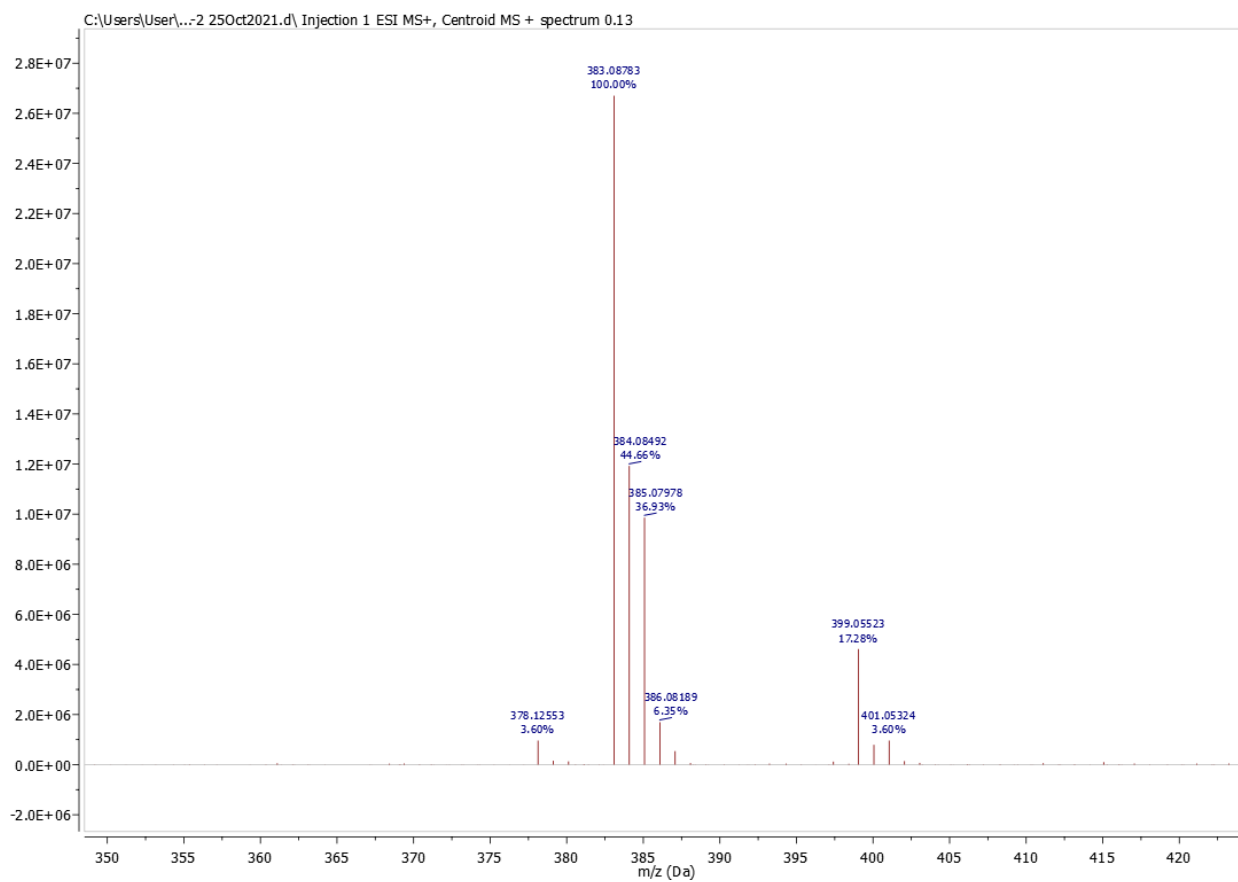
^{13}C NMR (101 MHz, Chloroform-d) for **17a**



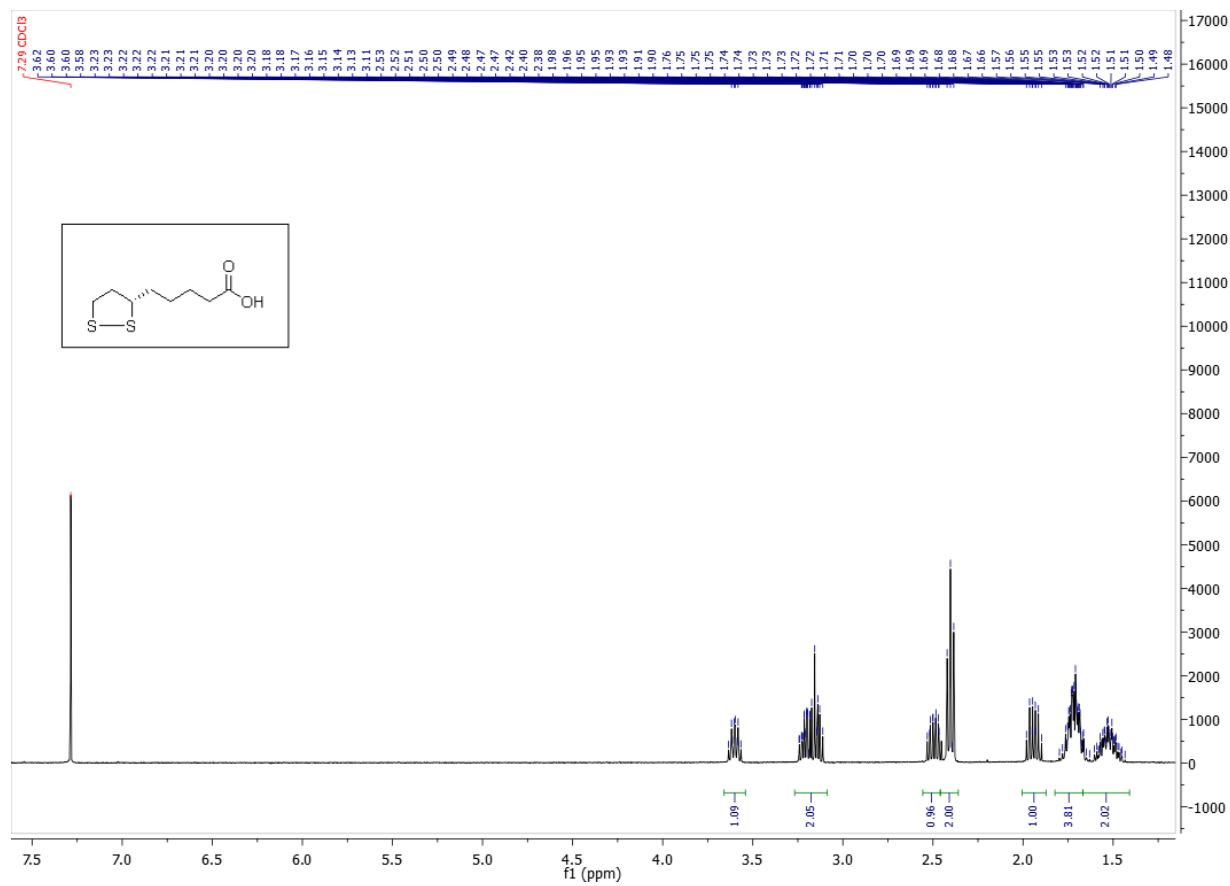
IR (KBr) for **17a**



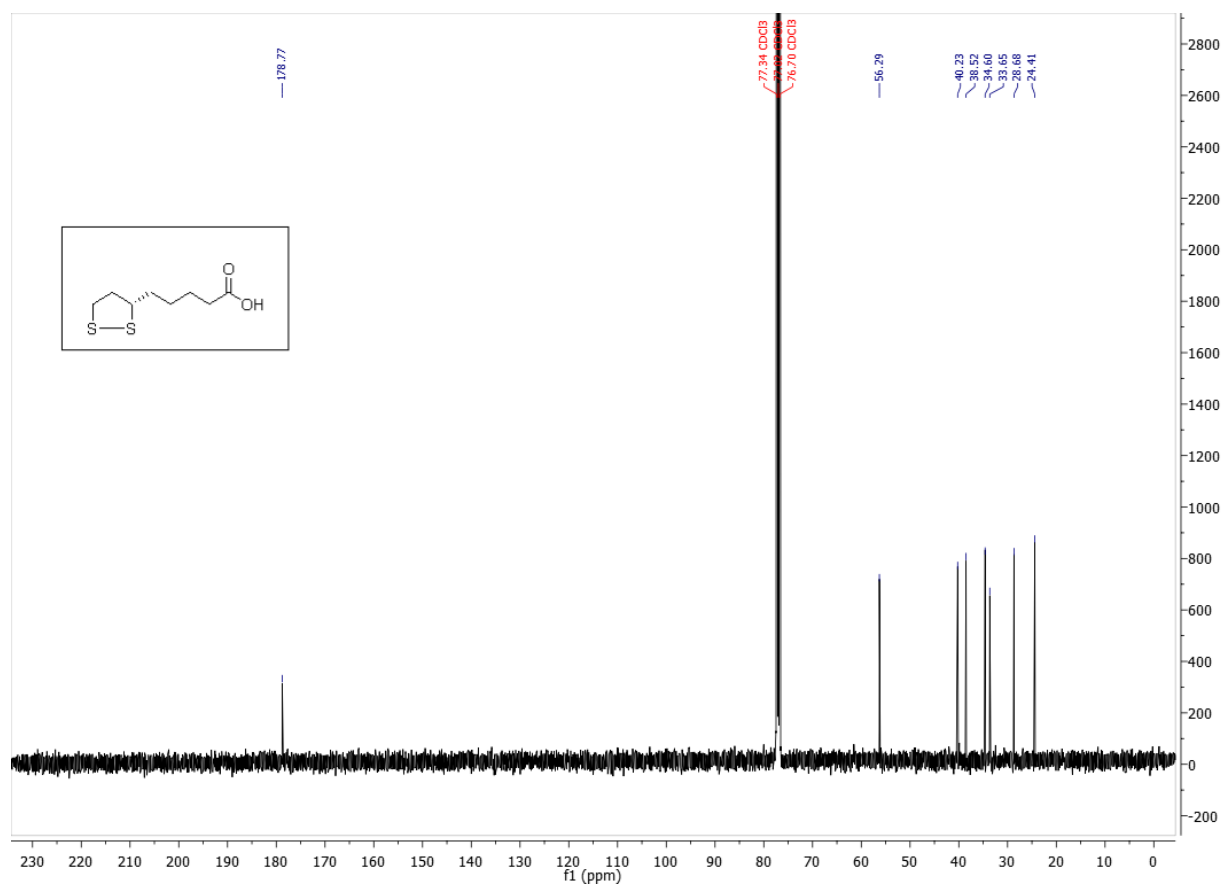
HRESIMS for 17a



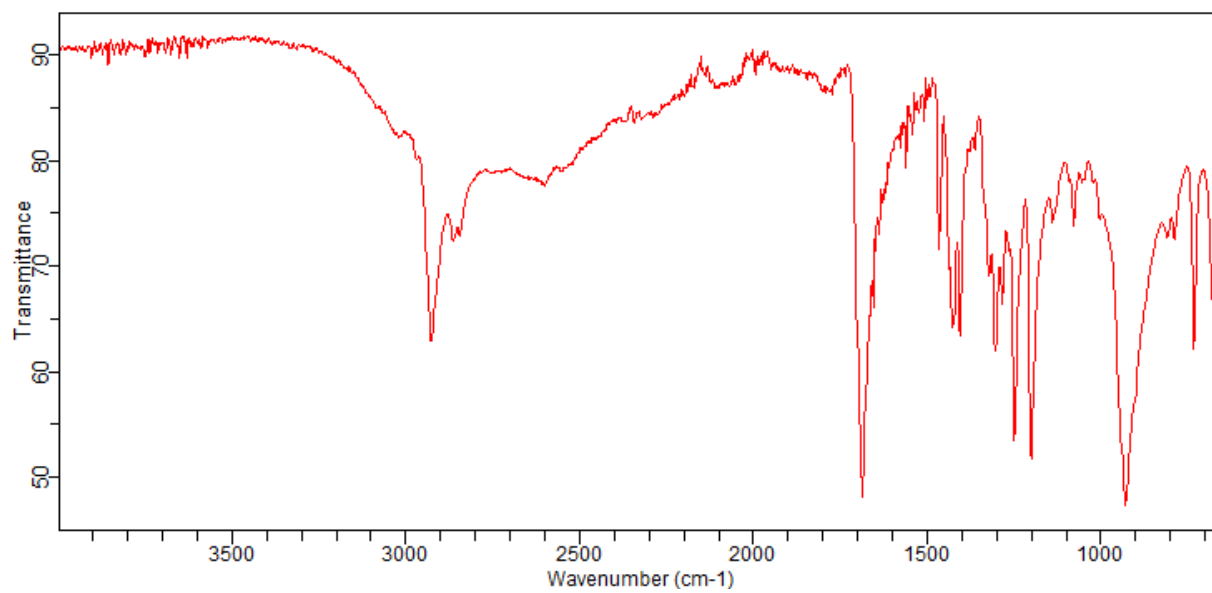
¹H NMR (400 MHz, Chloroform-d) for (S)-lipoic acid



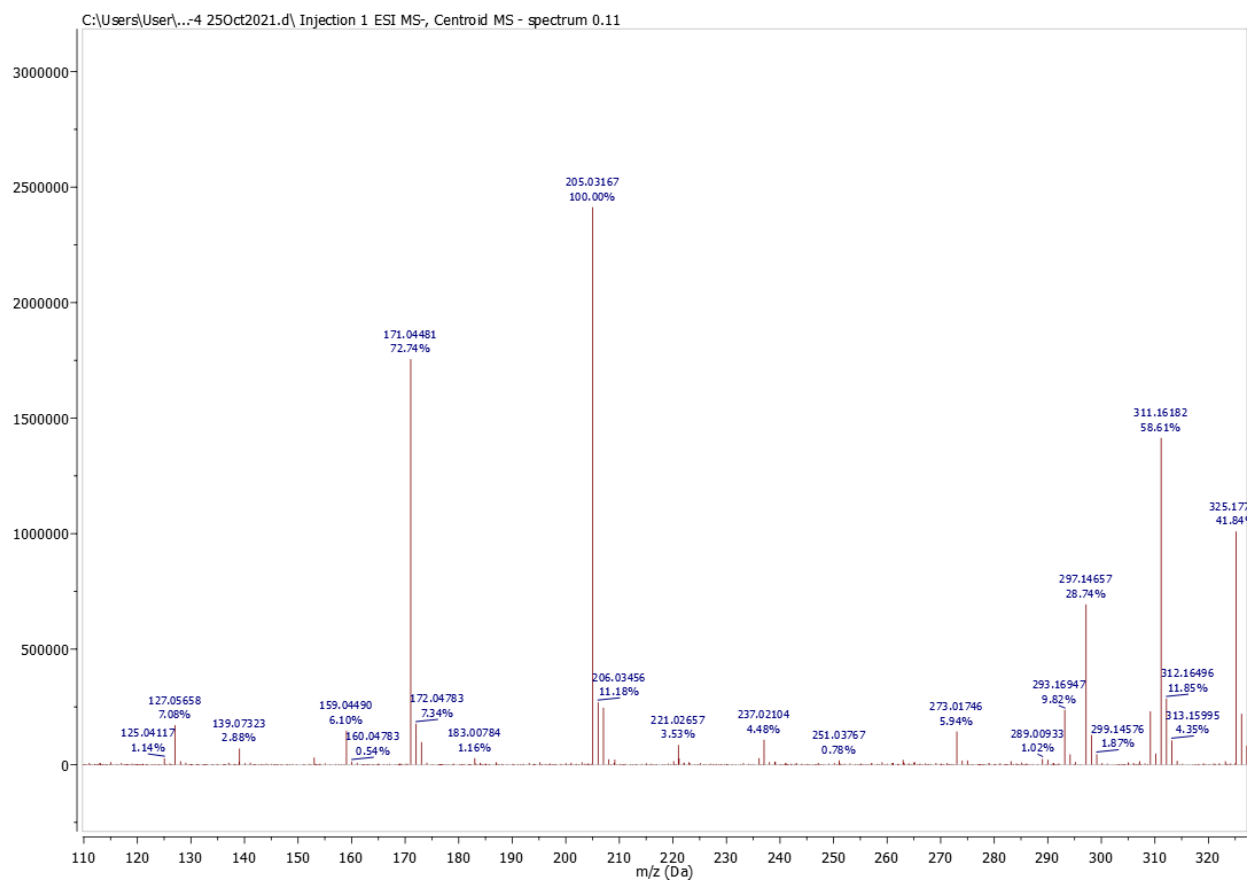
^{13}C NMR (101 MHz, Chloroform-d) for (S)-lipoic acid



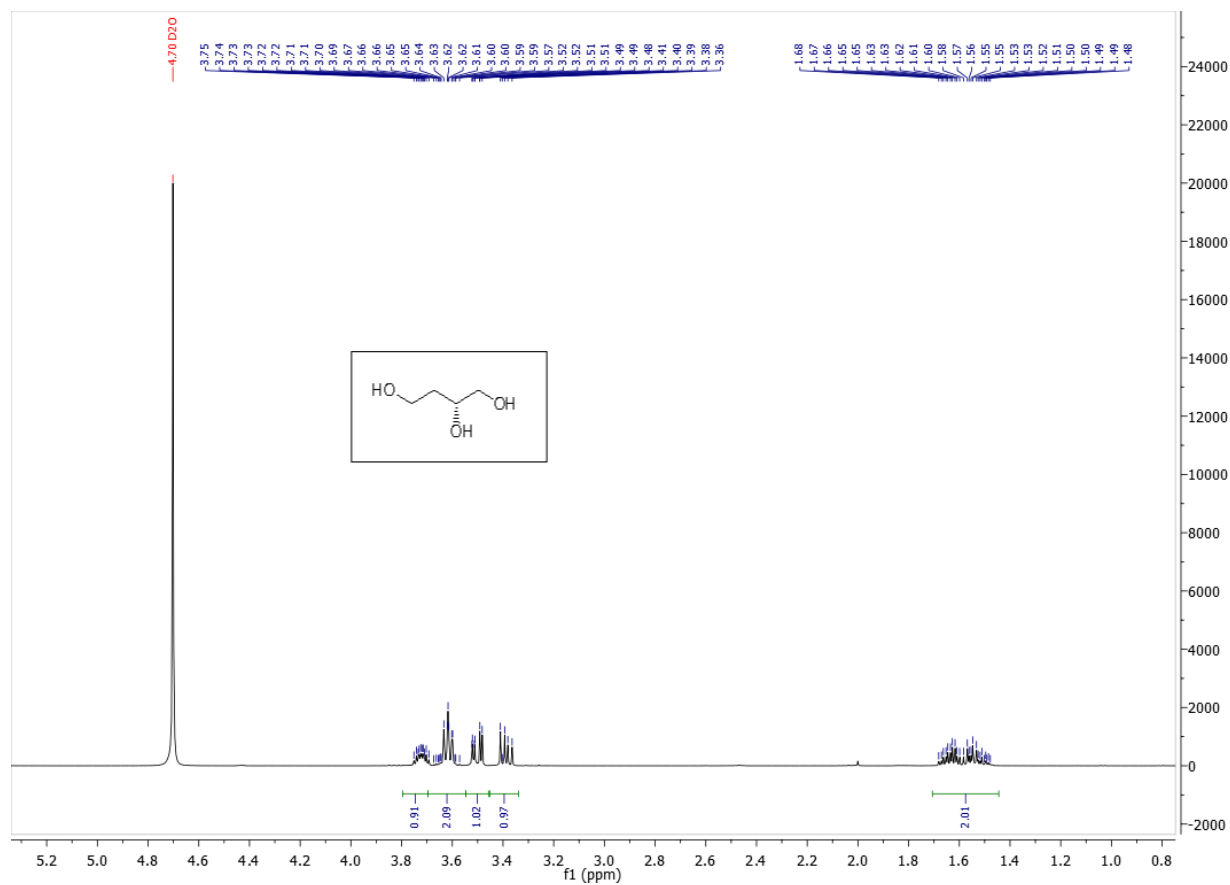
IR (KBr) for (S)-lipoic acid



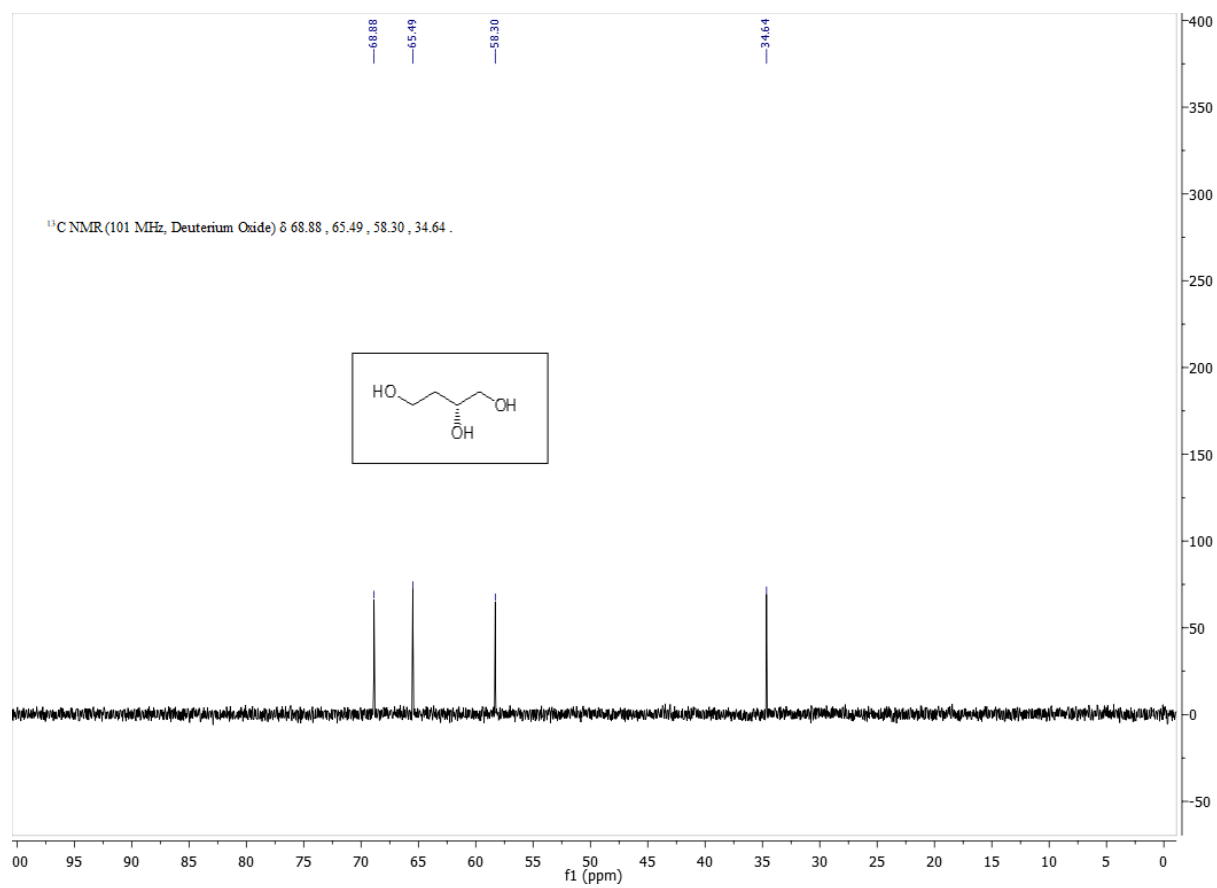
HRESIMS for (S)-lipoic acid



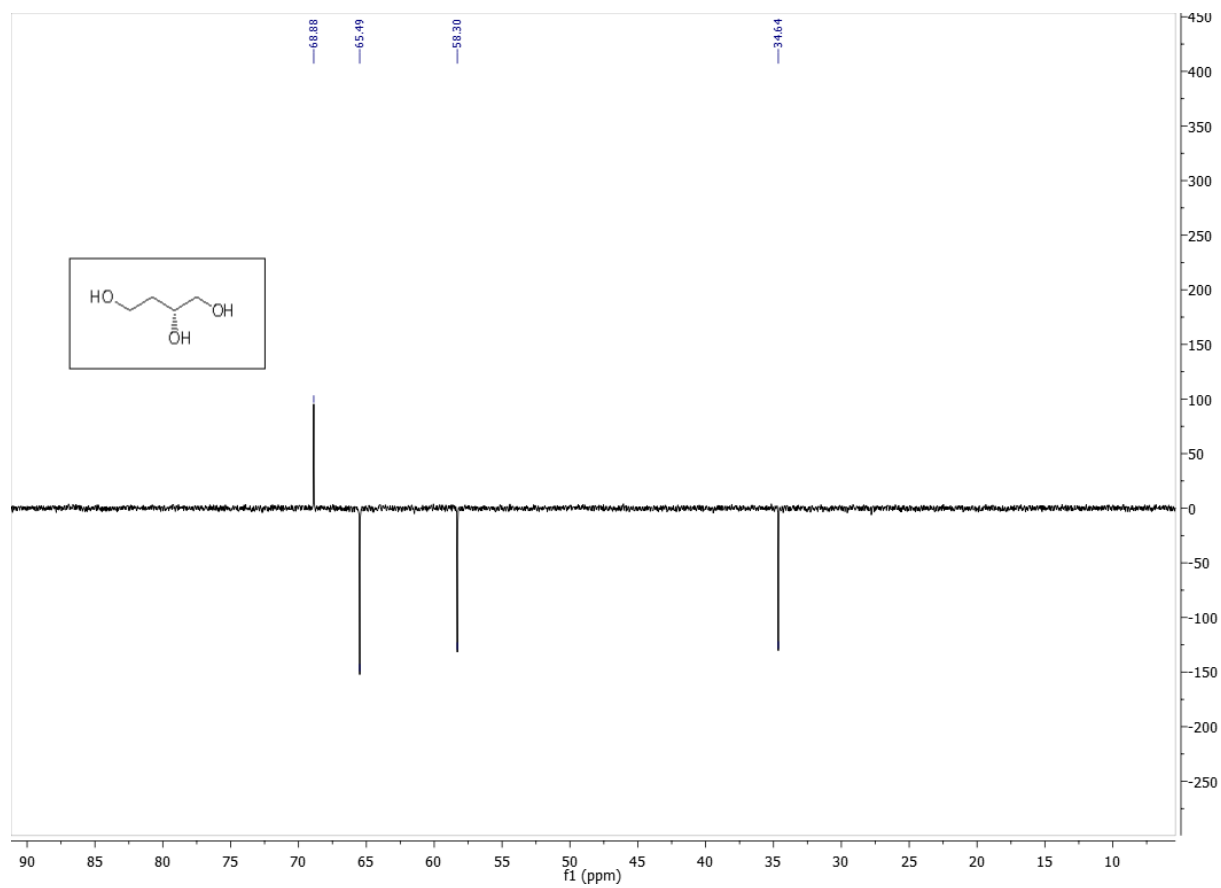
^1H NMR (400 MHz, Deuterium Oxide) for **13b**



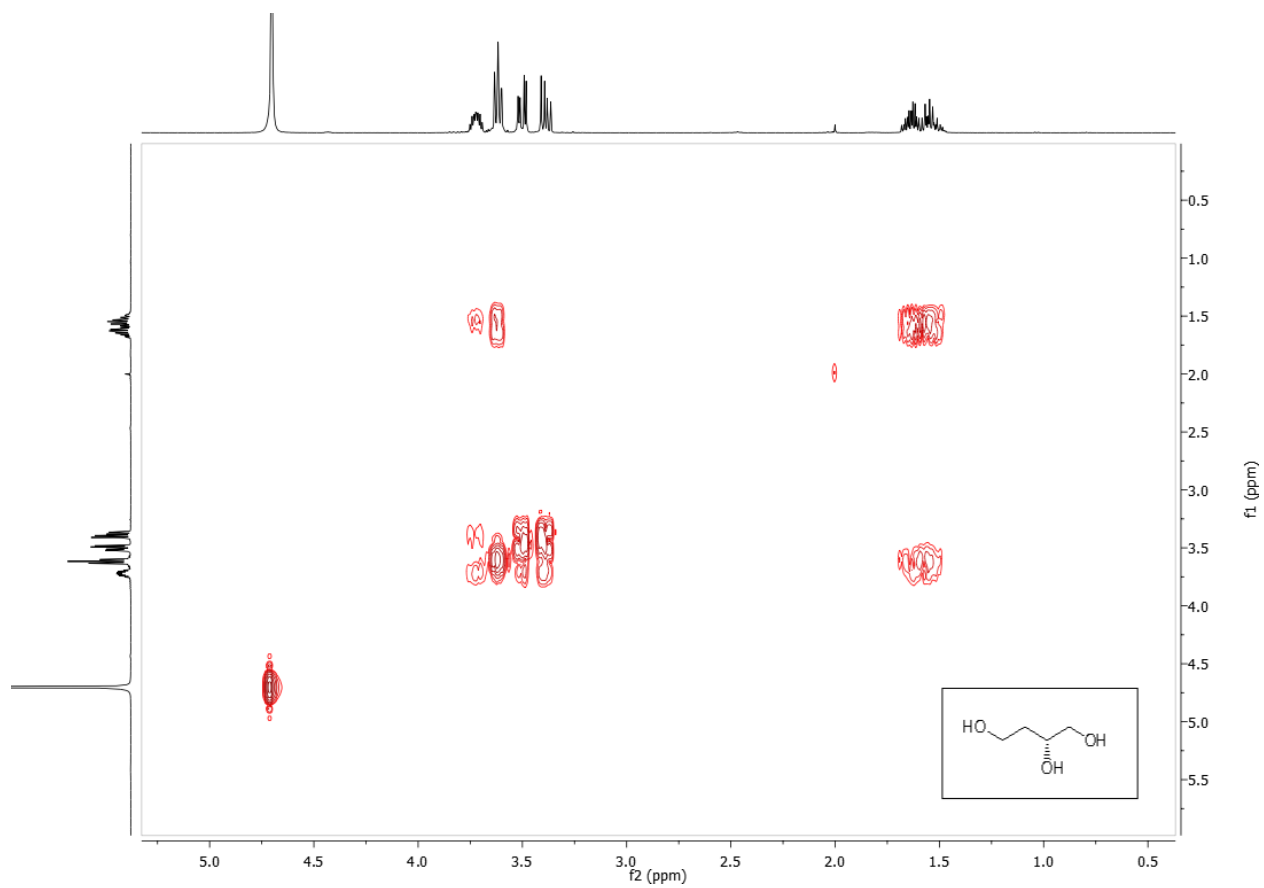
^{13}C NMR (101 MHz, Deuterium Oxide) for **13b**



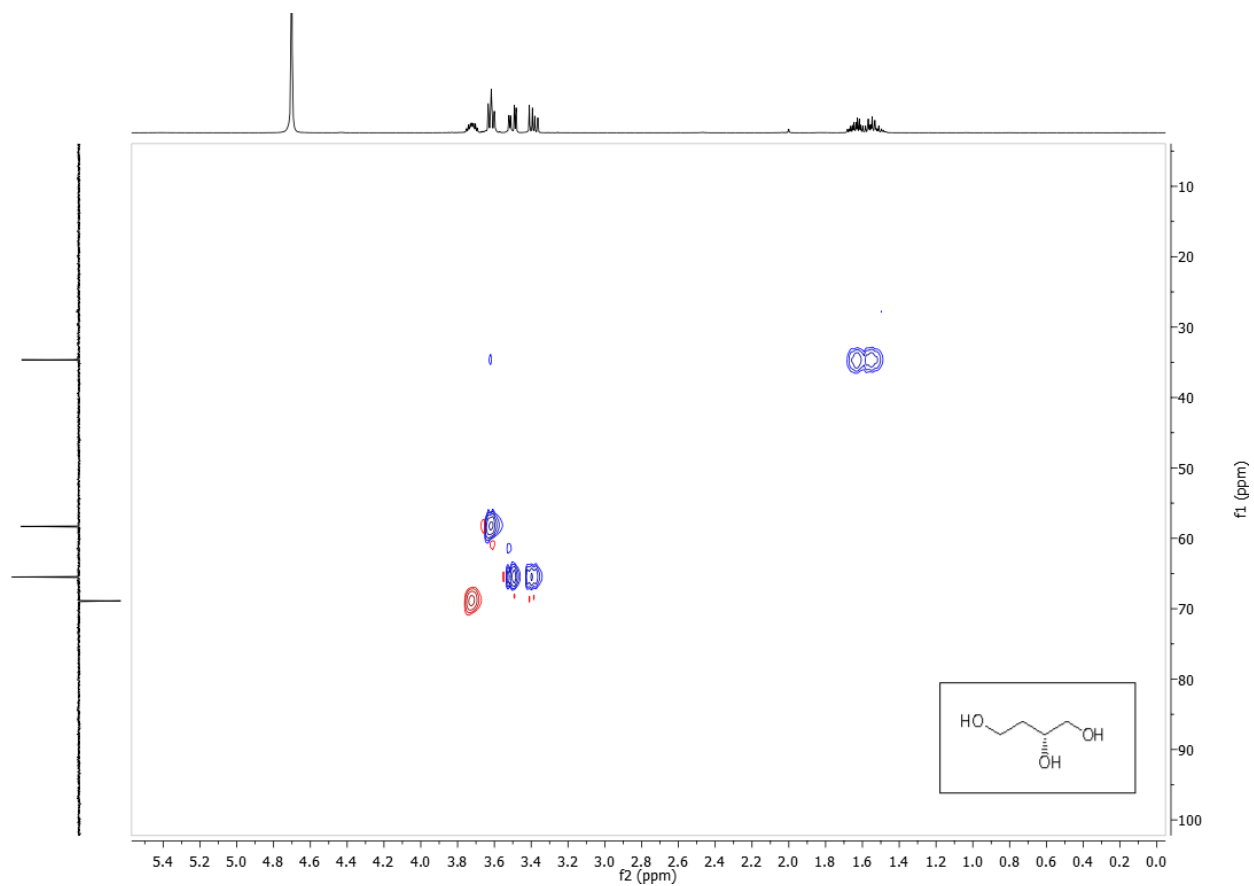
DEPT 135 (Deuterium Oxide) for **13b**



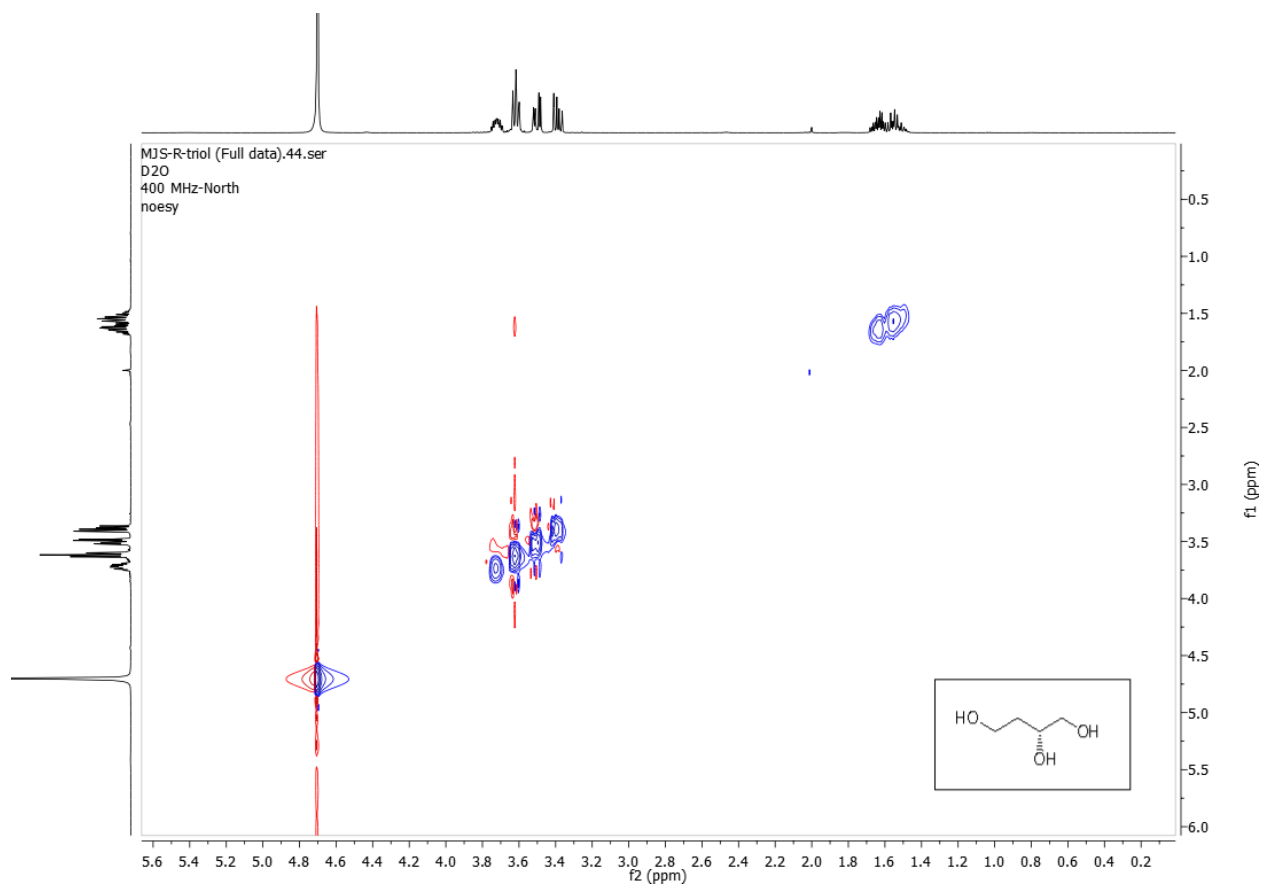
H-H COSY (Deuterium Oxide) for **13b**



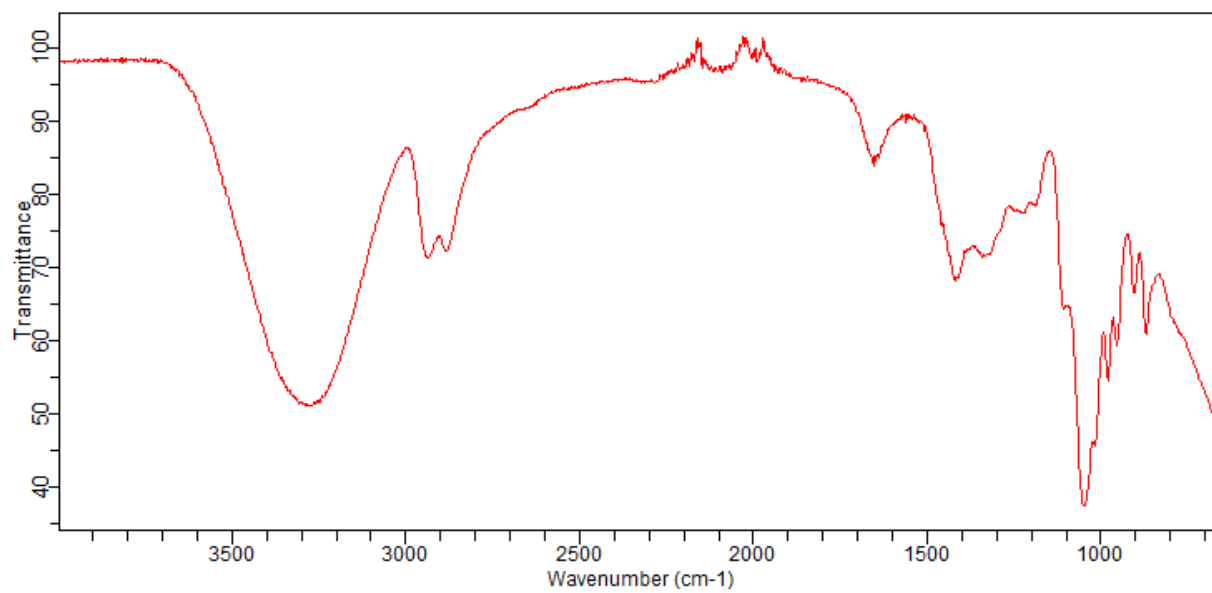
HSQC (Deuterium Oxide) for **13b**



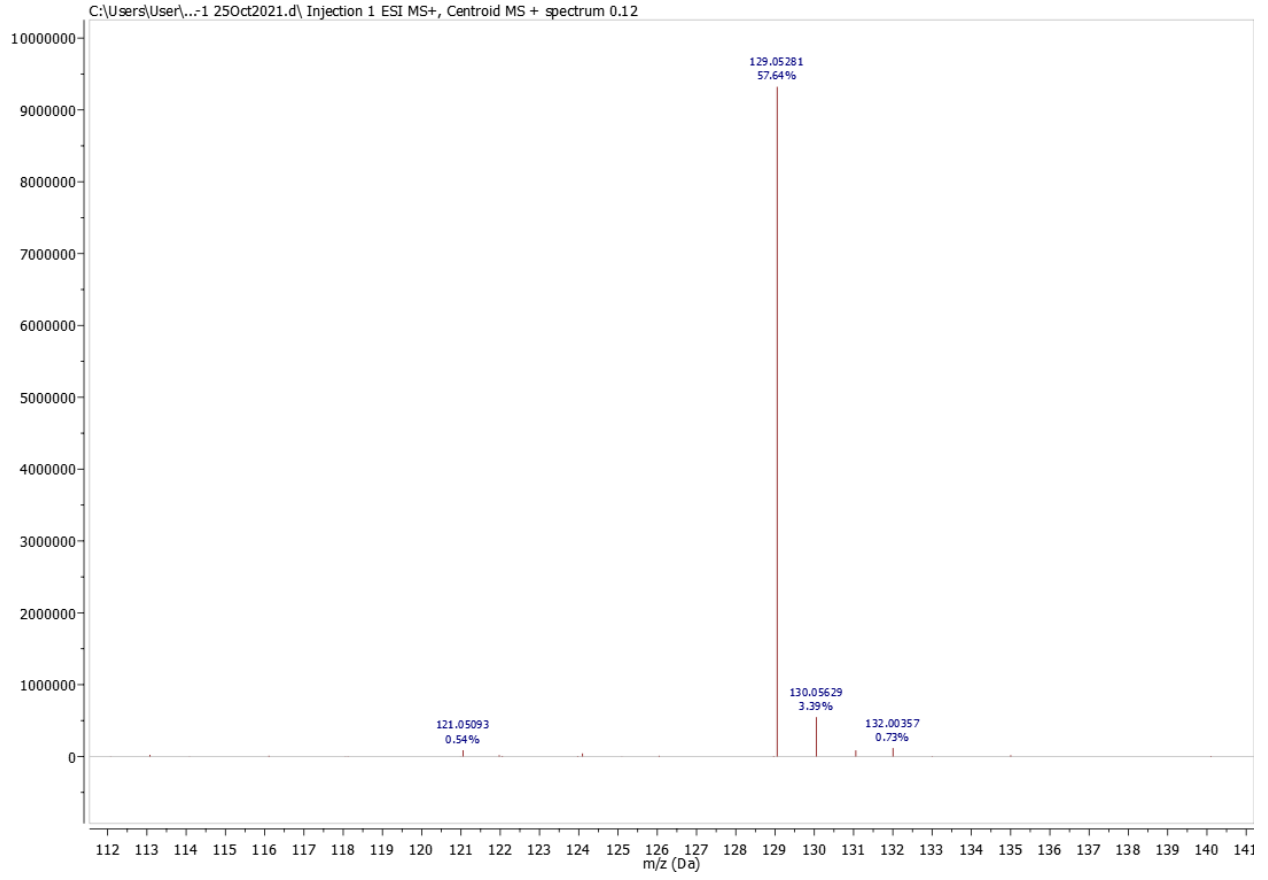
NOESY (Deuterium Oxide) for 13b



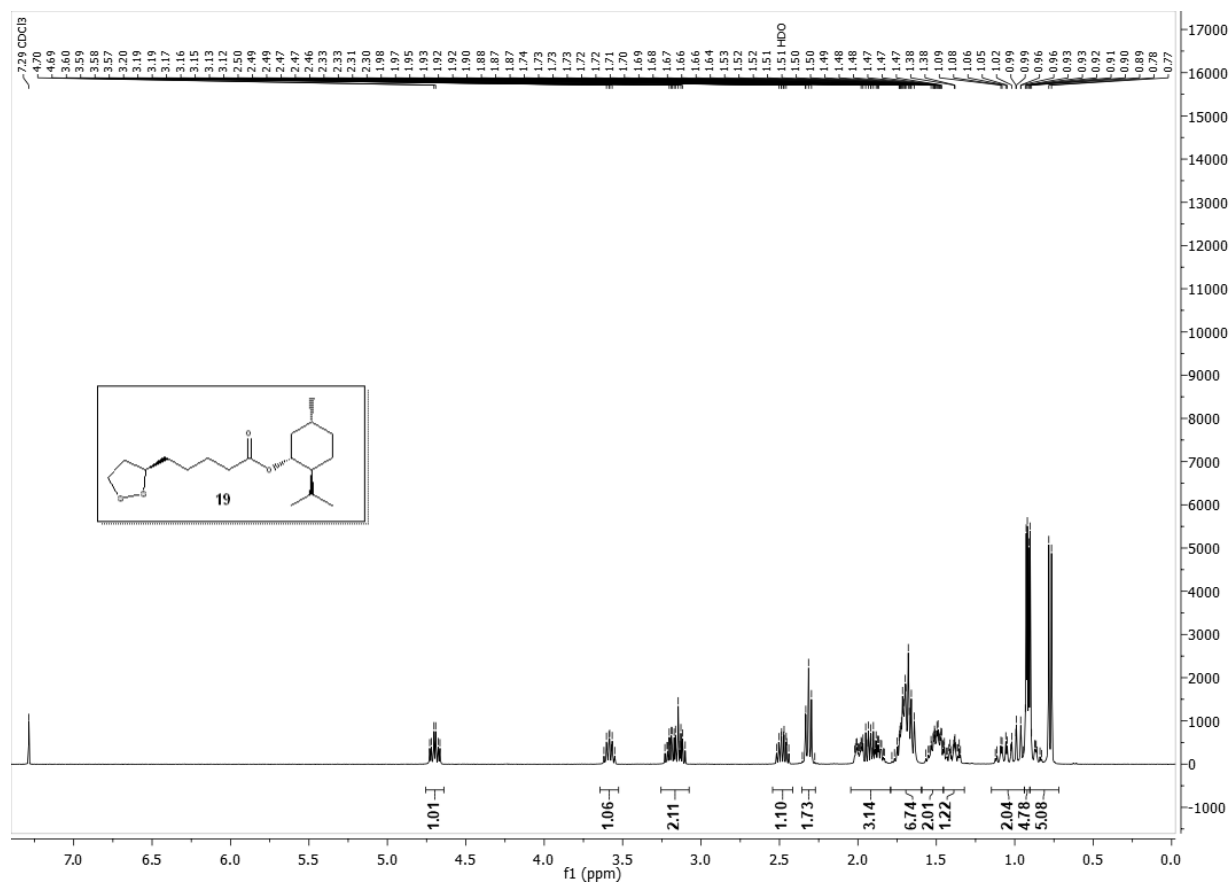
IR (KBr) for **13b**



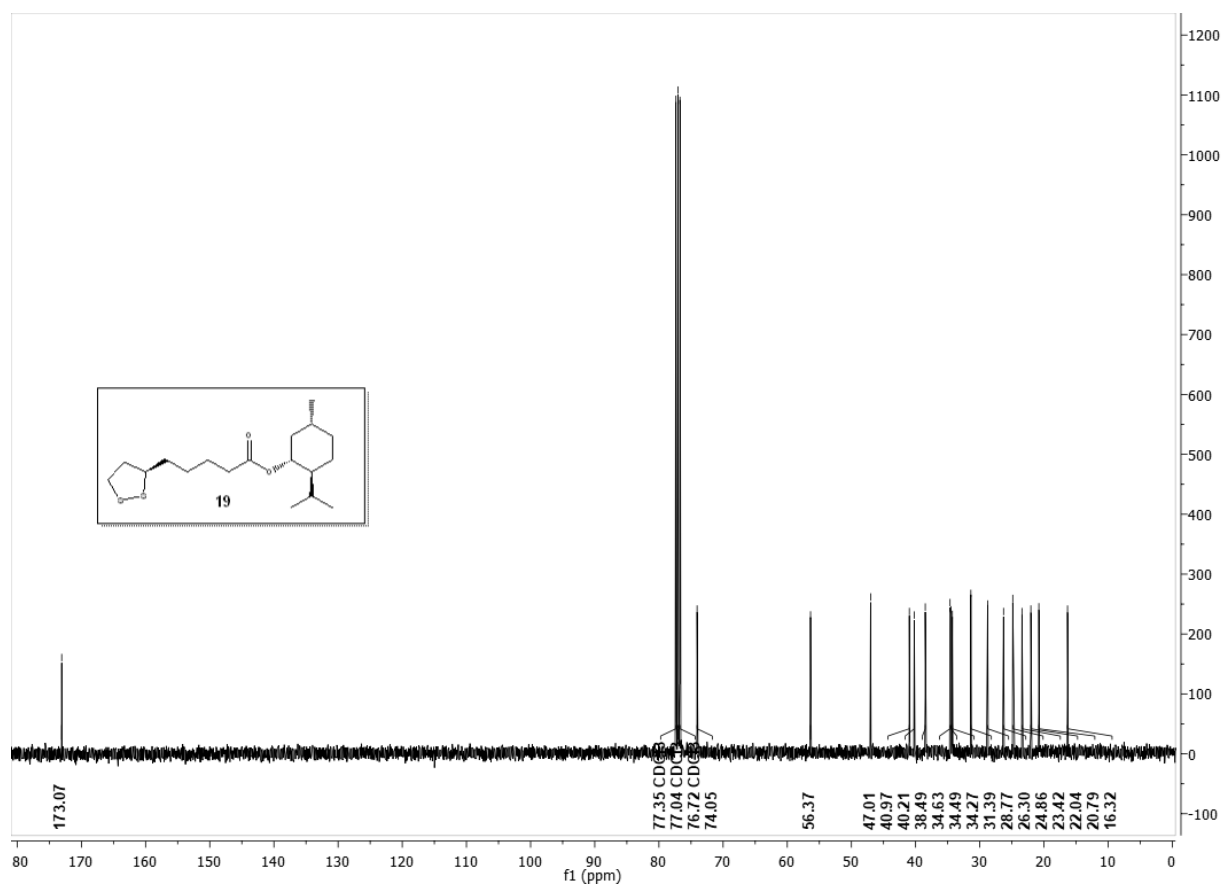
HRESIMS for 13b



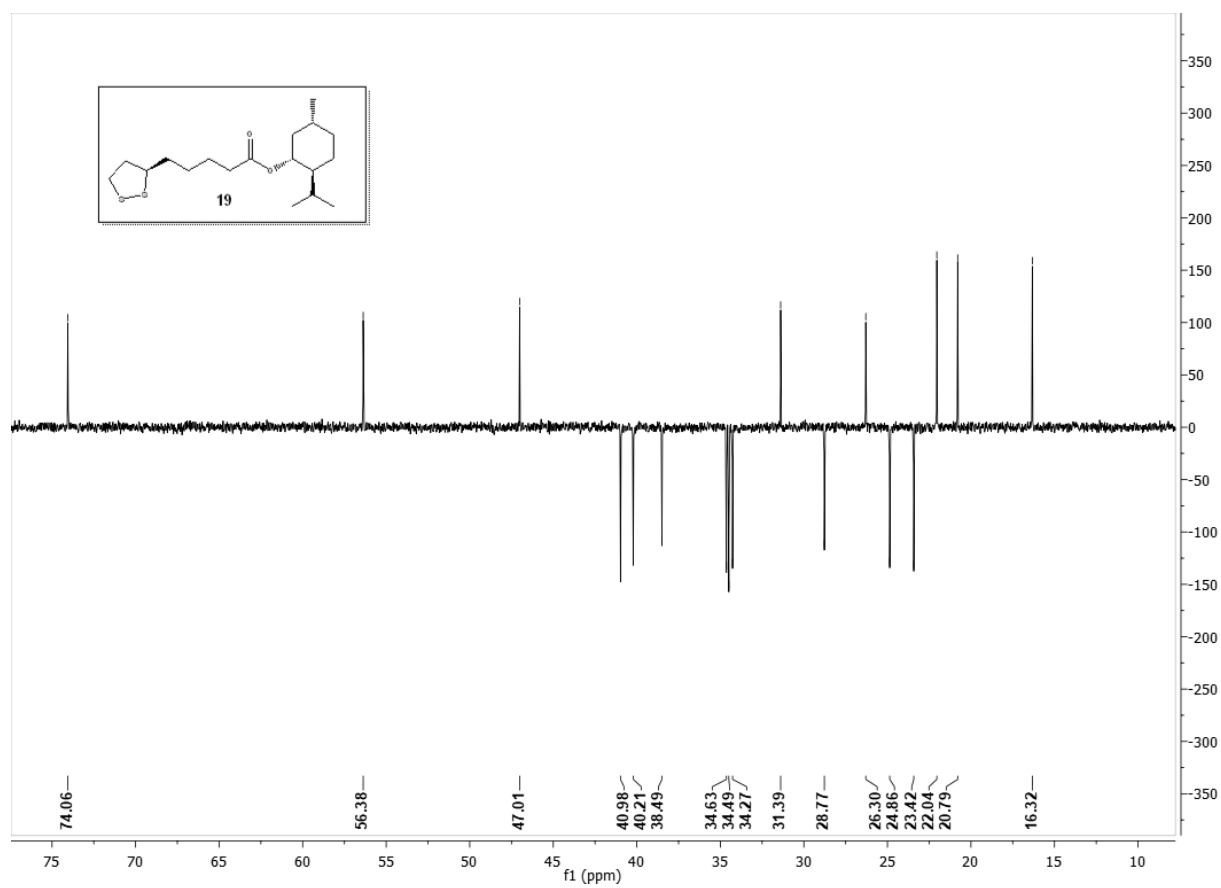
¹H NMR (400 MHz, Chloroform-d) for **19**



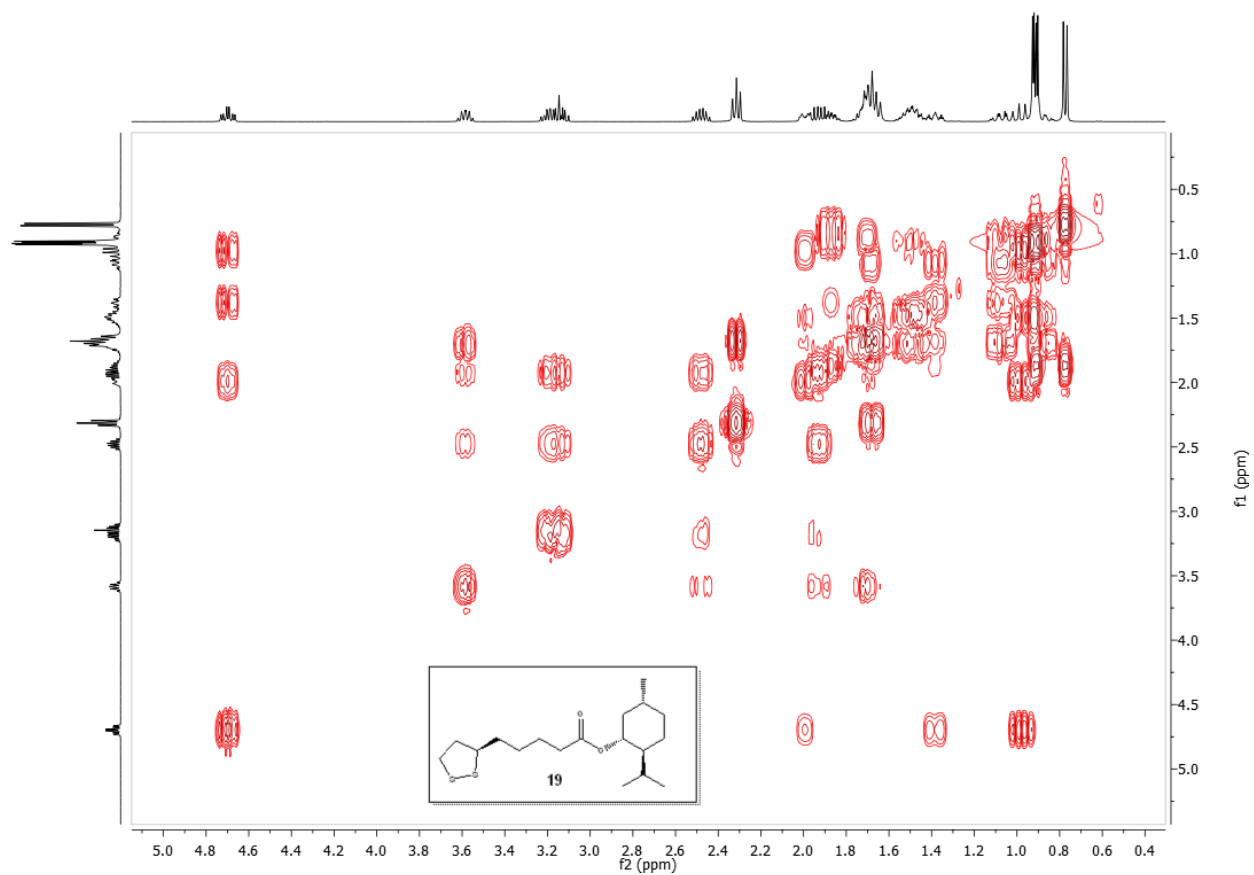
¹³C NMR (101 MHz, Chloroform-d) for **19**



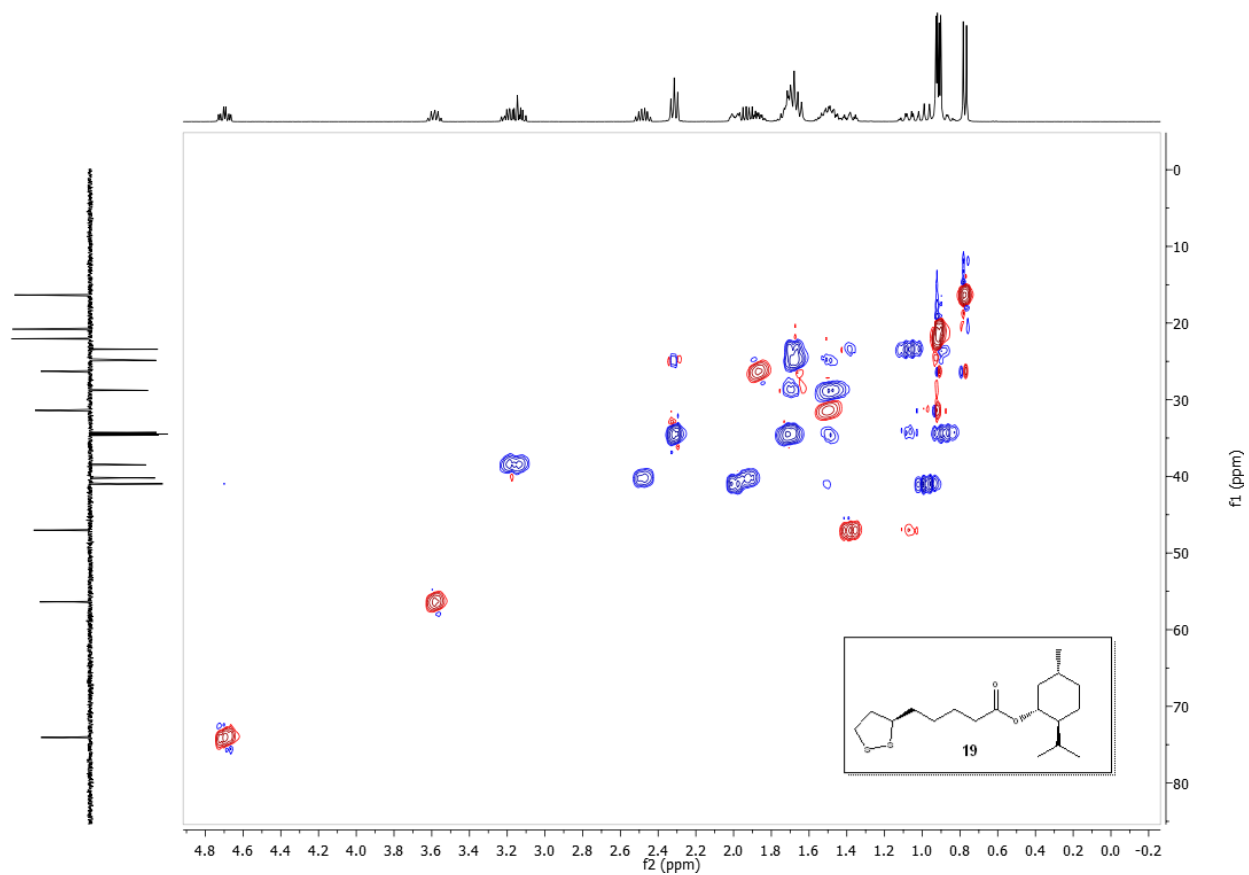
DEPT 135 (Chloroform-d) for **19**



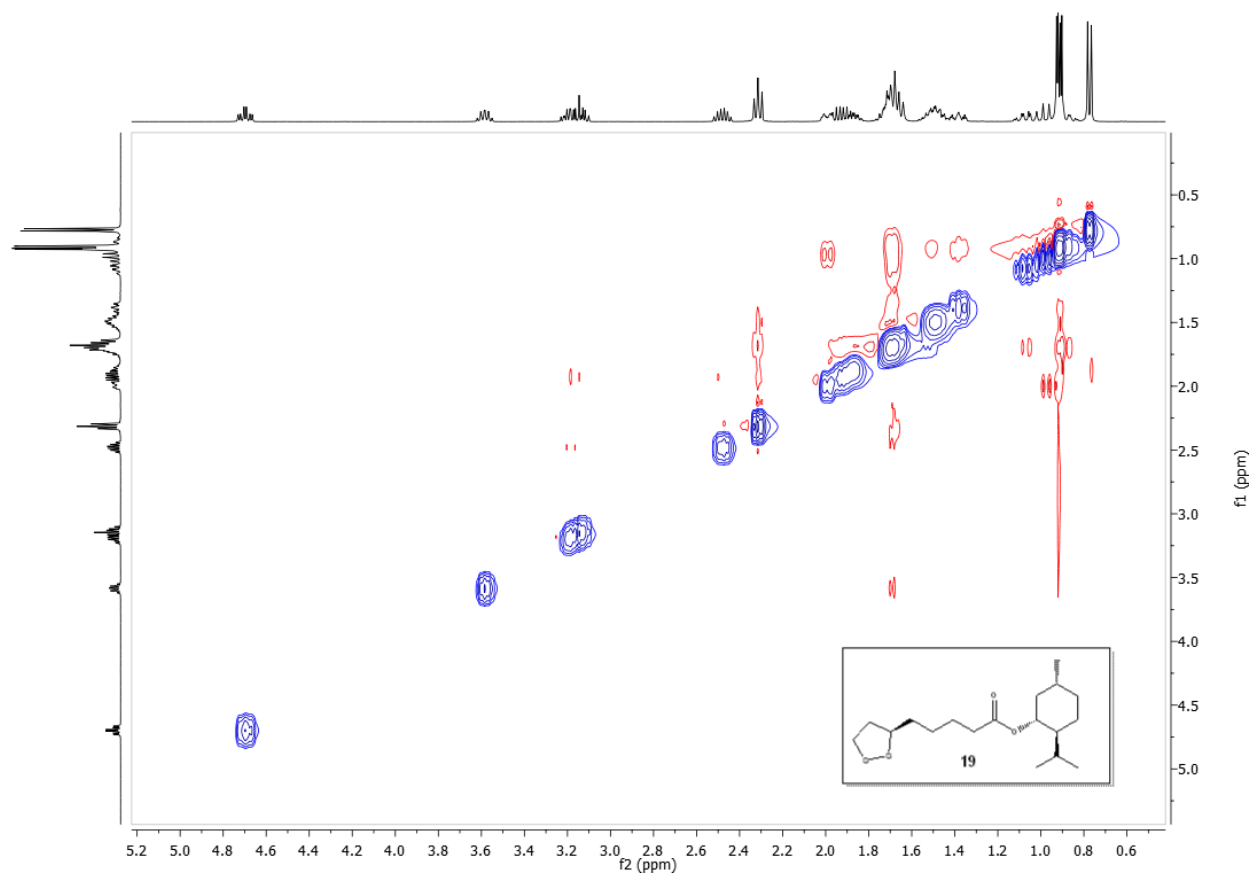
H-H COSY (Chloroform-d) for **19**



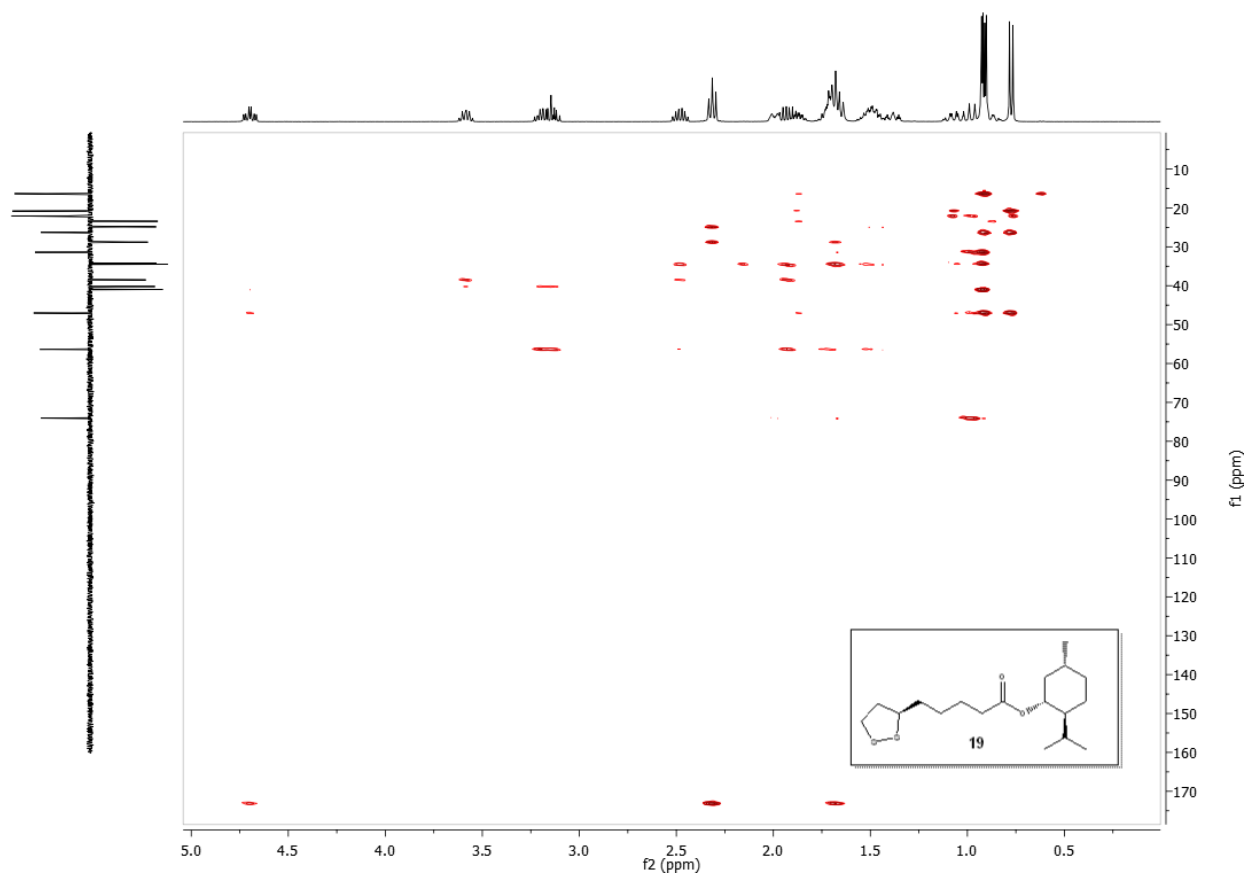
HSQC (Chloroform-d) for **19**



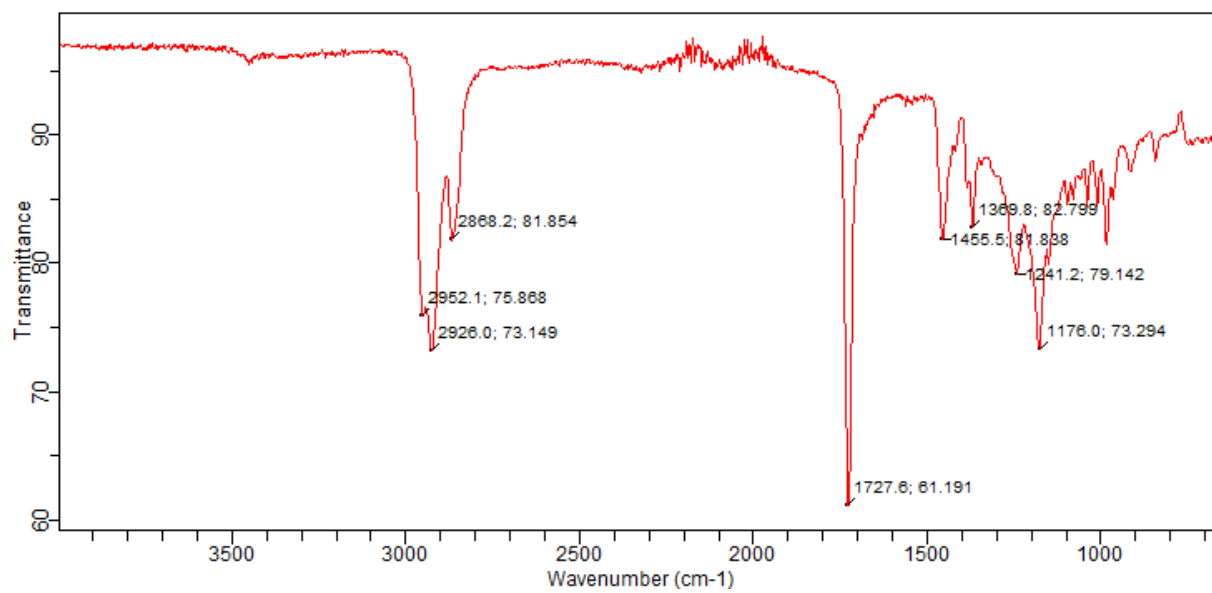
NOESY (Chloroform-d) for **19**



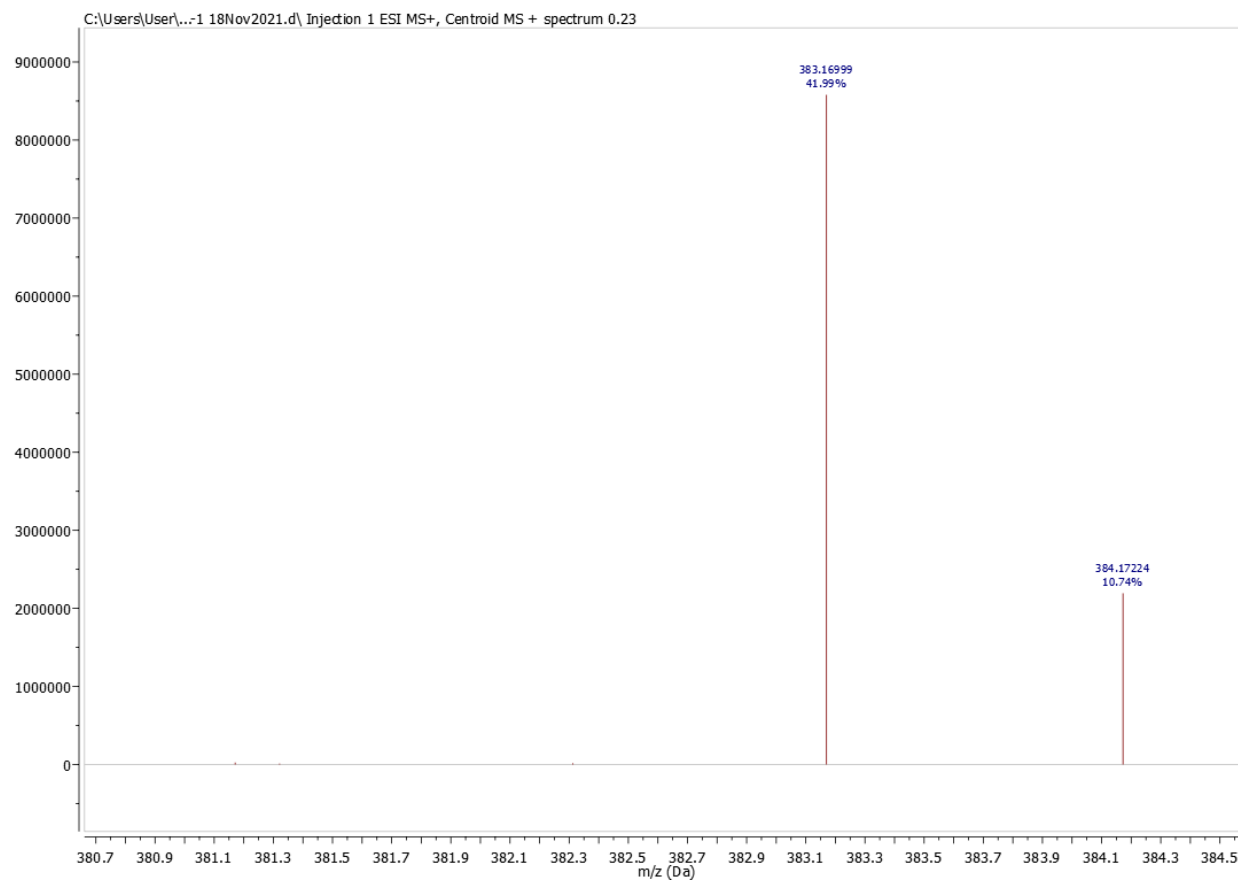
HMBC for 19



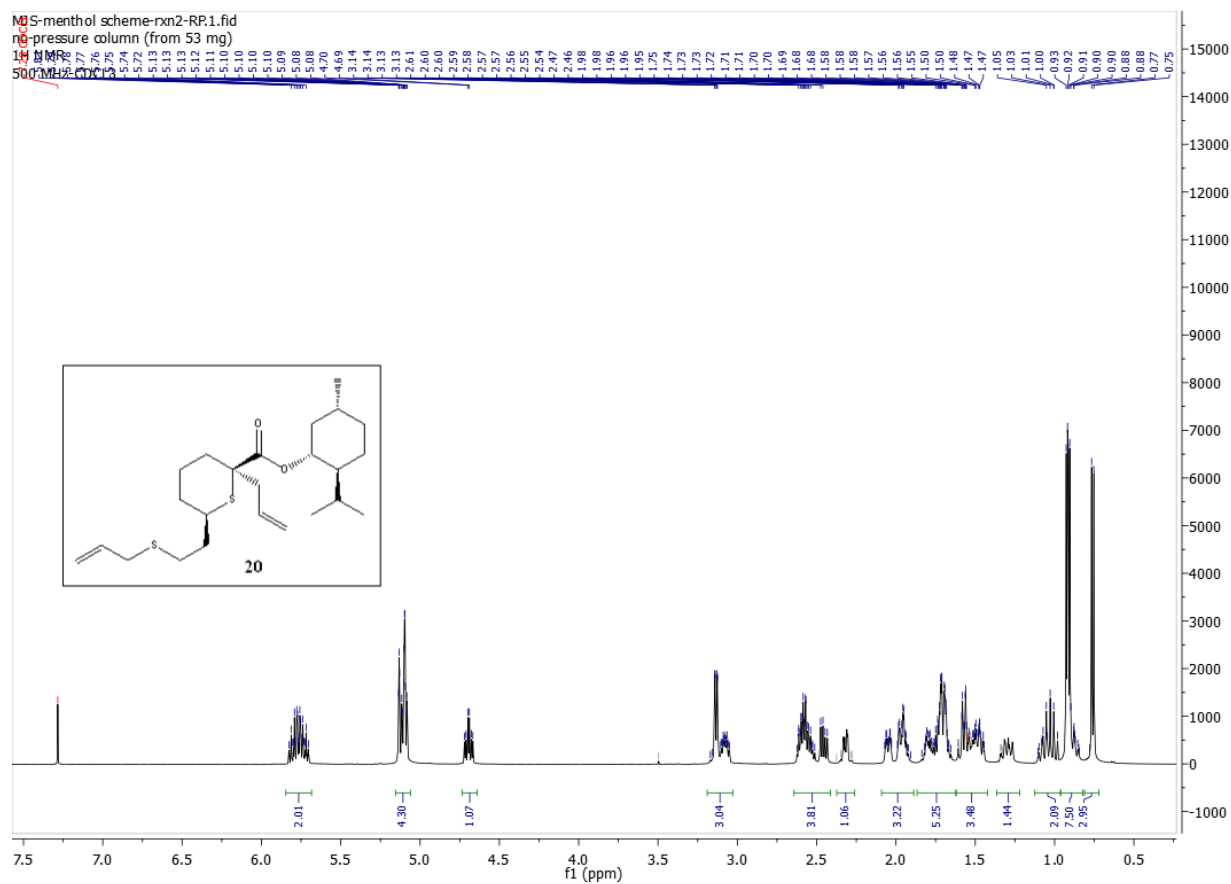
IR (KBr) for **19**



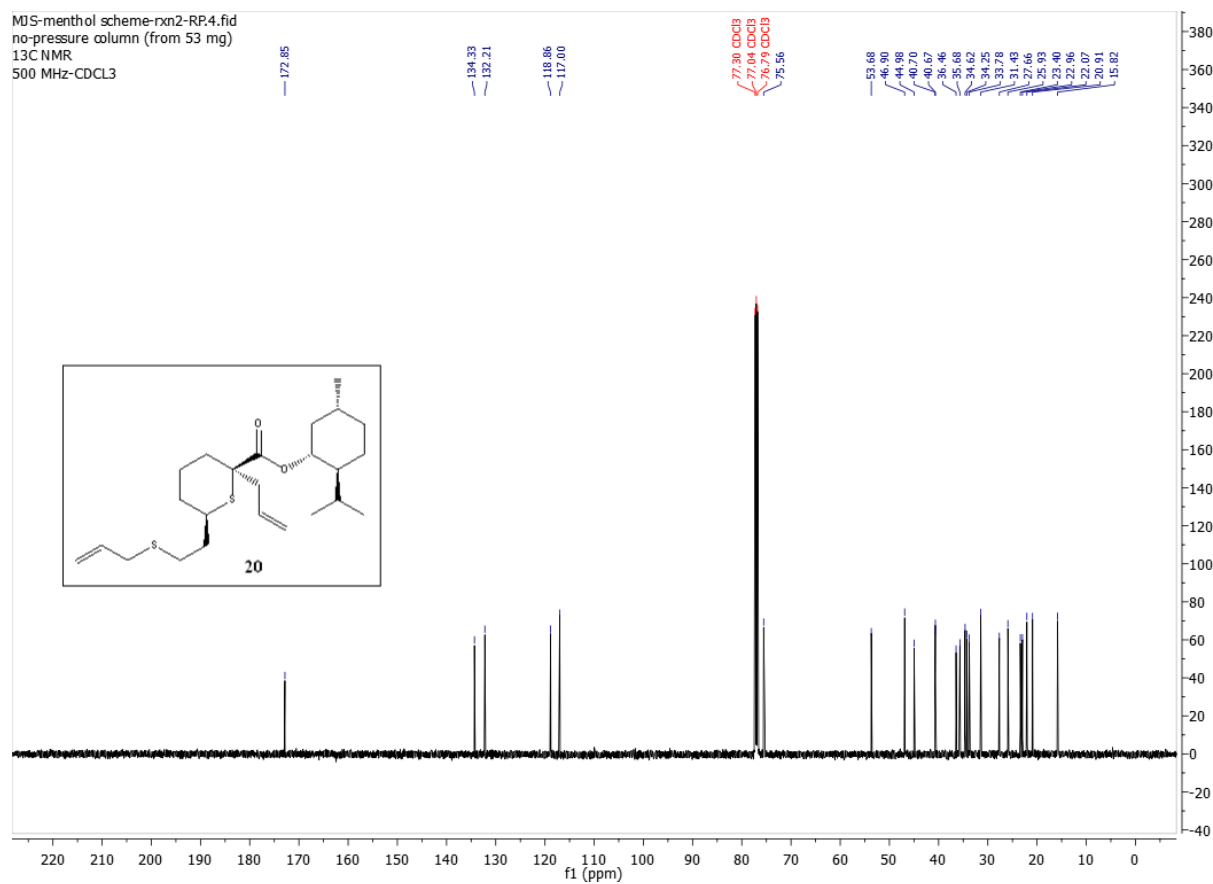
HRESIMS for 19



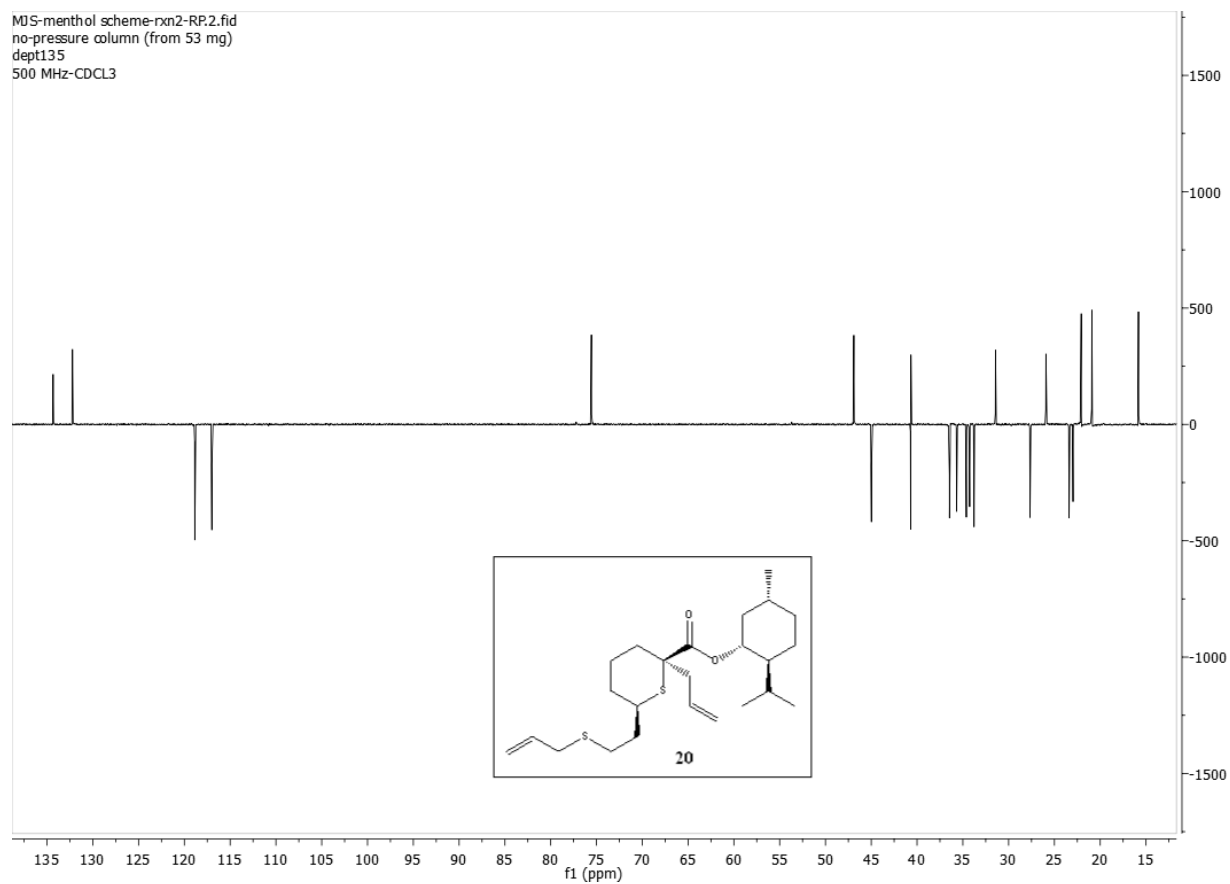
¹H NMR (500 MHz, Chloroform-d) for **20**



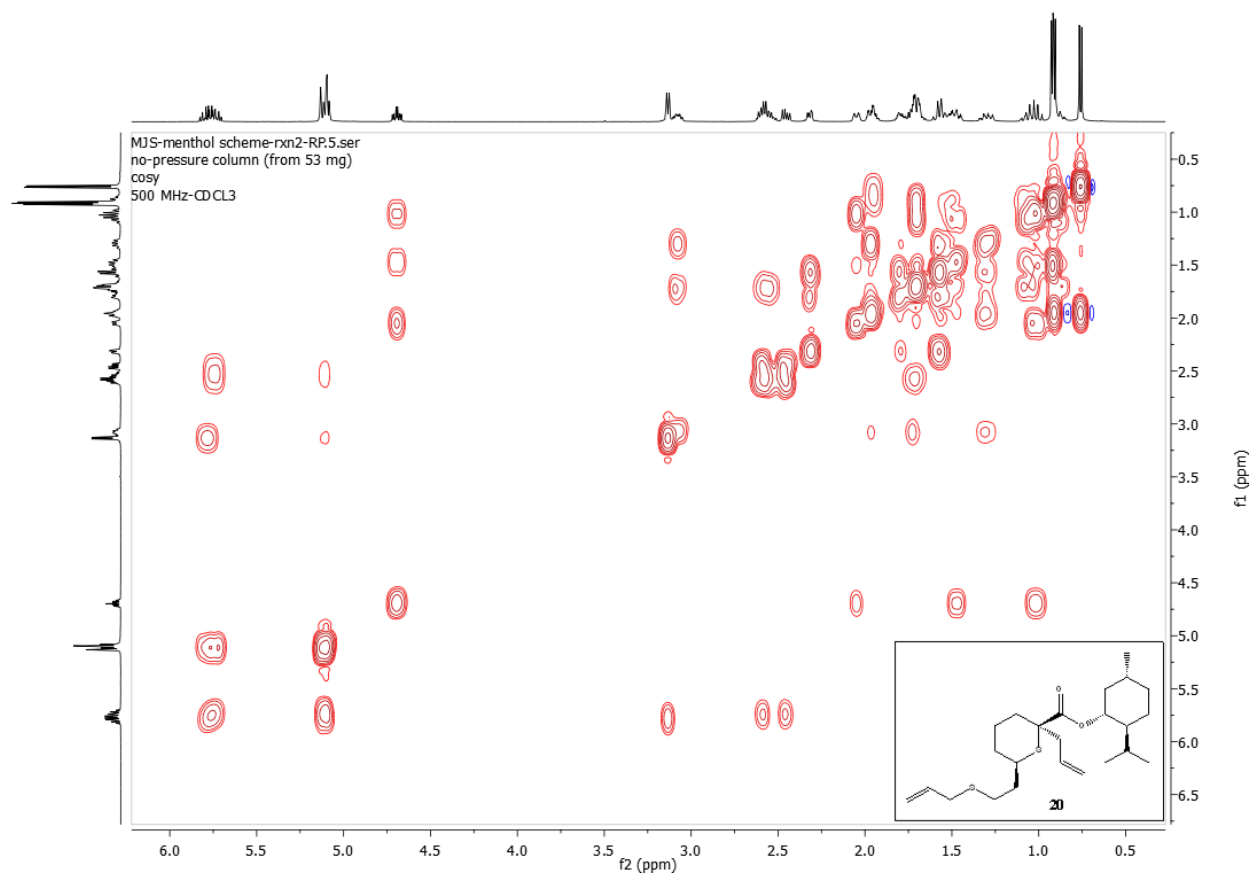
¹³C NMR (126 MHz, Chloroform-d) for **20**



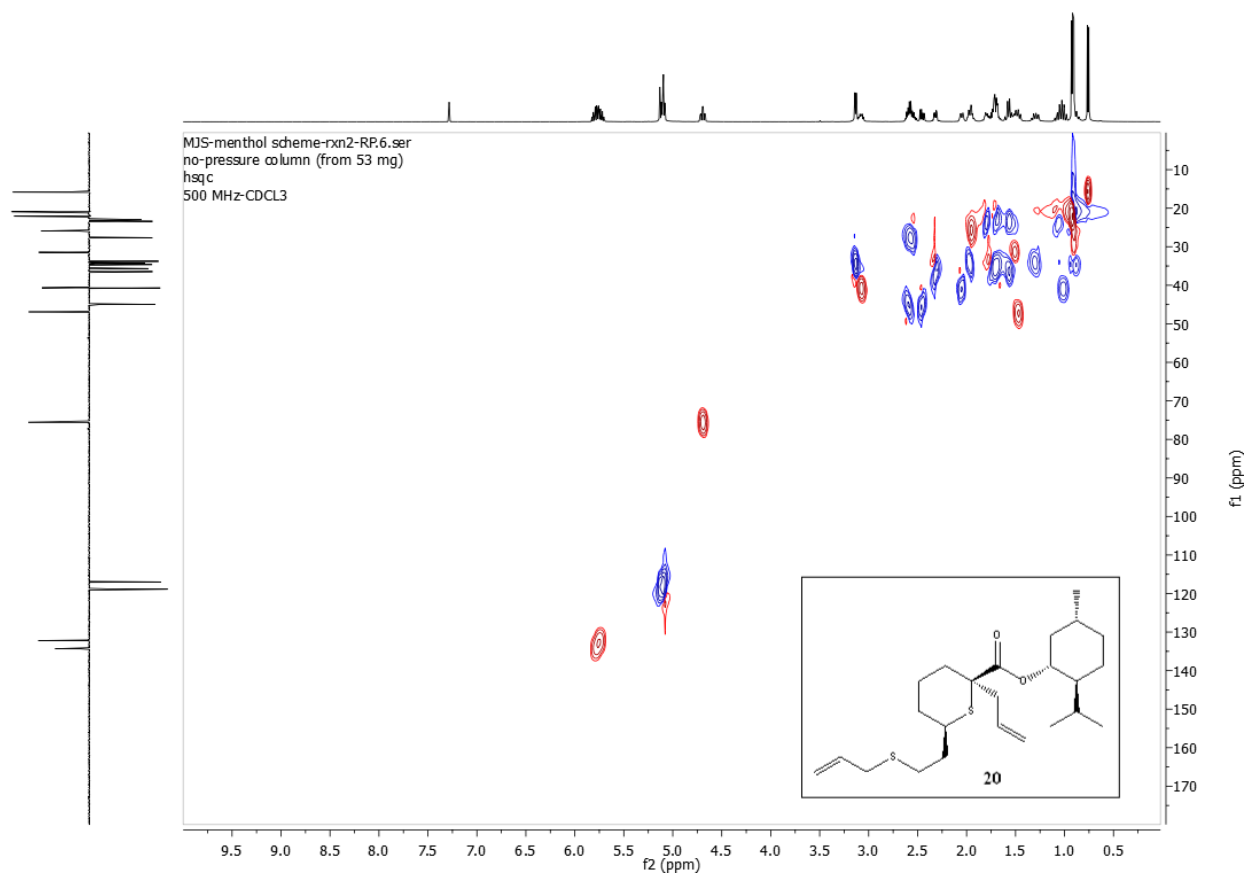
DEPT 135 (Chloroform-d) for **20**



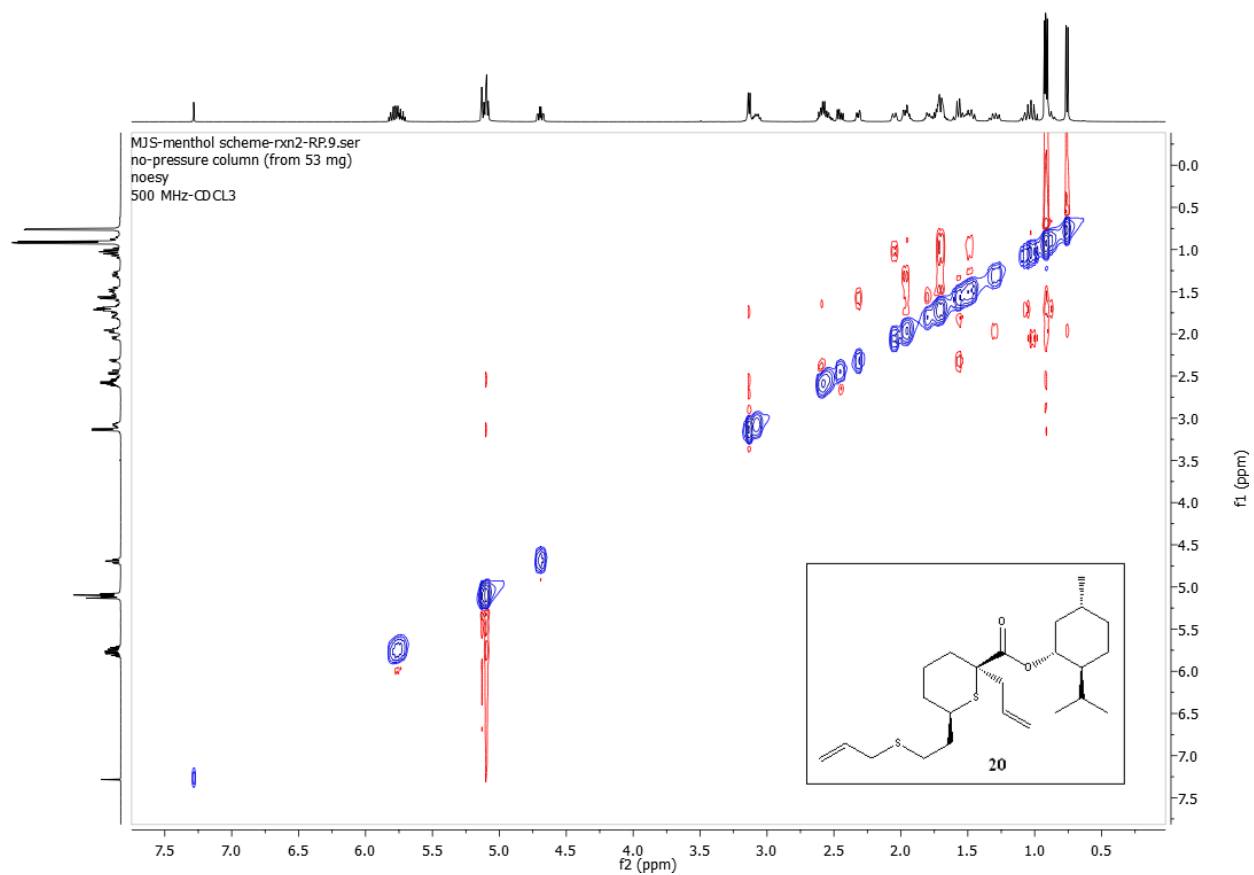
H-H COSY (Chloroform-d) for **20**



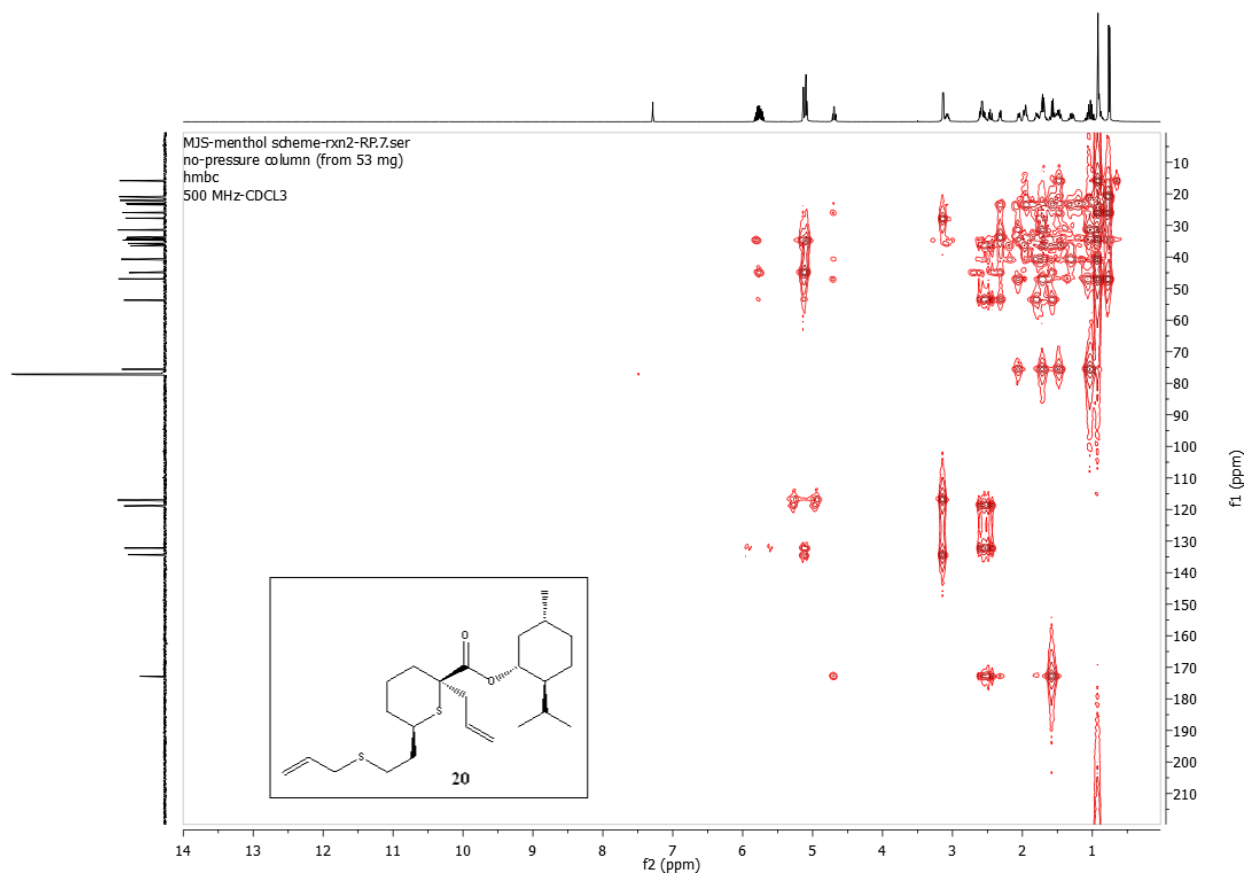
HSQC (Chloroform-d) for **20**



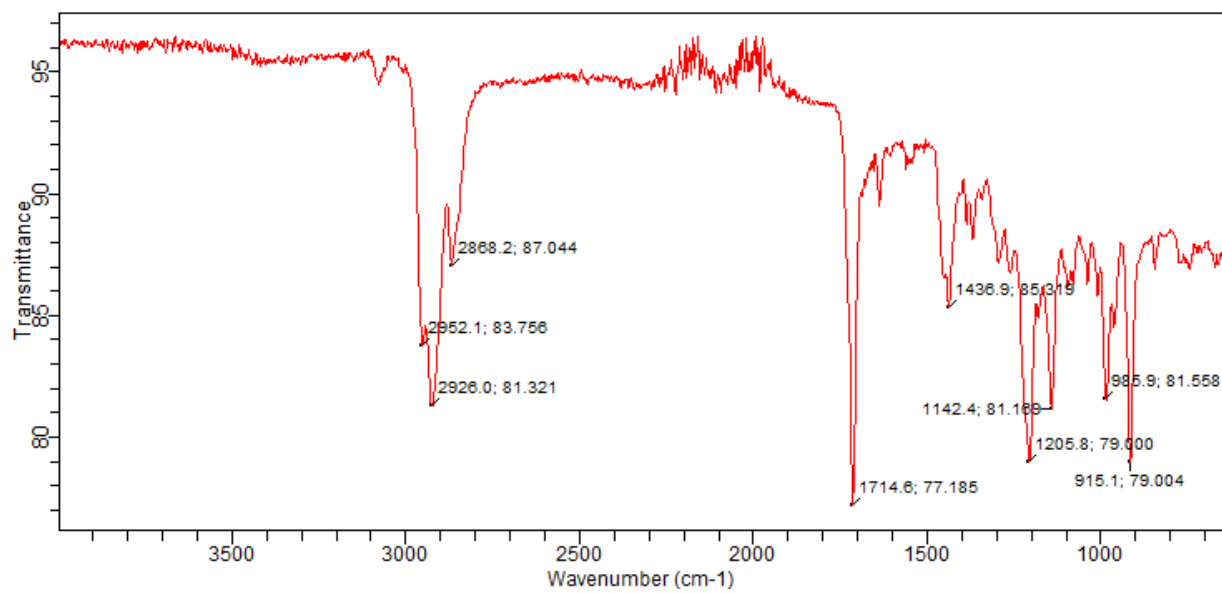
NOESY (Chloroform-d) for **20**



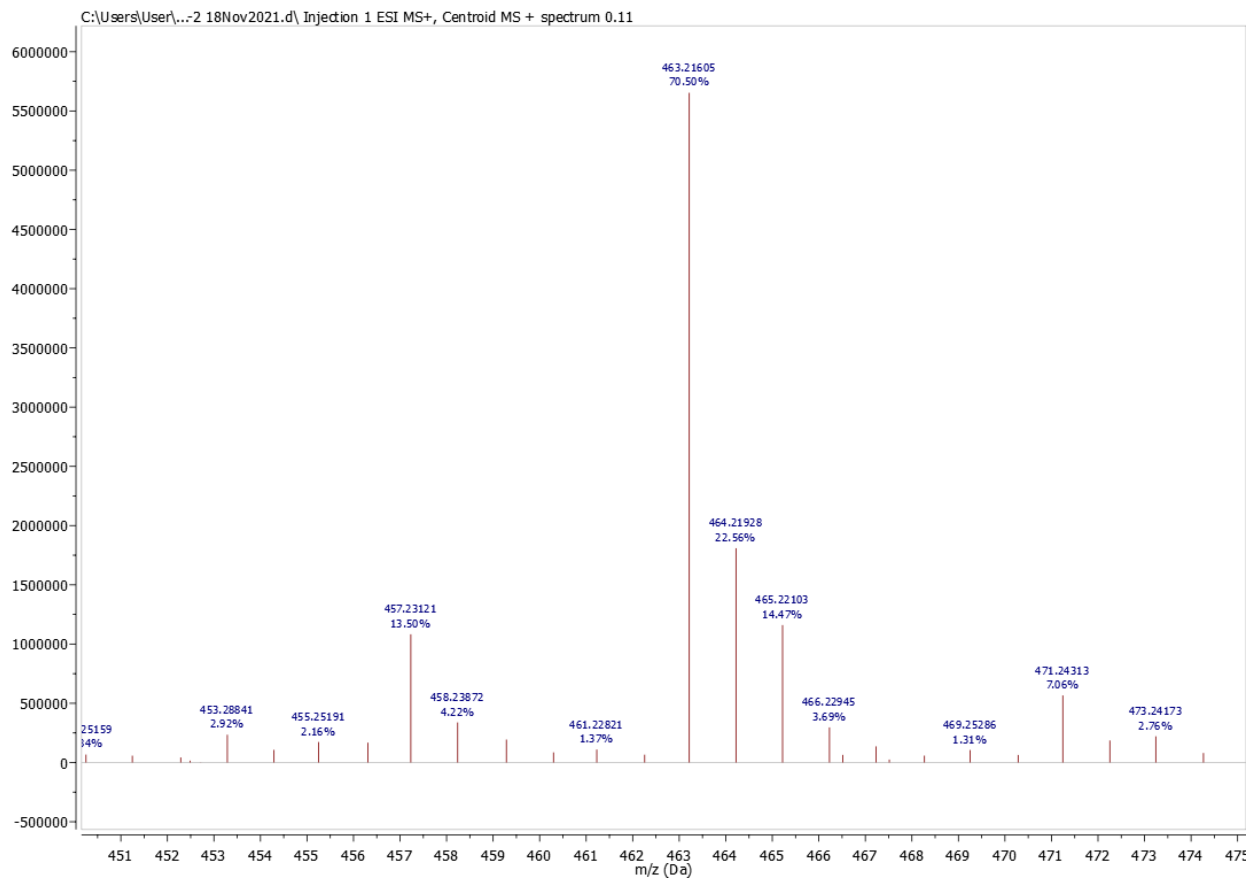
HMBC for 20



IR (KBr) for **20**

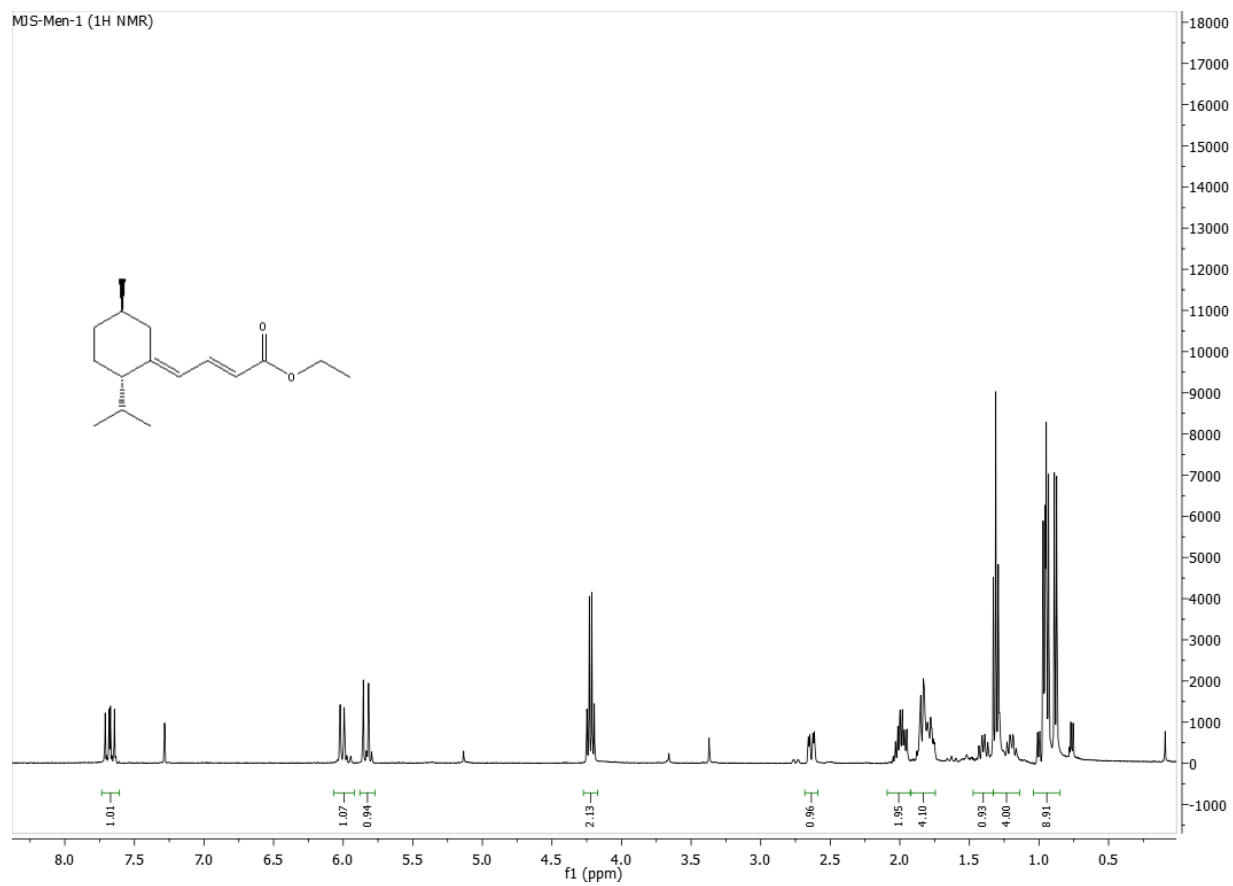


HRESIMS for 20

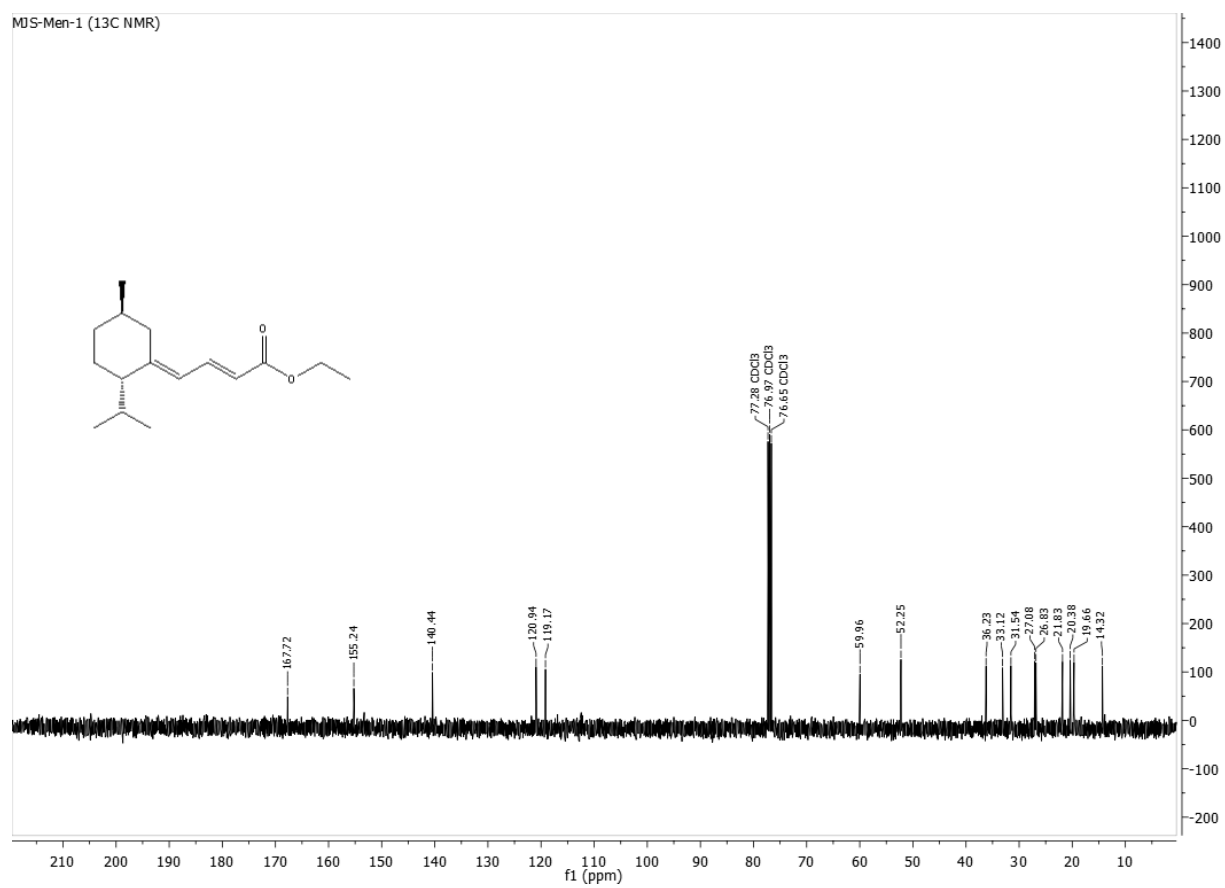


APPENDIX 2. SUPPLEMENTARY DATA-CHAPTER IV

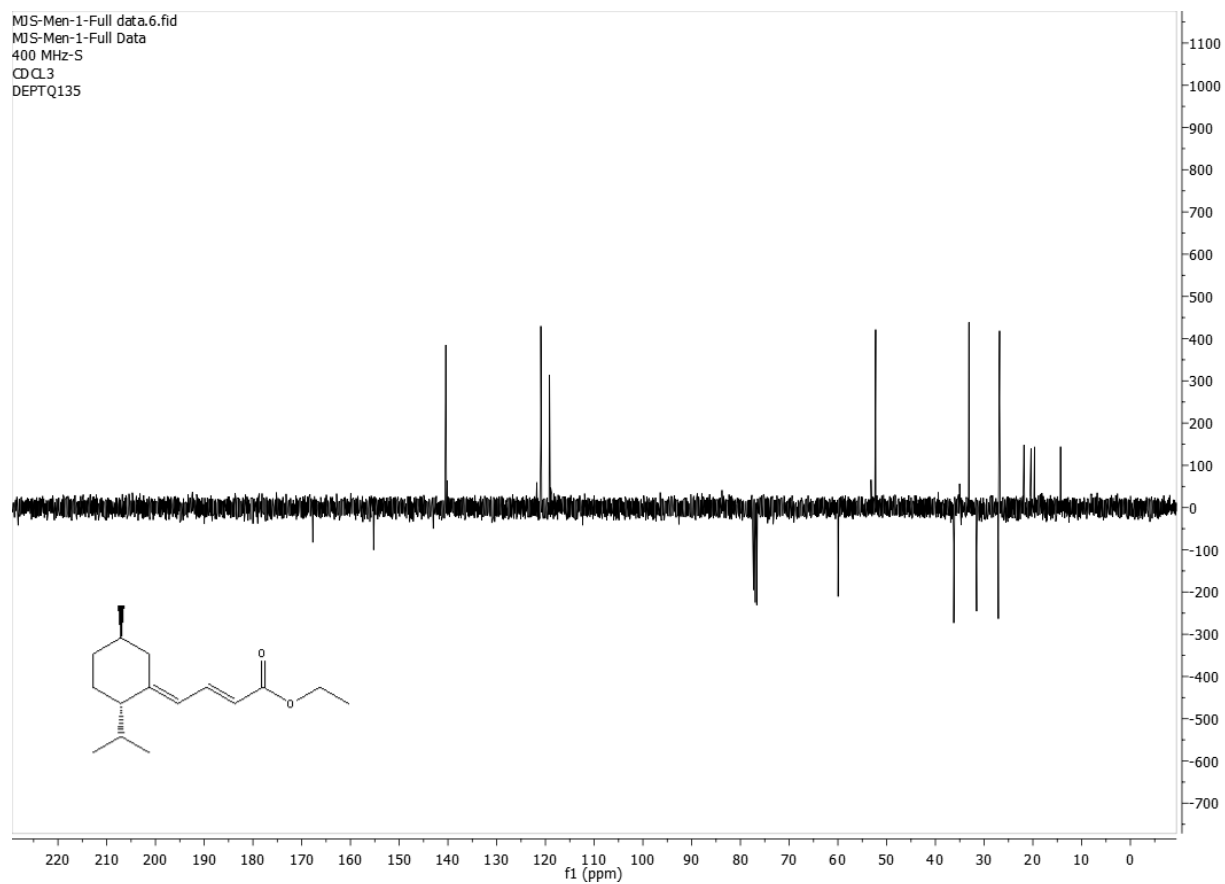
¹H NMR (400 MHz, Chloroform-d) for **AJM-IGR-100**



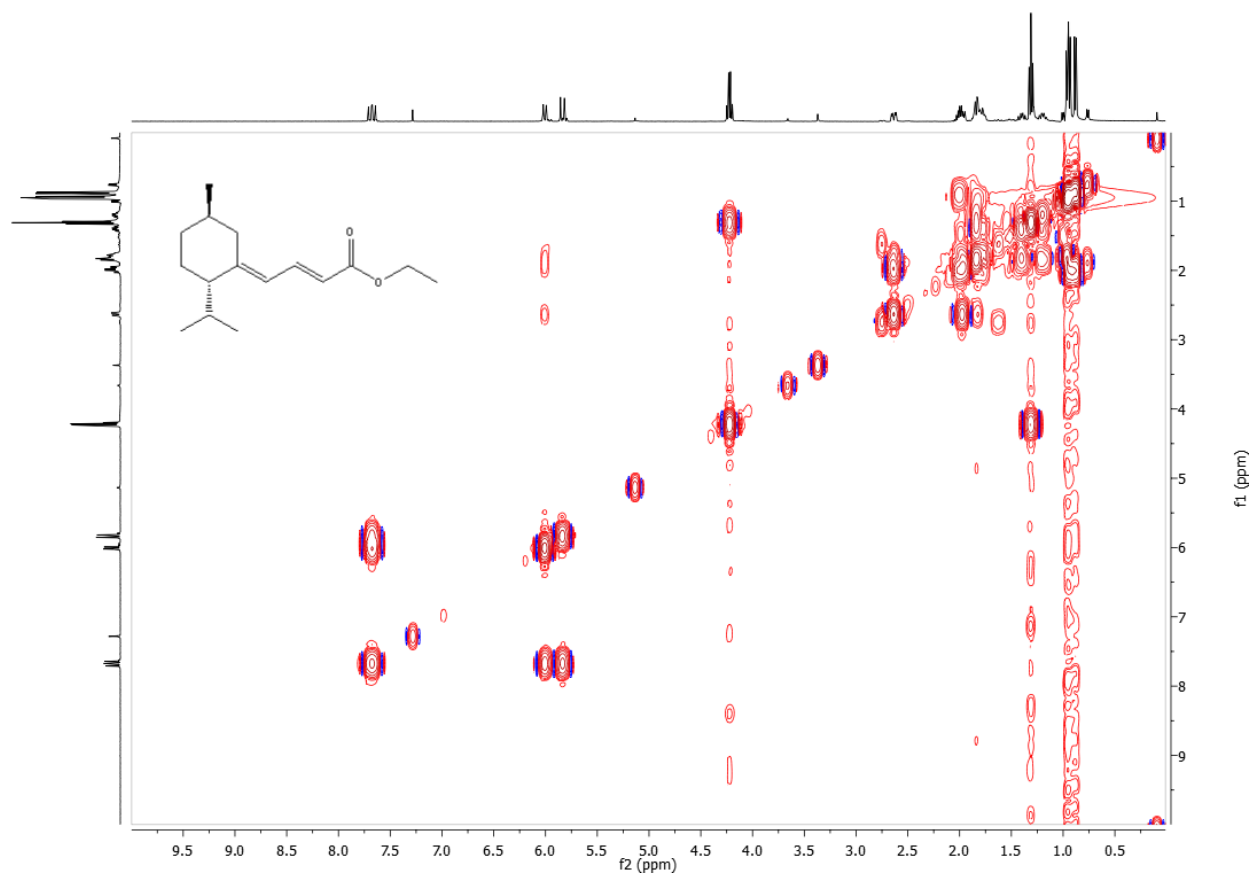
^{13}C NMR (101 MHz, Chloroform-d) for AJM-IGR-100



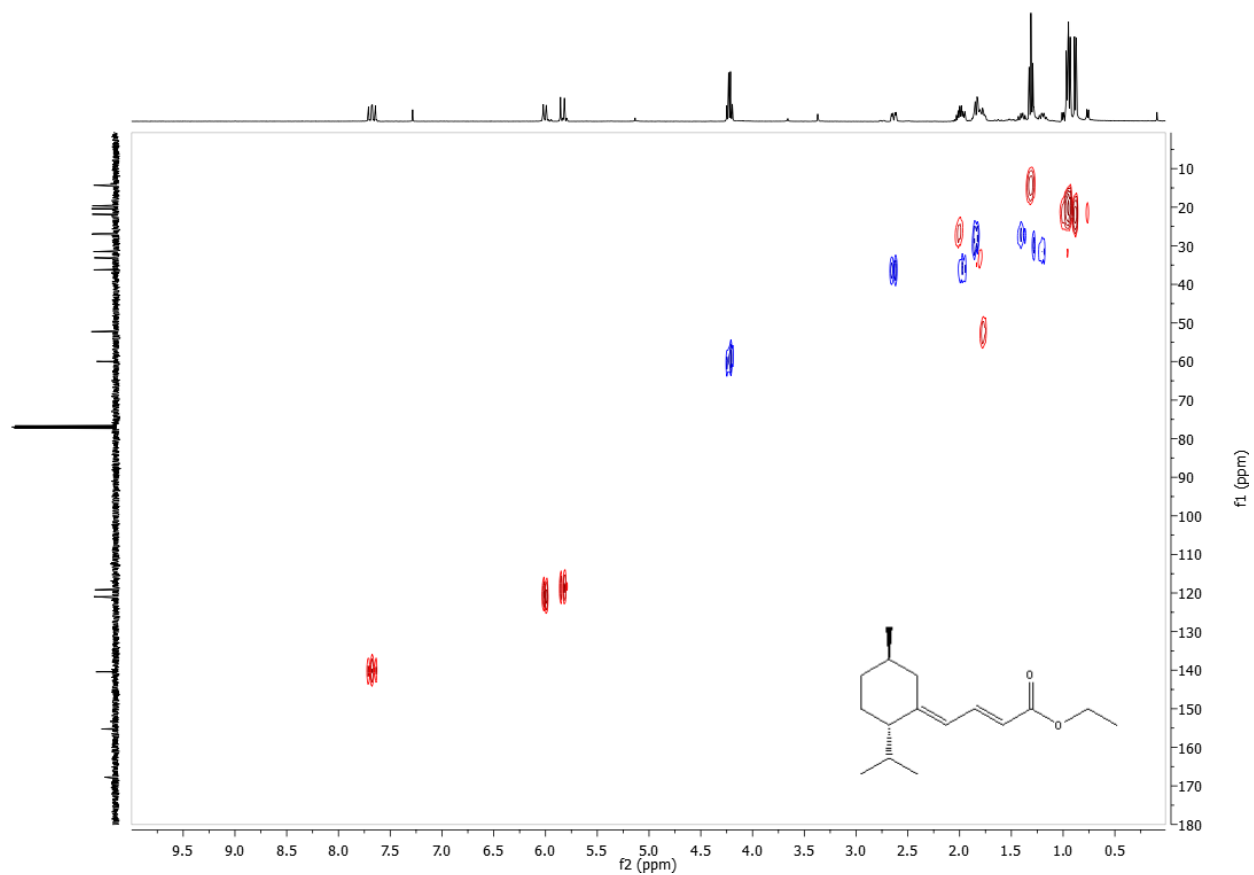
DEPTQ 135 (Chloroform-d) for AJM-IGR-100



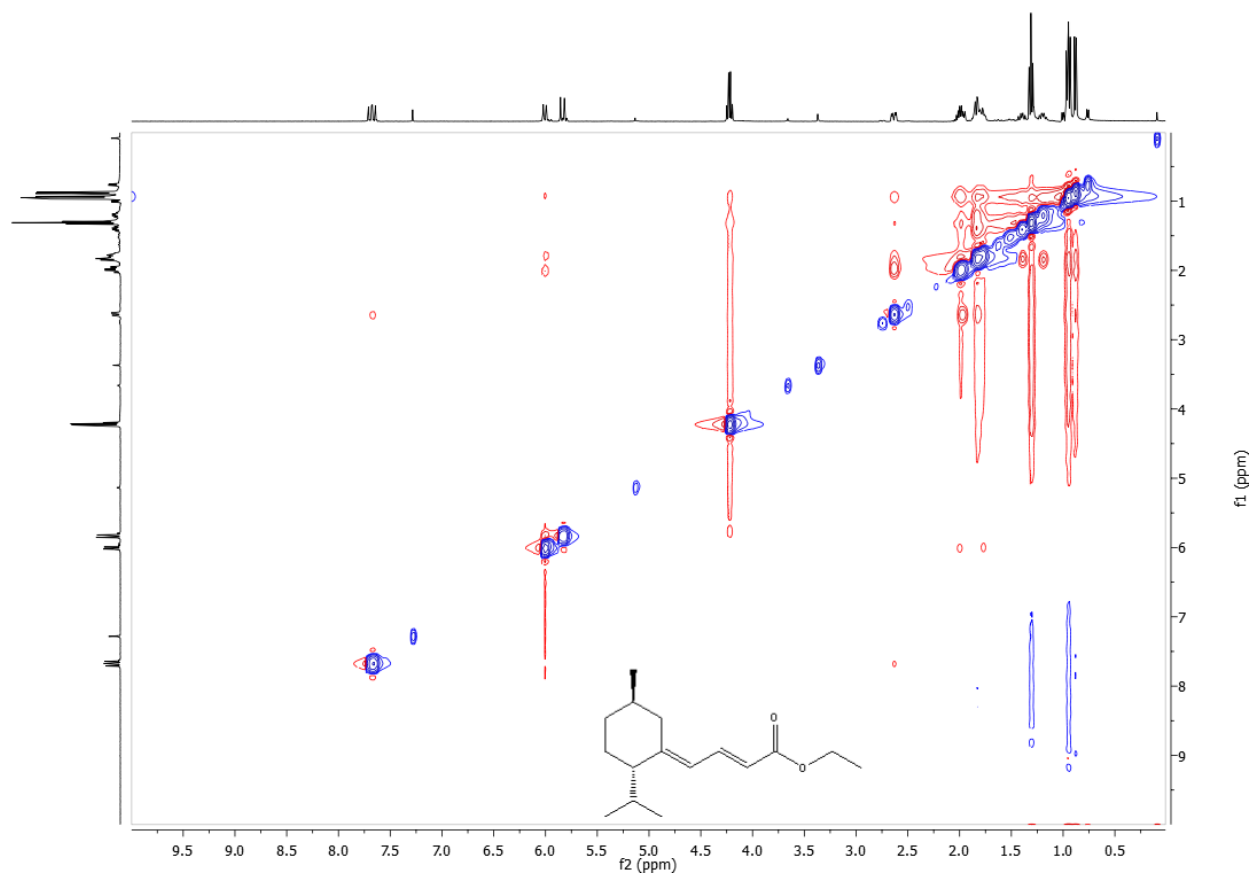
DQCOSY (Chloroform-d) for AJM-IGR-100



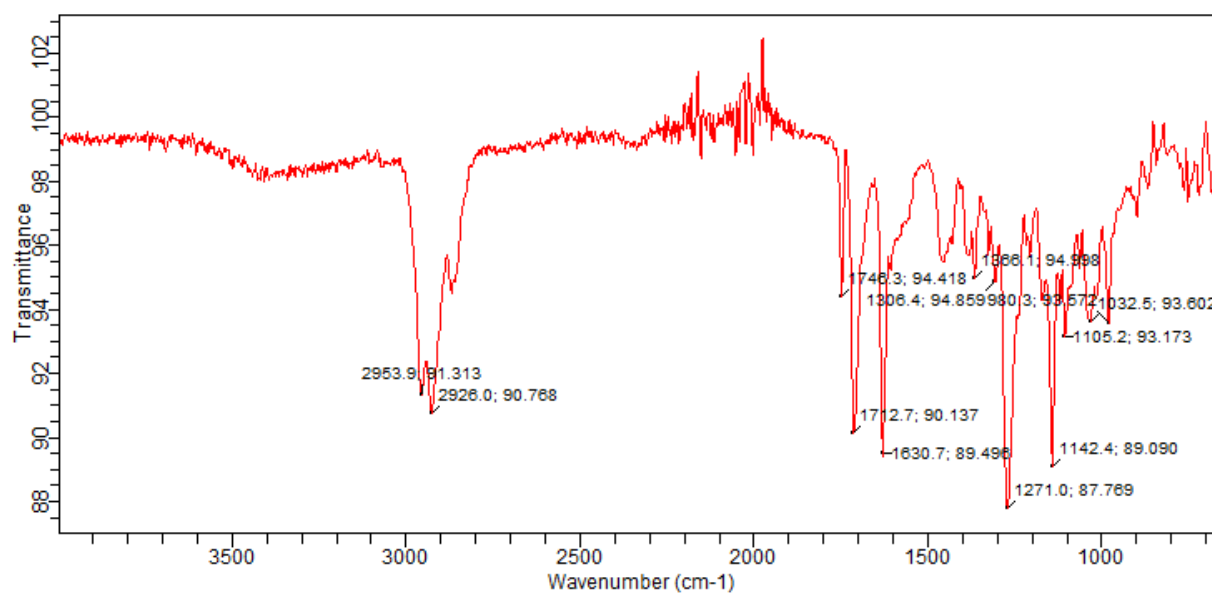
HSQC (Chloroform-d) for AJM-IGR-100



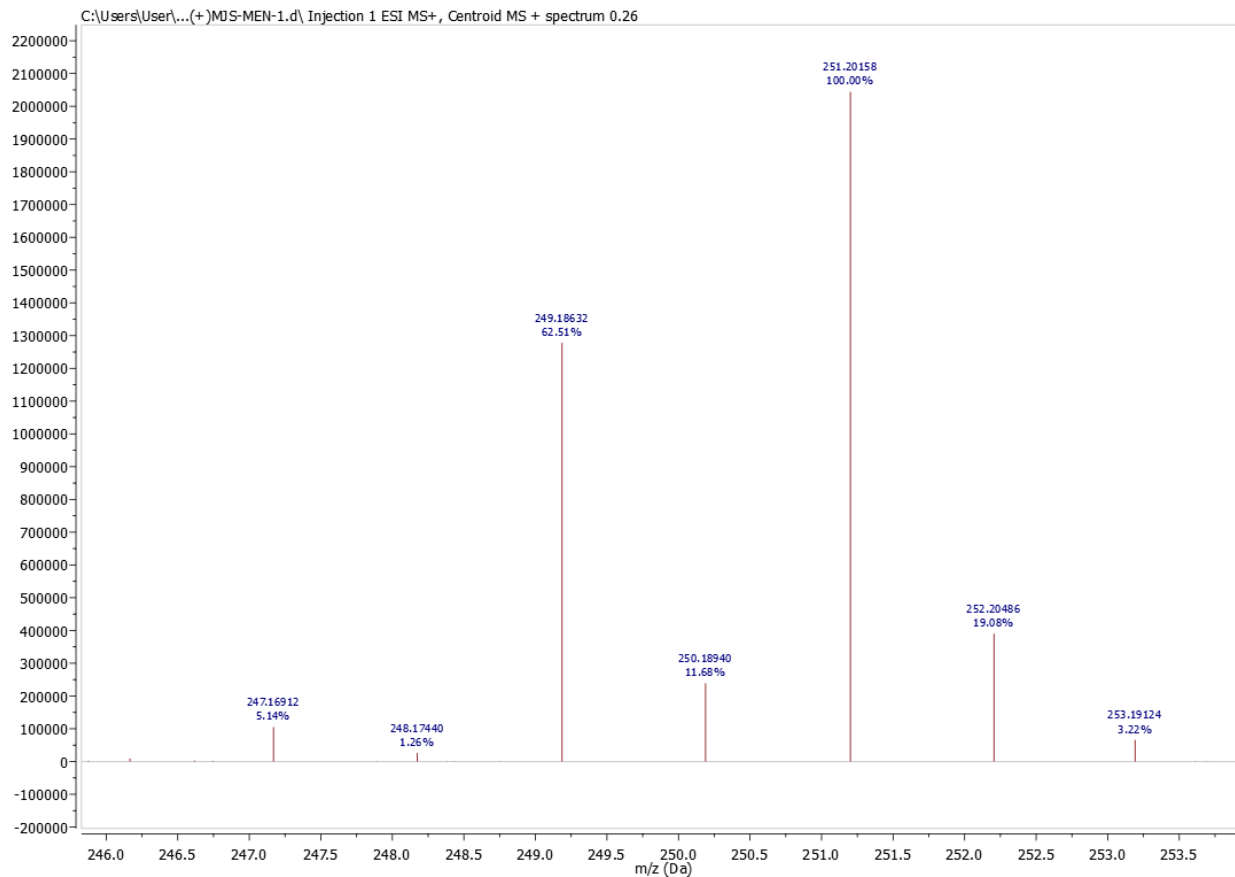
NOESY (Chloroform-d) for AJM-IGR-100



IR (KBr) for AJM-IGR-100



HRESIMS for AJM-IGR-100



VITA

WORK EXPERIENCE

(August 2016-Present), Research assistant/PhD candidate

The University of Mississippi, BioMolecular Sciences department, College of Pharmacy, Oxford, MS, United States of America.

(May 2012 – Present), Teaching assistant

King Saud University (KSU), Pharmacognosy department, College of Pharmacy, Riyadh, Saudi Arabia.

Received a full scholarship from KSU to pursue PhD in Pharmaceutical Sciences, Pharmacognosy.

(Aug 2011), Pharmacy Trainee

King Khalid University Hospital, Riyadh, Saudi Arabia.

(Aug 2010), Pharmacy Trainee

Riyadh Military Hospital, Riyadh, Saudi Arabia.

EDUCATION

(August 2016-Present), PhD candidate in Pharmaceutical Sciences with emphasis in Pharmacognosy.

The University of Mississippi, BioMolecular Sciences department, College of Pharmacy, Oxford, MS, United States of America.

(Sept 2006 — Jan 2012), B.S. in Pharmaceutical Sciences with First Class Honors.

King Saud University (KSU), College of Pharmacy, Riyadh, Saudi Arabia.

HONORS

(2018) The Honor Society of Phi Kappa Phi.

(2018) Golden Key International Honor Society.

(2019) The Honor Society of Gamma Beta Phi.

(2021) The Honor Society of Rho Chi

PUBLICATIONS

1. Negm WA, El-Aasr M, Attia G, **Alqahtani MJ**, Yassien RI, Abo Kamer A, Elekhrawy E. Promising Antifungal Activity of *Encephalartos laurentianus* de Wild against *Candida albicans* Clinical Isolates: In Vitro and In Vivo Effects on Renal Cortex of Adult Albino Rats. *Journal of Fungi*. **2022**; 8(5):426.
2. Slater, S.E., Lasonkar, P.B., Haider, S., **Alqahtani, M.J.**, Chittiboyina, A.G., & Khan, I.A. **(2018)**. One-step, stereoselective synthesis of octahydrochromanes via the Prins reaction and their cannabinoid activities. *Tetrahedron letters*, 59 9, 807-810.
3. **Alqahtani, M.J.**; Slater, S.; Chittiboyina, A.G.; Khan, I.A. Asymmetric synthesis of optical antipodes of lipoic acid. *In preparation*.
4. **Alqahtani, M.J.**; Rehman, J.U.; Chittiboyina, A.G.; Khan, I.A. Natural product analog as an insect growth regulator to control bed bug population. *In preparation*.
5. A patent is currently under review.